ЖУРНАЛ
ПРИКЛАДНОЙ ХИМИИ

Vol. 31 No. 8

August 1958

JOURNAL OF
APPLIED CHEMISTRY
OF THE USSR

(ZHURNAL PRIKLADNOI KHIMII)

IN ENGLISH TRANSLATION

CONSULTANTS BUREAU, INC.

2 MORE RUSSIAN JOURNALS
NOW IN ENGLISH TRANSLATION

IMMEDIATELY AVAILABLE—

(TRANSLATION BEGAN WITH 1957 VOLUMES)

DOKLADY SECTIONS

PHYSICAL CHEMISTRY,
GEOLOGICAL SCIENCES,

Doklady (Proceedings of the Academy of Sciences of the USSR) contains concise reports by leading Soviet scientists. It offers a comprehensive survey of the most advanced Soviet research.

Physical Chemistry—Approx. 500 pages per year. Includes all reports on chemical kinetics, interface phenomena, electrochemistry, absorption spectra, and related subjects.
Single issues, $35.00 — 6 issues per year, $160.00

Geological Sciences—Approx. 750 pages per year. Covers geology, hydrogeology, mineralogy, petrography, and geophysics.
Single issues, $40.00 — 6 issues per year, $200.00

Cover-to-cover translations by **bilingual scientists,** including all diagrams, photographs, and tabular material. Journals are staple bound in durable paper covers; clear multilith reproduction from IBM "cold type." Doklady is published in 36 issues annually—Consultants Bureau's English translation is published in 6. Issues are mailed to subscribers immediately upon publication.

CONSULTANTS BUREAU, INC.
227 W. 17th St., NEW YORK 11, N. Y.

Vol. 31 No. 8

August 1958

JOURNAL OF
APPLIED CHEMISTRY
OF THE USSR

(ZHURNAL PRIKLADNOI KHIMII)

A publication of the Academy of Sciences of the USSR

IN ENGLISH TRANSLATION

Year and issue of first translation:
vol. 23, no. 1 January 1950

	U. S. and Canada	*Foreign*
Annual subscription	*$60.00*	*$65.00*
Annual subscription for libraries of non-profit academic institutions	*20.00*	*25.00*
Single issue	*7.50*	*7.50*

Copyright 1959

CONSULTANTS BUREAU INC.
227 W. 17th ST., NEW YORK 11, N. Y.

Editorial Board
(ZHURNAL PRIKLADNOI KHIMII)

P.P. Budnikov, S.I. Vol'fkovich, A.F. Dobrianskii,
O.E. Zviagintsev, N.I. Nikitin (Editor in Chief),
G.V. Pigulevskii, M.E. Pozin, L.K. Simonova
(Secretary), S.N. Ushakov, N.P. Fedot'ev

NOTE: The sale of photostatic copies of any portion of this copyright translation is expressly prohibited by the copyright owners.

Printed in the United States

JOURNAL OF APPLIED CHEMISTRY

Vol. 31, No. 8 August, 1958

CONTENTS

	PAGE	RUSS. PAGE
The Present State and Development Prospects of the Production of Dilute Nitric Acid. M. A. Miniovich	1121	1129
Decomposition of Zinc and Cobalt Sulfates in a Current of Sulfur Dioxide and Air. V. V. Pechkovskii.	1130	1139
Mechanism of the Decomposition of Nephelines by Alkaline Solutions. V. D. Ponomarev and V. S. Sazhin	1134	1143
Acceleration of Porcelain Production. A. I. Avgustinik and V. M. Loginov	1140	1150
Study of the Burning Out of Chromium in the Production of Synthetic Ruby. G. A. Mukhin, N. I. Maliugina, and T. S. Uspenskaia	1150	1160
Effect of the Composition of Glasses on the Influence of Me_2O and Al_2O_3 Oxides on Their Electrical Conductivity. L. A. Grechanik	1154	1164
Oxygen and Nitrogen in Metallization Pseudoalloys. L. V. Krasnichenko and M. G. Ross	1160	1170
"Shavingless" Dissolution of Alloys. A. G. Loshkarev	1165	1175
The Occurrence of Hydrogen Embrittlement of Steel in Aqueous Solutions of Hydrogen Sulfide. S. A. Balezin and I. V. Nikol'skii	1171	1181
Hydrogen Embrittlement of Steel in Cathodic Treatment. M. A. Figel'man and A. V. Shreider	1175	1184
Influence of the pH of the Medium and the Temperature on the Proportions of Active Oxidizing Agents in Hypochlorite Solutions in Chlorination and Bleaching Processes. I. E. Flis	1183	1194
Colloidal Stability of Lithium Lubricants and the Influence of Their Dispersion Media on it. V. V. Sinitsyn, K. I. Klimov, and E. V. Aleeva	1191	1202
Effect of pH on the Oxidation–Reduction Potential of a Solution Containing Ferric and Ferrous Ions. O. N. Lapteva	1199	1210
Determination of the Interphase Area in Emulsions. A. V. Ianishevskii and I. S. Pavlushenko	1205	1215
Liquid–Vapor Equilibrium in the Binary Mixtures Ethyl Alcohol–Isopropyl Alcohol and Carbon Disulfide–Methyl Iodide. G. A. Gaziev, Ia. D. Zel'venskii, and V. A. Shalygin	1210	1220
The Use of Dienols as "Hardening" Accelerators for Unsaturated Polyester Resins. R. K. Gavurina, A. V. Mitrofanova, and N. S. Dmitrieva	1217	1227

(continued)

CONTENTS (continued)

	PAGE	RUSS. PAGE
Polymerization of Vinylacetylene. I. M. Dolgopol'skii, Z. F. Dobler, A. P. Iashina, and P. N. Trofimova	1224	1234
Preparation of 8-(Trichloromethyl)-theobromine and Theobromine. E. S. Golovchinskaia, V. M. Fedosova, and A. A. Cherkasova	1230	1241
Mechanical Properties of Casein Films. V. I. Eliseeva and E. V. Kuz'mina	1234	1245
Coke Formation in Catalytic Destructive Hydrogenation of Petroleums and Petroleum Residues. Ia. R. Katsobashvili and N. V. Sidorova	1240	1252
Investigation of the Composition of Phenols from the Thermal Liquefaction of Peat. M. K. D'iakova and N. A. Davtian	1246	1259
Brief Communications		
Thermodynamic Properties of Liquid Alloys in the System Sodium–Lead. A. G. Morachevskii	1252	1266
Experimental Investigation of the Gas Reduction of Na_2SO_4 to Na_2CO_3 in the Shaft Furnace. A. I. Gorbanev	1256	1270
Synthesis of Cation-Exchange Resins by Sulfonation of Phenol–Formaldehyde Novolacs at Elevated Temperatures. A. A. Vasil'ev and A. A. Vansheidt	1260	1273
Neoabietic Acid – A Primary Acid of the Oleoresin of Picea Excelsa Link. I. I. Bardyshev and Kh. A. Cherches	1263	1276
Determination of Cyclohexanone in Presence of Other Ketones. A. S. Maslennikov	1265	1277

THE PRESENT STATE AND DEVELOPMENT PROSPECTS OF THE PRODUCTION OF DILUTE NITRIC ACID

M. A. Miniovich

Nitric acid is among the products of the chemical industry of which the output is counted in millions of tons annually. It is the main raw material in the production of various substances of great importance in agriculture and industry. The most extensive use of dilute (weak) nitric acid, of 45-58% concentration, is for the production of fertilizers. Some of this acid is converted into concentrated (strong) 96-98% nitric acid, which is used in dye manufacture, in rocket technology, and other industries.

The scale of production of dilute nitric acid is primarily determined by the growth of its consumption in the manufacture of nitrogenous fertilizers, among which ammonium nitrate is the most important. In the postwar years, according to United Nations data [1], the production of some of these fertilizers has been increasing continuously, as shown in Table 1.

TABLE 1

Production of the Principal Nitrate Fertilizers in the Capitalist Countries in 1952-1955

Years	Total production of all nitrogenous fertilizers (in all capitalist countries) (millions of tons)	Broken down into individual types (%, by nitrogen content)		
		ammonium nitrate (solid)•	calcium nitrate	sodium nitrate
1952-1953	4.58	23.6	6.1	5.1
1953-1954	5.11	26.2	6.6	5.1
1954-1955	5.60	27.3	6.4	4.7

•Including production of calcium–ammonium nitrate, and ammonium sulfate–nitrate.

The considerable growth in the production of nitrogenous fertilizers (including mixed fertilizers), for which dilute nitric acid is needed, has made it necessary to expand considerably the existing nitric acid plants and to build many large new units.

Among the capitalist countries, the first place in nitric acid output is occupied by U.S.A., and the second by the Federal German Republic [2].

The growth of nitric acid production in U. S. A. during 1950-1955 is illustrated by the following data:

	Years					
	1950	1951	1952	1953	1954	1955
Production in 1000's of tons, as 100% acid	1212	1372	1475	1588	1777	2070

It should be noted that during the postwar years much attention has been devoted to expansion of nitric acid production even in those leading capitalist countries which were considerably behind such countries as U.S.A. and Germany in this respect. For example, in France the capacity of all the nitric acid plants increased by 82% from 1948 to 1954, and was over 800,000 tons in 1955.

The combined output of nitric acid in all the capitalist countries exceeds 7,000,000 tons per year.

I. The State of the Nitric Acid Industry

At the present time nitric acid is made almost exclusively by the contact oxidation of ammonia to nitric oxide in presence of platinum catalysts. The production of nitrogen oxides and their conversion into nitric acid is effected in units which differ mainly in the pressures used in the principal equipment, and in certain technological process conditions [3].

The industrial processes for the production of nitric acid are usually subdivided into three groups: 1) systems operated at pressures close to atmospheric; 2) systems operated under high pressures; 3) systems operated by a combined procedure – ammonia is oxidized at atmospheric pressure, and the nitrogen oxides are absorbed under high pressures.

Formerly, when the production of nitric acid was on a relatively small scale, it was expedient to build units operating at pressures close to atmospheric.

The advantages of the atmospheric-pressure (low-pressure) process included the relatively low costs of production, and raw materials (290-295 kg of ammonia, 90-110 kw-hrs of electrical energy, 0.049-0.55 g platinum metals, and 70-100 m^3 of water), the simplicity of the equipment, and ease of operation. After the scale of nitric acid production had greatly increased, the construction of new plants operating this process had to be abandoned. For the production of nitric acid at atmospheric pressure it is necessary to use considerable amounts of costly special steels, because it is necessary to install large absorption towers (30-35 m^3 per ton of acid per 24 hours), cumbersome heat exchangers (5-7 m^3 per ton of acid), etc.

For this and other reasons, the new nitric acid plants being built both in the USSR and in leading capitalist countries are designed to operate under increased pressures in the absorption section of the system.* This has led to a reduction of capital expenditure in the construction of new nitric acid plants owing to lower requirements for special steels, has made the use of ceramic packings unnecessary, etc.

The commonest process for the production of nitric acid in the capitalist industries is with the use of high pressures [4]; this is shown by the following data:

Process	Pressure in absorption system (kg/cm^2)
Montecatini	1.8 – 3.4
AZED	2.7 – 3.4
Société Belge du Marly	3.0 – 3.5
Chemical Construction Corporation	4.0 – 4.5
I. G.	1.5 – 5.0
DuPont	8.0

Most of the new nitric acid plants being built in Western Europe (including the Federal German Republic) operate the combined process (ammonia is oxidized to nitric oxide under atmospheric pressure, while nitrogen oxides are absorbed under pressure of 2.0 atmos and over).

Experience has shown that this type of system combines to some extent the advantages of processes for the production of nitric acid under atmospheric pressure (with regard to consumption of platinum metals, the degree of conversion of ammonia to nitric oxide, and, in part, power consumption) with the advantages of high pressure processes (relatively low volumes of absorption and heat-exchange equipment, possibility of block operation, etc.).

*The determining step in the production of nitric acid is oxidation of nitric oxide to dioxide. The rate of this process is proportional to the square of the pressure in the system. It follows that the volume of the equipment can be reduced considerably by the use of even moderate pressures in the oxide absorption system.

In the U.S.A the most common units (mainly of DuPont design) operate under pressures of 7-9 atmos both in the oxidation and in the absorption sections.

Comparative data on capital costs and the requirements with regard to special steels, platinum metals, and power for different processes of dilute nitric acid manufacture are of interest [5]. The values for nitric acid production under atmospheric pressure are taken as unity.

The main data for different processes for the production of dilute nitric acid are given below:

Process scheme	Consumption of platinum metals	Power requirements	Capital costs	Consumption of special steels
Atmospheric pressure	1.0	1.0	1.0	1.0
Combined	1.0	5.3	1.11*	0.75
High pressure	2.0–4.0	7.2	0.89	0.54

These data show that if ways could be found to decrease power consumption in the production of nitric acid by the combined process, the latter would be the most promising of the existing industrial methods.

Considerable experience has been gained in the USSR and abroad in the operation of various processes for the production of dilute nitric acid, and a number of investigations have been carried out in order to determine the optimum process conditions. As a result, it has proved possible in recent years to solve a number of important problems relating to better utilization of the raw materials in their conversion into nitric acid, and to decrease considerably the power consumption in the process.

Conversion of Ammonia Into Nitric Oxide

Preparation of the ammonia–air mixture. About 80% of the production costs of nitric acid is accounted for by the cost of ammonia. The maximum conversion of ammonia into nitrogen oxides is therefore of particular importance.

It has been found in practice that the most important conditions for a high degree of conversion of ammonia into nitric oxide are purity of the ammonia–air mixture, and catalyst activity. The air drawn in for the production of nitric acid is often contaminated with silica dust, oil, cinders, sulfur compounds, and other catalyst poisons, which decrease the degree of ammonia conversion, reduce the catalyst life, and increase irrecoverable losses of catalyst.

The air used in the production of nitric acid is generally purified by washing in water, filtration through rings moistened with viscin oil, or by means of coarse fabric materials. The ammonia–air mixture is finally purified by means of porolite filters (porous clay tubes) before combustion over catalysts.

The ammonia used for nitric acid production is either not treated at all to remove impurities (oil, catalyst dust from the ammonia-synthesis section), or is purified by means of asbestos or cotton cloth in conjunction with cotton wool or other filter materials. Experience has shown that these methods for removal of impurities from the air and ammonia do not always ensure the required purity of the ammonia–air mixture (the content of mechanical impurities should not exceed 0.007 mg/m^3).

In recent years searches have been carried out for materials which could be used in the production of ammonia–air mixtures virtually free from mechanical impurities. A special type of cardboard proved suitable for this purpose. Cardboard is being successfully used in certain plants in the USSR instead of porolite filters, if the temperature of the air or air–ammonia mixture does not exceed 100°. At higher temperatures of the air or air–ammonia mixture cardboard has proved unsuitable. Experience has also been gained on the use of activated-carbon filters for the removal of chemical contamination (sulfurous gases and other catalyst poisons) from the air. The results obtained in the purification of air by means of activated carbon suggest that this method should become extensively used in nitric acid manufacture. In view of the low efficiency of viscin filters (the degree of purification does not exceed 40%), this purification stage is being omitted in the new nitric acid plants being planned in the USSR.

*The calculation of capital costs for the construction of combined systems is dubious, in view of the savings effected by lower consumption of special steels, elimination of the costs of ceramic packing, etc.

Catalysts. The usual catalysts used abroad for the oxidation of ammonia to nitric oxide are binary platinum–rhodium alloys.

The rhodium content of these alloys varies from 5 to 10%.

The catalysts are used in the form of gauzes, 1100, 2000, and 2800 mm in diameter for low-pressure units, and 1150, 330, 500, and 540 mm for high-pressure units. The gauzes are made from wire 0.04-0.09 mm in diameter, generally with 1024 intersections per cm^2. The free area not covered by the wires is 45-65% of the total gauze area.

If the ammonia–air mixture is of adequate purity, a fairly high degree of conversion of ammonia into nitric oxide is achieved at 750-900° over platinum–rhodium catalysts. For example, in low-pressure units (or in the combined process) the conversion of ammonia reaches 97-98%, and in the high-pressure process, 95-96%.

In the USSR a new catalyst has been used for more than 10 years in the oxidation of ammonia; it is a ternary alloy of platinum, palladium, and rhodium. Many years of experience have shown that the mechanical strength of the ternary alloy is not inferior to that of the platinum–rhodium alloy (90-93% Pt and 10-7% Rh), while the activity of the former exceeds that of the latter by about 1%.

Replacement of 4-7% Rh in the platinum–rhodium alloy by the cheaper and more available palladium is a considerable advantage of the Russian catalyst. Gauzes made from the ternary alloy yield 1500-2000 kg of nitric acid per 1 g of metal, according to the conditions used in the oxidation of ammonia, before they have to be remelted. Irrecoverable losses of catalyst in low-pressure units are from 0.048 to 0.056 g, and in high-pressure units, from 0.164 g to 0.175 g per ton of HNO_3. The losses of platinum metals in foreign units are similar.

It has been reported [6] that in Girdler units (U.S.A.) producing nitric acid under 8-9 atmos pressure the platinum metal loss has been reduced to 0.156 g per ton of HNO_3. It must be assumed that this low value has been attained because of the use of new filter materials which retain fine catalyst particles from the gas and acid. In the USSR only glass wool is used for this purpose; experience has shown that it is not very suitable for retaining platinum metals from nitrous gases at high temperatures. Glass wool becomes compressed and undergoes partial destruction during use, losing its filtration properties.

A process was worked out in the USSR for 2-stage oxidation of ammonia to nitric oxide [7]; this was later improved and taken as far as the production stage. The process is essentially as follows: ammonia–air mixture passes over one platinum gauze (1st stage), and the combustion is completed over a nonplatinum catalyst (2nd stage). The nonplatinum catalyst consists of inexpensive and readily available heavy-metal oxides in tablet form, at some distance from the first stage.

Operation under industrial conditions has shown that the same degree of ammonia conversion is obtained with the 2-stage process as in operation with three gauzes made from binary or ternary platinum-metal alloys. If the 2-stage catalyst is used instead of three platinum-metal gauzes, the amount of precious metals used can be reduced by 60%, and their losses, by 20-30%.

Searches for nonplatinum catalysts for ammonia oxidation, which would give a high degree of conversion for long periods, have not been successful. The use of nonplatinum catalysts consisting of iron oxides promoted with bismuth, or catalysts based on the oxides of cobalt and other metals, results in a sharp decrease of ammonia conversion (from 94-95% to 87-90%) after 15-25 days of use. According to the literature, nonplatinum catalysts are not used anywhere abroad in nitric acid production.

Catalyst load. Low-pressure units for the production of nitric acid operate at a load of 600-650 kg of ammonia per 1 m^2 active catalyst surface per 24 hours, and high-pressure units, at 5.5 kg of ammonia per g of platinum metals per 24 hours. It has been found that in high-pressure operation the rate should be kept at 4-4.5 kg of ammonia per g of platinum metals in order to obtain a somewhat higher degree of conversion.

The lower degree of conversion (93-94%) obtained in foreign low-pressure units [8] is probably the consequence of operation at higher loads than those given above.

Preheating of ammonia–air mixture. In order to obtain a higher degree of ammonia conversion, for

many years it has been the practice to preheat the air used to 200°, before formation of the mixture with ammonia and combustion over the catalyst.

In recent years many units, both here and abroad, have been operating without preheating of the ammonia–air mixture. It has been found experimentally that the degree of conversion to nitric oxide obtained by the combustion of a mixture containing 11-12% of ammonia, without preheating, is the same as that obtained with a preheated mixture containing 9.5-10.5% of ammonia. Therefore air preheaters are not being installed in any of the newly built nitric acid plants; preheaters were formerly among the sources of mechanical contamination of the mixture.

Use of the heat of oxidation of ammonia to decrease power consumption. The power consumption in the production of nitric acid by the high-pressure process (8-9 atmos) is very high. Even if 25-40% of the energy of the compressed gases is recovered, 340-390 kw-hrs is required per ton of nitric acid (monohydrate). Because of this, work is continuing in the USSR and abroad on the power aspects of nitric acid production.

Until recently a considerable proportion of the heat liberated in ammonia oxidation was used to produce steam at 6-11 atmos pressure. In some cases steam at 18 atmos pressure was obtained in waste-heat boilers.

In modern plants, waste-heat boilers of various types (often of the La Mont type) are installed, for the production of steam at 39-40 atmos pressure, which is utilized in steam turbines at 10-11 atmos counterpressure. This yields up to 50-60 kw-hrs of electrical power per ton of nitric acid, and steam at 10-11 atmos for use in the process. However, this does not provide for rational utilization of the heat of combustion of ammonia. The nitrous gases are still at a very high temperature (150° and over) after passing through the waste-heat boilers, and a considerable amount of water and therefore power is required for cooling them. Tubular condensers are used to cool the nitrous gases and to condense the reaction water present in them. The low efficiency of these condensers is well known.

A new design of gas cooler has been developed in the USSR, and is being adopted industrially; its operation is based on the bubbling of the hot nitrous gas through cooling nitric acid. Such a cooler, with five sieve plates carrying water-cooled coils to remove heat, can reduce the temperature of the nitrous gas to 40-42° (gas temperature at entry 150-250°, steam content 18%, temperature of cooling water 28-30°). This new type of bubbling cooler, with 80 m^2 coil area, is equivalent to a tubular cooler 420-470 m^2 in area.

Special gas turbines have been installed in nitric acid plants in order to lower power consumption by more efficient utilization of the heat of oxidation of ammonia.

According to Drake [9] and Miller [10], nitric acid plants are being planned, and some have already been erected, with efficient gas turbines for power recovery. Units with a capacity of 250 tons per day are being installed in American DuPont plants built since the war. A high recovery of the energy used for compression of the air to 9 atmos is achieved in these units. The recuperation turbine attached to the shaft of the air compressor, driven by preheated waste gas, recovers nearly 75% of the power used by the compressor. It should also be noted that in some American plants the heat of the hot nitrous gases from the reactors is utilized for the production of low-grade steam. Thus, in some plants operating the DuPont system, the nitrous gases from the reactors pass consecutively through two waste-heat boilers; the first produces steam at 13 atmos, and the second, at 2.7 atmos.

Use of oxygen. In some plants the ammonia–air mixture is enriched with pure oxygen. Addition of oxygen accelerates both the oxidation of ammonia, and the conversion of the nitrogen oxides into nitric acid. However, the utilization of oxygen is at present restricted by its high cost. Oxygen can only be used in plants where it is available as a by-product. In units where oxygen-enriched ammonia–air mixture (containing 23-27% oxygen) is used, the conversion of ammonia is usually 1-2% greater than in units using an nonenriched mixture.

Absorption of nitrogen oxides. Relatively few changes have taken place abroad in recent years in the technology and equipment used in the absorption of nitrogen oxides.

As formerly, towers with ceramic packing (in low-pressure units) and bubble-cap towers (in high-pressure units) are used for absorption of nitrogen oxides. This type of absorption system does not conform to modern requirements with regard to the content of nitrogen oxides in the exit gases, the utilization of the

valuable combined nitrogen, etc. Moreover, because of the increasing scale of nitric acid production, it has proved uneconomic to recover nitrogen oxides from the waste gases. The tendency is therefore to achieve maximum conversion of nitrogen oxides into nitric acid without production of alkali nitrates.

Some foreign nitric acid plants built during the last few years have certain specific characteristics. Nitrogen oxides are absorbed at 3.5 atmos pressure in horizontal absorbers consisting of the so-called Fauser cylinders. Each such absorber consists of 20 cylinders, which are regarded as 20 stages in the absorption system. The specific volume is 2.7-3.0 m^3 per ton of HNO_3. The nitrous gases are oxidized in 4 hollow towers before absorption. The absorbers and oxidation towers are externally cooled by water. The total yield of combined nitrogen in this system does not exceed 95%.

An improved combined process has been developed in the USSR and is being put into production. In this process the power consumption is relatively low – 220 kw-hrs per ton of acid monohydrate – and alkaline absorption of nitrogen oxides from the waste gases is not used [11]. Among the most important characteristics of this process is the unit principle whereby the equipment is interconnected throughout the process, the production of ammonia–air mixture of a high degree of purity, the use of sieve-plate absorption towers, use of the heat of oxidation of ammonia for the raising of steam at 40 atmos, and the utilization of the heat of oxidation of NO and NO_2 for preheating of the waste gases to 160-180° before the recuperator turbine.

The construction of new dilute nitric acid plants operating the high-pressure process is being planned in the USSR. The capital investment can be reduced by 23,000,000 rubles and the consumption of special steels by over 400 tons, in the construction of each such plant [12].

II. Development Prospects for the Nitric Acid Industry

Searches for new methods for the production of nitrogen oxides. The production of ammonia, the principal raw material in the manufacture of dilute nitric acid, involves a number of very complex technological processes, requires cumbersome equipment, and the operating costs are heavy.

Research has continued for many years on the problem of the production of nitrogen oxides by fixation of atmospheric nitrogen. In particular, much work has been done on the electric arc process for production of nitrogen oxides, based on the oxidation of atmospheric nitrogen by the oxygen of the air at 3000-3500°. However, this method has not been adopted industrially, because of the high power consumption (12,000-16,000 kw-hrs per ton of nitric acid). In the arc process only about 3% of the power supplied is utilized in the formation of nitrogen oxides, while the rest is irrevocably lost.

Two processes are now being developed for the production of nitrogen oxides by fixation of atmospheric nitrogen: 1) the thermal process, in which somewhat over 1% of the atmospheric nitrogen is converted into nitric oxide when the air is heated by means of combustible gases above 2100°; 2) the radiation process, in which nitric oxide is obtained from nitrogen of the air by the action of ionizing radiations from uranium 235.

The first (thermal) process, developed in the University of Wisconsin (U.S.A.) was tested in 1946-1949 in a pilot unit with a daily production of 1 ton of nitric acid. Various materials suitable for construction of the recuperator furnaces were tested, the conditions for the optimum yields of nitric oxide were determined, the design characteristics of the recuperators for efficient fuel utilization were investigated, etc. It was found that pure magnesium oxide is the best of the materials tested for the furnace lining and packing. The concentration of nitrogen oxides in the reaction products leaving the hot zone of the furnace did not exceed 2% even when they were instantaneously chilled.

In the thermal process, as in the arc process, the equilibrium reaction $N_2 + O_2 \rightarrow 2NO$ is greatly dependent on the temperature conditions; this is illustrated by the following data:

Temperature (°K)	1000	1800	2200	2600	3000
Equilibrium content of NO obtained from the air (vol. %)	0.003	0.5	1.4	3.0	5.2

It must also be taken into account that the production of nitric oxide by the thermal process, for manufacture of nitric acid, includes the following stages: 1) preliminary cooling and drying of the nitrous gases; 2) catalytic oxidation of NO to NO_2; 3) absorption of NO_2, and its desorption in concentrated form at 150-200°. According to certain authors [13, 14], special brands of silica gel must be used in these stages of the process.

The fairly detailed published data [13-16] suggest that the thermal process for the production of nitrogen oxides, and their subsequent conversion, is extremely complicated on the large scale. According to press reports, the started construction of an experimental unit for the thermal process has been abandoned, and it has been decided to continue work on the process on the laboratory scale.

The second process for the production of nitrogen oxides is dependent on the development of nuclear power. The direct oxidation of atmospheric nitrogen by the action of ionizing radiations is being studied by Soviet and foreign workers. The fixation of nitrogen by the action of ionizing radiations and high-energy particles, for the production of nitric acid, is one peaceful application of atomic energy.

It has been found that oxidation of nitrogen commences under the action of electrons possessing energy corresponding to the potential at which molecular ions of nitrogen appear (16 ev); the formation rates of nitrogen oxides have been determined in relation to the irradiation time, composition of the gaseous mixture, pressure, and temperature, and the reaction mechanism has been determined [17, 18]. American workers [19] obtained 2.5 molecules of NO_2 per 100 ev at 140° and 1 atmos, and 5 molecules of NO_2 per 100 ev at 175° and 25 atmos.

Experiments in a nuclear reactor [19] showed that if air is subjected to ionizing radiations from uranium 235 under suitable conditions, nitrogen oxides can be obtained rapidly and, according to preliminary calculations, economically.

This method can only become technically important if the greater part of the energy of nuclear fission can be utilized directly [20]. However, the conversion of nuclear into chemical energy involves possible contamination of the gaseous reaction products with the fission products of uranium. The removal of such contamination from the reaction products is a very complex problem.

It follows from the foregoing that direct methods for the production of nitric oxide (thermal and radiochemical) are promising in principle, but very great difficulties must be overcome before they can be operated industrially.

Therefore the efforts of chemists and technologists are being directed toward continuing improvement of methods for the production of dilute nitric acid from ammonia.

Some of the investigations in this direction are noted below.

1. The choice of the combined method for the production of nitric acid must be regarded as an enforced solution. Despite the relatively advantageous capital costs and consumption of ammonia and platinum metals, the equipment required for ammonia oxidation remains cumbersome. The problem of reducing the power consumption in this process has not been completely solved. Methods are therefore being developed for the oxidation of ammonia under high pressures, with the primary aim of obtaining a degree of catalytic contact and consumption of platinum metals not higher than in systems operated under atmospheric pressure. Abroad there is also a tendency to convert the catalytic units to high-pressure operation. If this problem could be solved, it would be possible to reduce considerably the number and dimensions of the catalytic reactors, to decrease the surface area of the heat-exchange equipment, to abandon the use of costly turbocompressors for the nitrous gases, etc. Special attention must be devoted to searches for improved methods for the effective removal both of mechanical contaminations and of chemical impurities from the ammonia–air mixture. It is also necessary to study in detail the influence of pressure, gas-flow rates, catalyst load, etc., about which the information in the literature is totally inadequate, and which have been tested little in practice. The results of these investigations should reveal the optimum conditions for an acceptable degree of conversion of ammonia and consumption of platinum metals in the high-pressure oxidation process.

2. The increased output of electrical energy expected in the near future, with considerable reduction of its cost, should undoubtedly make the production of cheap oxygen possible. It is of great interest in this connection to develop a method for the oxidation of ammonia by means of pure oxygen, with the production of nitrogen oxides containing 25-27% NO. With the use of nitrogen oxides at this concentration (if cheap oxygen is available) is should become possible to reduce the volume of the equipment considerably, and to lower the energy consumption in the production both of dilute and of concentrated nitric acid.

3. The development of methods for effective removal of nitrogen oxides from the waste gases released

into the atmosphere from dilute nitric acid plants remains a very important task. Measures which have been taken in recent years to reduce the amount of nitrogen oxides released into the air have not produced satisfactory results.

The required permissible level of nitrogen oxides in the waste gases (0.05-0.1 vol. %), without a decrease of productivity, cannot be reached without the aid of special technical measures.

In some foreign factories [21, 22], catalytic methods for the removal of nitrogen oxides from the waste gases of nitric acid plants have been in use for many years.

Such a method was worked out in detail, and tested on a large pilot plant, even before the war [23]. The method was studied, not only with the object of removing nitrogen oxides from the waste gases, but also for the production of elemental nitrogen suitable for ammonia synthesis. The catalyst was a layer of nickel and copper supported on fireclay, and the required temperature of 500-600°, at which the nitrogen oxides were completely decomposed, was attained by the combustion of hydrogen.

It is now possible to use the catalytic method for decontamination of the waste gases, with the use of natural methane or combustible by-product gases from different industries instead of costly hydrogen.

The catalytic removal of nitrogen oxides from waste gases can be effected by economically advantageous methods, with rational utilization of the heat produced.

4. Among the other problems associated with the development of the dilute nitric acid industry, mention must be made of the need to develop large-scale equipment whereby the power consumption could be reduced to a minimum with the use of the heat of oxidation of ammonia.

LITERATURE CITED

[1] Food and Agriculture Organization (FAO) of the United Nations (Rome, 1953, 1954, 1955).

[2] A. F. Ivanov, The Fixed-Nitrogen Industry in the Capitalist Countries (OBTI, State Institute of the Nitrogen Industry, 1957). •

[3] M. A. Miniovich and N. I. Beliaev, Chem. Science and Ind. 1, 6 (1956).

[4] V. Auerbach, Ind. chim. Belge, 19, 1, 7 (1954).

[5] S. Strelzoff, Chem. Eng. 5, 170 (1956).

[6] Chem. Eng. 1, 275 (1956).

[7] D. A. Epshtein and N. M. Tkachenko, J. Appl. Chem. 11, 5, 731 (1938).

[8] Simposium over de fabricage van Salpeterzeur Chemisch Weekblad, 5, 61-37 (1956).

[9] J. Drake, Southern Power and Ind. 73, 6, 53 (1955).

[10] B. Miller, Chem. Eng. 11, 2 (1955).

[11] E. Ia. Mel'nikov, J. Appl. Chem. 30, 1445 (1957).••

[12] L. A. Kostandov, Chem. Science and Ind. 1, 6, 602 (1956).

[13] F. Daniels and N. Gilbert, Ind. Eng. Chem. 40, 1719 (1948).

[14] E. Foster and F. Daniels, Ind. Eng. Chem. 43, 986 (1951).

[15] Chem. Eng. 2, 193 (1953).

[16] Chem. Eng. Progr. 50, 12, 34 (1954).

[17] S. Ia. Pshezhetskii, Session of the Acad. Sci. USSR on the Peaceful Use of Atomic Energy, Div. Chem. Sci. (Moscow, Izd. AN SSSR, 1955).

[18] S. Ia. Pshezhetskii and M. T. Dmitriev, Atomic Energy 3, 10 (1957).••

•In Russian.

••Original Russian pagination. See C.B. Translation.

[19] P. Harteck and J. Dondes, Nucleonics, 14, 7, 22 (1956); Ind. Chem. 32, 381, 495 (1956).

[20] R. Coekelbergs, P. Gosselain and M. Vander, Ind. chim. Belge, 22, 2, 153 (1957).

[21] L'Industrie chimique, 347 (1946).

[22] Fauser, La chimica e L. Ind. 39, 3, 165 (1957).

[23] F. P. Ivanovskii, M. P. Korsh and E. B. Krishtul, J. Chem. Ind. 8, 8 (1935).

Received March 27, 1957

DECOMPOSITION OF ZINC AND COBALT SULFATES IN A CURRENT OF SULFUR DIOXIDE AND AIR

V. V. Pechkovskii

The A. M. Gor'kii State Institute, Perm'

In oxidative and sulfating roasting of sulfide ores, formation and decomposition of sulfates takes place in gases containing various amounts of sulfur dioxide and oxygen [1]. However, there are no experimental data in the literature on the decomposition of sulfates in a current of gas containing sulfur dioxide and oxygen.

The purpose of the present investigation was to study the rate of thermochemical decomposition of zinc and cobalt sulfates in gas streams consisting of sulfur dioxide and air. The decomposition rates of these sulfates were studied in relation to the sulfur dioxide content of the original gas, temperature, duration of the experiment, and presence of additives. The thermochemical decomposition of sulfates may be represented by the general equations

$$MeSO_4 \rightleftarrows MeO + SO_3, \quad (1)$$

$$SO_3 \rightleftarrows SO_2 + {}^1/_2O_2. \quad (2)$$

It was shown earlier [2] that if various metal oxides are present in the mixture they may accelerate sulfate decomposition by their catalytic effect on Reaction (2), and by formation of various compounds (ferrites, aluminates, silicates, etc.) with the metal oxides formed in Reaction (1). Substances which catalyze sulfate decomposition include compounds of iron, copper, cobalt, manganese, and certain other metals in the form of oxides. It was also found that the thermochemical decomposition of sulfates is intensified to an immeasurably greater extent by catalytically active metal oxides than by metal oxides which have no catalytic effect on Reaction (2). If catalytically-active metal oxides are formed directly in the decomposition of sulfates (for example, by the decomposition of the sulfates of copper, cobalt, manganese, etc.), they themselves serve as catalysts which accelerate Reaction (2). If the sulfates are decomposed in a current of gas containing oxygen and sulfur dioxide, under certain conditions the latter may be oxidized

$$SO_2 + {}^1/_2O_2 \rightleftarrows SO_3. \quad (3)$$

If the conditions are such that sulfur trioxide is formed by Reaction (3), the rate and extent of Reaction (1) decrease. It is therefore to be expected that if sulfur dioxide and oxygen are present in the gas passed over a sulfate, the decomposition rate of the sulfate should decrease.

The present investigation was undertaken to investigate these relationships.

The method was as follows. Thoroughly dried zinc and cobalt sulfates (analytical grade), and their mixtures with added ferric oxide, were roasted at definite temperatures in a laboratory tubular furnace in a current of dry gas made by thorough mixing of sulfur dioxide and air. Gas mixtures containing 0.0, 2.5, 5.0, 7.5 and 10.0 vol. % of sulfur dioxide were used. The weight of sulfate taken was 2.0 g in every experiment. When sulfates with added Fe_2O_3 were roasted, the amount added was 1.0% on the weight of the charge. The gas flow rate through the system was 3.0 liters/hour. The analysis consisted of determinations of sulfate sulfur left in the charge after the roasting.

The principal experimental results are given in Tables 1-5 and in the diagram. It was first established,

as can be seen from the data in Table 1 and the graph, that the decomposition rate of zinc sulfate in a current of air increases considerably in presence of ferric oxide. An addition of 1-2% of Fe_2O_3 to the charge is sufficient to raise the decomposition rate of zinc sulfate. Increases of this amount to above 1-2% produce virtually no further increase in the decomposition rate of zinc sulfate.

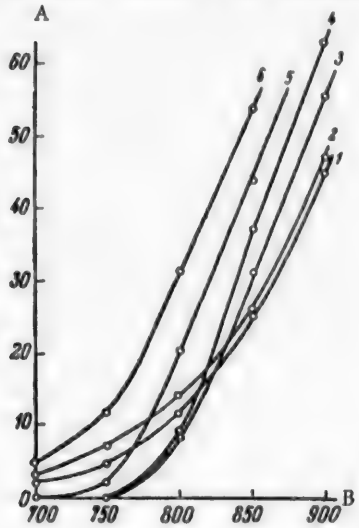

Variations of the degree of decomposition of zinc sulfate with the temperature and SO_2 concentration in the original gas; duration of experiments 15 minutes. A) Degree of decomposition of $ZnSO_4$ (%), B) temperature (°C). Decomposition of $ZnSO_4$ without additive; SO_2 concentration in the original gas (vol. %): 1) 7.5, 2) 0.0. Decomposition of $ZnSO_4$ with added Fe_2O_3; SO_2 concentration in the original gas (vol. %): 3 – 10.0, 4 – 7.5, 5 – 2.5, 6 – 0.0.

It follows from the data in Table 3 that the decomposition rate of cobalt sulfate is also increased somewhat on addition of ferric oxide. However, ferric oxide has much less effect on the decomposition rate of cobalt sulfate than of zinc sulfate. This is because catalytically-active substances are formed directly by the decomposition of cobalt sulfate, whereas zinc sulfate and its decomposition products have no catalytic activity toward Reaction (2).

Data on the influence of sulfur dioxide concentration in the original gas on the decomposition rates of zinc and cobalt sulfates are presented in Tables 1-3 and in the graph. It follows from these data that in the decomposition of zinc sulfate in absence of catalyzing additives increase of the sulfur dioxide concentration of the original gas decreases the rate of the process only slightly. The explanation is that in absence of catalysts the rate of Reaction (3) is low, and therefore increase of the SO_2 concentration in the original gas under these conditions does not lower the rate of thermochemical decomposition of zinc sulfate to any appreciable extent. Different results are obtained in the decomposition of zinc sulfate in presence of ferric oxide.

It follows from the data of Table 1 and the graph that under these conditions the rate of thermochemical decomposition of zinc sulfate varies considerably with the SO_2 concentration of the original gas. When zinc sulfate is decomposed in presence of the catalytic additive, the rate of the process decreases fairly considerably with increase of SO_2 concentration of the original gas. Thus, whereas decomposition of zinc sulfate mixed with the additive takes place in a current of air at 650°, if 7.5% of SO_2 is present in the original gas decomposition does not occur below 750°. Interesting results are revealed by comparison of the decomposition rates of zinc sulfate in a current of sulfur dioxide and air, with and without the catalytic additive in the charge.

TABLE 1

Variations of the Degree of Decomposition of Zinc Sulfate with the Temperature and SO_2 Concentration of the Original Gas. Duration of Experiment 15 Minutes; $ZnSO_4$ Decomposed: A) In Absence of Additive, B) With Fe_2O_3 Added

Temperature (°C)	Degree of decomp. of $ZnSO_4$ (%) at SO_2 concentr. in orig. gas (vol.%)									
	0.0		2.5		5.0		7.5		10.0	
	A	B	A	B	A	B	A	B	A	B
700	3.2	4.9	2.1	0.0	2.1	0.0	2.1	0.0	—	—
750	7.1	11.6	5.9	2.3	5.6	—	4.5	0.0	5.0	0.0
800	14.2	31.3	11.7	20.2	12.5	10.4	11.8	9.2	13.0	8.7
850	26.6	53.8	24.5	44.0	25.1	38.0	25.3	37.0	22.4	31.2
900	47.0	80.6	46.8	71.6	45.0	66.6	45.0	62.8	44.6	55.4

It follows from Table 1 and the diagram that in the low-temperature region (750° and less) the decomposition rate of zinc sulfate without additive in a current of sulfur dioxide and air is somewhat higher than the

decomposition rate under the same conditions, but in presence of the catalytic additive. Conversely, in the high-temperature region (800° and over) the decomposition rate of zinc sulfate without additive in a current of sulfur dioxide with air is somewhat lower than the decomposition rate of zinc sulfate under the same conditions, but in presence of the catalytic additive. In other words, in the low-temperature region (750° and less) the rate of thermochemical decomposition of zinc sulfate can be lowered by introduction of the additive and a simultaneous increase of the sulfur dioxide concentration in the original gas. In the high-temperature region (800° and over) introduction of the catalytic additive increases the rate of thermochemical decomposition of zinc sulfate even if the sulfur dioxide concentration of the original gas is increased.

TABLE 2

Variations of the Degree of Decomposition of Cobalt Sulfate with the Temperature and SO_2 Concentration of the Original Gas. Duration of Experiment 15 Minutes

SO_2 Concentration (vol. %)	Degree of decomposition of $CoSO_4$ (%) at temperature (°C)			
	750	800	850	950
0.0	1.1	5.8	18.9	100.0
2.5	0.0	0.0	3.7	84.8
7.5	0.0	0.0	1.3	59.2

TABLE 3

Variation of the Degree of Decomposition of Cobalt Sulfate with the SO_2 Concentration of the Original Gas (t = 900°). Duration of Experiment 15 Minutes

Substance	Degree of decomposition of $CoSO_4$ (%) at SO_2 concentration (%)				
	0.0	2.5	5.0	7.5	10.0
$CoSO_4$	59.3	37.5	26.6	17.3	21.9
$CoSO_4 + Fe_2O_3$	65.5	43.4	34.0	17.6	22.0

These results can be explained as follows. Introduction of the catalytic additive into zinc sulfate increases the rate of Reaction (2) under all conditions; at the same time, in presence of sulfur dioxide in the original gas the catalytic additive also increases the rate of Reaction (3). However, the equilibrium yield of SO_3 by Reaction (3) sharply decreases with increase of temperature, and therefore in the high-temperature region (800° and over) the presence of the catalytic additive in the charge has the ultimate effect of increasing the total decomposition rate of zinc sulfate even if the SO_2 concentration of the original gas is increased.

Data on the decomposition of cobalt sulfate in a current of sulfur dioxide and air are presented in Tables 2 and 3. It is seen that the rate of thermochemical decomposition of cobalt sulfate decreases considerably with increase of SO_2 concentration in the original gas from 0 to 7.5%, even in absence of additive. Thus, whereas in a current of air decomposition of cobalt sulfate can be detected at 750°, in a current of air containing 7.5% SO_2 decomposition occurs only at temperatures above 850°. Introduction of the catalytic additive increases the decomposition rate of cobalt sulfate only slightly. All this indicates once again that cobalt oxides formed by decomposition of cobalt sulfate are the catalytic agents in this case.

The data in Table 3 indicate that the relationship between the rate of thermochemical decomposition of cobalt sulfate and the sulfur dioxide concentration of the original gas is represented by a curve with a maximum at a point corresponding to 7.5% SO_2 in the original gas. In other words, when cobalt sulfate is decomposed in a current of sulfur dioxide and air, the rate of the process decreases with increase of the SO_2 concentration in the original gas from 0 to 7.5%. With further increase of the sulfur dioxide concentration in the original gas, the decomposition rate of cobalt sulfate increases somewhat. These results may be explained as follows.

Since the original gas used in the experiments consisted of mixtures of air and sulfur dioxide, increase of the latter in the mixture resulted in a corresponding decrease of the oxygen content. Therefore, with increase of the SO_2 under certain conditions the rate of Reaction (3) may decrease because of the decreased oxygen content in the original gas. Moreover, as was shown earlier [3], when sulfates giving rise to catalytically-active products are decomposed, the rate of Reaction (2) increases with decrease of the oxygen concentration in the gas phase. A consequence of these two factors in conjunction is that, when the SO_2 concentration of the original gas is increased above 7.5%, the decomposition rate of cobalt sulfate increases somewhat as compared with the decomposition rate at the optimum SO_2 content of the original gas. These data, and the results detailed earlier, therefore clearly demonstrate the important role of catalytic processes in the thermochemical decomposition of sulfates.

TABLE 4

Variation of the Degree of Decomposition of Cobalt Sulfate with the Duration of the Experiment (t = 850°)

SO_2 concentration in original gas (vol. %)	Decomp. (%) of $CoSO_4$ in expt. lasting (min)		
	30	45	60
0.0	29.3	49.5	64.8
2.5	13.5	17.0	27.6

TABLE 5

Variation of the Degree of Decomposition of Zinc Sulfate with the Duration of the Experiment. SO_2 Concentration in Original Gas 7.5%; $ZnSO_4$ Decomposed: A) Without Additive, B) With Fe_2O_3 Added

Duration of experiment (minutes)	Degree of decomposition of $ZnSO_4$ at temperature (°C)					
	800		850		900	
	A	B	A	B	A	B
30	25.2	18.2	42.6	47.0	56.2	66.6
45	35.3	22.0	45.0	48.1	58.0	67.8
60	43.5	27.2	45.6	48.2	59.5	69.4

Data on the effect of the duration of the experiment on the decomposition rates of zinc and cobalt sulfates are presented in Tables 4 and 5. It was shown that introduction of a catalytic additive into the charge and presence of sulfur dioxide in the original gas have no effect, under otherwise equal conditions, on the relationship between the rate of sulfate decomposition and the duration of the experiment. The decomposition rate of cobalt sulfate remains constant with increase of the duration of the experiment. The rate decreases with increase of the time only at high degrees of decomposition (about 85-90%). In the case of zinc sulfate the decomposition rate as a rule remains constant for some time, and then decreases with increasing duration of the experiment. This indicates that under otherwise equal conditions films of reaction products with different physical properties are formed on the zinc sulfate and cobalt sulfate grains respectively. The results show that the film formed on cobalt sulfate is less dense than that formed on zinc sulfate.

We believe that the results of this investigation may in some cases be useful in selection of the most favorable conditions for the thermochemical decomposition of sulfates.

LITERATURE CITED

[1] V. I. Smirnov, Oxidative Roasting of Copper Ores and Concentrates (ONTI, 1938).*

[2] V. V. Pechkovskii, J. Appl. Chem. 29, 7, 1137 (1956).**

[3] V. V. Pechkovskii, J. Appl. Chem. 28, 3, 237 (1955).**

Received February 7, 1957

*In Russian.

**Original Russian pagination. See C.B. Translation.

MECHANISM OF THE DECOMPOSITION OF NEPHELINES BY ALKALINE SOLUTIONS

V. D. Ponomarev and V. S. Sazhin

The Kazakh Mining and Metallurgical Institute

The process used at the present time for decomposition of nepheline $(Na, K)_2O \cdot Al_2O_3 \cdot 2SiO_2$, and conversion of the alumina into an alkaline solution consists of sintering of nepheline concentrates with limestone, with formation of water-soluble sodium (or potassium) aluminate.

Our investigations have shown that under certain conditions nephelines are completely decomposed by alkaline solutions, with extraction of the alumina, without sintering.

A study has been made of different conditions of alkali treatment of nephelines in autoclaves, and experiments have been carried out with synthetic mixtures containing alumina, silica, and sodium oxide; as a result, a possible mechanism of decomposition of nephelines under the action of alkaline solution has been tentatively postulated. In our opinion, this mechanism can be formulated as follows.

When treated with caustic solutions in the autoclave, nephelines are decomposed with formation of sodium (or potassium) aluminate and sodium silicate. The sodium silicate solution is evidently a system in which only a small part of the silica is present in the chemical compound Na_2SiO_3, while most of it is present in the form of $SiO_2 \cdot nH_2O$ sol in caustic soda solution.

The dissolution of nephelines is accompanied by other processes due to loss of silica from the solutions with formation of aqueous sodium (or potassium) aluminosilicate. In such treatment of nepheline alumina does not enter the solution, and only the original solid phases are changed.

It is well known that when sodium aluminate and sodium silicate solutions interact, a precipitate consisting of silica, alumina, and sodium oxide is formed.

This reaction is usually represented by the equation

$$2NaAlO_2 + 2Na_2SiO_3 + 4H_2O = Na_2O \cdot Al_2O_3 \cdot 2SiO_2 \cdot 2H_2O + 4NaOH$$

The molecular composition $Na_2O \cdot Al_2O_3 \cdot 2SiO_2 \cdot 2H_2O$ is usually ascribed to aqueous sodium aluminosilicate. In reality, the silica–alumina ratio in the precipitates formed during removal of silica from solutions rarely reaches 2:1; it usually varies in the range of 1.5:1 to 1.7:1. The sodium oxide–alumina ratio generally corresponds exactly to the formula. The variable silica–sodium oxide ratio, with a constant sodium oxide–alumina ratio, suggests that the precipitate is an aluminum sodium silicate of definite composition, containing a certain amount of adsorbed sodium aluminate. This opinion is held by several investigators.

Others attribute the variability of the composition of the precipitate to the colloidal nature of aluminate solutions.

I. I. Iskol'dskii states that when sodium aluminate and silicate come into contact, mutual coagulation of two oppositely-charged sols takes place. This interaction does not give rise to chemical compounds, but mixtures are formed containing, in addition to alkali, different amounts of alumina and silica. This continuous series of mechanical mixtures (berthollides) may approximate to a definite chemical composition.

Less is known about the composition and structure of precipitates formed in removal of silica from aluminate solutions in presence of lime, and the mechanism of the favorable action of lime.

V. A. Mazel' attributes the favorable influence of lime in the process to the formation of aluminum calcium silicates, which are less soluble than aluminum sodium silicate.

Strokov, Musiakov, and Prokof'eva [1, 2] consider that initially aqueous sodium aluminosilicate is formed, and part of the sodium in it is then displaced by calcium; they also admit the possibility of direct interaction of calcium oxide with silica in aluminate solutions, with formation of aqueous calcium monosilicate.

In the opinion of M. G. Leiteizen, N. K. Druzhinina, and T. A. Potapova, the function of the lime is to accelerate the removal of silica, without direct interaction between calcium oxide and silica. Silica reacts with sodium aluminate to form the sparingly soluble aqueous sodium aluminosilicate, in which sodium ions are partially exchanged for calcium ions. These authors noted that at 200° concentrated solutions of caustic soda in presence of calcium oxide decompose aluminum sodium silicate with formation of insoluble calcium sodium silicate, and the liberated alumina passes into solution.

In our opinion, the composition of the precipitate formed during silica removal depends on the concentrations of the components in the mixture and the reaction conditions.

If aluminum sodium silicate is treated with lime in water or weak alkaline solutions, ion exchange between sodium and calcium may take place. The extent of this exchange depends on the conditions.

E. N. Gapon derived the following equation for the exchange isotherm:

$$\frac{I_{M'}}{\sqrt{I_{M''}}} = K \frac{C_{M'}}{\sqrt{C_{M''}}},$$

where $I_{M'}$ and $I_{M''}$ are the amounts of uni- and bivalent ions sorbed by the aluminosilicate, in equilibrium with the solution; $C_{M'}$ and $C_{M''}$ are the respective concentrations of the uni- and bivalent ions in solutions; K is the equilibrium constant.

It follows from this equation that, under equal conditions, the ratio of sodium to calcium ions in the aluminosilicate is determined by the concentration of the solution with which it is in contact; therefore there is no reason to expect the formation of aluminosilicates of constant composition if the reaction is carried out under different conditions.

At high alkali concentrations in the solution, there is virtually no exchange of sodium ions for calcium ions in aluminosilicates.

We found that under certain conditions the introduction of calcium oxide into aluminate solutions containing silica may sharply change the course of silica removal from these solutions. In such cases a precipitate of hydrated calcium sodium silicate is formed; this probably has a lower solubility product than sodium aluminosilicate. The conditions which favor the formation of hydrated calcium sodium silicate are high temperature (or pressure), large excess of alkali in the solution, and a definite content of calcium oxide.

A large excess of alkali in solution, i.e., a high caustic ratio, is in our opinion necessary in order to retard the formation of hydrated sodium aluminosilicate (zeolite) and thereby to prevent silica removal from the solution at the expense of the alumina. I. I. Iskol'dskii reported that in strongly alkaline solutions precipitation of the berthollides (formation of zeolite) is occasionally retarded.

The amount of calcium oxide in the slurry must be sufficient for formation of calcium sodium silicate. Our investigations showed that the optimum amount is a slight excess over a unimolar ratio of calcium oxide to silica. If less lime is used, silica removal occurs both by means of calcium oxide and also by alumina.

It was found that the double silicate of calcium and sodium is formed under definite conditions from sodium silicate solution mixed with calcium oxide. High pressures (or temperatures) accelerate this process.

It follows from the foregoing* that when nephelines are subjected to treatment with alkaline solutions in presence of lime in the autoclave the mineral is first dissolved with formation of a solution of sodium aluminate and sodium silicate (or silicic acid gel), and calcium oxide then reacts with sodium silicate, forming a precipitate of the double silicate of calcium and sodium. A high degree of extraction of alumina into solution may be attained if the conditions are favorable for crystallization of the double silicate of calcium and sodium; the formation of sodium aluminosilicate (zeolite) does not occur to any appreciable extent. In other words, the secondary process of silica removal in presence of lime occurs through the agency of the calcium oxide and not of the alumina. Calcium oxide added to the leaching solution favors rapid and more complete decomposition of nephelines. It was shown experimentally that when nepheline concentrates are treated with water in the autoclave in presence of lime, nepheline is likewise decomposed with precipitation of calcium aluminosilicate and liberation of sodium (or potassium) oxide, which passes into solution.

In our opinion, the leaching of alumina from nephelines by alkaline solutions in presence of lime can be represented by the following over-all equation:

$$Na_2O \cdot Al_2O_3 \cdot 2SiO_2 + 2CaO_s + xNaOH_{aq} \rightarrow 2NaAlO_{2aq} + (x-2)\,NaOH_{aq} + Na_2O \cdot 2CaO \cdot 2SiO_2 \cdot 2H_2O_s$$

For simplicity, all the alkali is nominally represented as Na_2O.

The chemical composition and formation conditions of some of the precipitates are given in the table.

Chemical Composition of Precipitates

No. of x-ray diagram	Conditions of precipitate formation	Chemical composition (%)					
		alumina	total alkalies	calcium oxide	silica	ferric oxide	calcination loss
2	Treatment of nepheline concentrate with caustic soda solution without addition of calcium oxide	27.4	22.2	1.86	37.1	3.42	7.46
3	Reaction of sodium silicate solution with sodium aluminate solution at 30 atmos	30.6	19.19	–	37.52	0.30	9.8
4	Treatment of nepheline concentrate under the optimum conditions	1.9	14.96	35.7	30.76	2.8	12.93
5	Reaction of sodium silicate solution with calcium oxide at 30 atmos $\left(\frac{CaO}{SiO_2} = 1.1\right)$	–	16.8**	36.5	34.02	0.3	9.82
6	Interaction of sodium silicate solution, sodium aluminate solution, and calcium oxide at 30 atmos	3.4	16.99	36.4	33.70	0.2	8.46
7	Treatment of nepheline concentrate with caustic soda solution with addition of two moles of calcium oxide per mole of silica	1.6	10.94**	44.10	22.34	2.0	17.92
10	Additional treatment of precipitate to remove alkalies	1.4	0.85	48.66	21.56	1.28	25.05

*No special study of the mechanism of the nepheline decomposition by alkaline solutions was made at this stage of the investigation.

**Total alkalies in the precipitates were calculated from the difference between the amounts introduced and found in solution.

The precipitates formed by the treatment of nepheline concentrate with caustic soda solution, and by the interaction of sodium silicate and sodium aluminate solutions, are similar in chemical composition, and contain up to 30% alumina.

When nepheline concentrate was treated with caustic soda solution in presence of calcium oxide under the optimum conditions,* a precipitate containing 1.9% alumina was formed. Similar contents of the principal components (Na_2O, CaO, SiO_2) are found in the precipitates obtained by the interaction of sodium silicate solution, sodium aluminate solution, and calcium oxide, and by the interaction of sodium silicate solution with calcium oxide under the same conditions.

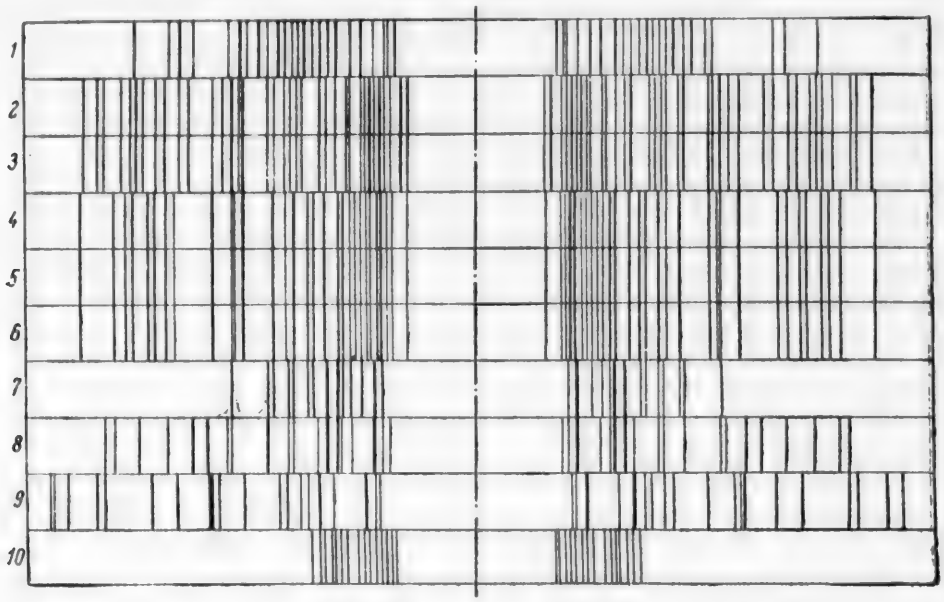

Relative positions of the lines in the x-ray powder diagrams.

The mechanism postulated for nepheline decomposition is confirmed by the results of x-ray and microscopic investigations of the original materials and of the precipitates formed in the treatment of nephelines and by the interaction of synthetic mixtures.

The figure shows the relative position of the lines of x-ray powder diagrams, taken with copper radiation, of: 1) concentrate of nepheline from the Kola peninsula; 2) precipitate formed by the treatment of nepheline with caustic soda solution without addition of calcium oxide; 3) precipitate formed by the interaction of sodium silicate and sodium aluminate solutions at 30 atmos; 4) precipitate formed in the treatment of nepheline with caustic soda solution in presence of calcium oxide under the optimum conditions; 5) precipitate formed by the interaction of sodium silicate solution, sodium aluminate solution, and calcium oxide at 30 atmos; 7) precipitate formed in the treatment of nepheline with caustic soda solution with addition of two moles of calcium oxide per mole of silica; 8) calcium hydroxide; 9) calcium oxide; 10) nepheline sludge obtained by repeated treatment of the precipitate after extraction of alkalies.

Examination of the powder diagrams leads to the following conclusions.

1. The crystal lattice of the precipitate formed by the treatment of nepheline by alkali alone (without calcium oxide) differs from that of nepheline (Diagrams 1 and 2). In contrast to nepheline, its crystals contain water of crystallization, and consist of hydrated sodium aluminosilicate.

The interaction of sodium aluminate and sodium silicate solutions at 30 atmos yielded a precipitate with the same crystal lattice (Diagram 3) as the precipitate formed in the treatment of nepheline with alkali without

*Molar ratio of sodium oxide to alumina in the original slurry 9.0, molar ratio $\frac{CaO}{SiO_2} = 1.1$, sodium oxide concentration 400-500 g/liter, pressure 30 atmos, treatment time 10-30 minutes.

addition of calcium oxide. This confirms our hypothesis that when nephelines are leached with alkali, secondary processes of silica removal from the solution take place, with formation of hydrated sodium aluminosilicate (zeolite).

2. Treatment of nephelines with alkali in presence of calcium oxide under the optimum conditions yielded a precipitate the crystals of which have a different crystal lattice (Diagram 4). This lattice is the same as that of the precipitates formed by the interaction of sodium silicate solution with calcium oxide, and by the interaction of sodium silicate solution, sodium aluminate solution, and calcium oxide (Diagrams 5 and 6).

This shows that the calcium oxide present in solution gives rise to a precipitate of hydrated calcium sodium silicate under certain conditions, irrespective of the presence or absence of alumina in the solution.

Comparison of Diagrams 4 and 5 also shows that the precipitate formed by the treatment of nepheline with alkali in presence of calcium oxide consists mainly of crystals which do not contain alumina. The presence of a small amount of alumina in the precipitate is accounted for by the presence of another solid phase, containing alumina.

The formation of a precipitate of hydrated calcium sodium silicate in the interaction of sodium silicate solution with calcium oxide in an alkaline medium confirms the probability of our suggested mechanism of nepheline decomposition. The precipitate of hydrated calcium sodium silicate is formed by the interaction of calcium oxide with the silica present in the alkaline solution, and not by displacement of alumina from the zeolite by calcium oxide.

3. The treatment of nepheline with alkali in presence of two moles of calcium oxide per mole of silica yielded a precipitate the x-ray powder diagram of which contains lines for crystals of hydrated calcium sodium silicate, and for calcium hydroxide (Diagrams 6, 7, and 8). This shows that the precipitate contains some free calcium hydroxide, not combined with silica.

4. The nepheline sludge formed by repeated treatment of the precipitate has a crystal lattice different from those considered above (Diagram 11). The diagram does not contain lines for crystals of hydrated calcium sodium silicate or of calcium hydroxide.

The precipitates formed by the treatment of nephelines and in the interaction of synthetic solutions were also studied under the microscope.*

The precipitate formed in the treatment of nepheline with alkali in presence of calcium oxide under the optimum conditions consists of newly formed crystals of fine prismatic form, often pointed. The average length of the crystals is 12-14 μ, and the average breadth, 2.5-3.0 μ. With a single nicol, the crystals are colorless or faintly green; the extinction is direct and the elongation negative. The crystals have low birefringence, in the region of 0.010-0.012, and are anisotropic. The refractive indices vary in the ranges N_g = 1.620 - 1.630, N_p = 1.590 - 1.600. Individual grains of aegirite and undecomposed nepheline are found.

The optical characteristics of the crystals formed by the interaction of sodium silicate solution with calcium oxide, and by the interaction of sodium silicate solution, sodium aluminate solution, and calcium oxide, are the same as those detailed above.

The precipitate formed by the treatment of nepheline concentrate with caustic soda solution without addition of calcium oxide, consists of a finely prismatic aggregate, yellow in color, when viewed under immersion. The refractive indices are in the range of 1.528-1.535. Considerable amounts of undecomposed nepheline are found.

The precipitate formed in the alkaline treatment of nepheline in presence of two moles of calcium oxide per mole of silica consists of the finely prismatic crystals described above, together with fine irregular crystals the optical characteristics of which were not determined.

*This analysis was carried out by Geological Engineer T. M. Al'zhanov.

SUMMARY

1. When nephelines are treated with caustic solutions in the autoclave, the mineral is decomposed with formation of a precipitate of hydrated sodium (or potassium) aluminosilicate. Alumina and alkali are not extracted into solution, and mere recrystallization of the original mineral takes place.

2. The autoclave treatment of nephelines with caustic solutions in presence of lime, under certain conditions, yields a precipitate of hydrated calcium sodium (or potassium) silicate, while the alumina is dissolved.

3. The following possible mechanism for the leaching of alumina from nephelines is postulated: when nephelines are treated with alkaline solutions in the autoclave in presence of lime, they are dissolved with formation of solutions of sodium aluminate and silicate (or silicic acid gel). Calcium oxide reacts with sodium silicate, forming a sparingly soluble precipitate of hydrated calcium sodium silicate; sodium aluminate remains in solution. This mechanism was confirmed by x-ray and microscopic investigations.

LITERATURE CITED

[1] F. N. Strokov, et al., Trans. State Inst. Appl. Chem. 29 (1936).

[2] I. S. Lileev, et al., Trans. State Inst. Appl. Chem. 32 (1940).

Received June 7, 1957

ACCELERATION OF PORCELAIN PRODUCTION

A. I. Avgustinik and V. M. Loginov

Accelerated firing of ceramic wares is of great practical importance, especially in relation to automation.

Under laboratory conditions, we fired porcelain insulators of types ShN-1 and ShS-6 in 6 hours (including the cooling stage). For accelerated firing under production conditions, at the Artem Accessory and Insulator Works in Slaviansk, an experimental kiln with a movable floor was constructed out of the resources of this works. S. I. Ivakhin, M. P. Boginskii, I. P. Boiko, and N. S. Grebennikov took part in the development work of this kiln, which was designed by the Ceramics Department of the Leningrad Technological Institute, and in its construction. The experimental kiln (Fig. 1) consists of a firing compartment (A) and a cooling compartment (B). A working car 1 and an auxiliary car 2 were used for accelerated firing. At one end of the working car is a combustion chamber 3, and at the other, the auxiliary car with two walls at its ends. Thus, during the firing the kiln space is bounded below by the floor blocks, above by the crown, by the wall of the auxiliary car at one end, and by the combustion chamber at the other. The experimental kiln has 10 fireboxes fitted with FDM-2 burners run on heavy oil. The upper and lower fireboxes 4 and 5 are connected by channels 6. The fuel oil is fed by gravity along a heated duct from supply tanks (2×0.8 m^3). The combustion air is supplied by a high-pressure blower ($V = 1000$ m^3/hour, $P_{max} = 240$ mm Hg). The kiln has 4 side and 2 end smoke vents 7, with channels 8 and dampers 9. A low-pressure Sirocco fan No. 6, 5 is used for removal of the flue gases. The same fan is used to supply cold air into the cooling compartment.

In the trials, the working car loaded with the ware was pushed into the firing compartment (A), and the auxiliary car was pushed close to it. The end gaps between the car and kiln were filled with fireclay paste to minimize heat losses and leaks of cold air. The burners were started up by means of "dies."* The lower burners 5 were used to raise the kiln temperature to 800°; the combustion gases passed through the connecting canals into the upper burners 4, were diluted with cold air entering through the ports of the upper burners, and then entered the kiln. The upper burners 4 were used to raise the kiln temperature from 800° to the maximum. The auxiliary burners 10 were in operation throughout the firing, and the combustion gases from them entered the kiln through the grate of the combustion chamber 11. The flue gases from the kiln passed through openings in the blocks of the raised floor 12, by-passing the damper 9, the common ducts 8, and baffles, were diluted with cold air, and ejected by means of a fan through the flue into the air. The kiln was operated at a rarefaction of 0.5-1.0 mm water column.

After the firing, the end gaps between the car and the kiln were opened, the ports of burners 4 and 5 were blocked up, and the working car was rolled from the firing compartment (A) into the cooling compartment (B). Simultaneously, the auxiliary car was pushed into the firing compartment. The car was cooled by cold air blown into the cooling compartment through the ports 13, and by the compartment lining. The temperature was measured by means of the thermocouples 14. The insulators were fired at 2% initial moisture content, and without being preheated. They were placed in saggers packed in 2 or 3 layers in the car. The total weight of porcelain per car was from 107 kg (first firing) to 274 kg (ninth firing). The range and numbers of the insulators fired together are given in Table 1. The fired insulators were tested by the oil test and the mechanical strength test (GOST 6490-53, 1232-53). From 20 to 50 insulators out of each batch fired were tested. In addition to the insulators, laboratory specimens were also fired, for determinations of the electrical and mechanical strength of the porcelain, shrinkage, and glaze luster. The temperature was recorded by means of platinum–rhodium thermocouples and pyrometers, and rarefaction, by means of a Krell suction gage, and the gas was analyzed in the Orsat apparatus.

*As in original – Publisher's note.

When the car was cooled, the temperature in the saggers and the cooling compartment was recorded, and the pressure of the cold air entering the cooling compartment was measured.

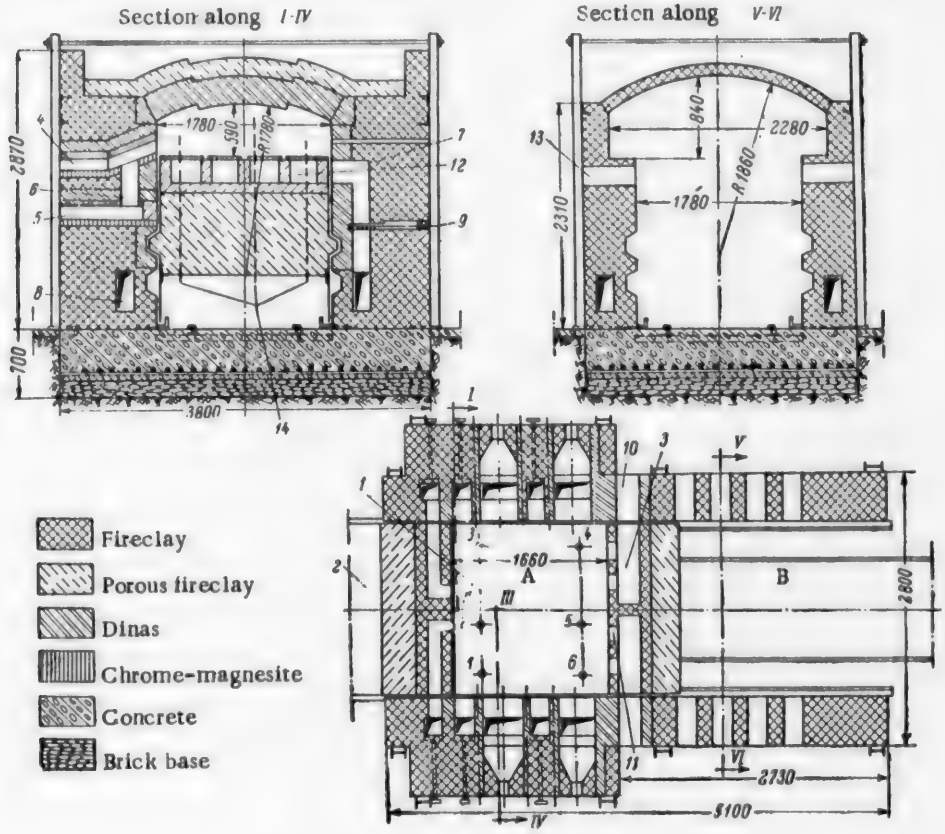

Fig. 1. Experimental kiln. Explanation in text.

Results of the Firings

Twenty firings were carried out. Eleven of these are discussed in this paper.

Firings 1-7, 10, and 11 took place with the use of oil fuel, without preheating of the kiln lining. In firing 8, the fuel used during the heating-up period consisted of 40% solar oil and 60% heavy oil. This did not give any significant increase in the rate of temperature rise. In firing 9 the working car was pushed into the kiln previously heated to 400°.

None of the sagger-fired insulators showed firing cracks; insulators which were not protected against the direct action of the combustion gases usually cracked during heating and cooling.

In firings 4, 8, 9, and 10 the temperature was raised to the maximum in 7 hours; in firings 1, 3, 5, 6, and 11, in 8 hours. Curves representing the limits of the high-speed firing conditions are given in Fig. 2. They represent firing 2 (Curve 1), and firing 8 (Curve 2). The results of tests on the laboratory specimens are summarized in Tables 2 and 3, and of tests on the insulators, in Table 4.

The firing-temperature region and cooling curves are presented in Fig. 3, which includes the most significant curves from which the conclusions were drawn. Certain comments are necessary concerning some of the experiments. In firing 1, the optimum temperature established later (1340°) was exceeded by 50-60°, so that half of the fired insulators were blistered. In firing 2 the maximum temperature was lowered to 1330°, but this temperature was not held. The water absorption of the fired insulators was in the range of 0.3-0%, while the electrical-breakdown and mechanical strengths of the insulators and laboratory specimens were higher than for

TABLE 1

Range and Numbers of Insulators Fired in the Saggers of the Experimental Kiln

Firings	Numbers of insulators fired					Total wt. of porcelain (kg)	Notes
	P-4,5	ShS-10	ShS-6	ShN-1	AIK-2		
1	5	62	—	12	13	107.3	
2	6	53	—	—	45	110.3	
3	5	39	—	—	32	110.0	$OB\text{-}10_{CF}$, P-7, P-8,5 and P-11 were fired in addition
4	13	12	76	—	40	146.9	
5	6	7	70	56	—	167.2	4000 RSh-4 rollers were fired in addition to the insulators
6	10	40	33	30	—	184.05	5000 RSh-4 rollers were fired in addition to the insulators
7	6	29	36	25	—	154.2	Ditto
8	8	32	32	21	—	159.7	Ditto
9	3	3	22	341	—	274.0	
10	—	22	—	—	—	257.6	330 trolley insulators (0.7 kg) were also fired
11	12	40	—	—	—	182.8	120, ditto

commercial specimens. In firing 3 the temperature was held at 1310°, and the cooling over the 950-550° range was more rapid than in the preceding firing. The electrical strength of ShS-10 insulators was lower as a result, but the mechanical strengh remained at the previous level. The electrical and mechanical strengths of the laboratory specimens increased. In firing 4 the temperature was held at 1310° for 2 hours, and cooling over the 800-600° range was more rapid than in firing 3. Tests of insulators from firing 4 revealed some rejects, although no defects could be detected in these insulators by external inspection. The water absorption of insulators from firings 3 and 4 was in the ranges of 0.4-0% and 0.3-0% respectively.

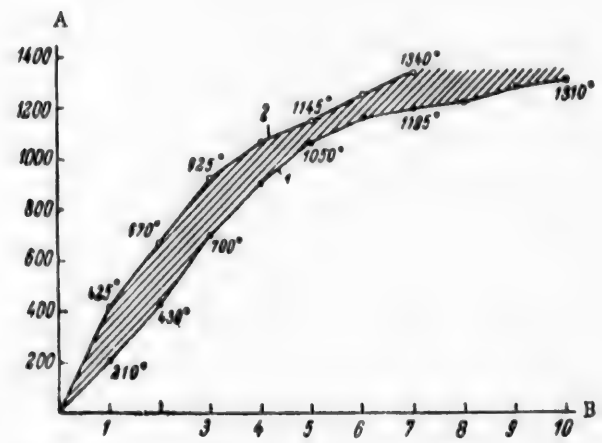

Fig. 2. Limits of high-speed firing conditions. A) Temperature (°C), B) time (hours). Explanation in text.

In firing 5, the temperature was held at 1310° for 3 hours. The cooling rate was approximately the same as in firing 2. As a result, the insulators had higher mechanical strength than commercial specimens, and also than insulators from firing 4; the electrical strength of the insulators was within the same range, but lower than that of commercial specimens. The water absorption of insulators from this firing was in the 0.2-0% range.

TABLE 2

Results of Electrical and Mechanical Strength Tests on Specimens Fired in the Experimental Kiln•

Characteristics		Firings (accelerated) in experimental kiln														Firing in works tunnel kiln	
		1	2		3		4		5		6		7	9	10	11	bottom	top
Maximum firing temperature (°C)	by pyrometers	—	—	—	—	—	—	1290	—	—	1320	1350	1350	1350	1380	1250	1350	1350
	by thermocouples	1385	1340	1330	1330	1310	1300	1305	1300	1320	1330	1340	1340	1340	1340	1310	—	—
Holding time at maximum temperature (hours)		2	0	0	1	1	2	2	3	2	2	2	2	2	3	0	4	4
Electrical breakdown strength in oil (kv/mm)		—	29.0	29.15	26.9	28.7	—	27.3	28.2	31.1	28.1	28.6	29.6	28.8	28.6	27.9	27.7	27.1
Bend strength kg/cm²	unglazed	—	—	—	—	—	—	—	—	—	—	—	—	722.2	722	865.1	691.8	—
	glazed	—	—	—	—	—	—	—	—	—	—	—	—	1084	—	—	891.8	—
Tensile strength (kg/cm²	unglazed	340	384	350.8	403.1	419.8	406.4	390.8	353	367	372.1	319.9	379.3	—	233	313	356.8	342.6
	glazed	—	—	—	—	—	—	—	—	—	—	—	544.7	—	—	—	532.0	544.8

•In firings 2, 3, 4, 5, and 6 the laboratory specimens were placed in two different saggers. The thermocouples and pyrometers were placed in the saggers together with the specimens.

TABLE 3

Glaze Luster and Shrinkage of Production Porcelain and Porcelain after Accelerated Firing

Characteristics		Nos. of accelerated firings in expt'l kiln				Firing in works tunnel kiln
		8		9		
Firing shrinkage (%)		7.96	8.56	8.44	9.0	8.3
Glaze luster (%)	white	—	—	5.0	5.25	4.83
	brown	—	—	8.36	8.40	7.10

In firing 6 the temperature was held at 1340° for 2 hours, and the cooling in the 1200-550° range was the same as in firing 3. The fired ShS-10 insulators had higher mechanical strength, but the mechanical strength of ShS-6 insulators was lower. The best results were obtained in firing 7, where the cooling rate in the 950-800° range was lower than in firing 6 (Fig. 3), while the maximum temperature of 1340° was held for 2 hours as in firing 6. The electrical strength of the insulators was 4-15% higher, and the mechanical strength, 6-26% higher, than those of commercial samples. The total firing time (heating up, holding, and cooling) was 14 hours, as against 60 hours in the works tunnel kiln. The glaze was spread evenly and had a stronger luster than in commercial specimens. These favorable results are consistent with the good results obtained with laboratory specimens (Table 2), which had a breakdown voltage of 29.6 kv/mm and a tensile strength of 379 kg/cm^2, as compared with 27.7 kv/mm and 357 kg/cm^2 respectively for ordinary production ware. In firings 8 and 9, with holding times of 2 hours, the cooling rate over the 900-700° range was somewhat lower than in firing 7, and this led to a decrease of mechanical strength. In firing 10, the holding time at 1340° was 3 hours, and the cooling was as in firing 7. As a result, the mechanical strength of the insulators was higher, and the electrical strength somewhat lower, than for production specimens.

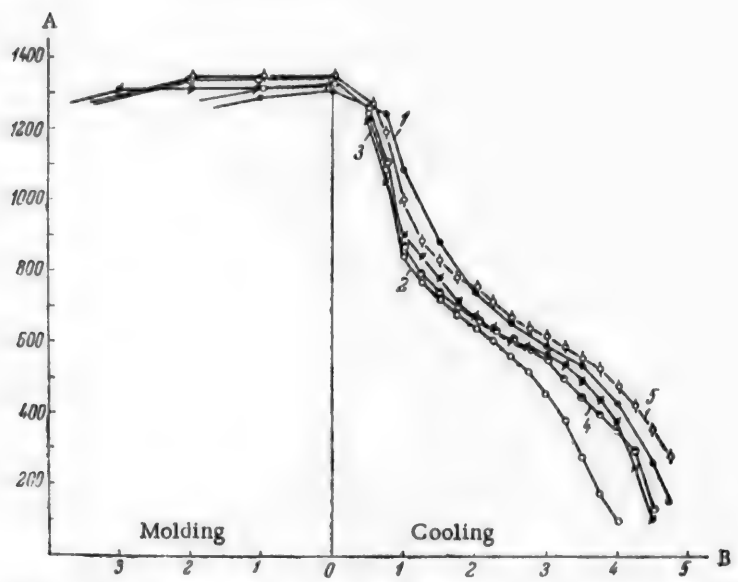

Fig. 3. Holding and cooling curves for accelerated firing. A) Temperature (°C), B) time (hours). Curves for firings: 1-2, 2-4, 3-5, 4-6, 5-7.

TABLE 4

Results of Tests on Insulators Fired in the Experimental Kiln•

Firings (accelerated)		1	2	3		4		5			6		
Types of insulators fired		ShS-10	ShS-10	ShS-10	P-4,5	ShS-6	P-4,5	ShS-6	ShS-10	P-4, 5	ShS-6	ShS-10	P-4,5
Test:													
Breakdown load (kg)	average	2100	2560	2430	8000	1730	8000	1950	2600	8300	1510	2200	7800
	variation limits	1900—2500	2000—3300	1800—3700	7100—8500	1100—2600	7000—8800	1700—2600	1900—2700	8200—8400	1200—1800	1800—2500	7400—8000
Electrical breakdown strength in oil (kv)	average	100	115	93	136.1	91.5	99	92	90	135	102	105	115.0
	variation limits	94.7—109.7	100—126	80—112	117—139	80—109	100—92	86—96	87—92	132—139.1	92—113	90—110	114—117

Firings (accelerated)		7			8		9		10	11	Firing in the production tunnel furnace		
Types of insulators fired		ShS-6	ShS-10	P-4,5	ShS-6	ShS-10	P-4,5	ShS-10	ShS-10	ShS-10	ShS-6	ShS-10	P-4,5
Test:													
Breakdown load (kg)	average	1800	2400	8300	1600	1840	1700	1900	2200	2500	1700	1900	7500
	variation limits	1600—2400	2000—2500	8200—8400	1400—1850	1600—2000	1450—1900	1800—2000	2000—2500	1800—2800	1550—2000	1700—2300	6600—8000
Electrical breakdown strength in oil (kv)	average	110	115	135	104	110.6	102	118	97.3	92.2	96	109	130
	variation limits	93—116	100—122	112—138.5	98—118	99—122	93—107	110—127	87—110	88—97	90—104	103—113	112—139

•In breakdown load tests on suspension insulators, the insulators broke down only at the attachments.

Firing 11 followed the procedure of firing 2. The fired insulators had higher water absorption and lower mechanical and electrical strength than those from firing 2.

Phase analysis of porcelain made by works and accelerated firing. Phase analysis was performed by optical and x-ray methods. Figure 4 shows microphotographs of polished sections of production porcelain (a) and porcelain from firings 7, 10, and 11 (b, c, and d respectively). It can be seen that porcelain from firing 11 (d) contains weakly defined mullite crystals, concentrated in the former feldspar grains; the boundaries of the latter are distinct. The production porcelain (a), and porcelain from firings 7 and 10 (b and c differ little from one another, and are more homogeneous than porcelain from firing 11 (d); they also contain distinct mullite crystals.

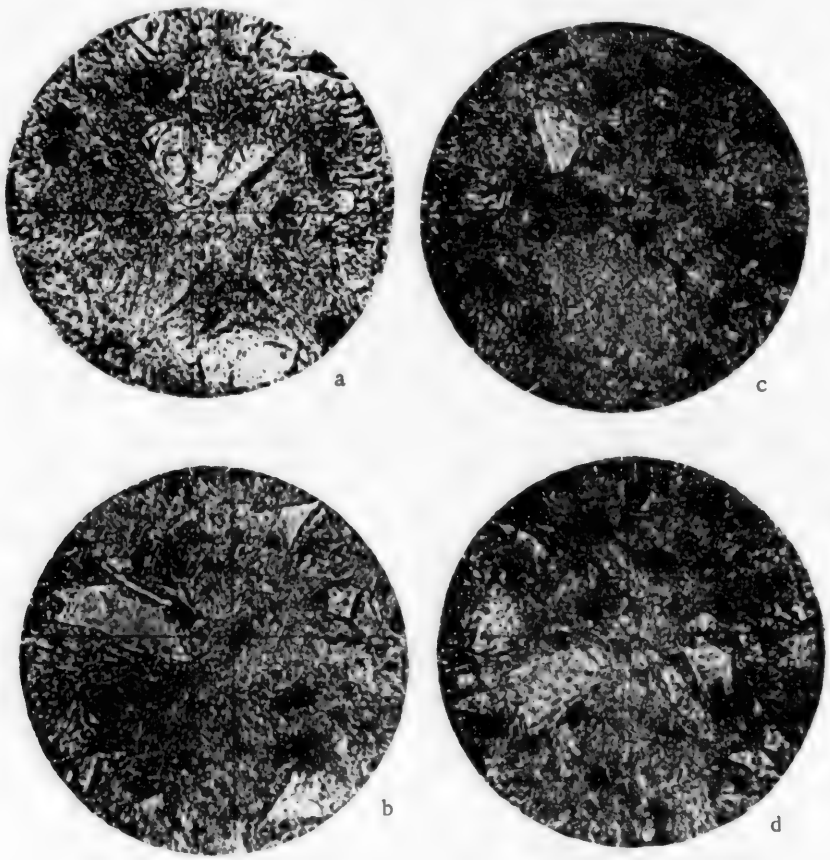

Fig. 4. Porcelain microstructure. Firing times (hours): a) 33; b, c, d) 7. Holding times (hours): a) 5 at 1320°; b) 2 at 1340°; c) 3 at 1340°; d) not held at 1320°.

Therefore, examination of polished sections by transmitted light does not reveal any significant differences of phase composition between production porcelain and porcelain fired in 12-14 hours by the accelerated procedure. To confirm this, the phase composition of insulator porcelain from the Artem and "Proletarii" works was investigated in an x-ray unit with an ionization chamber.* The body compositions are given on the following page.

* The x-ray unit was provided by the x-ray Laboratory of the State Institute for Planning and Research in the Cement Industry; the x-ray patterns given in this paper were obtained under the guidance of P. F. Konovalov.

Material	Body from Artem works	Body from "Proletarii" works	Material	Body from Artem works	Body from "Proletarii" works
Prosianala kaolin	10–10.5	15	Pegmatite	–	37
Pologoe kaolin	10–10.5	–	Eliseevo pegmatite	39–40.7	–
Kyshtym kaolin	–	15	Luga quartz sand	–	13
Chasov Iar clay	–	15	Avdeevka quartz sand	9–9.4	–
Druzhkov clay	22–23	–	Porcelain grog	6–10	5

In addition to determinations of phase composition, the fired porcelain was tested for mechanical strength (rods 10 mm in diameter), electrical breakdown strength (disks 80 mm in diameter), specific gravity, and water absorption. The porcelain body of the "Proletarii" works was made by the following procedure: grinding of pegmatite and grog between crusher rolls (to 50% residue on No. 006 sieve), vibratory grinding of quartz sand (to 3-4% residue on No. 006 sieve), followed by magnetic separation; drying and grinding of the clay materials (to pass through No. 1 sieve) → measuring of dry materials → combined grinding in a ball mill with added water (6 hours) → dehydration of the slip (in a plaster vessel) → kneading (by hand) → aging of the body (three days) → kneading (by hand). Production body from the Artem works was used in the trials; this was dried, ground (to pass through No. 1 sieve), mixed thoroughly, moistened, kneaded, aged (three days), and kneaded again (by hand). These masses were used for preparation of the specimens, which were fired in an electric furnace with carborundum heaters, and in the works tunnel kiln. A reducing medium in the electric furnace was created by combustion of kerosene; the approximate composition of the medium in all the firings was: CO_2 7.0%, O_2 0.8-1.0% and CO 6.0% (determined by means of the Orsat apparatus). The firing time in the electric furnace was varied from 6 to 16 hours; the holding times at 1300° were 4, 6, 8, and 10 hours, and at 1330°, 0, 2, 4, and 6 hours. The temperature curves for accelerated firing of porcelain with the best properties are given in Fig. 5 (1, 2). The firing time in the works tunnel kiln was 110 hours (Fig. 5, 3).

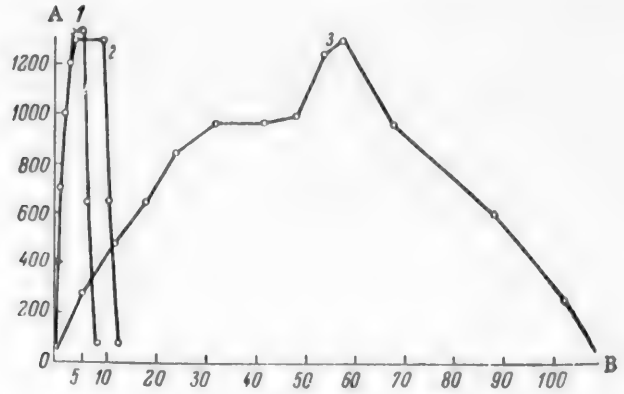

Fig. 5. Firing curves for porcelain; in the electric furnace by the accelerated regime (1, 2), and in the works tunnel kiln (3). A) Temperature (°C), B) time (hours).

The results obtained in tests of mechanical strength, electrical strength, water absorption, shrinkage, and density of laboratory specimens of the fired porcelain are given in Table 5. The data in Table 5 are consistent with the results obtained earlier for porcelain fired in the experimental production kiln (Table 2). The phase composition of the porcelain with the best properties (Table 5) was investigated by means of x-ray diffraction. Figure 6 shows x-ray diffraction diagrams of porcelain from the Artem works (1, 2, 3) and the "Proletarii" works (4, 5, 6). Diagrams 1 and 4 are for porcelain fired in the works tunnel kiln, Diagrams 2 and 5 are for porcelain fired in the electric furnace at 1300° for 6 hours, and Diagrams 3 and 6 are for porcelain fired in the electric furnace at 1330° for 2 hours. Comparison of the diffraction patterns of the same porcelain, fired by the ordinary

TABLE 5

Test Results and Properties of Porcelain Fired by the Accelerated Regime and Under Production Conditions

Porcelain	Temperature (°C) and holding time (hours)	Bend strength (kg/cm²)	Electrical breakdown strength in oil (kv/mm)	Water absorption	Shrinkage (%)	Density (g/cc)
Artem works	Production firing	710	27.0	0	6.10	2.510
	1300 — 4	720	21.0	0.7	6.32	2.516
	1300 — 6	720	28.0	0	6.10	2.500
	1300 — 8	600	30.0	0	6.00	2.490
	1300 — 10	590	25.0	0	5.55	2.470
	1330 — 0	700	18.0	1.5	6.60	2.550
	1330 — 2	730	28.0	0	6.10	2.510
	1330 — 4	710	28.3	0	5.70	2.495
	1330 — 6	540	26.0	0	5.20	2.475
"Proletarii" works	Production firing	720	25.0	0	6.10	2.505
	1300 — 4	710	24.3	0.4	6.29	2.500
	1300 — 6	700	26.0	0	6.20	2.498
	1300 — 8	680	26.0	0	6.18	2.486
	1300 — 10	580	24.0	0	5.70	2.420
	1330 — 0	710	20.0	1.0	6.70	2.540
	1330 — 2	720	28.0	0	6.10	2.510
	1330 — 4	690	29.0	0	5.85	2.490
	1330 — 6	530	27.6	0	5.45	2.470

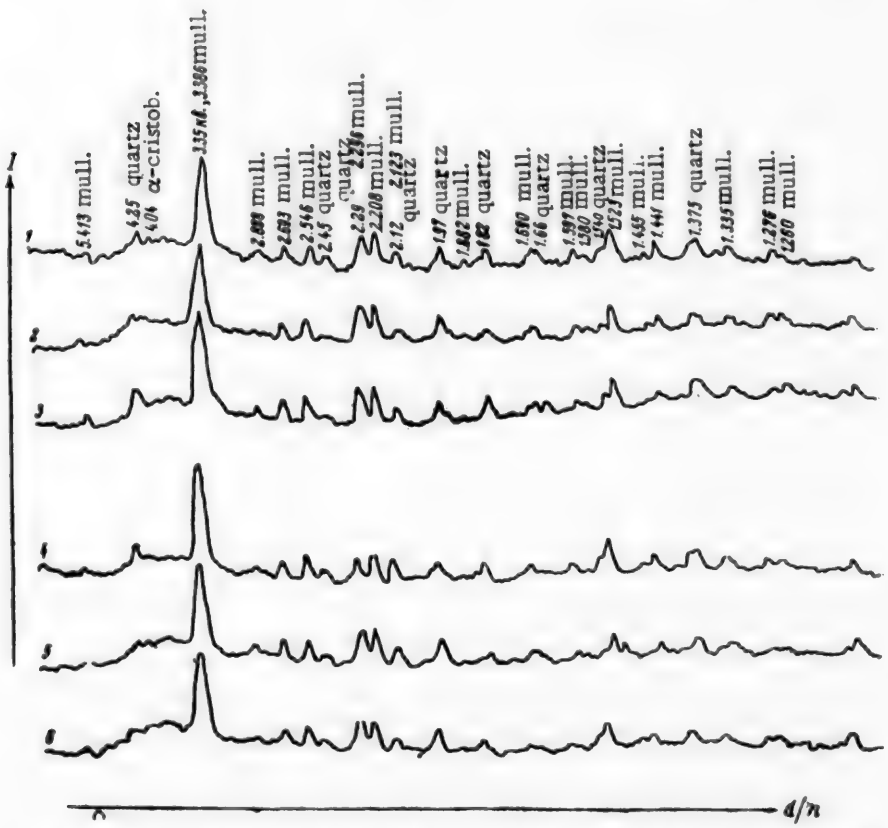

Fig. 6. x-Ray diffraction patterns for porcelain fired in the electric furnace by the accelerated regime (2, 3, 5, 6) and in the works tunnel kiln (1, 4). 1,2,3) Porcelain from the Artem works; 4,5,6) porcelain from the "Proletarii" works.

and accelerated procedure respectively (for example, 1, 2, and 3 in Fig. 6), clearly shows that the corresponding lines do not differ in intensity; this shows that the phase compositions of these porcelains are almost identical.

SUMMARY

1. Insulators of the P-4,5, ShS-10, ShS-6, ShN-1, and AIK-2 were fired in 2 and 3 tiers in saggers for a total time of 12-14 hours, with accelerated cooling; it was found that the insulators and laboratory specimens fired by this procedure had mechanical strength 10-20% higher than production ware, while the electrical strength was the same as, or a little higher than (firings 2, 7), that of production ware. Optical examination showed that the phase composition of porcelain fired in 12-14 hours is virtually the same as that of production porcelain fired for 60 hours.

2. It was found in x-ray investigations of the phase composition of porcelain fired by the accelerated regime in 8 and 12 hours, with holding times of 6 hours at 1300° and 2 hours at 1330° respectively, and of porcelain fired by the ordinary works procedure, that such porcelains are virtually identical in phase composition.

3. The mechanical strength of ShS-6, ShS-10, and P-4, 5 insulators can be increased as the result of cooling at a rate of 300-400°/hour in the 900-500° range.

The properties of the insulators deteriorate if this cooling rate is exceeded.

4. The accelerated firing procedure can serve as a basis of design calculations for an experimental production kiln of the slit type for mass firing of pin and suspension insulators of the above-named types.

5. The proposed accelerated firing procedure for ShN-1, ShS-6, ShS-10, and P-4,5 insulators should be subjected to trials in works tunnel kilns.

Received September 13, 1957

STUDY OF THE BURNING OUT OF CHROMIUM IN THE PRODUCTION OF SYNTHETIC RUBY

G. A. Mukhin, N. I. Maliugina, and T. S. Uspenskaia

One important characteristic of the quality of synthetic ruby is the intensity and uniformity of its color, which is often inadequate and irregular [1, 2].

The principal coloring matter in ruby is chromium, which is added to ammonium alum in the form of ammonium dichromate. The chromium is burned out when the colored alum is fired, and especially during crystallization of the ruby [3]. It has been found that the degree of burning out of the chromium depends on the crystallization conditions. The purpose of the present investigation was therefore to study the effect of crystallization conditions on the intensity and uniformity of the ruby color. The tracer atom method was used, with the aid of the γ-radiating chromium isotope Cr-51, with a half life of 26.5 days. The ammonium alum was colored with ammonium dichromate, previously tagged with radioactive chromium. The burning out of chromium during firing of the alum was determined from the ratio of the activity of all the powder formed to the activity of the original chromium nitrate solution added to the ammonium dichromate solution before the experiment. One-hundred mg samples of the powder were shaken with 5 ml of water, and transferred, by means of a porous-glass funnel, to paper filters of the same size and shape. Throughout the experiments determinations of activity were performed simultaneously on the powder samples and a standard made from 0.1 ml of the original radioactive chromium nitrate solution, so that it was possible to take into account the decay of Cr-51 and the counter efficiency.

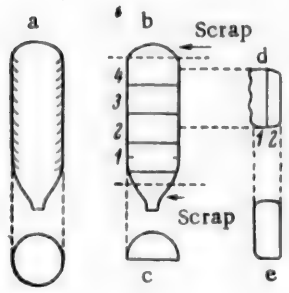

Fig. 1. Separation of ruby boule into plates. a) Boule; b) half-boule; c) plate perpendicular to the geometrical axis; d) middle portion of half-boule; e) plate parallel to the geometrical axis.

For determination of the burning out of chromium during growth of the boule,* the latter was ground to a homogeneous powderlike mass; the samples were prepared in the same way as the powder samples. The radiation standard for the ruby samples was a powder sample prepared and tested simultaneously with the ruby sample.

For studies of chromium distribution along and across the boule, the latter was split along its geometrical axis into two symmetrical half-boules, which were then cut into plates, 1-1.5 mm thick, parallel and perpendicular to the geometrical axis, by means of a diamond disk saw (Fig. 1). The activities of the plates were determined. As the plates differed in weight, the activities could not be compared directly from the counts, and for comparison the activities per 1 g of ruby in each sample were calculated.

The first series of experiments was performed under the conditions used in industry for alum firing and crystallization of the ruby. The chromium contents of the powder and ruby were determined (Tables 1 and 2).

The results in these tables show that on the average 10.7% of chromium is burned out during firing of the alum, and 50% during crystallization of the ruby; this is in good agreement with the results of chemical analyses [3]

*Crystals without definite faces are known industrially as boules.

TABLE 1

Actual Cr Contents of Powder, with 0.00317 g of Cr Introduced per 0.1 g of Powder

Sample No.	Activity of standard (pulses/min)	Activity of sample (pulses/min)	Actual Cr content in 0.1 g of powder (g)	Cr burned out (%)
1	2280	77	0.00278	12.3
2	2280	77	0.00278	12.3
3	2280	78	0.00281	11.3
4	2280	80	0.00289	8.8
5	2280	80	0.00283	8.8
			Average	10.7

TABLE 2

Actual Cr Contents of Ruby, with 0.00634 g of Cr Introduced into 0.2 g of Powder

Sample No.	Activity of 0.2 g of powder (pulses/min)	Activity of 0.2 g of ruby (pulses/min)	Actual Cr content in 0.2 g of ruby (g)	Cr burned out (%)
1	160	90	0.00356	43.8
2	160	76	0.00301	52.5
3	160	77	0.00305	51.9
4	160	78	0.00309	51.3
5	160	79	0.00313	50.6
			Average	50.0

TABLE 3

Activity Distribution Along the Height of Boule No. 5

Plate No.	Plate thickness (mm)	Weight of plate (g)	Activity of plate (pulses/min)	Activity of 1 g of ruby (pulses/min)	Initial activity of 1 g of ruby (pulses/min)
1	1.5	0.3894	47	120	144
2	1.6	0.5120	68	132	158
3	1.5	0.5558	72	129	155
4	1.3	0.6028	76	125	151
5	1.5	0.7336	92	130	158
6	1.3	0.6821	88	128	155
7	1.8	0.8976	112	125	150
8	1.5	0.8744	119	136	163
9	1.7	0.9812	141	143	171
10	1.3	0.7758	107	112	134
11	1.4	0.8904	127	142	171
12	1.4	0.8862	110	125	150
13	1.4	1.0062	139	128	153
14	1.4	0.9292	133	143	171
15	1.5	0.9070	128	141	170
16	1.6	0.9726	142	147	176
				Average	151

TABLE 4

Activity Distribution Across the Width of Boule No. 5

Plate thickness (mm)	Weight (g)	Activity (pulses/min)	Activity of 1 g of ruby (pulses/min)	Initial activity of 1 g of ruby (pulses/min)
Plates cut from top of boule				
1.8	1.0080	125	124	148
1.5	1.0583	133	125	150
2.0	0.4954	63	127	152
			Average	150
Plates cut from central part of boule				
1.5	0.816	91	111	133
1.3	0.751	88	117	133
1.5	0.680	75	110	133
1.4	0.561	67	119	134
			Average	133

Tables 3 and 4 contain data on the distribution of chromium in boule No. 5, which crystallized at an average rate of 8.4 mm/hour. In these and subsequent tables the activities of the plates are given; these values are proportional to their absolute chromium contents. For comparable results, the measured activities of all the plates were recalculated into values for the start of the count, by the usual formula for spontaneous radioactive decay.

The data presented in these tables, which are typical of all the boules investigated, show that the distribution of chromium along the height of the boule is not quite uniform (deviations from the mean reach

TABLE 5

Activity Distribution Along the Height of Boules No. 7 and No. 9

	Crystal formed at higher growth rate		Crystal formed at lower growth rate	
plate No.	initial activity of 1 g of ruby (pulses/min)	growth rates of indiv. regions of boule (mm/hr)	initial activity of 1 g of ruby (pulses/min)	growth rates of indiv. regions of boule (mm/hr)
1	292.2	14	156.8	6
2	238.0	14	170.5	6
3	251.2	14	162.7	6
4	220.0	9	201.9	7
5	214.1	9	201.9	7
6	216.7	9	229.4	8
7	220.7	9	243.0	8
8	210.1	8	243.1	8
9	193.7	8	184.3	6
10	195.4	8	154.3	6
11	200.3	8		
12	210.7	8		
13	195.4	8		
Average	226.7	9.7	Average 195.4	6.8

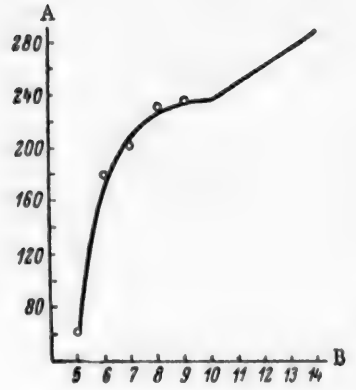

Fig. 2. Curve for the activity of ruby as a function of the crystallization rate of the boule. A) Activity or ruby (pulses/minute), B) boule crystallization rate (mm/hour).

15-20%), while the distribution of chromium across the boule may be regarded as virtually uniform. The purpose of the second series of experiments was to determine the degree of burning out of chromium, and its distribution in the boules, under different crystallization conditions.

Tables 5 contains typical results for the boules studied; here the distribution of chromium along the height of the crystal is indicated by the plate activities. The boules were crystallized at rates higher and lower than the production rate.

As the feed rate of the powder into the crystallization torch was not uniform, it proved impossible to grow the boules at a constant rate throughout their growth. However, operational records make it possible to determine the growth rates of individual regions of the boule in which the rates were relatively constant.

The results show that the crystallization rate of ruby has a significant influence on the distribution of chromium in the boule. This effect becomes more pronounced with larger fluctuations of the crystallization rate. Boule No. 10 was crystallized with frequent variations of the rate from 4 to 14 mm /hour.

The activity distribution along the height of boule No. 10, grown at a varying rate, is shown below:

Plate No.	1	2	3	4	5	6	7	8	9	10
Initial activity of 1 g of ruby (pulses/min)	97	339	48	77	325	339	271	218	364	135

By comparison of individual regions of the boules, grown at different rates, it is possible to plot the chromium content of ruby against the crystallization rate (Fig. 2). It follows from this graph that the chromium content of ruby increases, i.e., the amount of chromium burned out decreases, with increase of the growth rate of the boule. The flat portion of the curve indicates that the most favorable crystallization rate is 8-10 mm/hour. In production conditions the crystallization rate cannot as yet be exactly stabilized, and its variations during boule growth result in irregularities of the color of the ruby. To make the color of ruby more uniform, its crystallization rate must be stabilized.

LITERATURE CITED

[1] S. V. Grum-Grzhimailo and E. I. Utkina, Trans. Inst. Crystallography Acad. Sci. USSR 8, 99 (1953).

[2] F. I. Pashkovskaia, Trans. Inst. Crytallography Acad. Sci. USSR 8, 43 (1953).

[3] A. A. Kiselev and L. M. Dolgova, Trans. Inst. Crystallography Acad. Sci. USSR 8, 47 (1953).

Received January 14, 1956

EFFECT OF THE COMPOSITION OF GLASSES ON THE INFLUENCE OF Me_2O AND Al_2O_3 OXIDES ON THEIR ELECTRICAL CONDUCTIVITY

L. A. Grechanik

Central Scientific Research Laboratory for Electrotechnical Glass

One of the most important properties of glasses used for vacuum tubes is electrical resistance. Therefore a knowledge of the variations of electrical resistance with the chemical composition of glass over wide concentration ranges of the different components is necessary for development of new types of glasses for the vacuum tube industry.

The accepted explanation for the conductivity of solid glasses [1-8] is that Me^+ ions migrate through the spaces in the silicon-oxygen framework under the influence of the applied potential. The conductivity of glass therefore depends on its content of current-carrying ions and on their mobility, increasing with increasing contents of Me_2O oxides in the glass.

In addition to Me_2O oxides, Al_2O_3 produces some increase in the conductivity of glass when it replaces SiO_2 [4, 7, 8]. The mechanism of this effect is explained as follows [8]: Al_2O_3 forms AlO_4 tetrahedrons in the glass structure, which are capable of replacing SiO_4 tetrahedrons in the silicon–oxygen framework of the glass. As a result, the framework becomes "looser," as the Al–O spacing is greater (1.72 A) than the Si–O spacing (1.62 A), and migration of the Me^+ ions present in it therefore becomes easier. The conductivity therefore increases as the result of increased mobility of the Me^+ ions although their content remains unchanged.

Me_2O and Al_2O_3 are very common components of technical glasses. The effect of the contents of these oxides, when present simultaneously, on the conductivity of glasses is therefore a matter of interest.

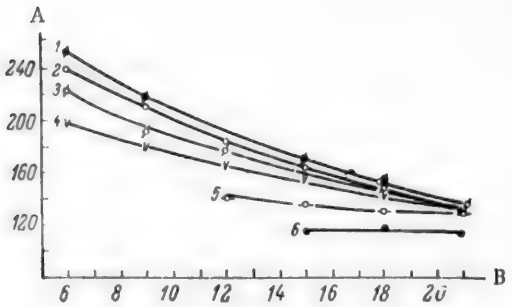

Fig. 1. Effect of replacement of SiO_2 by sodium oxide on T_{K-100} for glasses with different Al_2O_3 contents (constant B_2O_3 content). A) Values of T_{K-100} (°C), B) Na_2O content (%): 1 – 0, 2 – 1, 3 – 2, 4 – 4, 5 – 8, 6 – 12.

It has already been reported [6] that the ratio of Me_2O to Al_2O_3 has a considerable influence on the conductivity of alkali aluminosilicate glasses.

It was found in the present work on the composition of borosilicate glasses for the vacuum tube industry that the influence both of Me_2O and Al_2O_3 on the conductivity of glass is strongly associated with changes in the chemical composition of the glass, and in particular, with variations of the contents of each of these oxides. This relationship was studied in order to obtain fuller data on the dependence of the conductivity of glass on its composition, so that new formulations of vacuum-tube glasses could be designed more rationally.

EXPERIMENTAL

The group of glasses in the system SiO_2–B_2O_3–Al_2O_3–Na_2O was studied.

The glass compositions were formulated in molecular percentages within the following limits: SiO_2 from 55 to 82, Al_2O_3 from 0 to 12, Na_2O from 6 to 21, B_2O_3 (constant) 12.

The glasses were made from pure materials in quartz crucibles in a gas furnace at 1450°. The danger of Al_2O_3 from refractories entering the glass was thereby eliminated; this was particularly important in studies of glasses free from Al_2O_3, or containing only small amounts of it (1-2%).

The conductivity of the glass was represented in terms of the arbitrary standard T_{K-100}, the temperature at which the volume resistivity of the glass is 10^8 ohms·cm. The determinations of T_{K-100} were performed by the method developed at the Central Scientific Research Laboratory for Electrotechnical Glass [9]. The results are presented in Figs. 1 and 2.

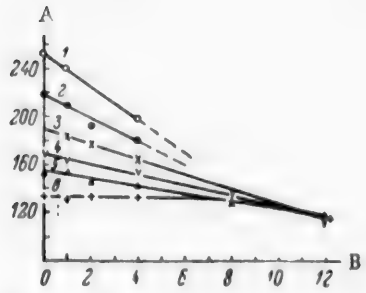

Fig. 2. Effect of replacement of SiO_2 by alumina on T_{K-100} for glasses with different Na_2O contents. A) Values of T_{K-100} (°C), B) Al_2O_3 content (%). Na_2O content (%): 1 – 6, 2 – 9, 3 – 12, 4 – 15, 5 – 18, 6 – 21.

It follows from Fig. 1 that replacement of SiO_2 by Na_2O in the glass, at constant Al_2O_3 content, produces different changes of T_{K-100}, which depend on the Al_2O_3 content. In absence of Al_2O_3 (Curve 1), as the Na_2O content increases T_{K-100} falls, i.e., the conductivity of the glass increases. However, in presence of increasing amounts of Al_2O_3 in the glass (Curves 2-5) this effect of Na_2O becomes less pronounced, and in glass containing 12% Al_2O_3 introduction of increasing amounts of Na_2O does not alter the conductivity of the glass (Curve 6). An interesting effect is observed: the number of current-carrying ions in the glass increases, but the conductivity of the glass remains unchanged. Thus, as the silicon–oxygen framework becomes increasingly "loosened" by the large AlO_4 tetrahedrons, increase of the Na^+ ion content has progressively less influence on the conductivity of the glass.

Replacement of SiO_2 by Al_2O_3 at constant Na_2O content (Fig. 2) is also accompanied by decrease of T_{K-100}, i.e., by increase of the conductivity of the glass; the increase greatly depends on the amount of Na_2O in the glass. At a relatively low Na_2O content (6%) replacement of SiO_2 by Al_2O_3 produces a considerable increase of conductivity: 1% Al_2O_3 lowers T_{K-100} by about 14°. With larger amounts of Na_2O this influence becomes weaker, and with 21% Na_2O replacement of SiO_2 by Al_2O_3 does not affect the conductivity. It was found that the relationship between the specific influence of Al_2O_3 (i.e., the effect produced by 1% Al_2O_3), introduced in place of SiO_2, on T_{K-100} of glasses, and the Na_2O content of the glasses, is linear (Fig. 3, Line 1).

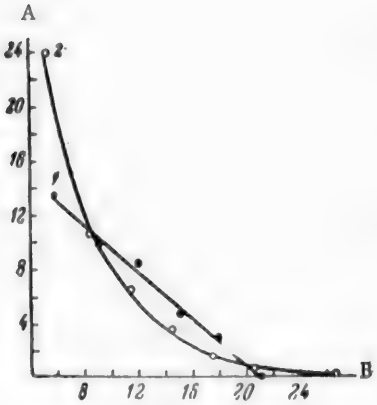

Fig. 3. Variation of the specific influence of Al_2O_3 on T_{K-100} with the Me_2O contents of glasses. A) Value of ΔT_{K-100} per 1% Al_2O_3 (°C), B) Me_2O content (%). 1) With % Na_2O, 2) with % Na_2O + + K_2O (Na_2O + K_2O = 1:1).

$$\Delta T_{K-100} = A - B\,[Na_2O],$$

where A = 18.9, B = 0.9, ΔT_{K-100} is the change of T_{K-100} of the glass on introduction of 1% Al_2O_3; $[Na_2O]$ is the content of Na_2O in the glass (molar %).

Thus, the more the silicon–oxygen framework is weakened by either Na_2O or Al_2O_3, the less influence does the other of these components have on the conductivity of the glass.

Figure 4 shows a region of the system studied, with lines for equal values of T_{K-100}. It is seen that there is a range of compositions in which the conductivity of the glass remains unchanged (T_{K-100} is constant) on replacement of Al_2O_3 by Na_2O. Thus, the respective effects of these components, which differ in principle with regard to the glass structure, are the same with regard to the conductivity of the glass.

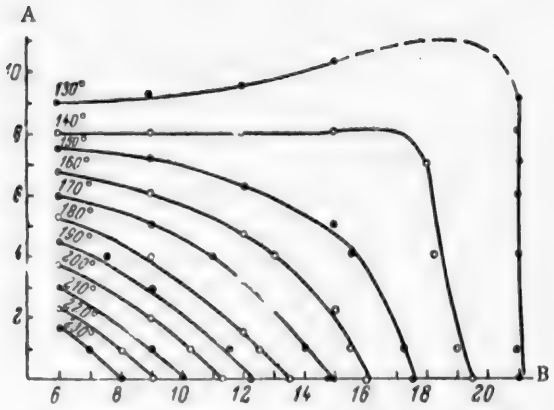

Fig. 4. Values of T_{K-100} for glasses of the system $SiO_2-B_2O_3-Al_2O_3-Na_2O$ (section corresponding to 12% B_2O_3). A) Al_2O_3 content (%), B) Na_2O content (%).

Analogous results, confirming these relationships, were obtained in studies of more complex multicomponent glasses of the system $SiO_2-B_2O_3-Al_2O_3-ZnO-Me_2O$, where Me_2O represents $Na_2O + K_2O$ in 1:1 ratio. The B_2O_3 and ZnO contents of all the glasses, with the exception of two separate series (see below) were constant.

The glass compositions were varied within the following limits (%): SiO_2 from 46 to 79, Al_2O_3 from 0 to 12, Me_2O from 5.5 to 26.5, B_2O_3 (const) = 6, ZnO (const) = 9.5.

The methods of glass preparation and determination of T_{K-100} were as described above. The results are presented in Figs. 5 and 6.

Figure 5 shows that replacement of SiO_2 by Al_2O_3 at constant Me_2O content results in different changes of T_{K-100}: at a low Me_2O content this replacement produces a sharp fall of T_{K-100}, i.e., increase of conductivity. At higher Me_2O contents this effect of Al_2O_3 becomes weaker, and finally at 26.5% Me_2O replacement of SiO_2 by Al_2O_3 has no effect on T_{K-100}.

Figure 3 shows variations of the specific influence of Al_2O_3 on T_{K-100} with the Me_2O contents of the glasses (Curve 2). This relationship is more complex than in the case of glasses of the system $SiO_2-B_2O_3-Al_2O_3-Na_2O$. However, the effect found in simpler glasses, namely, a decrease of the influence of Al_2O_3 as a "loosener" of the silicon–oxygen framework on the conductivity of glass with increased content of current-carrying Me^+ ions in the glass, is also found in multicomponent glasses approaching industrial glasses in composition.

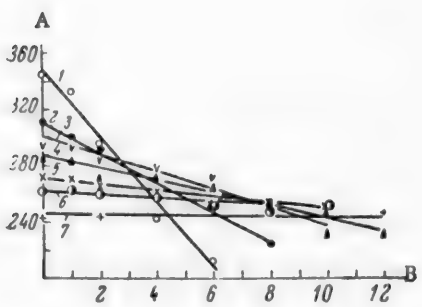

Fig. 5. Effect of replacement of SiO_2 by alumina on T_{K-100} for glasses at different Me_2O contents. A) Values of T_{K-100} (°C), B) Al_2O_3 content (%). Me_2O content (%): 1) 5.5, 2) 8.5, 3) 11.5, 4) 14.5, 5) 17.5, 6) 20.5, 7) 26.5.

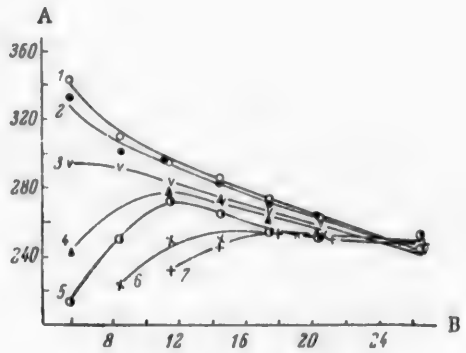

Fig. 6. Effect of replacement of SiO_2 by Me_2O(Na_2O : K_2O = 1 : 1) on T_{K-100} for glasses at different Me_2O contents. A) Values of T_{K-100} (°C), B) Me_2O content (%). Al_2O_3 content (%): 1) 0, 2) 1, 3) 2, 4) 4, 5) 6, 6) 8, 7) 10.

The replacement of SiO_2 by Me_2O oxides at constant Al_2O_3 content is represented by a particularly complex relationship for the glasses studied (Fig. 6); in absence of Al_2O_3 (Curve 1), the conductivity of the glass increases (T_{K-100} falls) with increasing Me_2O content, as is to be expected. However, in presence of Al_2O_3 (Curves 2-7) the variation of the conductivity with increasing Me_2O content in the glass changes character, and the T_{K-100} curves become complex in form. It is found in some instances (Curves 4-7) that replacement of SiO_2 by Me_2O in the glass lowers the conductivity (T_{K-100} rises) rather than raising it, up to a definite

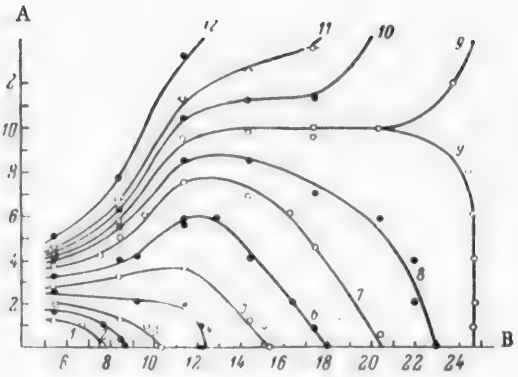

Fig. 7. Values of T_{K-100} for glasses of the system $SiO_2-B_2O_3-Al_2O_3-ZnO-Me_2O$ (section corresponding to 6% B_2O_3 and 9.5% ZnO). A) Al_2O_3 content (%), B) Me_2O content (%). Values of T_{K-100} (°C): 1) 320, 2) 310, 3) 300, 4) 290, 5) 280, 6) 270, 7) 260, 8) 255, 9) 250, 10) 245, 11) 240, 12) 230.

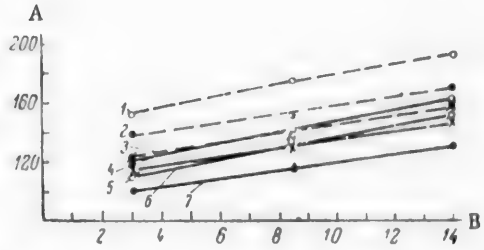

Fig. 8. Effect of replacement of SiO_2 by boron oxide on T_{K-100} for glasses with different Al_2O_3 and Na_2O contents. A) Values of T_{K-100} (°C), B) B_2O_3 content (%). Al_2O_3 contents (%): 1, 4—1; 2, 5-4; 3, 6-6; 7-10. Continuous lines for 18% Na_2O; dash lines for 12% Na_2O.

concentration, and only then begins to raise it (T_{K-100} falls). This effect is possibly caused by the action of two factors: on the one hand, the change of glass composition results in an increase in the concentration of the current-carrying Me^+ ions, which should raise the conductivity of the glass; on the other hand, the "neutralization effect" [5, 10] is intensified on increase of the total $Na_2O + K_2O$ content of the glass, which should produce a considerable decrease of conductivity. The simultaneous action of these factors probably accounts for the maxima on the curves in Fig. 6.

Figure 7 represents a region of the glass system in question, with lines for equal values of T_{K-100}. These results show that in complex multicomponent glasses there is also a very strong connection between the effects of Al_2O_3 and Me_2O on conductivity.

Two additional series of compositions were studied in order to determine the influence of B_2O_3 and ZnO on the conductivity of this group of glasses, and to establish a connection between the influence of Al_2O_3 on conductivity of glass and the contents of B_2O_3 and ZnO in the latter. The Al_2O_3 contents were varied from 0 to 10%, and ZnO and B_2O_3 contents from 3 to 15%, at the expense of SiO_2; the Na_2O content was kept constant at either 12% or 18%. The results obtained in determinations of T_{K-100} are given in Figs. 8 and 9.

The results (Fig. 8) show that replacement of SiO_2 by B_2O_3 produces a small linear increase of T_{K-100} (2.5° per 1% B_2O_3), although the Na_2O content remains constant. These results are in agreement with the known influence of B_2O_3 on the conductivity of glass [4, 8], and also show that the influence of B_2O_3 is independent of the Al_2O_3 (in the range of 1-10%) and Na_2O (in the range of 12-18%) contents of the glass.

Replacement of SiO_2 by ZnO has almost no effect on T_{K-100}, i.e., the conductivity of glass remains unchanged (Fig. 9). If we accept the view than ZnO may form ZnO_4 tetrahedrons which replace SiO_4 in the silicon—oxygen framework in glass [11], we may suppose that the "density" of the framework does not change, and neither does the ability of Na^+ ions to migrate through its "voids." It follows from Fig. 9 that variations of the Na_2O (12-18%) and Al_2O_3 (1-6%) contents of glass have no effect on the dependence of T_{K-100} on replacement of SiO_2 by ZnO.

The specific influence of Al_2O_3 on the conductivity of glass also depends very little on the B_2O_3, and ZnO contents; for example, with 3% B_2O_3 it is 2°, and with 15% B_2O_3 3.5°; with 3% ZnO 3.5° and with 15% ZnO 1.0°.

It also follows from Figs. 8 and 9 that the decrease of T_{K-100} with increase of the Na_2O content from 12 to 18% does not depend on either the B_2O_3 or the ZnO contents of the glass.

Thus, in this study of the effects of Al_2O_3, B_2O_3, and ZnO on the conductivity of glass we are dealing with components capable of forming tetrahedrons of the EO_4 type, which can replace SiO_4 tetrahedrons in the silicon—oxygen framework of the glass. The results obtained in this investigation show that such reconstruction of the framework may in some instances have a very strong influence on the conductivity, either hindering somewhat (in the case of B_2O_3) or facilitating (in the case of Al_2O_3) the migration of Me^+ ions under the influence of an

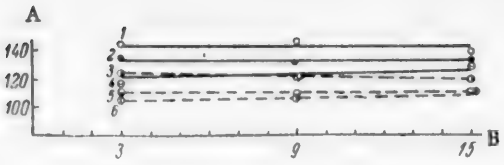

Fig. 9. Effect of replacement of SiO_2 by zinc oxide on T_{K-100} for glasses with different Na_2O and Al_2O_3 contents. A) Values of T_{K-100} (°C), B) ZnO content (%). Al_2O_3 contents (%): 1, 3-1; 2, 5-4; 4, 6-6. Continuous lines for 18% Na_2O; dash lines for 12% Na_2O.

electric field. Of the three components in question, Al_2O_3 has the greatest influence on the mobility of Me^+ ions, increasing the conductivity of glass.

Changes in the conductivity of glass under the influence of each of these components depend very little on changes in the contents of the other two components in the glass. This shows that, in the concentration ranges investigated, B_2O_3, ZnO, and Al_2O_3 modify the silicon–oxygen framework of the glass independently of each other. These results provide a sounder basis for formulation of new glass compositions. It is obvious, for example, that low-alkali borosilicate glasses for vacuum tubes, which must have high resistance, should contain only very limited amounts of Al_2O_3, 1-2% (Al_2O_3 is usually added to lower the tendency of the glass to crystallize). A high Al_2O_3 content would lower the resistance of the glass considerably. In the formulation of high-alkali glasses, considerable amounts of Al_2O_3 may be used without any further increase of conductivity. If the glass contains $Na_2O + K_2O$ a decrease of their total content is not always accompanied by a conductivity decrease. This depends on the Al_2O_3 content of the glass. For example, with 8% Al_2O_3 in the glass, the total $Na_2O + K_2O$ content can be lowered from 12 to 6% while the conductivity increases considerably: T_{K-100} decreases from 270 to 210°.

If the glass contains B_2O_3, and especially ZnO, it is only necessary to consider their influence on other properties of the glass rather than on the conductivity.

SUMMARY

1. A relationship has been demonstrated between the influence of Me_2O oxides on the conductivity of glass and the Al_2O_3 content, and also between the influence of Al_2O_3 and the Me_2O content.

2. The influence of Al_2O_3 in lowering the resistance of glass becomes much weaker with increasing Me_2O content. The variations of the specific influence of Al_2O_3 (i.e., the influence of 1% Al_2O_3) on T_{K-100} of glass with the Na_2O content and the $Na_2O + K_2O$ content ($Na_2O : K_2O = 1 : 1$) have been determined.

3. The influence of Na_2O on the resistance of glass becomes much weaker with increasing Al_2O_3 content; at a definite Al_2O_3 content, the conductivity of the glass remains unchanged despite the increased content of current-carrying Na^+ ions.

4. With increasing replacement of SiO_2 by $Na_2O + K_2O$, the changes in the conductivity of glass differ according to the Al_2O_3 content; in a certain region such replacement even results in a decrease in the conductivity.

5. Replacement of SiO_2 by B_2O_3 and ZnO has the same effect on the conductivity of aluminoborosilicate glasses as of simple soda–lime glasses (according to literature data), i.e., B_2O_3 lowers the conductivity somewhat, while ZnO has no effect.

6. The B_2O_3 and ZnO contents have no effect on the specific influence of Na_2O, and very little effect on the specific influence of Al_2O_3.

7. The data obtained for the effects of glass composition on the conductivity in the systems $SiO_2–B_2O_3–Al_2O_3–Na_2O$ and $SiO_2–B_2O_3–Al_2O_3–ZnO–Me_2O$ can be used for more rational formulation of new glass compositions for the vacuum tube industry.

LITERATURE CITED

[1] K. S. Evstrop'ev and N. A. Toropov, Chemistry of Silicon and Physical Chemistry of the Silicates (Industrial Construction Press, 1950).*

[2] J. Stevels, Progress in the Theory of the Physical Properties of Glass (Eindhoven, 1948).

*In Russian.

[3] B. I. Markin, Doctorate Dissertation (Lensoviet Technological Institute, Leningrad, 1954).

[4] G. Gelgoff and M. Tomas, Z. techn. Phys. 6, 544 (1925).

[5] O. V. Mazurin, Candidate's Dissertation (Lensoviet Technological Institute, Leningrad, 1953).

[6] N. M. Verebeichik and V. I. Odelevskii, J. Tech. Phys. 26, 8, 1696 (1956).

[7] M. M. Shults and L. G. Aio, J. Leningrad State Univ. 8, 153 (1955).

[8] H. Moore and R. C. DeSilva, J. Soc. Glass Techn., 36, 168, 5 (1952).

[9] V. I. Shelubskii, Glass and Ceramics 9, 13 (1953).

[10] G. I. Skanavi, Physics of Dielectrics (GTTI, 1949).•

[11] N. Kreidl, Glass Ind., 2-4 (1943).

Received November 5, 1956

•In Russian.

OXYGEN AND NITROGEN IN METALLIZATION PSEUDOALLOYS

L. V. Krasnichenko and M. G. Ross

One important aspect of the general problem of increasing the service life of components subject to sliding friction is the use of various steel-based pseudoalloys as antifriction materials. In view of the extensive uses of electrometallization in the national economy, studies of the properties of steel pseudoalloys, and determination of their chemical composition, are of definite scientific and practical interest.

Fig. 1. Microstructure of metallization steel pseudoalloy.

Metallization involves intensive oxidation of the melted metal which moves in a stream of air at a high partial pressure of oxygen.

Oxidation and interaction of the metal with the nitrogen of the spraying air proceed vigorously. The composition and properties of the metallization layer differ sharply from those of the metals used for the process.

The electrometallization process is essentially as follows: two wires with a potential difference between them approach each other at a definite velocity until they come in contact. When the ends of the wires touch, they melt. A stream of compressed air emerging at a high velocity from a nozzle hits the melted metal and breaks it up into minute spherical droplets coated with an oxide film. These particles hit the surface to be coated and become attached to it. Further particles hit those already deposited and coalesce with them, gradually forming a layer of the required thickness [1].

Figure 1 shows the microstructure of a group of metallization steel particles after impact. The general gray background is the basis metal with inclusions of diffusely spread oxides, and the dark veins are formed by oxides situated along the boundaries of the particles and streaks formed as the result of particle breakdown on impact. Sometimes the oxides are deposited in the form of large gray compact inclusions; these are parts of the oxide layers broken down on impact, while the black dots are pores.

Characteristic features of this structure are porosity and heterogeneity, which account for the good antifriction properties of such layers. The layer porosity varies from 10 to 15%.

The results of determinations of oxygen and nitrogen in a steel pseudoalloy obtained from a steel wire of the following composition (%) are given below: C – 0.11; S – 0.020; Mn – 0.50; P – 0.032; Si – traces.

The literature contains no descriptions of methods for determination of oxygen in metallization layers.

The oxides contained in the pseudoalloy were converted into a form convenient for analysis, by anodic dissolution of the pseudoalloy, when the nonmetallic inclusions, including oxides, separated out in powder form.

These inclusions were brownish to black in color, in the form of scales, fragments, and globules; they were opaque when viewed under the microscope by transmitted light, and had a metallic luster by reflected light.

To ensure complete separation of unstable nonmetallic inclusions, the electrolytic sulfite salt method was used; this method has a number of advantages over others, the most important being absence of oxygen at the anode and hydrogen at the cathode [2].

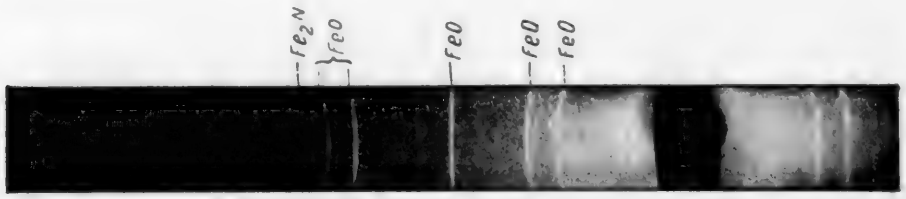

Fig. 2. x-Ray pattern of nonmetallic inclusions isolated from steel pseudoalloy.

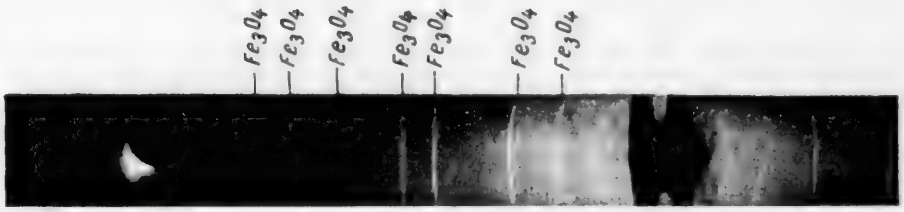

Fig. 3. x-Ray pattern of nonmetallic inclusions isolated from annealed steel pseudoalloy.

TABLE 1

Analytical Data for the Pseudoalloy

Nitrogen		Oxides		Oxide oxygen		Total oxygen content of oxides
N	calc. as Fe_2N	FeO	Fe_3O_4	FeO	Fe_3O_4	
0.140	1.26	10.66	1.02	2.38	0.28	2.66
0.126	1.13	10.52	0.58	2.35	0.15	2.50
0.132	1.18	12.28	0.38	2.74	0.10	2.84
0.120	1.10	11.72	0.40	2.61	0.11	2.72
0.132	1.18	11.86	0.34	2.64	0.09	2.73
0.130	1.17	11.41	0.54	2.54	0.15	2.70

The powder of nonmetallic inclusions consisted of oxides, carbides, and nitrides. To eliminate analytical errors caused by partial dissolution of the carbides, the latter were first decomposed, when the liberated iron passed completely into the filtrate. The cuprammonium salt method [3] was used for this purpose.

Ferrous iron was determined in the nonmetallic powder after decomposition of the carbides, and total iron was determined in an aliquot portion of the same solution; ferric iron was found by difference.

Determination of nitrogen in an aliquot portion of the solution gave the amount of bivalent iron in nitride form. Bivalent iron in oxide form is given by the difference between the previously found amount of ferrous iron and the amount of ferrous iron in nitride form. The ferrous and ferric iron contents were calculated as FeO and Fe_2O_3.

The combined oxygen in the pseudoalloy was given by the sum of the oxygen contents of all the oxides in the nonmetallic inclusions isolated from the pseudoalloy. The analytical results (as % of the alloy dissolved) are given in Table 1.

TABLE 2

Computation of the x-Ray Pattern Given by the Nonmetallic Inclusions in the Steel Pseudoalloy, ρ = 0.3 mm

Intensity	$2l_{meas}$	l_{meas}	Θ_{meas}	$\rho \cos^2 \Theta$	$2l_{corr}$	Θ_{corr}	hkl	d	Phase
M.	54.65	27.32	27°18′	0.46	55.11	27°33′	111	2.47	FeO
M.	57.66	28.83	28°48′	0.77	58.00	29°00′		2.35	Fe_2N
VS.	64.12	32.06	32°06′	0.42	64.54	32°16′	002	2.14	FeO
M.	66.12	33.06	33°06′	0.41	66.62	33°18′		2.08	Fe_2N
W.	68.62	34.31	34°18′	0.40	69.02	34°30′	011	2.02	Feα
W.	83.47	41.73	41°42′	0.34	83.81	41°54′		1.71	Fe_3O_4
S	98.56	49.28	49°15′	0.24	98.32	49°09′	022	1.514	FeO
VS.	108.41	54.20	54°12′	0.20	108.21	54°06′	002	1.41	FeO
M.	124.51	62.25	62°15′	0.12	124.39	62°11′	113	1.293	FeO
M.	126.92	63.46	63°28′	0.11	126.81	63°24′		1.278	Fe_3O_4
M.	134.69	67.34	67°21′	0.08	134.61	67°18′	222	1.238	FeO
M.	156.62	78.31	78°19′	0.024	156.58	78°17′	112	1.166	Feα

TABLE 3

Computation of the x-Ray Pattern Given by the Nonmetallic Inclusions in Annealed Steel Pseudoalloy, ρ = 0.3 mm

Intensity	$2l_{meas}$	l	Θ	$\rho \cos^2 \Theta$	$2l_{corr}$	Θ_{corr}	α/β	d	Phase
VW.	41.80	20.90	20°54′	0.52	42.32	21°18′	β	—	—
M.	44.71	22.35	22°21′	0.51	45.21	22°09′	α	2.97	Fe_3O_4
M.	49.20	24.60	24°36′	0.30	49.50	24°44′	—	2.73	Fe_2O_3
VS.	53.15	26.62	26°36′	0.47	53.62	26°48′	α	2.53	Fe_3O_4
VW.	57.80	28.90	28°54′	0.45	58.25	29°09′	—	2.03	Feα
M.	65.59	32.80	32°48′	0.41	66.00	33°00′	α	2.09	Fe_2N
M.	68.84	34.42	34°24′	0.39	69.23	34°36′	—	2.01	—
S.	90.53	45.26	45°15′	0.29	90.82	45°24′	α	1.164	Fe_3O_4
VS.	100.94	50.47	50°26′	0.24	101.18	50°34′	α	1.481	Fe_3O_4
W.	126.42	63.21	63°12′	0.12	126.64	63°18′	α	1.279	Fe_3O_4
VW.	141.36	70.78	70°40′	0.06	141.42	70°42′	α	1.210	Fe_3O_4
VW.	156.28	78.14	78°10′	0.02	156.30	78°18′	—	1.169	—

The contents of oxygen and manganous oxide are not given in the table. If it is assumed that half of the manganese in the pseudoalloy is in oxide form, the oxide oxygen content must be greater by 0.05%. The average content of combined oxygen is therefore 2.75%.

It follows from the tabulated data that the nonmetallic inclusions consist mainly of ferrous iron.

The phase composition of the nonmetallic inclusions, isolated in powder form, was investigated by the Debye x-ray method. The x-ray pattern was taken by means of the ordinary camera used for polycrystals in the URS-70 x-ray unit, by means of chromium radiation. Computation of the x-ray pattern (Table 2) given by the nonmetallic inclusions in the steel pseudoalloy (Fig. 2) showed that after removal of carbides the powder largely consists of the lower oxide FeO with a small amount of carbides. The phases corresponding to the interference lines, as found by computation, are indicated in the diagram.

The presence of FeO in the metallization layer is explained by the very rapid cooling of the particles, when the ferrous oxide formed remains in the metastable state at low temperatures before it can pass into higher oxides.

The total oxygen content of the pseudoalloy is actually somewhat higher than that found above, because of oxygen in the form of solid solution.

Because of the very rapid cooling of the particles, the metallization layer is in a nonequilibrium state, and therefore annealing is accompanied by decomposition of FeO, formation and coagulation of higher oxides, liberation of atomic oxygen from solid solutions, and a consequent increase in the oxide content of the layer.

We annealed the steel pseudoalloy in a lead bath at 550° for 6 hours. The annealed samples were investigated by the same procedure as was used for the nonannealed.

The average oxygen content of the annealed samples was 3.11%, of which 0.29% was in Fe_2O_3, 2.77% in Fe_3O_4, and 0.05% in MnO.

Thus, the oxygen content increased by 0.32% over the nonannealed samples, and the relative proportions of the oxides changed – the annealed pseudoalloy consisted mainly of Fe_3O_4 instead of the metastable FeO with a small amount of Fe_3O_4.

TABLE 4

Analytical Data for the Pseudoalloys

Material	C	Mn	S	Si	P	Combined	
						oxygen	nitrogen
Low-carbon wire	0.11	0.50	0.02	traces	0.032	—	—
Pseudoalloy	0.07	0.30	0.014	—	0.026	2.75	0.13
High-carbon wire	0.90	0.49	0.022	0.23	0.030	—	—
Pseudoalloy	0.62	0.30	0.017	0.17	0.022	1.95	0.14

These results were confirmed by phase analysis of the nonmetallic inclusions; all the intense interference lines in the x-ray pattern (Fig. 3) correspond to the Fe_3O_4 phase. The computation is given in Table 3.

In metallization, intensive oxidation is accompanied by direct chemical interaction between the metal and atmospheric nitrogen; it was therefore of interest to determine the nitrogen content of the pseudoalloy. Nitrogen may be present in the form of solid solution in ferrite, and in the form of nitride phases. The total nitrogen content was determined by the volatilization method [4]. The average nitrogen content of the steel pseudoalloy, determined in a series of experiments, was 0.17%. Nitride nitrogen was determined in an aliquot portion of a solution of the nonmetallic inclusions isolated from the pseudoalloy. The nitride nitrogen content was 0.13%.

On the assumption that nitrogen reacts with the metal during metallization the same manner as it reacts with iron powder, it follows that a nitride corresponding to the formula Fe_2N is formed.

The methods used for investigation of the pseudoalloy from low-carbon steel were applied to a pseudoalloy from high-carbon steel. The analytical results are compared in Table 4.

Table 4 shows that the oxide oxygen content is much lower in the high-carbon than in the low-carbon pseudoalloy. The explanation is that the carbon, while being burned out during the metallization process, protects the iron from oxidation to some extent. The nitrogen contents of the two alloys are almost equal.

The methods used for oxygen and nitrogen determination were somewhat simplified; this may be regarded as permissible for these high contents of the gases in the metallization pseudoalloys.

SUMMARY

1. Metallization is accompanied by intensive oxidation processes, as the result of which the oxygen content of the pseudoalloy becomes hundreds of times as high as that of the original metal.

2. The pseudoalloy is in a metastable state, and contains oxygen mainly in the form of ferrous oxide; this was confirmed by chemical and x-ray analysis.

3. The metal becomes saturated with nitrogen, present mainly as nitrides, during metallization.

4. Pseudoalloys made from high-carbon wire have a much lower oxide content than those made from low-carbon wire.

LITERATURE CITED

[1] L. V. Krasnichenko and M. N. Shchirzhetskii, J. Tech. Phys. 25, 5, 791 (1955).

[2] Methods for Isolation and Analysis of Nonmetallic Inclusions in Steel (from Conference Proceedings) (Izd. AN SSSR, 1954).*

[3] Iu. A. Kliachko, A. T. Atlasov and M. I. Shapiro, Analysis of Gases, Nonmetallic Inclusions, and Carbides in Steel (1953).*

[4] A. N. Morozov, Hydrogen and Nitrogen in Steel (1953).*

Received September 15, 1956

*In Russian.

"SHAVINGLESS" DISSOLUTION OF ALLOYS

A. G. Loshkarev

The V. V. Vakhrushev Mining Institute, Sverdlovsk

The preceding papers contained the results of kinetic studies of the shavingless dissolution (i.e., without reduction to chips or shavings) of copper, iron, and lead in nitric acid [1], of aluminum in alkali [2], and of magnesium, zinc, tin, and iron in hydrochloric acid [3]. In the shavingless method of analysis of metals and alloys [4], and in corrosion studies by the shavingless method, special interest lies in the rate of shavingless dissolution of alloys and, in particular, the question of uniform extraction of the alloy components into the shavingless sample.

The present paper contains our experimental data on the shavingless dissolution of certain alloys, and a definition of the general conditions for uniform transfer of the alloy components into the shavingless sample. The experimental procedure used was described in the first communication [1]. The methods of shavingless ultimate analysis were used for chemical analysis of the shavingless alloy samples.

EXPERIMENTAL

Carbon steels. Standard specimens of 12^d, 83^e, and 18^e steels, in the form of plates (d = 50 mm, h = 8 mm), from the Urals Institute of Ferrous Metals were used for the experiments. The specimens differed in their carbon contents and microstructure. Specimen 12^d had a laminar perlite structure, and standard specimens 83^e and 18^e, laminar perlite, globular perlite, and martensite structure. The required steel microstructure was produced by appropriate heat treatment. The results of kinetic experiments on the shavingless dissolution of carbon steels in 0.127 ml of 6.5 N HNO_3 at 16° are presented in Tables 1 and 2.

Comparison of the experimental data in Table 1, Table 2, and data on the kinetics of iron dissolution [1] shows that wide variations of the carbon content have no effect on the iron contents of shavingless samples. The microstructure of the carbon steel also has no influence on the dissolution rate, as steels with perlite and martensite structures are dissolved at an equal rate, at least within the error limits of colorimetric determination of iron.

Since the solution rates of carbon steels and iron in nitric acid are equal, the nature of the solution kinetics of carbon steels in nitric acid must be the same as that of iron; i.e., during the first stage the dissolution rate of the alloy is determined by the rate of steady diffusion of nitric acid to the alloy surface, and during the second stage it is determined by the rate of nonsteady diffusion [1].

Tool steel. Table 3 contains the results obtained in analysis of shavingless samples of R9 tool steel, for different times of dissolution at 16°. The chemical composition of R9 steel is (in %): C 0.92, Cr 3.60, W 8.90, V 2.00. Four drops (about 0.16 ml) of 6.50 N HNO_3 was used as solvent.

The oxidation potential of nitric acid (for example, $\varphi^0_{HNO_3/NO} = 0.96$ v) is considerably higher than the potentials of the alloy components – iron ($\varphi^0_{Fe^{2+}/Fe} = -0.44$ v), nickel ($\varphi^0_{Ni^{2+}/Ni} = -0.23$ v), chromium ($\varphi^0_{Cr^{3+}/Cr} = -0.71$ v), manganese ($\varphi^0_{Mn^{2+}/Mn} = -1.05$ v), and tungsten ($\varphi^0_{W^{3+}/W} = -0.2$ v). Although the potential of R9 steel is unknown, it may be assumed that it differs little from the potential of iron, as the

contents of alloying components in this steel lie below Tammann's first stability boundary [5]. Therefore R9 steel and, as other experiments showed, low-alloy and medium-alloy steels, dissolves similarly to iron in nitric acid. The alloy components enter the sample in the proportions in which they are present in the alloy. The carbides present in the steel are partialy oxidized and dissolved by nitric acid, and partially (especially alloy carbides) enter the shavingless sample in the form of fine particles.

TABLE 1

Shavingless Dissolution of Carbon Steels of Different Carbon Contents in 0.127 ml of 6.5 N HNO_3 at 16°

Dissolution time (min)	Iron content in sample from standard (mg		
	12[d] (0.12% C)	83[e] (0.5% C)	18[e] (0.02% C)
1	12.84	13.12	12.17
2	14.91	14.85	14.07
3	15.97	16.75	16.52
5	16.64	17.07	17.54
7	17.18	17.31	17.94
10	17.62	17.81	18.39
15	18.10	18.37	18.42

TABLE 2

Shavingless Dissolution of Carbon Steels of Different Structures in 0.127 ml of 6.5 N HNO_3 at 16°

Dissolution time (min)	Iron contents in samples from standards (mg)			
	18[e]		83[e]	
	steel structure			
	perlite	martensite	perlite	martensite
3	16.75	16.64	16.48	16.25
5	17.03	17.20	17.19	16.91
7	17.58	17.86	17.58	17.18
10	18.09	18.42	17.81	17.86
15	18.50	18.84	18.70	18.70

Silumins. Experiments were performed on a specimen of modified Silumin AL9 (Si 6.10%, Mn 0.37%, Fe 0.55%). The microstructure of this Silumin corresponds to a hypoeutectic alloy; its structure consists of primary segregations of aluminum and a fine-grained eutectic of aluminum and silicon. The alloy was dissolved in 0.086 ml (2 drops) of 20% caustic soda solution at 16°. The results of the experiments are presented in Table 4.

The oxidation potential of hydrogen ions (at pH = 14 $\varphi^0_{H^+/\frac{1}{2}H_2} = -0.828$ v) is considerably more positive than the potentials of aluminum ($\varphi^0_{AlO_3^{3-}/Al} = -2.35$ v) and silicon ($\varphi^0_{SiO_3^{2-}/Si} = -1.93$ v). Therefore here, as in the previous instances, the main aluminum phase may dissolve at a rate determined by diffusion of the solvent [1-3]. The data of Table 4 on the contents of aluminum (q) in shavingless samples are plotted in the diagram against the square root of the dissolution time ($\sqrt{t}$). The relationship between q and $\sqrt{t}$ is satisfactorily linear, in conformity with the equation for diffusion kinetics.

Thus, the shavingless dissolution rate of Silumin in caustic soda solution, like that of aluminum [2], is determined by the rate of diffusion of the solvent to the alloy surface.

The crystals of the silicon phase partly dissolve, and partly enter the sample unchanged. It should be noted that when high-silicon Silumins are dissolved the amount of solid phase in the sample is always considerable. Analytical data for shavingless Silumin samples show that silicon, and the admixtures present in small amounts (Mn, Fe, etc.), enter the sample in the proportions in which they are present in the alloy.

The foregoing experimental data show that the rate of shavingless dissolution of steels in nitric acid, and of Silumin in caustic soda solution, is determined by the rate of diffusion of the solvent to the metal surface. The alloy components enter the shavingless sample in the weight proportions in which they are present in the alloy.

General Conditions for Uniform Layer Breakdown of Alloys

The shavingless method of analysis of technical metals and alloys is based on shavingless sampling. However, if a shavingless sample is to be suitable for chemical analysis, the components of the material must enter the sample without change of their relative proportions by weight.

TABLE 3

Chemical Composition of Samples of R9 Steel for Different Times of Shavingless Dissolution

Dissolution time (min)	Components	Contents (%)	Absolute error (%)
1	Cr	3.68	+ 0.08
	W	8.77	−0.13
	V	1.91	−0.09
5	Cr	3.51	−0.09
	W	8.85	−0.05
	V	1.93	−0.07
10	Cr	3.67	+ 0.07
	W	8.87	−0.03
	V	2.02	+ 0.02
15	Cr	3.69	+ 0.09
	W	9.02	+ 0.02
	V	1.89	−0.11

TABLE 4

Aluminum and Silicon Contents of Shavingless Samples of Silumin for Different Dissolution Times Solvent − 0.086 ml of 20% NaOH

Dissolution time (min)	Components	Contents		Absolute error of aluminum determination (%)
		(mg)	(%)	
1	Al	2.40	−	−
	Si	0.153	6.06	−0.04
5	Al	3.31	−	−
	Si	0.224	6.35	+ 0.25
10	Al	6.05	−	−
	Si	0.402	6.23	+ 0.13
15	Al	7.44	−	−
	Si	0.464	5.88	−0.22

All alloys can be subdivided into two principal groups, differing in microstructure: 1) heterogeneous (mechanical) mixtures, consisting of two or more phases; these include carbon steels, cast irons, Silumins, Duralumin, etc; 2) homogeneous (one-phase) systems, such as solid solutions in one of the alloy components, intermetallic compounds, solid solutions in chemical compounds, electronic compounds, and interstitial phases; examples of such alloys are austenitic steels, Monel metal, brasses, and many others. Thus, any heterogeneous alloy consists of a containing phase, which may be the principal alloy component, a solid solution, an intermetallic compound, etc., and of included phases, consisting of solid complexes of alloying elements and impurities. For brevity, alloying components and impurities will be referred to as secondary components.

For sampling, the material is subjected to shavingless dissolution in a small volume (0.05-1 ml) of solvent − acid, mixture of acids, or alkali. Attention must be specially drawn to the important fact that the purpose of shavingless dissolution is to obtain a sample of the alloy, and not to dissolve it completely. In order that the sample should correctly represent the alloy composition, it is sufficient to break down a part of the alloy and to transfer it by some means into a chemical vessel. The alloy components in such a sample may be present either in the dissolved state, or as individual particles. The sample so obtained is subjected to additional treatment, primarily to dissolve its solid portion. The passage of metal into solution in the form of ions under the action of the solvent is the consequence of an oxidation−reduction reaction, in which the metal (M) acts as the reducing agent, and the solvent as the oxidizing agent O_x

$$M + O_x = M^+ + Red.$$

In the modern view, dissolution of a metal consists of two simultaneous electrochemical processes at the metal−solution boundary: anodic ionization of the metal $M - e \rightarrow M^+$, and cathodic reduction of the solvent $O_x + e \rightarrow Red$.

In the dissolution of technical metals and alloys, a distinction is made between the homogeneous electrochemical and the heterogeneous galvanic mechanisms of the process. In homogeneous electrochemical dissolution of an alloy, the anodic and cathodic processes take place simultaneously, on the same region of the metal surface, and the alloy surface remains equipotential during the dissolution. In the heterogeneous galvanic process, the alloy surface is differentiated into cathodic and anodic regions. The cathodes are the solid complexes ("inclusions") of the included phases. The anode is the surface of the main (containing) phase of the alloy. In such cases the surface of the alloy is not equipotential during dissolution.

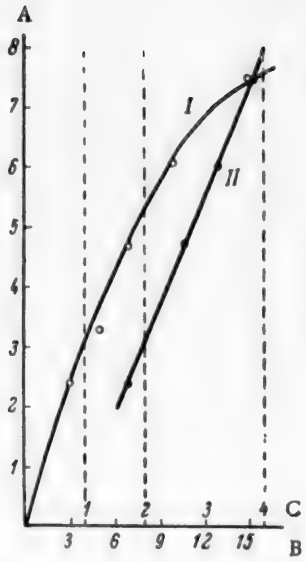

Kinetics of shavingless dissolution of Silumin A19 in 0.086 ml of 20% caustic soda solution. A) Aluminum content q (mg), B) time t (minutes), C) $\sqrt{t}$. I) q as a function of t, II) q as a function of $\sqrt{t}$.

The principal conditions for the uniform breakdown of an alloy in shavingless sampling shall now be considered in the light of the foregoing general considerations.

Uniform layer dissolution of the containing phase of the alloy. Uniform transfer of the alloy components to the shavingless sample is effected only if the containing phase is dissolved in a uniform layer. The latter occurs if the alloy dissolves by the homogeneous electrochemical mechanism, i.e., if the alloy surface remains equipotential during the dissolution. This condition is satisfied by all homogeneous (one-phase) alloys, and by heterogeneous (multiphase) alloys the inclusions in which do not disturb the equipotential nature of the alloy surface.

The surface of a heterogeneous alloy is equipotential if the potential difference ($\Delta\varphi$) between the inclusions and the containing phase is either zero or small.

By the Frumkin and Levich equation [6]

$$\Delta\varphi = \frac{2r_0 i_c}{\pi\kappa},$$

where r_0 is the radius of a disk-shaped inclusion; i_c is the cathodic current density; κ is the conductivity of the solution; $\pi = 3.14$.

At a given rate (i_c) of the process, the surface of the heterogeneous alloy is closer to equipotentiality at smaller values of r_0 and higher values of κ.

In shavingless sampling it is not difficult to select conditions in which the alloy dissolves by the homogeneous electrochemical mechanism i.e., layer by layer. This is confirmed by the following approximate calculation of $\Delta\varphi$ for the dissolution of an iron alloy in nitric acid: the current density i_c of the dissolution of iron in 4.84 N HNO_3 during the period of steady diffusion reaches 0.5 amp/cm^2 [1]; the conductivity κ of 4.84 N HNO_3 at 18° is 0.67 ohm$^{-1}\cdot$cm^{-1}; the radius r_0 of the solid complex ("cathodic inclusion") is taken as 10^{-3} cm; under these conditions the maximum potential difference $\Delta\varphi$ is 0.00047 v.

This calculation shows that although the surface is not strictly equipotential, deviations from equipotentiality are very small even if the inclusions are of considerable size.

The rate of homogeneous electrochemical dissolution of an alloy is determined either by the rate of the cathodic–anodic process, or by the rate of diffusion of the solvent to the alloy surface. Shavingless sampling is carried out under conditions in which the dissolution rate of the alloy is controlled by diffusion. The explanation is that under such conditions the sample can be taken rapidly and most of the alloy components are transferred into the dissolved portion of the sample. Shavingless homogeneous electrochemical dissolution becomes diffusion-controlled under the condition that the oxidation potential of the solvent greatly exceeds the potential of the containing phase of the alloy. The containing phase then dissolves layer by layer.

The behavior of inclusions during dissolution of the alloy depends on the magnitude of their reduction potential.

Suppose that the potential of the solvent greatly exceeds the potential of the inclusions. The inclusions then dissolve at a rate limited by diffusion of the solvent. In this case the inclusions dissolve at the same rate as the containing phase. The whole alloy dissolves uniformly (layer by layer).

Suppose that the potential of the solvent is less than the potential of the inclusions. The inclusions do not dissolve and enter the sample in the form of solid particles.

Suppose that the potential of the solvent is greater than the potential of the inclusions, but the dissolution rate of the inclusions is lower than that of the containing phase (the dissolution rate of the inclusions is

limited by the cathodic–anodic process). In this case part of the inclusions enters the sample in the form of solid particles, and part as ions.

If the inclusions are electrochemically passive, but can dissolve as the result of chemical reaction with the solvent, the dissolution rates of the containing phase and the inclusions should be in the same relationship as in the cases considered above.

Heterogeneous galvanic dissolution consists of depolarization of the solvent on the inclusions, which act as cathodic regions, and ionization of the containing phase, mainly close to the inclusions. In this case the alloy is not dissolved uniformly by layers, and the chemical composition of the shavingless sample differs from that of the alloy. Under favorable conditions, heterogeneous galvanic dissolution of an alloy can also yield a correct shavingless sample. Factors favoring uniform dissolution of the alloy include increase of the number of inclusions at the alloy surface, and diffusional control of the dissolution rate. However, if the dissolution process is heterogeneous galvanic, experimental determinations are necessary to establish whether a correct sample is obtained.

Error of shavingless sampling. The error (P) of shavingless sampling is taken to mean the difference between the percentage content of a particular secondary component in the shavingless sample (G') and its true content in the alloy (G). The sampling error can be expressed as an absolute (P_{abs}) or a relative (P_{rel}) percentage:

$$P_{abs} = G' - G, \qquad P_{rel} = \frac{G' - G}{G} \cdot 100. \tag{1}$$

The magnitude of the error is a measure of the uniform transfer of a given secondary component into the sample in shavingless dissolution; in other words, it indicates the degree to which the ratio of the given component to the others is maintained when they pass from the alloy into the sample.

It can be shown that the sampling error due to inadequate or excessive dissolution of the solid complexes ("inclusions") relative to the containing phase of the alloy is given by the equations:

$$P_{abs} = \frac{l}{L} G \frac{G_{ph}}{100}, \quad P_{rel} = \frac{l}{L} G_{ph}, \tag{2}$$

where G is the content of a given component in the alloy (%); G_{ph} is the content of a given secondary component in the included phase (as % of the total content of this secondary component in the alloy); l is the maximum size of an inclusion; L is the extent of breakdown (dissolution) of the alloy under the action of the solvent.

Equations (2) represent the direct dependence of shavingless sampling error on the alloy structure. They show that the error diminishes with decreasing size of the inclusions and with increasing breakdown of the alloy.

Displacement reactions in shavingless sampling. In shavingless dissolution of alloys, displacement reactions may occur in certain conditions between the ions of a more electropositive component present in solution in the shavingless sample, and the atoms of a less positive component of the alloy:

$$M_1^{II} + M_2^{2+} \rightarrow M_1^{2+} + M_2^{II},$$

$$\varphi_{M_1^{2+}/M_1} < \varphi_{M_2^{2+}/M_2^{II}}.$$

The component ratio in the shavingless sample then shifts in favor of the more electronegative component. If measures are not taken to prevent the displacement reaction, an unreliable sample of the alloy is obtained. The alloy surface must remain equipotential in the course of shavingless sampling. The equilibrium potential of the dissolving alloy is at a compromise value between the potential of the containing phase and the oxidation potential of the solvent. The general rule for prevention of the displacement reaction is that in the course of shavingless dissolution the equilibrium potential (φ_e) of the alloy–solvent system must remain more positive than the potential of the displaced component (φ_{dc})

$$\varphi_c > \varphi_{dc} \tag{3}$$

Shavingless dissolution may proceed with different relationships between the equilibrium potential and the potential of the most electropositive component of the alloy: 1) the containing (main) phase of the alloy may be the most positive component of the alloy; in this case Condition (3) holds and displacement does not occur; 2) the containing phase of the alloy may be the least positive component of the alloy, while the oxidation potential of the solvent is lower than the potential of the other secondary components of the alloy; the latter then enter the solution in the form of solid particles during the dissolution, and displacement does not occur; 3) under the conditions indicated in 2) the potential of the solvent may be higher than the potential of one of the secondary components, and the solution of the sample contains ions of the secondary component. If the equilibrium potential is lower than the potential of the secondary component, displacement occurs. To prevent displacement, it is necessary to use a solvent of high oxidation potential (nitric acid, aqua regia, etc.) so that Condition (3) holds.

Prevention of displacement is also aided by the fact that many metals lose their ability to undergo this reaction in oxidizing media such as nitric acid, aqua regia, hydrogen peroxide, and other oxidizing agents containing oxygen. Such metals include readily-passivated steel components, important from the practical aspect: iron, nickel, chromium, vanadium, tungsten, and molybdenum. This fact is clearly illustrated by Tananaev's [7] interesting observations.

Consideration of shavingless dissolution leads to the conclusion that three conditions must be satisfied in the preparation of a reliable shavingless sample: the surface of the dissolving alloy must be equipotential, the sampling error must be less than the permissible value (Equation 2), and the equilibrium potential of the dissolving alloy must be more positive than the potential of any displaceable component. Our rules for shavingless sampling are confirmed by the author's experimental data and by the results of shavingless analysis of various alloys, reported by Tananaev [8], Kalinichenko [9], Onosova [10], Loshkareva [11], Tananaeva [12], and others.

SUMMARY

The rate of shavingless dissolution of carbon steels and low and medium alloy steels in nitric acid, and of Silumins in caustic soda solution, is determined by the rate of diffusion of the solvent to the metal surface. The components of these alloys enter the shavingless samples in the weight proportions in which they are present in the alloys.

LITERATURE CITED

[1] A. G. Loshkarev, J. Appl. Chem. 30, 10, 1558 (1957).*

[2] A. G. Loshkarev, J. Appl. Chem. 30, 12, 1862 (1957).*

[3] A. G. Loshkarev, J. Appl. Chem. 31, 10, 1493 (1958).*

[4] N. A. Tananaev, Factory Labs. 13, 4, 389 (1947).

[5] G. Tammann, Die Chemischen und Galvanischen Eigenschaften von Mischkristallen (Leipzig, 1919).

[6] A. N. Frumkin and V. G. Levich, J. Phys. Chem. 15, 748 (1941).

[7] N. A. Tananaev, Progr. Chem. 5, 621 (1949).

[8] N. A. Tananaev, The Shavingless Method (Sverdlovsk, Metallurgy Press, 1948).**

[9] I. I. Kalinichenko, Candidate's Dissertation (Urals Polytech. Inst. Sverdlovsk, 1950).

[10] S. P. Onosova, Candidate's Dissertation (Urals Polytech. Inst. Sverdlovsk, 1951).

[11] G. V. Loshkareva, Candidate's Dissertation (Urals Polytech. Inst. Sverdlovsk, 1954).

[12] A. N. Tananaeva, Factory Labs. 5, 522 (1957).

Received October 14, 1956

*Original Russian pagination. See C.B. Translation.

**In Russian.

THE OCCURRENCE OF HYDROGEN EMBRITTLEMENT OF STEEL IN AQUEOUS SOLUTIONS OF HYDROGEN SULFIDE

S. A. Balezin and I. V. Nikol'skii

It is known that when ferrous metals are pickled in solutions of inorganic and certain organic acids some of the hydrogen is absorbed in the atomic state by the metal, causing pickling blisters and hydrogen or pickling embrittlement [1].

In view of the fact that chemical removal (mainly by means of acids) of scale and rust from metal articles is of great practical importance, there have been many investigations of hydrogen absorption. It has been found that the presence of very small amounts of certain substances in the pickling liquors stimulates hydrogen absorption considerably. For example, Polukarov and Appolov [2] found that As_2O_3 and SeO_2 stimulate diffusion. Morris [3] regards As_2O_3 and SO_2 as diffusion stimulators for citric acid solutions. Polukarov [4-6] used these substances, and also $TeCl_2$ and H_2S, as additives to sulfuric acid in his investigations. Bablik [7] found that hydrogen sulfide had a stimulating effect in the pickling of steel in sulfuric and hydrochloric acid solutions. He added sodium sulfide to acid solutions and found that the amount of hydrogen diffusing through a steel disk is proportional to the square root of the sodium sulfide concentration in the solution, i.e., $H_{diff} = K\sqrt{C}$, where K is a constant for the given experimental conditions, C is the sodium sulfide concentration, and H_{diff} is the amount of hydrogen diffused. Addition of carbon disulfide to the acid solution decreased the amount of hydrogen liberated in the gaseous form, and increased considerably the amount of diffusing hydrogen. Colloidal sulfur and medicinal charcoal had similar effects.

In addition to the above-named authors, Iofa and Liakhovetskaia [8], Krasso [9], and Prange [10] reported that arsenious compounds have an accelerating effect. Korber and Ploum [11] and Uhlig [12] demonstrated the stimulating effect of phosphorus. Alekseev and Polukarov [13] performed tensile tests on wires undergoing cathodic saturation, and found that As, Sb, and Sn salts have a stimulating effect when added to caustic soda solution.

Bardenheuer and Ploum [14] studied the effects of hydride-forming elements of the Vth and VIth groups of Mendeleev's periodic system on hydrogen diffusion, and found that selenium has the strongest stimulating effect of all the elements studied. The stimulating effects decrease in the following sequence: Se, As, Te, Sb, S, P. Zapffe [15] also discussed this series of elements, regarded as stimulators of hydrogen diffusion into steel.

Boer and Fast [16] showed that addition of sodium sulfide to a buffer mixture of pH = 7 causes hydrogen absorption, which did not occur in absence of this additive. Dubovoi and Romanov [17] used sodium sulfite to accelerate the electrolytic saturation of steel with hydrogen. Sabinina and Polonskaia [18] found that addition of small amounts of the oxides of lead, tin, or cadmium to sulfuric acid solution increased the amount of hydrogen diffused. Balezin and Solovei [19] named pyridine and α-picoline as stimulators of hydrogen absorption. The stimulating effect of thiourea in nitric acid was studied in one of our earlier investigations [20]. Bonner and Burnham [21] and Marsh [22] demonstrated the powerful stimulating action of hydrogen sulfide in solutions of low hydrogen-ion concentrations.

To summarize the above data, the following substances may be regarded as stimulators of hydrogen diffusion into steel: SeO_2; TeO_2, SO_2; $As^{\cdots}$, $As^{\cdots\cdots}$; Na_2S, H_2S; CS_2; Na_2SO_3; $CS(NH_2)_2$; Sn, Pb, Cd (sulfates); pyridine, α-picoline; medicinal charcoal; P.

Some authors (Polukarov [13], Korber and Ploum [11], and others) consider that diffusion of hydrogen into steel is in general possible only in presence of stimulators in corrosive media. They were unable to detect hydrogen diffusion in thoroughly purified acids. Thoroughly purified acids are not used in industrial practice; generally the acids and the metals being pickled contain various impurities which act as diffusion stimulators. Among these impurities are sulfur and some of its compounds.

In investigations of hydrogen absorption by carbon steels during pickling in acid solutions, sulfides occupy a prominent position as absorption stimulators. Easily soluble sulfides or sulfur in the colloidal state stimulate the diffusion of hydrogen into steel when they are added to inorganic acid solutions. The purpose of the present investigation was therefore to investigate hydrogen embrittlement (hydrogen absorption is always associated with hydrogen embrittlement, although the latter does not occur in every case) in sodium sulfide solutions.

Three batches of wire were used for the investigation.

1) For tests in sodium sulfide solutions, wire 6 mm in diameter, initial number of twists (in torsion test) 17, of the following chemical composition (%): C 0.13, Mn 0.45, Si traces, P 0.011, S 0.03.

2) For tests in H_2S solutions, wire 6 mm in diameter, initial number of twists 9, of the following chemical composition (%): C 0.18, Mn 0.40, Si 0.14, P 0.020, S 0.025.

3) Tests with sulfide films were carried out on wire specimens 5.7 mm in diameter, initial number of twists 7.7, of the following chemical composition (%): C 0.13, Mn 0.47, Si 0.16, P 0.022, S 0.023.

The saturation of the wires with hydrogen was carried out with the wires in a vertical position in the solution at 18°. The brittleness was determined by comparison of the number of twists to failure in a torsion test, before and after pickling. The tests were performed by means of the AM-1 machine with specimens 100 mm long over the test portion.

RESULTS

The first experiments were performed with aqueous sodium sulfide solutions. From 2 to 10 g sodium sulfide per liter was added to boiled distilled water, and the test specimens were then immersed in it. The wire became coated with an even black layer of iron sulfide. Variations of the pickling time and of the sodium sulfide concentration had no effect on the brittleness of the wire. The small decrease in the number of twists can always be accounted for by destruction of the surface layer, rather than hydrogen saturation (Table 1).*

TABLE 1

Effect of Concentration of Aqueous Sodium Sulfide Solution and Exposure Time of the Specimens on Wire Brittleness

Exposure time in solution (hours)	Number of twists	
	2 g Na_2S per liter	10 g Na_2S per liter
Control	17.0	17.0
24	15.5	15.3
48	16.0	16.0
96	16.5	16.0
120	15.2	16.2

These results show that no hydrogen absorption occurs in sodium sulfide solutions.

Different results were obtained with aqueous hydrogen sulfide solution.

Boiled distilled water was saturated for 2 hours at 18° with hydrogen sulfide, and this solution was used as the medium for wire pickling. The brittleness increases considerably with the pickling time, especially during the first hour. On more prolonged pickling the brittleness diminished and the metal gradually regained its plasticity (Table 2).

The decrease of brittleness with increasing pickling time may be attributed to decreasing concentration of hydrogen sulfide in the solution as the result of its oxidation to elemental sulfur, and formation of insoluble iron sulfide (the specimens became coated with black FeS, and the amount of sulfide increased with the pickling time).

The hydrogen sulfide concentration of the solution was varied, by variations of the time during which the gas was passed through water; it was found that brittleness increased with the H_2S concentration.

*Average results of 5-7 determinations are given in the tables.

The fact that hydrogen embrittlement occurs at low hydrogen sulfide concentrations (0.031 N) indicates that even small amounts of hydrogen ions in solution, in presence of sulfur (S or S") may produce changes in the mechanical properties of steel as the result of hydrogen absorption (Table 3). In view of the possible changes which might be produced in the mechanical properties of the specimens by the action of sulfide ions on their surface, some of the specimens were put into a thermostat immediately after the pickling and held at 180-200° for two hours in order to remove most of the absorbed hydrogen. In such cases changes in the number of twists to destruction must be attributed to surface changes only. Such changes were slight in our experiments.

TABLE 2

Effect of Pickling Time in Saturated Hydrogen Sulfide Solution on Wire Brittleness

Pickling time (minutes)	Number of twists	Pickling time (hours)	Number of twists
Control	9.0	–	9.0
15	3.6	24	1.5
30	2.3	48	1.7
45	2.5	72	2.5
60	2.0	96	2.8
		120	3.4
		144	4.5

TABLE 3

Results of Torsion Tests on Wire Pickled in Hydrogen Sulfide Solutions of Different Concentrations. Pickling Time 15 Minutes

Hydrogen sulfide concentration (normality)	Number of twists to destruction
Control	9.0
0.031	5.7
0.060	5.3
0.085	4.5
0.145	3.5

In the next experiment, specimens coated with sulfide film were tested. (The wire was placed in a chamber filled with moist hydrogen sulfide before the pickling). These specimens were immersed in distilled water for 30 and 60 minutes and then subjected to the torsion test. The results revealed some degree of brittleness, clearly caused by absorbed hydrogen, as the specimens regained their initial properties when heated at 200° after the immersion.

The brittleness found in this case can be attributed to the presence of a certain amount of H_2S adsorbed from the gas phase by the iron sulfide film, and dissolved in the water when the specimens were immersed in it.

The explanation for the stimulating action of sulfur (S or S") in presence of even small amounts of hydrogen ions is that sulfur (S or S") lowers hydrogen overvoltage [8, 23, 24], i.e., facilitates the discharge process $H^+ + e \rightarrow H$, and at the same time retards recombination of hydrogen atoms into molecules, $H + H \rightarrow H_2$ [12]; thereby a definite concentration of hydrogen atoms, sufficient for diffusion, is established at the metal surface.

SUMMARY

The occurence of hydrogen embrittlement in steel exposed to aqueous hydrogen sulfide solutions was studied; it was found that hydrogen embrittlement may originate under the action of water, if the metal is coated with a sulfide film. An explanation of this effect is given.

LITERATURE CITED

[1] S. A. Balezin, Sci. Mem. Lenin Pedagogic Institute, Moscow City 99 (1957).

[2] M. P. Polukarov and N. A. Appolov, J. Appl. Chem. 10, 2 (1937).

[3] T. Morris, J. Soc. Chem. Ind. 54, 3 (1935).

[4] M. P. Polukarov, Sci. Mem. Perm State Univ. 1, 1 (1935).

[5] M. P. Polukarov, Sci. Mem. Perm State Univ. 2, 3 (1936).

[6] M. P. Polukarov, J. Appl. Chem. 21, 6 (1948).

[7] H. Bablik, Korrosion u. Metallschutz, 8 (1935).

[8] Z. A. Iofa and E. I. Liakhovetskaia, Proc. Acad. Sci. USSR 86, 3 (1952).

[9] T. Krasso, Z. Elektroch. 40, 12 (1934).

[10] F. A. Prange, Corrosion, 8, 10 (1952).

[11] F. Korber and H. Ploum, K. W. Mitt Inst. Eisenforschung, 14, 16 (1932).

[12] H. Uhlig, Metals Technology, 11, 4 (1944).

[13] D. V. Alekseev and M. P. Polukarov, J. Russ. Phys.-Chem. Soc., Chem. Section 3-4, 58 (1926).

[14] P. Bardenheuer and H. Ploum, K. W. Mitt Inst. Eisenforschung, 16, 11 (1934).

[15] C. Zapffe, Materials and Methods, 34, 4 (1950).

[16] Y. Boer and Y. Fast, Rec. Trav. Chim. Pays-Bas, 54, 9 X 1939.

[17] V. Ia. Dubovoi and V. A. Romanov, Steel 8 (1947).

[18] L. E. Sabinina and L. A. Polonskaia, J. Phys. Chem. 6, 1 (1935).

[19] S. A. Balezin and D. Ia. Solovei, Sci. Mem. Lenin Pedagogic Institute, Moscow City 83, 4 (1950).

[20] S. A. Balezin, I. V. Nikol'skii and G. S. Parfenov, Sci. Mem. Lenin Pedagogic Institute, Moscow City 76 (1953).

[21] W. A. Bonner and H. D. Burnham, Corrosion, 9, 5 (1953).

[22] G. A. Marsh, Corrosion, 10, 3 (1954).

[23] N. D. Tomashov and A. Z. Fedotova, Trans. Inst. Phys. Chem. Acad. Sci. USSR 5 (1955).

[24] V. A. Kuznetsov and Z. A. Iofa, J. Phys. Chem. 21, 2 (1947).

Received January 17, 1957

HYDROGEN EMBRITTLEMENT OF STEEL IN CATHODIC TREATMENT

M. A. Figel'man and A. V. Shreider

Despite the existence of a number of publications [1-8] concerning research into hydrogen embrittlement of steel, there are many controversial and sometimes contradictory opinions on the nature of the effect and means for its prevention. It is important to study the conditions under which embrittlement originates in steels which are most prone to hydrogen absorption when treated in electrolytes commonly used in industrial practice.

EXPERIMENTAL METHODS

A thin strip of U9 steel was chosen as the main object of study. This steel is widely used in machine construction for the production of different types of springs, which are particularly vulnerable if affected by hydrogen embrittlement.

The experiments were performed with annealed, cold-worked and heat-treated (quenched and tempered) metal. The principal test method used was the bilateral flexing test, which is one of the most sensitive methods for evaluation of hydrogen embrittlement of steel. A specially designed instrument was used, with which the tests could be performed relatively simply and rapidly [9]. Not more than ~45 sec. elapses between removal of the specimens from the solution and the start of the tests; this is very important in view of the high rate at which hydrogen is liberated from steel, and of the consequent possible error in evaluation of the experimental results.

The measure used for hydrogen embrittlement was the quantity B_f, which we term the relative brittleness or degree of embrittlement, defined by the expression

$$B_f(\%) = \frac{B_0 - B_h}{B_0} \cdot 100,$$

where B_0 is the bend angle at which failure occurs in the specimen before cathodic treatment, and B_h is the corresponding angle after cathodic treatment.

The instrument used differs from most devices used previously for such purposes by its high sensitivity – the angle at which failure occurs can be measured to an accuracy of 1-2°. The instrument is equipped with an automatic device which reverses the direction in which the lever oscillates. The constant tension and uniform displacement rate of the specimen ensure good reproducibility of the test results (the scatter does not exceed 8-10%).

Fatigue tests (to 10^7 cycles) were performed by means of a machine designed by I. I. Sidorin; this can be used for simultaneous tests on 12 flat specimens at 1400 oscillations per minute.

The hydrogen content of steel was determined by the vacuum heating method (600-800°, $4-5 \cdot 10^{-5}$ mm Hg), in apparatus designed by Morozov [10]. The hydrogen contents of the specimens were determined both immediately after removal from the electrolyte, and after 1 hour, 16 hours, and 7 days of exposure to air.

EXPERIMENTAL RESULTS

Cathodic polarization without application of deposits. The steel was subjected to hydrogen saturation by cathodic polarization in 0.1, 1, and 10% solutions of sulfuric acid and caustic soda containing different additives, at 20, 50, and 80°, cathodic current densities 0.2, 2, and 20 amps/dm^2, and exposure times (seconds) 6, 60, and 600. In cathodic polarization of quenched U9 steel in sulfuric acid solutions the brittleness becomes very considerable during the first few seconds of electrolysis, and its magnitude is greater at higher temperatures. With more prolonged polarization, the further course of embrittlement depends (under comparable conditions) on the electrolyte temperature. If the process takes place at room temperature (20°), the embrittlement increases continuously with the exposure time. At higher temperatures not only does the rate of embrittlement diminish with time of polarization, but there is even some restoration of plasticity. In cathodic polarization in 10% sulfuric acid, at current density 20 amps/dm^2, the embrittlement increases continuously with time, irrespectively of the electrolyte temperature (Fig. 1). With increase of current density the brittleness diminishes in 0.1% and increases in 10% sulfuric acid solution. Under equal conditions, the brittleness increases during very short exposures (up to 6 seconds) and decreases during longer exposures, with increase of temperature.

The embrittlement caused by cathodic treatment in alkaline solutions is considerably less than in acid solutions. The relationship between the degree of embrittlement and the temperature of the alkaline electrolyte is complex in character – in cathodic polarization in dilute solution and low current densities the brittleness decreases with increase of temperature from 20 to 80°. Increase of current density, and also increase of the solution concentration, result in increase of brittleness over the 50-80° range. Simultaneous increases of concentration and current density result in a continuous increase of brittleness with increase of electrolyte temperature from 20 to 80° (Fig. 2).

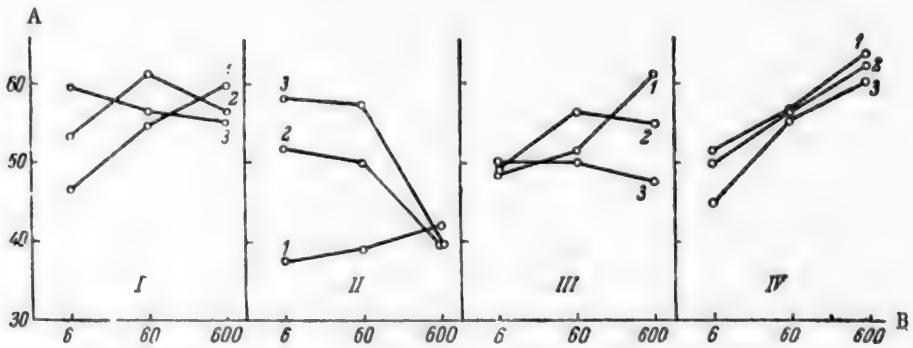

Fig. 1. Effect of the duration of cathodic polarization on the relative brittleness of quenched U9 steel. A) Relative brittleness (%), B) duration of cathodic polarization (seconds). Temperature (°C): 1) 20, 2) 50, 3) 80. H_2SO_4 concentration (%) and current density (amps/dm^2) respectively: I) 0.1 and 2, II) 0.1 and 20, III) 10 and 2, IV) 10 and 20.

Introduction of cyanides into the alkaline solutions increases the hydrogen embrittlement of steel. The brittleness of cathodically polarized steel diminishes with increase of temperature in alkaline cyanide electrolytes. The brittleness increases with current density over all the temperature range studied. Most additives increase the brittleness of steel to some extent when added to alkaline solutions (in contrast to acid solutions, in which additives as a rule decrease brittleness). Of three grades of steel (10, 40, and 30 KhGSA), 30 KhGSA showed the least tendency to hydrogen embrittlement, and steel 40 the greatest. Irrespective of the chemical composition of the steel, the maximum embrittlement corresponds to the most highly stressed state of the metal (after cold working without annealing) although quenched and tempered steel is harder than cold-worked steel (Fig. 3).

Cathodic polarization with deposition. The effects of the conditions in which galvanic coatings are deposited, on brittleness, were studied in the deposition of copper, nickel, tin, zinc, cadmium, and chromium.

The electrolytes used for copper deposition were of the cyanide (CuCn 90 g/liter, $NaCN_{free}$ 20 g/liter,

Na_2CO_3 60 g/liter; current density 1, 1.5, and 3.5 amps/dm^2; temperature 20 and 40°; layer thickness 1, 5, 10, and 25 μ) and sulfate ($CuSO_4 \cdot 5H_2O$ 200 g/liter, H_2SO_4 50 g/liter; current density 2 amps/dm^2; temperature 20°; layer thickness 1, 10, and 25 μ) types. Copper from sulfate solution was deposited on an under-layer of copper deposited from the cyanide electrolyte. As the result of copper deposition, annealed and quenched steel undergoes pronounced embrittlement when the copper layer is only 1 μ thick. On further deposition of copper, the brittleness increases more slowly, especially in annealed steel, where the maximum degree of embrittlement, 40-50%, is reached with layers 10 μ thick; this is followed by a decrease to 27-40% with layers 25 μ thick. Increases of temperature and current density in the electrodeposition of copper result in some increase of steel embrittlement for all the layer thicknesses investigated. Brittleness also increases with increasing current density at constant electrolyte temperature. The nature of embrittlement in sulfate electrolyte depends to a considerable extent on the thickness of the copper under-layer deposited from the cyanide electrolyte. No significant differences of brittleness were found between annealed and quenched steel after copper deposition from sulfate electrolyte.

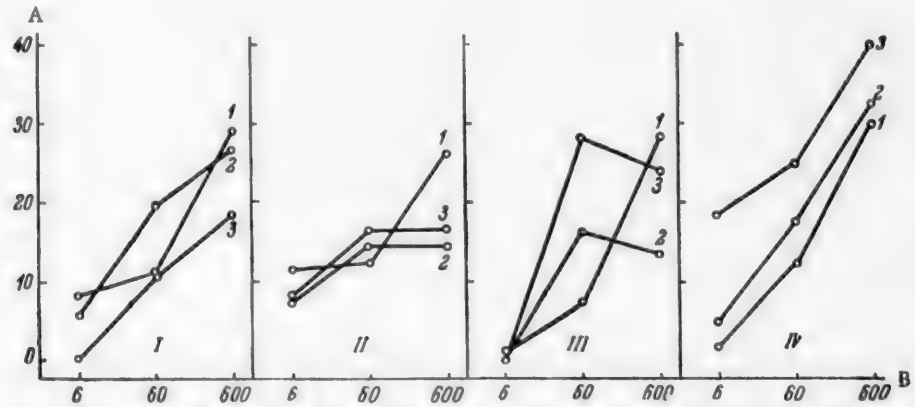

Fig. 2. Effect of the duration of cathodic polarization on the relative brittleness of quenched U9 steel. A) Relative brittleness (%), B) time of cathodic polarization (seconds). Temperature (°C): 1) 20, 2) 50, 3) 80. NaOH concentration (%) and current density (amps/dm^2) respectively: I) 0.1 and 2, II) 0.1 and 20, III) 10 and 2, IV) 10 and 20.

Two electrolytes were used for nickel deposition:

1) $NiSO_4 \cdot 7H_2O$ 175 g/liter, NaCl 5 g/liter, H_3BO_3 25 g/liter, $Na_2SO_4 \cdot 10H_2O$ 50 g/liter, $MgSO_4 \cdot 7H_2O$ 30 g/liter; pH = 4.8-5.8; temperature 20 and 40°; current density 0.5 and 3 amps/dm^2; and 2) $NiSO_4 \cdot 7H_2O$ 350 g/liter, pH = 1.5-2.0; temperature 40 and 80°; current density 2 and 5 amps/dm^2. The thickness of the nickel coatings was 1, 3, and 15 μ. The first of these is the universal electrolyte widely used for application of nickel coatings on various articles made from ferrous metals. The second electrolyte is used for the formation of thick and plastic deposits. Nickel coating causes less embrittlement of the basis metal than does copper coating. Despite the differences of electrolyte composition and deposition conditions, in both electrolytes the brittleness of annealed steel increases from 0 to 20-35% with increase of layer thickness of 3 μ, and then rises more slowly, reaching 35-50% when the layer is 15 μ thick. The embrittlement of quenched steel caused in the deposition of a thin (1 μ) nickel layer remains virtually unchanged with further increase of the deposit thickness.

Tin deposits 1, 10, and 20 μ thick were formed from a sulfate electrolyte ($SnSO_4$ 50 g/liter, H_2SO_4 75 g/liter, phenol 20 g/liter, glue 3 g/liter; temperature 20°; current density 0.5 and 1.5 amps/dm^2). In tin plating, embrittlement occurred only in quenched steel at high current densities.

Zinc coatings 1, 5, and 25 μ thick were deposited from cyanide (Zn 45 g/liter, $NaCN_{total}$ 90 g/liter, NaOH 75 g/liter; temperature 20°; current density 1 and 6 amps/dm^2) and sulfate ($ZnSO_4$ 210 g/liter, $Na_2SO_4 \cdot 10H_2O$ 95 g/liter, $Al_2(SO_4)_3 \cdot 18H_2O$ 30 g/liter, dextrin 10 g/liter; temperature 20°; current density 0.5 and

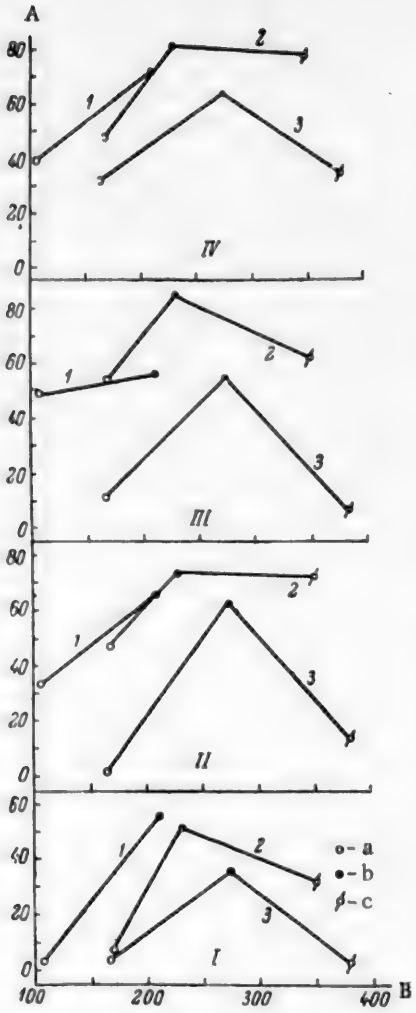

Fig. 3. Relationship between Vickers hardness and relative brittleness of steel 10 (1), 40 (2), and 30KhGSA (3) after cathodic polarization in 10% H_2SO_4 solution (I), 10% NaOH (II), 10% NaOH and 1% NaCN (III), and cyanide zinc electrolyte (IV). A) Relative brittleness (%), B) Vickers hardness. Steel: a) annealed, b) cold-worked, c) quenched.

2 amps/dm^2; pH 3.8-4.4) electrolytes. The embrittlement caused in zinc plating is considerably greater with cyanide than with sulfate electrolyte. Despite the differences of the electrolyte composition, the changes in the embrittlement of steel with increase of layer thickness are approximately the same in both cases – the brittleness increases sharply in the deposition of layers up to 5 μ thick, and less rapidly during subsequent deposition. The brittleness both of annealed and of quenched steel decreases with increase of current density in both electrolytes (Fig. 4).

Cadmium deposits 1, 10, and 20 μ thick were produced in a cyanide electrolyte (Cd 45 g/liter, $NaCN_{total}$ 115 g/liter, NaOH 30 g/liter, $NiSO_4 \cdot 7H_2O$ 2 g/liter, sulfite liquor 10 g/liter; temperature 20°; current density 1 and 3 amps/dm^2). In cadmium plating, as in zinc plating, there is a sharp increase of brittleness in the deposition of thin layers. When the deposit becomes thicker, not only is the increase of brittleness retarded, but there is even some restoration of plastic properties. In contrast to zinc plating, in cadmium plating the brittleness increases with increasing current density.

The universal electrolyte (CrO_3 250 g/liter, H_2SO_4 2.5 g/liter, Cr^{+++} 3.5 g/liter) was used for chrome plating. Different conditions were used for the deposition, mainly with application of bright coatings 5, 25, and 50 μ thick. Under all deposition conditions, the brittleness increases sharply on deposition of chromium layers up to 5 μ thick. The brittleness of steel decreases with increase of the layer thickness over 5 μ. Annealed steel undergoes greater embrittlement than quenched steel during deposition of thin layers of chromium. In general, greater embrittlement occurs as the result of chrome plating at higher electrolyte temperatures and current densities than at low values of these parameters (Fig. 5). The least brittleness arises in the deposition of chromium coatings intermediate between gray and bright. Temperature variations in the range of 35 to 65° at constant current density (50 amps/dm^2) influence mainly the brittleness of annealed steel coated with relatively thick chromium coatings; the minimum brittleness is found at 45°, and the maximum at 35 and 65°.

Anodic treatment of the chromium coatings – dechroming – results in a decrease of the brittleness of chromium-plated steel; the extent of this decrease depends on the chrome-plating conditions and the state of the basis metal. Removal of the chromium coating produces a considerable decrease in the brittleness of steel (by about 30-40%). Complete restoration of the plastic properties occurs on removal of the entire deposit 50 μ thick from annealed steel. The embrittlement which arises as the result of a second chroming is of approximately the same magnitude as that found after the first deposition of chromium. Interruption of the chroming process has no significant influence on the brittleness of quenched steel; the difference in the brittleness of steel chrome-plated with and without interruption of the current supply is less than 10% at all deposit thicknesses. In the case of annealed steel the brittleness increases as the result of a prolonged interruption (24 hours) of the current supply.

The effects of the different galvanic coatings on the fatigue limits of annealed and quenched steel were determined in the deposition of coatings 25 μ thick. The galvanic coatings lower the fatigue limit of steel, but to different extents which depend both on the type of coating and on the state of the basis metal. The fatigue limit is lowered more in quenched than in annealed steel. In both cases the greatest decrease of fatigue limit was produced as the result of nickel plating, and the least, as the result of copper plating.

Prevention of hydrogen embrittlement. Before the surfaces were coated, the influence of the surface preparation on the embrittlement which arises both directly and during subsequent deposition of galvanic coatings was investigated.

In electrochemical degreasing in the ordinary alkali solution at 70° embrittlement arises both in quenched and in annealed steel, but to a much greater extent in the former than in the latter. Subsequent anodic treatment in the same solution (usually applied for dehydrogenation and additional cleaning of the steel surface) leads to gradual restoration of the plastic properties of the metal. However, anodic treatment in the solution at room temperature has hardly any effect on the brittleness. The temperature of the medium to which the steel is exposed has a decisive influence on the restoration of the plastic properties of steel after hydrogen embrittlement. The higher the temperature of the medium, the more rapidly is the embrittlement eliminated.

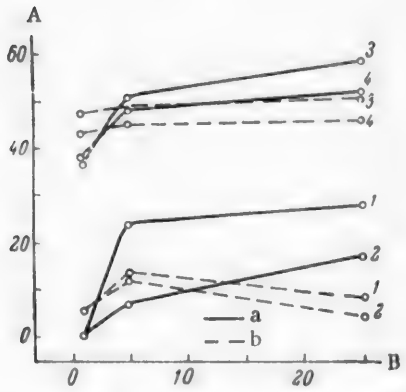

Fig. 4. Effect of thickness of the zinc layer on the relative brittleness of annealed (a) and quenched (b) steel U9. A) Relative brittleness (%), B) thickness of zinc layer (μ). Zinc coatings applied at current densities (amps/dm^2): in sulfate electrolyte 1) 0.5, 2) 2; in cyanide electrolyte 3) 1, 4) 6.

Pickling in 5% hydrochloric acid solution (without application of current) confers considerable brittleness on steel within the first few seconds. Additives – ChM, KS, and flour – do not decrease the brittleness to any significant extent. Pickling prior to copper plating results in some increase in the brittleness of annealed steel, and has almost no effect on quenched steel. Pickling prior to nickel plating results in some decrease in the brittleness of annealed steel, and slight increase of brittleness in quenched steel.

A study was made of the effect of an under-layer of copper deposited from a cyanide electrolyte on the embrittlement produced during nickel and chromium plating. It was found that the presence of copper-under layers 3 and 10 μ thick somewhat increases the brittleness of quenched steel in the deposition of a nickel coating 3 μ thick (as compared with nickel plating without an under-layer). In the deposition of a thicker nickel coating (15 μ), a copper under-layer has hardly any influence on brittleness. The presence of an under-layer of copper or nickel results in some decrease in the brittlesness of steel with a thin coating of chromium. If the chromium coating is relatively thick, an under-layer of copper intensifies the embrittlement. An under-layer of nickel 3 μ thick prevents embrittlement during subsequent coating of annealed steel with chromium 50 μ thick.

Oxidizing additives (CrO_3, $KMnO_4$) added to solutions of sulfuric acid (used for cathodic polarization) and hydrochloric acid (for pickling without application of current) tend to reduce embrittlement only if added in large amounts. They were found to be more effective in the pickling solution.

Agitation of the electrolyte (by means of air, and mechanically), periodic reversal of the current, increase of the current efficiency for the metal, and thickening of the cathode cross section, all favor some decrease in the brittleness of annealed steel but have no significant influence on the plastic properties of quenched steel.

Elimination of hydrogen embrittlement. The main method for elimination of hydrogen embrittlement is exposure of the hydrogen-saturated steel to room or higher temperatures. It has been found that the plastic properties of steel saturated with hydrogen without application of galvanic coatings are gradually restored during exposure at room temperatures. The brittleness is eliminated more rapidly from steels treated in alkaline than in acid solutions. In the presence of galvanic coatings, aging (at room temperature) is an ineffective means of plasticity restoration, and in some instances it may even increase the brittleness. This shows that the deposits prevent release of hydrogen. After removal of the deposit (for example, mechanically), the brittleness disappears fairly rapidly. The most effective means for elimination of embrittlement arising during cathodic treatment is exposure to elevated temperatures. The higher the exposure temperature, the more rapidly are the plastic properties of the steel restored (Fig. 6). The maximum permissible exposure temperature should be such as to ensure that the properties of the coating and the basis metal are not affected. The plastic properties

of steel coated with cadmium, zinc, and in some instances chromium were restored almost completely after exposures at 200-300° for various times. However, the brittleness of annealed steel with a thin (5 μ) coating of chromium was not restored even after exposure at 500°.

The results of determinations of the hydrogen content of the steel immediately after cathodic polarization and some time later are in agreement with the data obtained on the course of variations of hydrogen embrittlement (see table). The data in the table show that the hydrogen content of the steel increases with the time of cathodic treatment. This increase is not uniform – about as much hydrogen diffuses into the steel during the first two hours as during the subsequent 14 hours. The hydrogen is slowly liberated from the steel during exposure to air. The greatest amount of hydrogen is liberated during the first hour after removal of the specimens from the electrolyte. However, even after 7 days of exposure the steel contained more hydrogen than it did in its original state before the treatment.

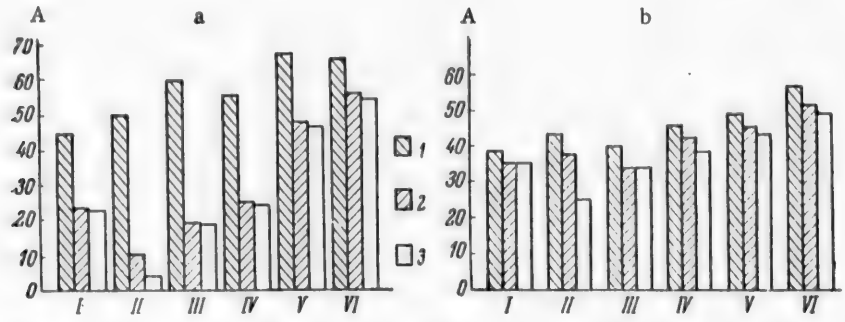

Fig. 5. Effect of chroming conditions on the relative brittleness of annealed (a) and quenched (b) steel U9. A) Relative brittleness (%). Current density (amps/dm^2) and temperature (°C) respectively: I) 15 and 40-45; II) 30 and 40-45; III) 40 and 40-45; IV) 50 and 50-55; V) 60 and 55-60; VI) 70 and 65-70. Layer thickness (μ): 1) 5, 2) 25, 3) 50.

The development of hydrogen embrittlement in cathodic treatment without application of coatings may be explained in the light of the mechanism postulated for hydrogen saturation. It is presumed that when steel is treated in acid solutions the incorporation of hydrogen as the result of cathodic liberation during polarization by means of an external current source is accompanied by hydrogen saturation owing to incomplete suppression of the action of the microcells on the steel cathode surface. It is considered that hydrogen which enters the crystal lattice in the course of its microelectrochemical destruction is bound more firmly to the metal than the hydrogen which enters the stable crystal lattice during cathodic polarization caused by an external current source [11, 12]. The lower hydrogen absorption of steel in alkaline solutions, as compared with acid solutions, can be ascribed to the fact that the cathode is not dissolved in alkaline solutions at the concentrations studied, and also to the formation of passive films on the cathode surface.

The losses which take place in the weights of the specimens, despite the fact that the specimens are placed into and removed from the electrolyte with the current flowing, indicate that the microcells are not completely suppressed in the course of cathodic polarization in acid solution. For example, in cathodic polarization of steel U9 in 0.1% sulfuric acid solution at 20°; in an exposure time of 600 seconds, the weight loss at D_C = 0.2, 2, and 20 amps/dm^2 was 20.2, 13.7, and 4.3 mg/cm^2·day respectively. This is analogous to the diminished microelectrochemical corrosion which occurs when electrochemical protection against corrosion is incomplete; dissolution of the protected metal continues, although at a lower rate.

The relationship between steel brittleness and the conditions of cathodic hydrogen saturation cannot be explained only on the basis of data correlating the magnitude of hydrogen overvoltage with temperature, current density, and electrolyte composition.

The course of embrittlement in the formation of galvanic coatings can be explained both by changes in the magnitude of the internal stresses in the deposits, and by changes of the hydrogen content of the metal.

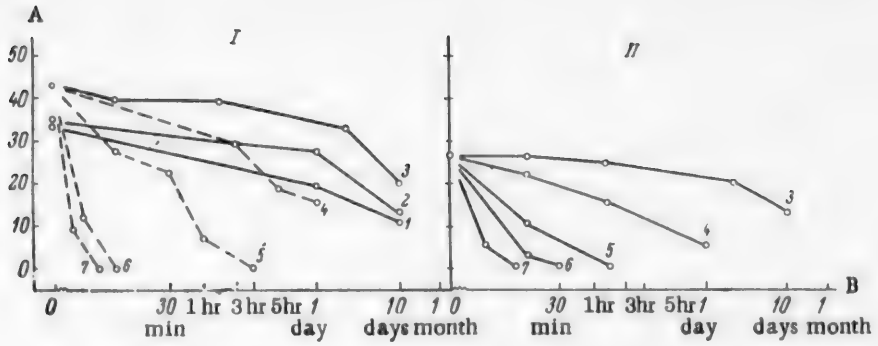

Fig. 6. Effect of exposure time at different temperatures on the relative brittleness of quenched (I) and annealed (II) steel U9 after cadmium plating in a cyanide electrolyte. A) Relative brittleness (%); B) exposure time. Temperature (°C): 1, 2,3) 20; 4) 100; 5) 200; 6) 230; 7) 270. Current density (amps/dm^2): 1, 2) 1; 3-7) 15. Layer thickness (μ): 1) 1, 2) 20, 3-7) 10.

Hydrogen Contents of Steel U9

Material	Exposure time		Hydrogen content	
	in electrolyte	in air	in cc/100 g	% on specimen wt.
Annealed	—	—	0.37	0.000033
	1 min.	—	1.33	0.00012
	10 min.	—	5.77	0.00052
	1 hr. 40 mm.	—	9.0	0.00081
	16 hr	—	19.2	0.00173
	1 hr 40 mm.	1 hr	3.11	0.00028
	1 hr. 40 mm..	16 hrs	1.88	0.00017
	1 hr. 40 mm.	7 days	0.88	0.00008
Cold-worked	0	—	0.51	0.000046
	1 min.	—	1.66	0.00015
	10 min.	—	6.6	0.00060
	1 hr. 40 mm.	—	9.56	0.00086
	16 hrs.	—	19.1	0.00172
	1 hr. 40 mm.	1 hr.	3.77	0.00034
	1 hr. 40 mm.	16 hrs.	1.11	0.00010
	1 hr. 40 mm.	7 days.	0.88	0.00008
After quenching and tempering	0	—	0.46	0.000041
	1 min.	—	1.66	0.00015
	10 min.	—	2.11	0.00018
	1 hr. 40 mm.	—	2.55	0.00022
	16 hrs.	—	5.77	0.00052
	1 hr. 40 mm.	1 hr.	2.0	0.00018
	1 hr. 40 mm.	16 hrs.	0.77	0.00007
	1 hr. 40 mm.	7 days	0.55	0.00005

In the former case, increase of brittleness in the application of thin coatings is associated with the development of stresses, which can only be relaxed when the coatings are thick enough, in the coatings. In the latter case, increase of brittleness in the initial period of electrolysis can be ascribed to penetration of hydrogen into the metal through the thin coating; thin coatings of certain metals can accelerate diffusion of hydrogen into steel, whereas thick coatings act as obstacles to the diffusing hydrogen.

SUMMARY

1. The embrittlement of steel as the result of cathodic polarization is considerably greater in acid than in alkaline solutions.

2. Addition of cyanides to alkaline solutions results in a considerable intensification of hydrogen absorption.

3. The extent of the embrittlement depends to a considerable extent on the state of the treated metal. One important criterion of the tendency of steel to undergo hydrogen embrittlement is the magnitude of the internal stresses.

4. In most cases quenched steel undergoes greater embrittlement than annealed steel, but the presence of certain amounts of cyanides in the electrolyte may sharply reduce the difference in the degree of embrittlement.

5. In the application of galvanic coatings, the degree of embrittlement is influenced not only by hydrogen absorption of the basis metal but also by the stresses which arise in the coatings. In any particular instance the predominance of one or the other of these factors depends on the nature of the coating and on the deposition conditions.

6. The degree of embrittlement decreases with thickening of the deposit; this is attributed, first, to the formation of a barrier which prevents incorporation of hydrogen in the metal, and second, to the relaxation of stresses in the deposit as the result either of cracking or of plastic deformation of the deposit.

7. The embrittlement which arises in presence of galvanic coatings is greater in electrodeposition in cyanide than in noncyanide electrolytes.

8. Various methods for prevention of embrittlement (current reversal, additions to pickling liquors, anodic treatment, increase of current efficiency, increase of the thickness of the articles, etc.) are not very suitable for quenched steel, but may prove effective in the treatment of articles made from annealed steel.

9. Exposure to air results in fairly easy elimination of hydrogen embrittlement of steel without galvanic coatings. However, if a coating is present the brittleness may increase as the result of exposure.

10. The most effective method for elimination of brittleness is exposure of the articles, after cathodic treatment, at 200-300°; however, in some instances, when the brittleness is caused mainly by stresses in the deposit, such treatment may prove unsuccessful.

LITERATURE CITED

[1] C. A. Zapffe and P. W. Worden, Trans. Am. Soc. Metals, 42, 517-602 (1950).

[2] C. A. Zapffe and C. E. Sims, Metals Technology 8, 5 (1941).

[3] C. A. Zapffe and C. E. Sims, Metals and Alloys 11, 5 (1940).

[4] C. A. Zapffe and M. E. Haslem, Wire and Wire Products, 21, 149 (1946).

[5] S. S. Nosyreva, Factory Labs. 3, 307 (1948).

[6] McGrow, Electrodeposition Research Proceedings of the NBS. 4-6 (1951).

[7] H. Fischer and H. Bărman, Korrosion u. Metallschutz, 16, 12 (1940).

[8] S. S. Nosyreva, Steel 6, 542 (1945).

[9] M. A. Figel'man and A. V. Shreider, Factory Labs. 5, 580 (1956).

[10] A. N. Morozov, Hydrogen and Nitrogen in Steel (Metallurgy Press, 1950).•

[11] Iu. V. Baimakov and M. I. Zamotorin, Proc. Conf. on Electrochemistry (Izd. AN SSSR, 1953).•

[12] Iu. V. Baimakov and G. I. Kvint, Trans. Leningrad Polytechnic Inst. 6, 72 (1953).

Received December 26, 1956

•In Russian.

INFLUENCE OF THE pH OF THE MEDIUM AND THE TEMPERATURE ON THE PROPORTIONS OF ACTIVE OXIDIZING AGENTS IN HYPOCHLORITE SOLUTIONS IN CHLORINATION AND BLEACHING PROCESSES

I. E. Flis

The Leningrad Technological Institute

Dilute hypochlorite solutions contain three principal substances which are active in chlorination and bleaching of cellulose and fabrics, and in many other oxidation reactions; these are chlorine Cl_2, hypochlorous acid HClO, and hypochloride ClO^-. The proportions of these components may be determined by analysis of certain principal equilibria which occur in such systems. These equilibria are considered here.

Equilibrium of chlorine hydrolysis. Iakovkin [1] showed that the following hydrolytic reaction takes place in chlorine solutions:

$$Cl_2 + H_2O \rightleftharpoons HClO + H^+ + Cl^-. \qquad (1)$$

His paper contains detailed thermodynamic characteristics of Equilibrium (1) over a wide range of temperatures. The hydrolysis constants (K_h) found by Iakovkin for various temperatures have the following values [2]:

t (°C)	10	20	25	35	40	50	60
$K_h \cdot 10^4$	2.58	4.06	4.84	6.43	7.15	8.51	9.75

Shilov and Solodushenkov [3, 4] confirmed the existence of Equilibrium (1), and found that it is established very rapidly. For example, the rate constants of chlorine hydrolysis at 0.2 and 17.8° are 108 and 528 respectively.

With the use of the above values for K_h, and after determinations of the solution pH and its active chlorine• and chloride contents, it is possible to calculate the activity or concentration ratios of chlorine and hypochlorous acid, and also a_{HClO} and a_{Cl_2} separately.

$$\frac{a_{HClO}}{a_{Cl_2}} = \frac{K_h}{a_{H^+} \cdot a_{Cl^-}}. \qquad (2)••$$

In the case of previously prepared chlorine water, we have in the original solution,

$$a_{H^+} \cong a_{Cl^-} \quad \text{and} \quad \frac{a_{HClO}}{a_{Cl_2}} \cong \frac{K_h}{a^2_{H^+}}. \qquad (2a)$$

• Molar sum of Cl_2 and HClO.

•• a represents the activity or concentration of a given substance at equilibrium. Since dilute solutions are used in practice, it may be assumed that the activity coefficients of Cl_2 and HClO are close to unity.

However, in the chlorination process usually ($a_{H+} \neq a_{Cl^-}$, and then a_{Cl^-} must be calculated from appropriate analytical data. For example, if a sample of solution of known pH is taken, and alkali solution is added to it in excess sufficient to shift Equilibrium (1) almost completely to the right, and its chloride ($a^0_{Cl^-}$) and total active chlorine (a_{total}) contents are determined by known methods [5-7], the chloride content of the solution can be calculated from the formula [6, 7]

$$a_{Cl^-} = \frac{\left[K'_h \cdot a_{H+} \cdot a_{total} - a^0_{Cl^-} + 1\right] \sqrt{\left[K'_h \cdot a_{H+} \cdot a_{total} - a^0_{Cl^-} + 1\right]^2 + 4K'_h \cdot a_{H+} \cdot a^0_{Cl^-}}}{2K'_h \cdot a_{H+}}, \quad (3)$$

where

$$K'_h = \frac{1}{K_h}.$$

Then the activity or concentration of chlorine is

$$a_{Cl_2} = K'_h \cdot a_{H+} \cdot a_{Cl^-} \cdot a_{total} - a^0_{Cl^-} + a_{Cl^-}. \quad (4)$$

Equations (2) and (4) may be used for determination of the composition of acid solutions. They can provide an exact measure of the chlorinating or bleaching action in the solution; this is of great practical importance. This question is to be considered later in this paper.

Equilibrium in the dissociation of hypochlorous acid and hydrolysis of hypochlorite. The relative chlorine content of the solution falls with increase of pH, and when the chlorine has almost vanished there is an abrupt change of pH, indicating a transition to another equilibrium [6]

$$HClO \rightleftharpoons H^+ + ClO^-. \quad (5)$$

Further decrease of H^+ activity leads to virtual disappearance of HClO, with an abrupt transition to a new pH region, where the equilibrium of hypochlorite hydrolysis predominates.

$$ClO^- + H_2O \rightleftharpoons HClO + OH^-. \quad (6)$$

If the dissociation constant of HClO (K_d) is used, and the active chlorine content (a_{total}) is determined by the usual method, it is possible to calculate, without any serious error, the HClO and ClO^- contents of the solution [6]

$$a_{HClO} = \frac{a_{H+} \cdot a_{total}}{K_h + a_{H+}} = \frac{a_{H+} \cdot a_{total} \cdot K''_h}{K_w + a_{H+} \cdot K''_h}, \quad (7)$$

$$a_{ClO^-} = \frac{K_h}{K_h + a_{H+}} \frac{a_{total}}{} = \frac{K_w \cdot a_{total}}{K_w + a_{H+} \cdot K''_h}, \quad (8)$$

where K''_h is the hydrolysis constant of hypochlorite, and K_w is the ionic product of water.

It is known that $K''_h = \frac{K_w}{K_d}$.

The dissociation constants of hypochlorous acid have been studied by numerous workers [8-19]. Most of them found values of the order of 10^{-8}. However, nearly all of them were determined at 18-25°. However, under industrial conditions oxidation processes are effected over a wider temperature range (for example, bleaching is usually carried out at 25-40°). It is therefore necessary to know the composition of bleaching liquors and the ratio of a_{ClO^-} and a_{HClO} in them, which determines the degree and rate of oxidation at various temperatures.

Therefore it was obviously necessary to determine K_d and K_h^* at the temperatures used in the practical utilization of these systems. These determinations were carried out by us jointly with Mishchenko and Pakhomova [18] by a thermochemical method, and jointly with Byniaeva by a potentiometric method.

Here we consider briefly the results of potentiometric determinations whereby K_d could be found directly. A series of investigations based on thermochemical experiments, leading to a more complete thermodynamic characterization of Equilibria (5) and (6), is described in another paper [18].

It follows from (7) and (8) that $K_d = \varphi\left(a_{H^+}, \frac{a_{ClO^-}}{a_{HClO}}\right)$. Therefore to calculate K_d it is necessary to find values of $\frac{a_{ClO^-}}{a_{HClO}}$, corresponding to different values of a_{H^+}. This can be done by a potentiometric method with the use of electrodes reversible with respect to H^+ ions. Only the glass electrode is suitable for hypochlorite systems. The glass electrode has been used both in potentiometric titrations of hypochlorite solutions [6, 14, 17, 19-23], and for pH determinations in the course of oxidation.

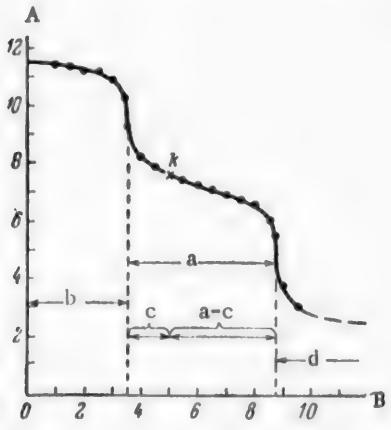

Fig. 1. Potentiometric titration of hypochlorite solution by sulfuric acid, with the use of a glass electrode. A) pH, B) amount of 0.1 N H_2SO_4 (ml). a) Region in which the equilibrium $ClO^- + H_2O \rightleftharpoons HClO + OH^-$ predominates; b) region in which the equilibrium $ClO^- + H^+ \rightleftharpoons HClO$; d) region in which the equilibrium $HClO + H^+ + Cl^- \rightleftharpoons Cl_2 + H_2O$ predominates.

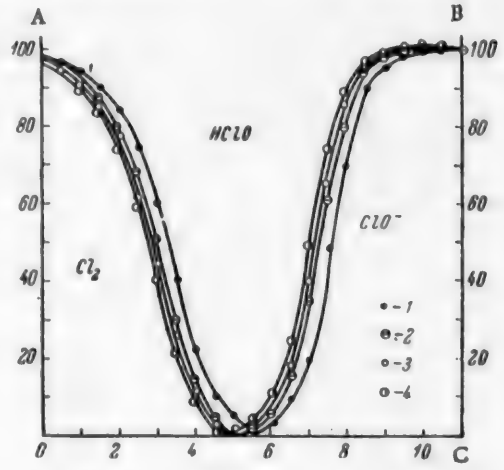

Fig. 2. Relationships between pH and concentration of active oxidants in hypochlorite solutions at different temperatures. A) Cl_2 concentration (%), B) ClO^- concentration (%), C) pH. Temperature (°C): 1) 10, 2) 25, 3) 25, 4) 50.

Let us consider Fig. 1, which shows the potentiometric titration curve of hypochlorite solution by sulfuric acid. Regions of each of the above-mentioned equilibria (1, 5, 6) are clearly defined. Since the system is in equilibrium, Equations (7) and (8) or analogous expressions are valid for any point on this curve

$$pK_d^* = \mathrm{pH} + \log\frac{a_{HClO}}{a_{ClO^-}}. \qquad (9)$$

However, for calculation of K_d it is more convenient to use the middle region a of the curve, where hypochlorite (ClO^-) and hypochlorous acid (HClO) are present in considerable and comparable amounts, whereas regions b and d correspond to negligible concentrations of hypochlorous acid and ClO^- ions respectively.

• The value of K_d lies in the range of $10^{-4} - 10^{-10}$.

The concentration ratio $\frac{C_{ClO^-}}{C_{HClO}}$ can be determined directly from the titration curve. For example, at the point K it is equal to the ratio $\frac{a-c}{c}$.

If it is assumed that

$$\log \frac{fa_{(ClO^-)}}{fa_{(HClO)}} = -A\sqrt{\mu}\ [24], \tag{10}$$

where $fa_{(ClO^-)}$ and $fa_{(HClO)}$ are the corresponding activity coefficients; A is the constant in the Debye and Hückel equation for calculation of activity coefficients; and μ is the ionic strength of the solution, we have

$$pK_d = pH + \lg \frac{c}{a-c} - A\sqrt{\mu}. \tag{11}$$

This equation, valid only for fairly dilute solutions, was used in our calculations, on the assumption that it does not involve any serious errors under our experimental conditions.

Potentiometric titrations of hypochlorite solutions by sulfuric acid were carried out at 10, 25, 35, and 50°. The pH determinations were performed by means of an electronic potentiometric unit [6] to an accuracy of 0.03-0.02 pH. The glass electrode was carefully calibrated at various temperatures against the hydrogen electrode in a number of buffer solutions. The second half-cell in the circuit was a saturated calomel electrode, the potential of which was calculated from the formula

$$\varphi_{sat.\ cal} = 0.26303 - 0.0007\ t\ [25].$$

The sodium hypochlorite solutions used in the experiments were prepared by chlorination of caustic soda solutions. Chlorine was prepared by the action of chemically pure hydrochloric acid on potassium dichromate. The caustic soda solutions were virtually free from carbonate impurity; this was confirmed by special potentiometric experiments [7]. The sulfuric acid solutions were made from "Fixanal" standard, and their concentrations were checked before the experiments. The values of μ were calculated from the analytical results by means of the known formula [24], by the method described by us elsewhere [7]. Values of A in Equation (11) were calculated by Karapet'iants, and are given in his monograph [26]; these were used in our calculations.

The experimental data and the calculated values of K_d and K_h^* at various temperatures are given in the table.

The average values of K_d and K_h^* (with error limits) are given below:

Temperature (°C)	$K_d \cdot 10^8$	$K_h^* \cdot 10^7$
10	3.23 ± 0.05	0.93 ± 0.05
25	5.00 ± 0.06	2.05 ± 0.06
35	6.61 ± 0.07	3.18 ± 0.06
50	8.91 ± 0.06	6.14 ± 0.03

Equilibrium between hypochlorous acid and chlorine monoxide in solution. In discussion of the composition of hypochlorite solutions, it is necessary to consider yet another equilibrium.

$$Cl_2O_{aq} + H_2O_l \rightleftharpoons 2HClO_{aq} \tag{12}$$

This equilibrium was mentioned by Förster [27]. Goldschmidt [28], who studied the distribution of Cl_2O between water and CCl_4, found that the constant for Equilibrium (12) at 0° is 0.00096. Later, Roth [29]

Determinations of the Dissociation Constants of HClO and Calculations of the Hydrolysis Constants of Hypochlorite at 10, 25, 35, and 50° from the Results of Potentiometric Determinations

pH	C_{ClO^-} (mole/liter)	C_{HClO} (mole/liter)	μ	$K_d \cdot 10^8$	$K_h'' \cdot 10^7$	Notes
			10°			
6.40	0.0007	0.0073	0.0295	2.95	1.00	$K_w = 2.97 \cdot 10^{-15}$ $A = 0.4960$ Initial concentration $C^0_{ClO^-} = 0.0096$ mole/liter
6.80	0.0016	0.0065	0.0293	2.95	1.00	
7.00	0.0025	0.0057	0.0290	3.31	0.89	
7.20	0.0034	0.0049	0.0289	3.47	0.85	
7.40	0.0043	0.0041	0.0287	3.16	0.94	
7.55	0.0052	0.0033	0.0284	3.55	0.84	
7.80	0.0062	0.0024	0.0283	3.24	0.94	
8.05	0.0072	0.0016	0.0281	3.24	0.94	
8.45	0.0082	0.0007	0.0270	3.24	0.94	
			25°			
6.00	0.0014	0.0076	0.0318	4.90	2.08	$K_w = 1.02 \cdot 10^{-14}$ $A = 0.5085$ Initial concentration $C^0_{ClO^-} = 0.0107$ mole/liter
6.55	0.0016	0.0075	0.0303	5.37	1.90	
6.70	0.0029	0.0063	0.0311	5.37	1.90	
6.90	0.0033	0.0060	0.0309	5.37	1.90	
7.10	0.0042	0.0052	0.0307	5.01	2.03	
7.30	0.0052	0.0043	0.0305	4.68	2.18	
7.45	0.0061	0.0035	0.0303	4.90	2.08	
7.65	0.0071	0.0026	0.0302	4.79	2.13	
7.90	0.0081	0.0017	0.0300	4.68	2.18	
8.25	0.0091	0.0008	0.0299	4.90	2.08	
			35°			
6.10	0.0010	0.0084	0.0323	6.46	3.25	$K_w = 2.1 \cdot 10^{-14}$ $A = 0.5175$ Initial concentration $C^0_{ClO^-} = 0.0112$ mole/liter
6.45	0.0019	0.0076	0.0321	6.46	3.25	
6.70	0.0028	0.0069	0.0319	6.03	3.48	
6.85	0.0037	0.0062	0.0317	6.61	3.18	
7.00	0.0046	0.0054	0.0315	6.76	3.11	
7.15	0.0056	0.0046	0.0313	6.92	3.04	
7.30	0.0065	0.0037	0.0312	7.08	2.99	
7.50	0.0075	0.0028	0.0311	6.92	0.04	
7.75	0.0085	0.0019	0.0309	6.46	3.25	
8.10	0.0825	0.0010	0.0308	6.46	3.25	
			50°			
5.60	0.0004	0.0080	0.0305	8.51	6.47	$K_w = 5.51 \cdot 10^{-14}$ $A = 0.5319$ Initial concentration $C^0_{ClO^-} = 0.0100$ mole/liter
6.15	0.0013	0.0072	0.0303	9.33	6.90	
6.45	0.0021	0.0065	0.0301	8.91	6.18	
6.70	0.0030	0.0057	0.0298	8.32	6.61	
6.85	0.0039	0.0049	0.0296	8.91	6.18	
7.00	0.0048	0.0041	0.0294	9.33	5.90	
7.20	0.0057	0.0033	0.0293	8.91	6.18	
7.40	0.0067	0.0024	0.0291	8.91	6.18	
7.65	0.0076	0.0016	0.0289	9.12	6.04	
8.20	0.0086	0.0007	0.0288	9.55	5.76	

calculated this constant again, and found the value of 0.00351 for the same temperature. Data [30] on the heats of formation of Cl_2O_{aq} and $HClO_{aq}$ in solution at 25°:•

• The Thermodynamic and other properties of Cl_2O [31].

$$\Delta H^0_{Cl_2O\,aq} = 9.2\ \frac{kcal}{mole}\ and\ \Delta H^0_{HClO\,aq} = -28.48\ \frac{kcal}{mole},$$

$$\Delta H^0_{H_2O\,l} = -68.32\ \frac{kcal}{mole},$$

give −2.76 kcal/mole for the heat of Reaction (12).

The equation for the reaction isobar can be used for calculation of approximate values of the constants for Equilibrium (12) in the 10-50° temperature range. Substitution of the above values into the simplest isobar equation

$$\lg K_{273} = \frac{2760}{2.303 \cdot 1.987 \cdot 273} + i = -2.45, \qquad (13)$$

gives i = 4.64. Values of the equilibrium constant for (12), calculated from Equation (13), are given below:

t °C	0	10	25	35	50
$K_{(12)} \cdot 10^3$	3.51	2.98	2.32	1.97	1.61
$\frac{Cl_2O}{HClO}$ (%)	0.35	0.30	0.23	0.20	0.16

The relative contents of chlorine monoxide in hypochlorous acid solutions are also given. It is seen that the percentage contents of Cl_2O are low. They decrease with rise of temperature.

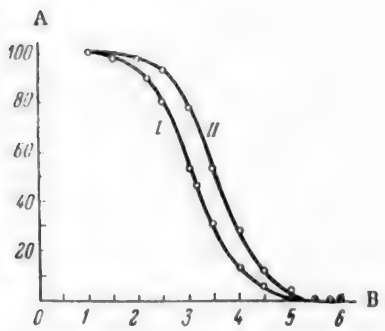

Fig. 3. Influence of chloride concentration on the relative contents of chlorine and HClO in acid hypochlorite solutions at 25°. A) Ratio $\frac{a_{Cl_2}}{a_{total}}$ (%), B) pH. Chloride concentration (mole/liter): I) 0.3, II) 1.

Hypochlorite bleach liquors usually contain up to 0.025 mole of active chlorine per liter at the start of bleaching. As these solutions are alkaline, their hypochlorous acid content is negligibly low. The amounts of chlorine monoxide must be even lower. The solution pH falls during bleaching, and reaches 6.5-6.0 by the end of the process. Although at these pH values the solution contains HClO only, the amount of active chlorine present falls by at least 80-90% of the initial value. Even if it is assumed that the HClO content of the solution is 0.010 mole/liter, then the Cl_2O concentration at 35° must be $2 \cdot 10^{-5}$ mole/liter or $1.74 \cdot 10^{-3}$ g/liter. If 100 ml of this bleach liquor is taken for analysis, it contains $8 \cdot 16^{-6}$ g-equiv of chlorine monoxide. Thus, of 10 ml of 0.1 N thiosulfate solution used for titration of active chlorine in the volume of the bleach liquor taken, not more than 0.1 ml is used in titration of ClO. This minute fraction in titration is at the limit of possible error.

Therefore when the compositions of bleach liquors at different pH and temperatures are given, the Cl_2O contents are omitted, as the concentrations of this compound in bleach liquors are negligibly small.

Relationship Between Chlorination and Oxidation Processes in Bleach Liquors

Iakovkin's data for the hydrolysis constant of chlorine, and our values for the dissociation constant of HClO, were used to calculate the concentrations of substances, active in bleaching, in the liquors. As the result of these calculations it is possible, for the first time, to estimate the influence of temperature on chlorination and oxidation processes in hypochlorite bleach liquors. The compositions of hypochlorite solutions over a narrow temperature range (18-25°) has been determined by various workers [32-34]. The results of our calculations are presented graphically in Fig. 2. The curves in Fig. 2 can be used for estimations of the relative contents of Cl_2, HClO, and hypochlorite in the liquor at a given pH and temperature. Examination of the positions of these curves at different temperatures leads to the conclusion that, under otherwise constant conditions, increase of temperature leads to an increase of the relative HClO

content in solutions where Equilibrium (1) is operative, and to increases in the relative contents of hypochlorite in the pH regions where Equilibria (5) and (6) are of practical significance. This corresponds to a positive sign of ΔH for Reactions (1) and (5), and a negative sign (exothermic reaction) for (6). It follows that for effective chlorination at higher temperatures relatively greater acidification or increase of chloride concentration is required. Chlorination and oxidation in an acid bleach liquor (pH < 5) depend on the concentration ratio of chlorine to hypochlorous acid at a given pH and temperature. This may be characterized by the quantity x

$$x = \frac{a_{Cl_2}}{a_{total}}, \tag{14}$$

where $a_{total} = a_{Cl_2} + a_{HClO}$.

It follows from Equation (4) that

$$x = \frac{a_{H^+} \cdot a_{Cl^-}}{K_h + a_{H^+} \cdot a_{Cl^-}}, \tag{15}$$

i.e., $x = \varphi (a_{H^+}, a_{Cl^-})$.

Curves representing this functional relationship are given in Fig. 3. Curve I corresponds to a solution containing 0.3 mole of chloride per liter, and Curve II, to a solution with $C_{Cl^-} \cong 1$ mole per liter. On the one hand, Formula (15) can be used to calculate the amount of chloride which must be present in solution so that at a given pH virtually only the chlorination process occurs (x = 100%). On the other hand, it is possible to calculate the degree of acidification (pH) at which virtually chlorination only occurs at a given chloride concentration. If the initial concentration of active chlorine in solution is known, and its value during chlorination are subsequently determined, such calculations can be used for evaluation of chlorine consumption. Under production conditions chlorine consumption in fiber chlorination is often determined without account being taken of the fact that acid hypochlorite solutions and chlorine water also contain hypochlorous acid, which acts mainly as an oxidant. Such errors may be avoided by the use of the calculation formulas given above.

SUMMARY

1. The dissociation constants of hypochlorous acid at 10, 25, 35, and 50° respectively are: $(3.23 \pm 0.05) \cdot 10^{-8}$; $(5.00 \pm 0.06) \cdot 10^{-8}$; $(6.61 \pm 0.07) \cdot 10^{-8}$; and $(8.91 \pm 0.05) \cdot 10^{-8}$.

2. Calculations show that the chlorine oxide content of the liquors generally used for bleaching is negligible. Hence it may be concluded that chlorine oxide does not play any appreciable part in bleaching.

3. Iakovkin's experimental results, and the results of experimental determinations of the dissociation constants of HClO which are presented in the paper, were used to determine the influence of pH on the composition of hypochlorite bleach liquors at 10, 25, 35, and 50°, and to consider the conditions favoring chlorination and oxidation in acid hypochlorite solutions.

LITERATURE CITED

[1] A. A. Iakovkin, J. Russ. Phys.-Chem. Soc. 32, 673 (1900).

[2] G. Lewis and M. Randall, Chemical Thermodynamics (ONTI, Chem.. Theoret. Press, Leningrad, 1936), p. 425 [Russian translation].

[3] E. A. Shilov and S. N. Solodushenkov, J. Phys. Chem. 19, 405 (1945).

[4] E. A. Shilov and S. N. Solodushenkov, J. Phys. Chem. 21, 1159 (1947).

[5] K. Shval'be and P. Ziber, Chemical Production Control in the Cellulose and Paper Industry. (In Russian) (Goslestekizdat, Leningrad, 1934).

[6] B. P. Nikol'skii and I. E. Flis, Trans. Leningrad Technol. Inst. 1, 61 (State Wood and Paper Press, 1949).

[7] I. E. Flis and M. K. Byniaeva, Trans. Leningrad Technol. Inst. 3, 179 (State Wood and Paper Press, 1955).

[8] J. Sand, Z. phys. Chem. 48, 610 (1904); 50, 474 (1905).

[9] E. Abel, Hypochlorite and elektrische Bleiche. Halle, 14 (1905).

[10] F. Giordani, Gazz. Chim. Ital. 54, 859 (1924).

[11] W. Noyes and T. Wilson, J. Am. Soc. 44, 1630 (1922).

[12] F. Soper, J. Chem. Soc. 125, 2231 (1924).

[13] I. Gallart, Anal. Soc. espan.' fis. quim. 31, 422 (1933).

[14] G. Davidson, J. Text. Inst. 24, 185-206 T (1933).

[15] A. Skrabal, Z. Elektroch. 48, 448 (1942).

[16] H. Hagisava, Bull. Inst. phys. Chem. Research, Japan, 19, 1220 (1940).

[17] B. P. Nikol'skii and I. E. Flis, J. Gen. Chem. 22, 1298 (1952).*

[18] I. E. Flis, K. P. Mishchenko and N. V. Pakhomova, J. Inorg. Chem. 3, 8 (1958).

[19] T. Gorston, Pulp and Paper Mag. Canada 31, 374 (1931).

[20] E. Voigtmann and B. Rowland, Paper Trade J. 95, 9, 36 (1932).

[21] I. S. Khutorshchikov, Paper Ind. 7 and 11 (1940).

[22] B. G. Milov, Paper Ind. 2 (1939).

[23] W. Hisey and C. Koon, Paper Trade J. 36, 6 (1936).

[24] S. Glasstone, Introduction to Electrochemistry (Moscow, IL, 1951). p. 446 etc. [Russian translation].

[25] E. Mislowitzer, Determination of Hydrogen-Ion Concentration in Liquids (State Chem. Tech. Press, Leningrad, 1932) [Russian translation].

[26] M. Kh. Karapet'iants, Chemical Thermodynamics [in Russian] (Moscow-Leningrad, Goskhimizdat, 1953), p. 405.

[27] F. Förster, J. pr. Ch. (2), 63, 163 (1901).

[28] S. Goldschmidt, Ber. 52, 753 (1919).

[29] W. Roth, Z. Phys. Chem. A 145, 289 (1929).

[30] Bur. of Stand. circular, 500, N. Y. (1952).

[31] Gm.-Kr (Achte Auflage) 227 (1927).

[32] R. Bergquist, Svensk Pap. tidn. 30, 686 (1927).

[33] R. Bergquist, Pap. Fabr. 25, 72 (1928).

[34] K. M. Markuze, Reconstruction of the Textile Industry 5, 43 (1935).

Received July 30, 1957

*Original Russian pagination. See C.B. Translation.

COLLOIDAL STABILITY OF LITHIUM LUBRICANTS AND THE INFLUENCE OF THEIR DISPERSION MEDIA ON IT

V. V. Sinitsyn, K. I. Klimov, and E. V. Aleeva

The colloidal stability of plastic greases is one of the most interesting problems of their physical chemistry, and is very important in the practical sense. Colloidal stability of greases is the term used for their ability to retain their colloidal structure for a long time without decomposition or liberation of the liquid dispersion medium. In other words, greases which show very little separation of the liquid phase (oil), as the result of syneresis, over considerable periods of time, are termed colloidally stable.

The syneresis of plastic greases was studied by a number of Russian and foreign scientists in the 1930's. Mention must be made of the work of Herschel [1], Varentsov et al., [2, 3], Velikovskii et al., [4, 5], Farrington et al., [6], and others. An unfortunate defect of most of these investigations is the meager theoretical basis and, in some instances, unconvincing interpretation of the experimental facts; this is mainly due to the incorrect conceptions of the structure of plastic greases which were widely held at that time. The instruments and methods used in these investigations were far from perfect and, as was shown by the American National Lubricating Grease Institute and by ourselves [7], they did not provide a sufficiently accurate evaluation of the colloidal stability of greases. We devised a simple apparatus and method for estimation of the tendency of greases to undergo syneresis during storage [10], based on the modern view of the structure of greases [8, 9] regarded as spatial networks formed by the particles of the disperse phase, with the liquid dispersion medium included in them. The method is based on mechanical pressing of oil from the grease.

Trials of the method at the plants of the Ministry of the Petroleum Industry showed that it is simple, fairly accurate, and convenient in use; most important, it gives a correct evaluation of the relative colloidal stability of greases of similar types [11]. In view of the favorable results of these trials, the KSA apparatus and method were adopted as the basis for the standard method of evaluation of the colloidal stability of greases, GOST 7142-54. The existence of the KSA apparatus made it possible to study the effects of various factors on the colloidal stability of greases. Some results of studies of the influence of disperse phase concentration and the viscosity of the dispersion medium on the stability of mineral oil—sodium soap systems were published by us earlier [7]. The influence of the dispersion medium on the colloidal stability of greases was studied by a number of workers [3, 12, 13, and others]. The main conclusion to be drawn from the experimental data is that increase of the viscosity of the dispersion medium improves the stability of greases. This conclusion is consistent with the results of experience of the storage of greases [14]. Very little information is available on the influence of chemical composition or purification of the dispersion medium, and the existing statements are highly contradictory and unreliable. There are no experimental data on the relationship between the viscosity—temperature characteristics of the dispersion medium and colloidal stability of greases.

This paper presents the results of a study of the influence of chemical composition and viscosity of the dispersion medium on the colloidal stability of lithium greases.

Materials used, and method of investigation. Greases made from oils thickened with lithium stearate soap were used. The following products and their mixtures were used for preparation of the grease samples: Arctic Diesel fuel (GOST 4749-49); aviation oil MK-22 (GOST 1013-49); naphthenic hydrocarbons isolated from MS-20 oil;* organosilicon liquids (silicone oils); commercial oils: velosite (GOST 1840-51), AU spindle

*The authors thank Prof. S. E. Krein for kindly supplying the naphthenic hydrocarbons.

oil (GOST 1642-50), avtol (automobile) oil 4 (GOST 1862-42), and SU machine oil (GOST 1707-51). The viscosity of the dispersion media of the lubricants was increased by the addition of polyisobutylene of molecular weight 15,000.

Lithium stearate soap was prepared by a very convenient method described in the literature [15]. A weighed quantity of the soap, dehydrated by heating for 8 hours at 105°, was stirred into the oil at room temperature. The soap – oil suspension was heated to 210° in a closed flask with continuous stirring for about 20-30 minutes. After the soap was completely melted, as shown by complete transparency of the melt, the latter was poured onto a tray at room temperature (~20°) in a layer 5 mm thick. The grease was left for 24 hours on the tray, then rubbed through a metal 200-mesh sieve. All the greases had a neutral reaction. The colloidal stability of each grease was determined directly after the rubbing. The colloidal stability of greases was determined by the standard method, GOST 7142-54 "Greases. Method of estimation of colloidal stability."

Grease properties can be greatly influenced by small fluctuations of composition, presence of small amounts of free acid or alkali, and variations in the technological cooking process. The action of such factors may distort the influence of the conditions under investigation on the grease properties. Despite the measures taken (exact formulation, preparation of greases from preformed soap, strict cooking conditions, similar reaction of the finished greases), it was necessary to determine the extent to which incidental factors, not taken into account, influence the colloidal stability of the greases.

It was also desirable to study variations of the viscosity of the dispersion medium during grease preparation. When the melted grease is poured out, especially if it had been prepared from lighter petroleum fractions (Diesel fuel, etc.), evaporation of light fractions (up to 4-7%) takes place. The viscosity of the dispersion medium may then increase.

TABLE 1

Viscosity Variations of the Dispersion Medium During Grease Preparation

Dispersion medium	Viscosity at 20° (centistokes)			ν_t/ν_i (%)
	initial ν_i	cooked in a closed flask ν_c	poured onto tray ν_t	
Arctic Diesel fuel	4.11	4.20	7.4	180
Arctic Diesel fuel + 1.8% polyisobutylene	16.5	17.1	–	–
The same, with 4.5% polyisobutylene	50.9	53.9	81	160
The same, with 15% polyisobutylene	180	182	265	145

The most suitable method for extraction of the dispersion medium from greases without changes in their composition and properties is by expression of the oil from the grease sample by means of compressed air [12]. We used the following method. A sample of the grease (10 g) was placed in a No. 2 Schott filter. Excess pressure was created over the grease by means of compressed air (0.25-0.5 kg/cm^2). The oil pressed out of the grease flowed through the porous glass plate into a receiving tube. By this method the dispersion medium, even Diesel oil, can be extracted virtually unchanged from the grease. Data which confirm that the compressed-air method is suitable for expression of oil from greases are presented in Table 1. The dispersion medium was pressed out of four grease samples prepared under conditions in which evaporation of the oil was excluded (cooked and cooled in a closed flask). The data in Table 1 show that the viscosities of the dispersion medium pressed out of the grease, and of the original oil are almost the same. However, if the greases are made by our method(poured out onto a tray), the viscosity of the dispersion medium increases. It is seen that the increase is 50-80% of the initial viscosity of the oil. In the case of heavier dispersion media (spindle oil, mixtures of MK-22 oil with Diesel fuel, etc.), the oil losses and consequent increase of viscosity of the dispersion medium when the greases are poured out onto trays are considerably lower. In view of the considerable

viscosity changes in the dispersion media when the greases are poured out onto trays, this effect must be taken into account in discussion of the experimental results.

To test the consistency of the method used for preparation of the greases, a series of samples was prepared from the same materials. Data on the colloidal stability of greases made in parallel cooks are presented in Table 2. It follows from Table 2 that the reproducibility of the method is approximately the same for different oils, the variations being in the range of 3 to 5% of oil pressed out. The reproducibility of the colloidal stability determinations by the method used corresponds to about ±0.5% of oil pressed out.

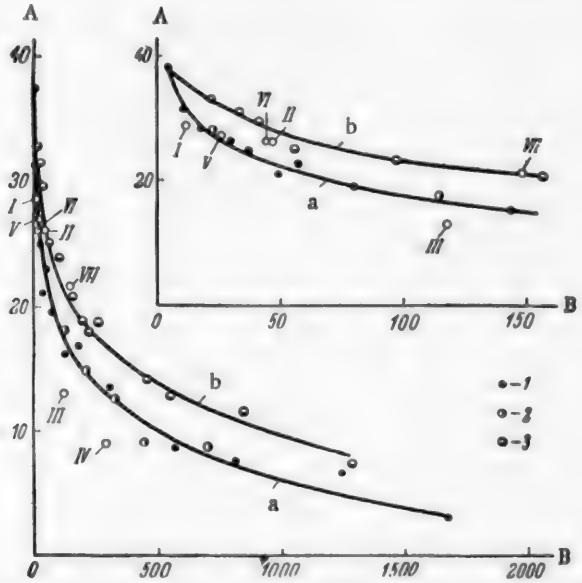

Fig. 1. Colloidal stability of lithium greases as a function of the viscosity of their dispersion media at 20°. A) Oil pressed out (%), B) oil viscosity (centistokes). Oils: I) velosite, II) spindle AU, III) avtol 4, IV) machine SU, V) MVP, VI) silicone (Sample No. 1), VII) silicone (Sample No. 2). 1) Arctic Diesel Fuel + MK-22, 2) the same + naphthenes from MS-20, 3) the same + polyisobutylene.

TABLE 2

Colloidal Stability of Lithium Greases Made in Parallel Cooks

Dispersion medium	Cook No.						Average
	1	2	3	4	5	6	
Arctic Diesel fuel	38.6	36.2	37.6	36.6	31.9	30.5	34.8
The same, with 5% polyisobutylene	30.9	27.3	21.8	22.4	22.3	–	24.9
The same, with 38% MK oil	25.1	25.3	23.5	–	–	–	24.6

For greater reliability, all the experimental data presented in this paper are based on the results of tests on not fewer than 2 or 3 parallel preparations of grease samples of the same composition. The average values obtained in such tests are given in the tables and in Figs. 1-3.

EXPERIMENTAL

For studies of the influence of the viscosity of the dispersion medium on the colloidal stability of greases, three series of samples were prepared from mixtures of Arctic Diesel fuel with different components. In addition, greases were made on the basis of commercial oils – velosite, MVP, AU spindle oil, avtol 4, SU machine oil, and two samples of organosilicon liquids of different viscosities. Data on the composition, viscosity of the dispersion media, and colloidal stability of the samples are presented in Table 3 and Fig. 1; the latter shows variations of the colloidal stability of greases with the viscosity of their dispersion media at 20°. It follows from the data in Fig. 1 and the table that increase of the viscosity of the dispersion medium improves the colloidal stability of the grease in all cases. The increase of colloidal stability is particularly pronounced if the viscosity is raised to 100-150 centistokes. Further increase of viscosity to 1700 centistokes also improves colloidal stability, but to a considerably smaller extent. It is important to note that the increase of colloidal stability with viscosity of the dispersion medium is qualitatively the same when MK-22 viscous oil is added to Diesel fuel, when pure naphthenic hydrocarbons are added, and when it is thickened by means of polyisobutylene.

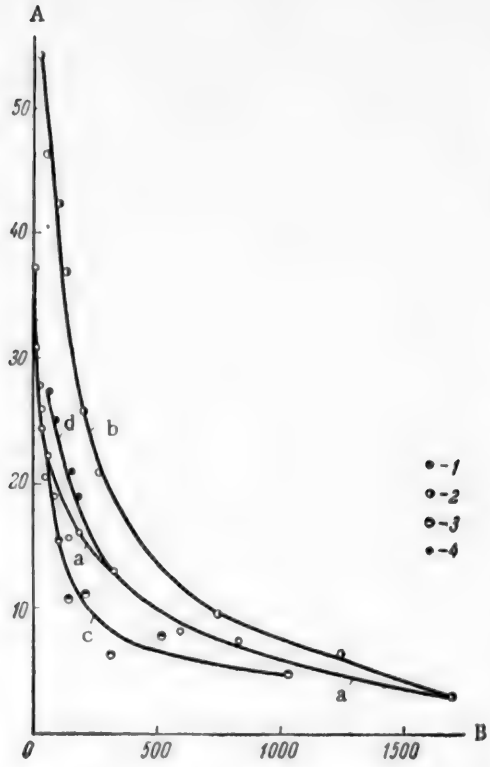

Fig. 2. Variation of the colloidal stability of lithium greases with the viscosity of their dispersion media and the temperature. A) Oil pressed out (%), B) oil viscosity (centistokes). 1) Arctic Diesel fuel + MK-22 (at constant t) 2) MK-22, 3) Arctic Diesel fuel + MK-22 (55.6%), 4) the same + MK-22 (80%), (2, 3, 4, at variable t).

Viscosity increases have a similar effect in greases made from organosilicon liquids (silicone oils) and commercial hydrocarbon oils. It follows that the colloidal stability of lithium greases containing dispersion media of different chemical nature is improved considerably by viscosity increases of the dispersion media over a very wide range (from 4 to 1700 centistokes at 20°). After the nature of the relationship between the colloidal stability of lithium greases and the viscosity of their dispersion media had been established, it was important to determine the influence of the chemical nature of the dispersion medium on grease stability. Figure 1 shows that all the systems studied fall into two fairly distinct groups. The first of these (Curve a) includes greases made from mixtures of Diesel fuel with MK-22 oil and naphthenic hydrocarbons. Greases made from commercial hydrocarbon oils (Points I-V, Fig. 1) are close to these systems in colloidal stability, although in some instances (with avtol 4 and SU machine oil) the stability is somewhat better (the comparison is made at equal viscosities of the dispersion media).

It is clear from these results that in the case of hydrocarbon oils and their mixtures with low-viscosity petroleum products (Arctic Diesel fuel) the degree of purification and origin (chemical composition) of the dispersion media have a weak influence on the colloidal stability of lithium greases. Greases based on mixtures of Diesel fuel with naphthenic hydrocarbons (MS-20 oil with polar compounds such as tars, aromatic hydrocarbons, etc., removed) do not differ in colloidal stability from greases based on mixtures containing residual MK-22 oil, or from greases based on commercial distillate oils – AU spindle oil, velosite, etc. It follows that oils of different origins and degrees of purification can be used for the production of quite stable grease, provided that other quality requirements are taken into consideration.

Greases based on Arctic Diesel fuel thickened with polyisobutylene (Curve b), and on organosilicon liquids (Points VI and VII) differ appreciably from all the others in colloidal stability. Figure 1 shows that, at the same viscosity of the dispersion media, their colloidal stability is worse than that of greases based on petroleum oils (Curve a). There is a consistent difference of 4-6% in the amounts of oil pressed out of them by the method used, over a wide viscosity range of their dispersion media. The causes of the lower colloidal stability of

TABLE 3

Characteristics of Dispersion Media and Data on the Colloidal Stability of Lithium Greases at 20°

Arctic Diesel fuel with addition of naphthenes from MK-22 oil (%)	0	30	40	47	52	54	55.6	64.3	72.7	74.6	80	90	92.5	96	100
Viscosity	4.11	11.2	18.1	30.3	37.9	48.7	57.2	80.7	145	183	326	593	829	1270	1700
Oil pressed out* (%)	37.4	30.9	27.8	26.0	24.5	20.5	22.3	19.0	15.7	16.2	13.0	8.3	7.5	6.3	3.1
Arctic Diesel fuel with addition of naphthenes from MS-20 oil (%)	0	45	75	87.4	91	95.3	100								
Viscosity	4.11	22.9	116	219	336	441	690								
Oil pressed out* (%)	37.4	28.1	18.0	14.8	12.5	9.1	8.7								
Arctic Diesel fuel with addition of polyisobutylene (%)	0	2.0	3.0	3.8	5.0	9.0	11.1	15.6	16.0	16.5	18.0	22.5	30.0	35.0	
Viscosity	4.11	21.2	33.8	40.9	56.1	96.4	157	191	223	257	461	557	848	1300	
Oil pressed out* (%)	37.4	32.4	30.8	29.5	24.9	23.7	20.9	18.9	18.1	18.7	14.2	13.1	11.7	7.4	

	Velosite	MVP	AU spindle oil	Avtol 4	SU machine oil	Organosilicon liquids	
						№ 1	№ 2
Viscosity	11.6	26.5	47.4	118	294	45.6	150
Oil pressed out* (%)	28.4	27.0	26.1	13.1	9.2	26.2	21.7

*Oil pressed out determined according to GOST 7142-54.

greases based on Diesel fuel with polyisobutylene, and on organosilicon compounds, may be revealed by an examination of the relationship between grease stability and the viscosity of the dispersion medium.

Figure 2 shows curves for the variations of the colloidal stability of lithium greases with the viscosity of their dispersion media and the temperature. Curve a was determined at 20°, for a series of greases made with mixtures of Diesel fuel and MK-22 oil, of different viscosities; it represents the dependence of the colloidal stability of greases on the viscosity of the dispersion medium under isothermal conditions (20°). Curves b, c, and d relate to grease samples made with MK-22 oil and with mixtures of Arctic Diesel fuel and MK-22 oil (55.6 and 80%) respectively. The viscosity of the dispersion medium was varied by increases or decreases of temperature during determinations of colloidal stability. It is seen that variations of the viscosity of the dispersion medium caused by temperature changes have a much greater influence on the colloidal stability of greases than those caused by changes of the medium (at constant temperature). This effect is explained as follows. As is known, temperature variations have little effect on the properties of the structural framework in greases [16]. Therefore, on the one hand, it may be assumed that if the pressing-out temperature is varied (Curves b, c, and d) only the viscosity of the dispersion medium exerts an influence, the structure of the grease being unchanged. On the other hand, formation of structure in greases during the cooking process greatly depends on the viscosity of their dispersion media. The shape, dimensions, and type of cohesion between the particles of disperse phase which constitute the structural framework of the grease are determined to a considerable extent by the viscosity of the dispersion medium during crystallization from the melt.

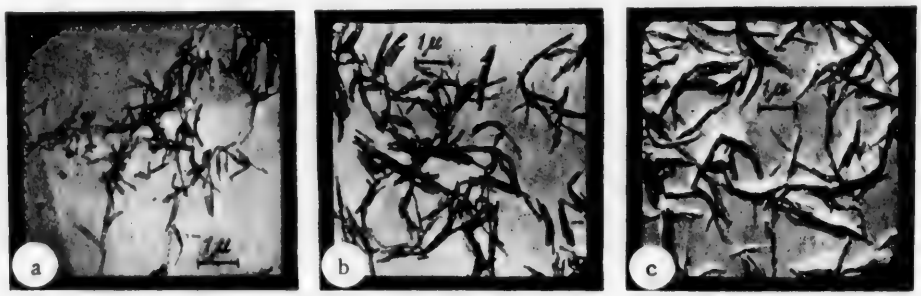

Fig. 3. Electron micrographs of the structure of lithium greases. A) Diesel fuel + MK (55.6%) at $\nu_{20°}$ = 57.2 centistokes, b) the same + MK (90%) at $\nu_{20°}$ = 593 centistokes, c) MK-22 at $\nu_{20°}$ = 1,700 centistokes.

For elucidation of the influence of the viscosity of the dispersion medium on the colloidal stability of greases, we carried out, jointly with S. A. Gol'din, an electron microscope investigation of grease structure. Figure 3 shows electron micrographs of three grease samples, made with mixtures of Diesel fuel with MK oil and with pure MK oil. It is seen that increase of the viscosity of the dispersion medium results in diminished dispersity of the thickener soap fibers. It is evident that the coarser structure of greases made with viscous oils has lower thickening power. The experimental data in Fig. 2 also show that with dispersion media of higher viscosity the structure of greases is less perfect with regard to colloidal stability. Thus, under test conditions ($t° \neq$ const), the highest colloidal stability is found in greases in which the viscosity of the dispersion medium is lower at the temperature of structure formation. This nature of the relationship between the colloidal stability of greases and the viscosity of their dispersion media fully accounts for the worse stability of greases made with organosilicon liquids and with Diesel fuel containing polyisobutylene additive. Such dispersion media have flat viscosity – temperature curves. Therefore, at the temperatures at which the grease structure is formed, their viscosity is considerably higher than that of usual hydrocarbon oils or mixtures of Diesel fuel with viscous oils. Deterioration of the structurization conditions (higher viscosity of the medium) results in decreased colloidal stability of lithium greases made from Diesel fuel with polyisobutylene additive, or from organosilicon compounds, as compared with ordinary mineral oils.

The relationship between the colloidal stability of lithium greases and the viscosity – temperature characteristics of their dispersion media ($\nu_{20°} \approx$ const) is given on the next page.

Dispersion medium	$\nu_{20°}$ (centistokes)	$\nu_{20°} / \nu_{100°}$	Stability M (%)
Avtol 4	118	21.2	13.1
Diesel fuel + MK-22 (72%)	151	19.8	15.7
Diesel fuel + naphthenes (75%)	109	16.3	18.0
Silicone oil (No. 2)	150	6.0	21.7
Diesel fuel + polyisobutylene (8.9%)	150	4.5	20.9

It may be seen that, on the one hand, the most stable grease is that made with avtol 4, with the highest ratio of viscosities at 20 and 100°. On the other hand, greases made with dispersion media with flat viscosity–temperature characteristics (silicone oil, Diesel fuel + polyisobutylene) are the least stable. Despite the fact that greases containing polyisobutylene or silicone oils have lower colloidal stability, it does not necessarily follow that these dispersion media are not suitable for the production of quite stable low-temperature greases. It is known that these oils have very flat viscosity–temperature curves. Therefore, if such oils and ordinary hydrocarbon oil with the same viscosity at −50° are taken, the viscosity of the latter at ordinary temperatures would be much lower. Therefore the colloidal stability of a grease made with ordinary petroleum oil may be the same as, or even less than, that of greases made with oils thickened with polyisobutylene, or with silicone liquids.

The foregoing can be readily illustrated by an example. A mixture of Diesel fuel and MK-22 oil (56%) has a viscosity of 690 centistokes at −50°. The viscosity of Diesel fuel containing 16.5% polyisobutylene is 100 centistokes at −50°. A grease made with the latter oil would have better low-temperature properties. Nevertheless, because of the considerable viscosity decrease of the dispersion medium with increase of temperature, greases based on mixtures of Diesel fuel with MK-22 have lower colloidal stability; the amounts of oil pressed out are 22.3 and 18.7% respectively. An even more convincing example is provided by a comparison of these dispersion media with a commercial oil, AU spindle oil (often used in the production of low-temperature greases). The viscosity of this oil at −50° is 2880 centistokes, and the amount of oil pressed out is 26.1%.

SUMMARY

1. The colloidal stability of plastic greases made by the thickening of various liquid oils (petroleum oils; mixtures of Diesel fuel with oils, naphthenic hydrocarbons, and viscosity additives; organosilicon compounds), varying in viscosity ($\nu_{20°}$ = 4– 1700 centistokes), with lithium stearate soap has been studied; it was found that the colloidal stability of the lithium greases is improved by increase of the viscosity of the dispersion medium in all cases. The colloidal stability depends especially strongly on viscosity at relatively low viscosities of the dispersion medium ($\nu_{20°}$ < 100 – 200 centistokes).

2. Variations of the viscosity of the dispersion medium as the result of temperature changes have a greater influence on the colloidal stability of greases than do changes of the dispersion medium at the same temperature (with greases made from oils of different viscosities).

3. Electron microscope investigations showed that increase of the viscosity of the dispersion medium results (under equal conditions) in an increase in the average fiber size of the thickener (lithium soap) and a decrease of the thickening power of the disperse phase.

LITERATURE CITED

[1] W. H. Herschel, Proceedings ASTM, 33, 1, 349 (1933).

[2] V. P. Varentsov and E. D. Leonova, Petroleum Economy 1, 50 (1938).

[3] E. L. Al'perovich and V. P. Varentsov, Trans. Central Scientific Research Inst. of Aviation Fuels and Oils 1, 297 (1941).

[4] D. S. Velikovskii, Lubricant Greases [in Russian] (State Fuel Tech. Press, 1945).

[5] D. S. Velikovskii and I. P. Lukashevich, Trans. Gubkin Petroleum Inst. Moscow 2, 259 (1940).

[6] B. B. Farrington and R. L. Humphreys, Ind. Eng. Ch. 31, 2, 230 (1939).

[7] K. I. Klimov, et al., Petroleum Economy 11, 62 (1954).

[8] B. B. Farrington and D. H. Birdsall, Oil and Gas J. 45, 46, 268 (1947).

[9] G. V. Vinogradov, Progr. Chem. 21, 6, 758 (1952).

[10] K. I. Klimov, et al., Author's Certif. No. 99049, Class 421, 7/03.

[11] K. I. Klimov, et al., Factory Labs. 21, 1, 106 (1955).

[12] T. G. Roehner and R. C. Robinson, Oil and Gas J. 43, 29, 76 (1944).

[13] B. W. Hotten and D. H. Birdsall, Ind. Eng. Ch. 47, 3, 1, 447 (1955).

[14] V. V. Sinitsyn and E. V. Aleeva, Petroleum Processing 6 (1955).

[15] A. A. Trapeznikov, Author's Certif. No. 66893, Class 120, 11.

[16] G. V. Vinogradov and K. I. Klimov, Proc. Acad. Sci. USSR 71, 2, 307 (1952).

Received June 5, 1956

EFFECT OF pH ON THE OXIDATION–REDUCTION POTENTIAL OF A SOLUTION CONTAINING FERRIC AND FERROUS IONS

O. N. Lapteva

The A. I. Gertsen Pedagogic Institute, Leningrad

The literature contains numerous descriptions of determinations of the standard potential of the equilibrium [1-15]

$$Fe^{\cdot\cdot} \rightleftharpoons Fe^{\cdot\cdot\cdot} + e. \qquad (1)$$

However, the values of $\varphi^{\circ}_{Fe^{\cdot\cdot\cdot}/Fe^{\cdot\cdot\cdot}}$ reported by different authors differ considerably (from 0.735 to 0.782 v). The effects of pH on the oxidation–reduction potential of the system ferric ions–ferrous ions–aqueous medium have been studied much less [16-18]. The literature data on the solubility product of ferric hydroxide also differ considerably. The values given by different authors for the solubility product of ferric hydroxide differ by ten orders of magnitude ($10^{-36} - 10^{-46}$) [19, 20].

In view of the great practical importance of aqueous systems containing ferric and ferrous ions, we carried out a series of potentiometric investigations of the potentials of such systems at different pH values.

The results are presented below.

EXPERIMENTAL

Special attention was devoted to purity of the reagents and removal of oxygen from the solutions. Distilled water and sulfuric acid (chemically-pure grade) were subjected to two further distillations. The salts (chemically pure) were recrystallized twice. The redistilled water used for preparation of the solutions was boiled for an hour, and then cooled in a stream of nitrogen, purified as described below. Crystalline sodium hydroxide (chemically pure) was dissolved in the minimum volume of water in a cylinder with a ground-glass stopper, and then left for a considerable time to allow carbonates to settle. When required, the solution was removed by means of a pipet and diluted with distilled water, from which oxygen had been previously removed by a current of nitrogen. The alkali concentration was determined by titration. Ferric sulfate was stored in solution form.

The systems for investigation, which initially contained mixtures of ferric and ferrous sulfates, were prepared by the solution of weighed quantities of anhydrous ferrous sulfate in definite volumes of water, followed by addition of calculated amounts of ferric sulfate solution. The final composition of the solutions was determined by analysis. The concentrations of ferric and ferrous ions were determined by titration with potassium dichromate before and after reduction of ferric ions by zinc in an acid medium. The ferric ion concentration was found from the difference between the first and second titrations. Sulfate was determined gravimetrically or by Freze's method [21]. The analytical data were used to determine the ionic strength of the solution, and the activities of $Fe^{\cdot\cdot}$ and $Fe^{\cdot\cdot\cdot}$ ions were found from the Debye and Hückel formula.

A series of experiments was carried out with solutions of different initial contents of ferric and ferrous ions. The characteristics of these solutions are given on next page.

Ratio		I	II	III
Molar concentrations	$\frac{C_{Fe^{\cdots}}}{C_{Fe^{\cdot\cdot}}}$	$\frac{0.01}{0.01}$	$\frac{0.05}{0.01}$	$\frac{0.001}{0.001}$
activities	$\frac{a_{Fe^{\cdots}}}{a_{Fe^{\cdot\cdot}}}$	0.103	0.210	0.210

The cell used for the experiments was a flask 200 ml in capacity. The flask was covered by a lid into which was sealed a bulb-shaped glass electrode; a funnel with a tap for addition of alkali was inserted into the lid. A platinum electrode, a bridge containing saturated potassium chloride solution (for contact between the half cells), and a nitrogen inlet tube, were introduced into the cell through side tubes. All the joints were ground glass. Nitrogen was prepared by decomposition of ammonium nitrite, and was stored in gas holders containing ferrous hydroxide in aqueous and precipitated form. Before the nitrogen entered the cell it was purified further to remove traces of oxygen; for this, it was passed through a tubular furnace containing freshly-reduced copper at 350°, and through several flasks with ferrous hydroxide. To fill the cell with the test solution and simultaneously to remove air from the cell, the solution was displaced from its storage vessel into the cell by means of a stream of nitrogen. Nitrogen was passed continuously and fairly rapidly into the solution during the experiment. The cell, prepared as described above, was placed in an air thermostat maintained at 25°. The emf was determined by the compensation method. The reference electrode was a saturated calomel half cell. The hydrogen exponent was calculated from the results of determinations of the glass-electrode potential by means of an electronic potentiometer. The oxidation potentials were measured with the aid of a platinum electrode by means of a high-resistance potentimeter to an accuracy of 1 mv.

As already stated, the original systems were solutions of ferrous and ferric sulfates, and therefore the potentials determined in them with the aid of the platinum electrode corresponded to Equilibrium (1). The pH and oxidation potential of the system corresponding to the transition from one equilibrium to another on gradual addition of caustic soda solution to the original system could be determined by means of potentiometric determinations. As the result of a large number of experiments it was established that up to about pH = 5.0 the potential becomes stable within a few minutes. At higher pH the potential fluctuations are considerable, and the equilibrium becomes established progressively more slowly; at the same time, the system becomes very sensitive to oxygen. In such systems the potential measurements were sometimes continued for several days.

Principal Electrochemical Equilibria in the Systems Studied, and their Characteristics

The initial pH values of Solutions I, II, and III were 1.64, 0.97, and 2.45 respectively. They contained sulfuric acid in definite excess, added to suppress hydrolysis. On addition of alkali solution, the oxidation potential changed very little at first. This is consistent with the hypothesis that here Equilibrium (1) is applicable, in which hydrogen ions are not involved. However, when definite pH values are reached, 2.2, 2.4, and 2.7 respectively for solutions I, II, and III, a light brown precipitate of ferric hydroxide began to form, and the potential began to change in a quite regular manner with increase of pH. This can be represented by the following equilibrium:

$$Fe^{\cdot\cdot} + 3H_2O \rightleftharpoons Fe(OH)_3 + 3H^{\cdot} + e. \qquad (2)$$

At pH above 7.0 the precipitate changed color, and became black. This indicates the formation of a new phase, magnetic iron oxide, in the system.* The regular variation of potential with changes of pH under the new conditions indicates that under these conditions the potential is determined by the following equilibrium:

$$3Fe^{\cdot\cdot} + 4H_2O \rightleftharpoons Fe_3O_4 + 8H^{\cdot} + 2e. \qquad (3)$$

Thus, in the system studied, three electrochemical equilibria determining the potential of the platinum electrode — (1), (2), and (3) — are encountered as the pH changes.

*The dried black precipitate was attracted by a magnet.

TABLE 1

Data for Calculation of Standard Potential in the System: $Fe^{++} \rightleftharpoons Fe^{+++} + e$; Molar Concentration of $SO_4^{=}$ is 0.04

Molality		pH	$\sqrt{\mu}$	$^1a_{Fe^{++}}$	$^1a_{Fe^{+++}}$	$a_{Fe^{++}}$	$a_{Fe^{+++}}$	$\frac{a_{Fe^{+++}}}{a_{Fe^{++}}}$	$\lg \frac{a_{Fe^{+++}}}{a_{Fe^{++}}}$	Expt'l value of φ_{redox} (v)	Calc. value of φ°_1 (v)
$m_{Fe^{++}}$	$m_{Fe^{+++}}$										
0.00949	0.00922	1.64	0.391	0.160	0.0163	0.00147	0.000155	0.105	—0.98	0.681	0.738
		1.42	0.400	0.154	0.0148	0.00142	0.000149	0.105	—0.98	0.682	0.738
		1.54	0.394	0.158	0.0158	0.00146	0.000146	0.102	—0.99	0.685	0.743
		1.61	0.391	0.160	0.0163	0.00147	0.000150	0.102	—0.99	0.683	0.741
0.00977	0.00877	1.47	0.398	0.155	0.0151	0.00143	0.000143	0.100	—1.0	0.678	0.736
0.00977	0.00877	1.51	0.396	0.157	0.0155	0.00145	0.000147	0.101	—1.0	0.679	0.737
0.00947	0.00903	0 78	0.386	0.164	0.0172	0.00151	0.000162	0.108	—0.97	0.682	0.739

Selected values are given in Tables 1, 2, and 3. The average values of the standard potentials were calculated from all the experimental data.

Table 1 contains results of determinations of the oxidation potentials in solution I in a strongly acid medium, and calculated standard potentials for Equilibrium (1).

The average value of the standard potential for Equilibrium (1) was found to be 0.738 v. Our value differs considerably from those given in certain modern reference books [22, 23].

One possible cause of this discrepancy might be insufficient accuracy in calculations of the ion activities at equilibrium. We did not extrapolate to zero concentrations, as is often done in such investigations [24], because this graphical device always involves an element of uncertainty, especially if data for low concentrations are lacking. In particular, such extrapolation for the system ferric ions—ferrous ions—water, performed by Brey and Herchey [7; 22, p. 367] where the last experimental point was determined for $\sqrt{\mu} \approx 0.24$, is dubious. Extrapolation to zero ionic strength, a device used by Schumb, Scherrill, and Sweetser [8], who obtained the value of $\varphi^{\circ} = 0.782$ v, is actually based on the the use of a somewhat modified equation derived from the Debye and Hückel theory. This method also requires data on potentials at very low ionic strengths; here, as is noted by Latimer, the experimental errors are very considerable [22, p. 368]. It was therefore preferred to calculate the activities for our systems by means of the theoretical equation of Debye and Hückel, which is valid for very dilute solutions, on the assumption that under the conditions of our experiments its use involves relatively smaller errors. Indeed, the modified equation, generally recommended for moderately dilute solutions, gives values of φ°_1 which differ little from those calculated by means of the simpler equation, but are even lower than the latter.

It must also be pointed out that all our determinations were performed in a nitrogen atmosphere, and the influence of oxygen was therefore excluded. Hydrolysis of the ferric salt was suppressed by special addition of acid; according to Hedstrom [25], it could not give rise to errors.

Our value of φ°_1, found to be 0.738 v, while different from the data in the above sources [22, 23], is close to the average value of φ°_1, 0.745 v, found by most workers [1-15]. The experimental values of the potentials and the calculated standard potentials of Equilibria (2) and (3) are given in Table 2. The average standard potentials of Equilibria (2) and (3) are 0.908 and 1.206 v respectively. These values, and data from thermodynamic tables [22, 26], were

used to calculate the standard changes of free energy in the formation of $Fe(OH)_3$ and Fe_3O_4; these were found to be −169.21 and −232.10 kcal/mole respectively. In addition, the experimental data were used to calculate $\log a_{Fe(OH)_3}$, which represents the activity of ferric hydroxide in its saturated solution. Some of these results are given in Table 3.

TABLE 2

Data for Calculation of Standard Potentials in the Systems: $Fe^{++} + 3H_2O \rightleftharpoons Fe(OH)_3 + 3H^+ + e$ and $3Fe^{++} + 4H_2O \rightleftharpoons Fe_3O_4 + 8H^+ + 2e$. Molal concentration of SO_4^{--} is 0.04

pH	Molality $m_{Fe^{++}}$	$\sqrt{\mu}$	$\gamma a_{Fe^{++}}$	$a_{Fe^{++}}$	$\lg a_{Fe^{++}}$	Expt'l φ_{redox} (v)	φ°_2 (v)	φ°_3 (v)
2.36	0.00922	0.317	0.227	0.00209	−2.68	0.661	0.917	—
2.54		0.316	0.228	0.00210	−2.68	0.639	0.926	—
2.87		0.315	0.229	0.00211	−2.68	0.580	0.925	—
3.86		0.314	0.230	0.00212	−2.68	0.414	0.933	—
6.65		0.314	0.230	0.00212	−2.68	−0.137	—	1.184
2.70		0.314	0.230	0.00212	−2.68	0.600	0.915	—
4.38		0.314	0.230	0.00212	−2.68	0.312	0.921	—
6.42		0.314	0.230	0.00212	−2.68	−0.064	0.902	1.203
6.73	0.00877	0.314	0.230		−2.68	−0.109		1.230
7.60		0.314	0.230		−2.68	−0.207	—	1.196
8.00		0.314	0.230		−2.68	−0.443	—	1.194

TABLE 3

Calculations of the Average Values of the Logarithm of the Activity of Ferric Hydroxide, from Experimental Data

Solution	pH	pOH	$-3\lg C_{OH^-}$	$\lg a_{Fe^{+++}}$	$\lg a_{Fe(OH)_3}$
I	2.36	11.77	−35.31	− 4.00	−39.31
	4.43	9.70	− 29.10	−10.17	−39.27
	2.70	11.43	−34.29	− 5.05	−39.34
	4.75	9.38	− 28.14	−11.3	−39.44
	6.42	7.71	− 23.13	−16.4	−39.53
	6.73	7.40	−22.20	−17.16	−39.68
II	2.94	11.19	−33.57	− 5.85	−39.42
	2.59	11.64	−34.62	− 4.95	−39.57
	3.01	11.12	− 33.36	− 6.0	−39.36
	5.56	8.57	−25.71	−13.44	−39.15
	4.60	9.53	− 28.59	−10.87	−39.46

It follows from the calculated values that the average value of $\log a_{Fe(OH)_3}$ is −39.43. The value of $\Delta Z^\circ_{Fe(OH)_3}$ found from this, −169.21 kcal/mole, is in good agreement with direct electrochemical experimental data. Finally, the calculated values of $\Delta Z^\circ_{Fe(OH)_3}$ and $\Delta Z^\circ_{Fe_3O_4}$ were used to calculate the standard potentials of the equilibria:

$$Fe_3O_4 + OH^- + 4H_2O \rightleftharpoons 3Fe(OH)_3 + e \quad (4)$$

$$3Fe + 8OH^- \rightleftharpoons Fe_3O_4 + 4H_2O + 8e. \quad (5)$$

The standard potentials and changes of isobaric potentials of the electrochemical equilibria are given on next page:

Equilibrium	φ° (v)	ΔZ° (kcal/mole)
$Fe^{\cdot\cdot} \rightleftharpoons Fe^{\cdot\cdot\cdot} + e$	0.738	17.02
$Fe^{\cdot\cdot} + 3H_2O \rightleftharpoons Fe(OH)_3 + 3H^{\cdot} + e$	0.908	20.78
$3Fe^{\cdot\cdot} + 4H_2O \rightleftharpoons Fe_3O_4 + 8H^{\cdot} + 2e$	1.206	55.59
$Fe_3O_4 + OH^{\cdot} + 4H_2O \rightleftharpoons 3Fe(OH)_3 + e$	−0.490	−11.84
$3Fe + 8OH^{\cdot} \rightleftharpoons Fe_3O_4 + 4H_2O + 8e$	−0.863	−159.26

I thank Professor A. I. Shultin for help in the present investigation.

SUMMARY

1. The effect of pH in the range from 1.5 to 11.0 on the oxidation–reduction potential of the system ferric ions–ferrous ions–aqueous medium was studied; it was found that precipitation of ferric hydroxide begins at pH from 2.2 to 2.7, according to activity ratio of $Fe^{\cdot\cdot\cdot}$ and $Fe^{\cdot\cdot}$ ions.

2. The standard changes of free energy of the system in formation of ferric hydroxide and magnetic iron oxide have been calculated, and found to be −169.21 kcal/mole and −232.10 kcal/mole respectively.

The value of log $a_{Fe(OH)_3}$ in saturated solutions is −39.43.

LITERATURE CITED

[1] R. Peters, Z. phys. Ch. 26, 193 (1898).

[2] W. Meitland, Z. Elektroch. 12, 263 (1906).

[3] A. Noyes and B. Brann, J. Am. Soc. 34, 1016 (1912).

[4] Gerke, Chem. Rev. 1, 388 (1925).

[5] S. Popoff and Kunz, J. Am. Chem. Soc. 51, 382 (1929).

[6] S. Popoff, W. Fleharty and E. Hanson, J. Am. Chem. Soc. 53, 1643 (1931).

[7] W. Brey and A. Herchey, J. Am. Chem. Soc. 56, 1889 (1934).

[8] W. Schumb, M. Scherrill and S. Sweetser, J. Am. Chem. Soc. 59, 2630 (1937).

[9] G. Smith and C. Getz, Ind. Eng. Ch. 10, 191 (1938).

[10] G. Smith and F. Richter, Ind. Eng. Ch. 16, 580 (1944).

[11] D. Bezier, Ann. Chim. 20, 161 (1945).

[12] E. N. Gapon, J. Phys. Chem. 20, 1028 (1946).

[13] S. Bagchi, J. Indian. Ch. Soc. 27, 4 (1950).

[14] R. Connick and M. McVey, J. Am. Chem. Soc. 73, 1798 (1951).

[15] L. Magnusson and J. Huizenga, J. Am. Chem. Soc. 75, 2242 (1953).

[16] M. Quintin, Compt. rend. 232, 1303 (1951).

[17] D. Bezier, Compt. rend. 216, 798 (1943).

[18] P. A. Kriukov and G. P. Avseevich, Trans. Leningrad Div. All-Union Sci. Res. Inst. 17, 135 (1933).

[19] E. Müller, Das Eisen und seine Verbindungen. Dresden (1917).

[20] N. Elder, Trans. Am. E ektroch. Soc. 57, 383 (1930).

[21] N. A. Freze, Factory Labs. 10-11, 1181 (1939).

[22] W. M. Latimer, Oxidation States of the Elements and Their Potentials in Aqueous Solutions [Russian translation] (IL, 1954), p. 229.

[23] Natl. Bur. Standards Circular 500 (1952).

[24] M. Randall and W. Vietti, J. Am. Chem. Soc. 50, 1526 (1928).

[25] Hedström, Arkiv Kemi, 1-2, 1 (1953).

[26] M. Pourbaix, Thermodynamique des Solutions Aqueuses Diluées (Delft, 1945).

Received April 20, 1957

DETERMINATION OF THE INTERPHASE AREA IN EMULSIONS

A. V. Ianishevskii and I. S. Pavlushenko

The Lensoviet Technological Institute, Leningrad

Unstable emulsions are very often encountered in practice. Rapid and reasonably accurate determinations of the dispersity of such systems involve considerable difficulties.

A method and apparatus which offer a relatively simple solution to this difficult problem are described in this paper.

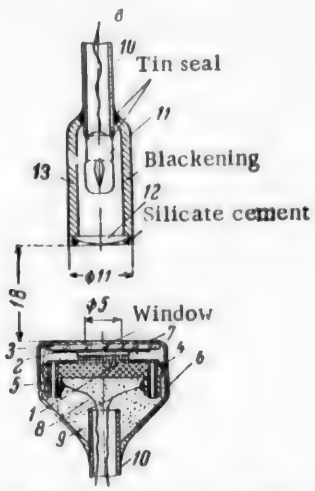

Fig. 1. Light probe. 1) FS-K1 photocell, 2) light filter, 3) glass, 4) panel, 5 and 6) contacts, 7) casing with window, 8) conductors, 9) filler (wax, plaster of Paris, etc.) 10) tube 5 × 0.5, 11) lamp, 12) lens, 13) casing of light source.

Every emulsion is a system consisting of a medium of definite optical density, and scattering centers – disperse phase droplets – distributed fairly uniformly in it. A parallel light beam encountering an individual droplet is refracted, i.e., "scattered."

If the diameter of the scattering centers is of the same order of magnitude as the wavelength of the incident light (or less than the latter), the scattering properties of the droplets are strongly dependent on the wavelength The greater the droplet diameter, the less does scattering depend on wavelength. The influence of dispersion on the scattering of a parallel beam by a spherical droplet is even less if the light is monochromatic.

The above effect occurs in absence of optical absorption. This means in practice that the dispersion medium and disperse phase must be colorless liquids which do not contain metal salts [1].

The optical properties of emulsions have been studied for a long time by a number of workers [2-5]. Bailey, Nichols, and Kraemer [4] confirmed experimentally that light absorption is a measure of the light-scattering power of a dispersion. Moreover, they showed that the absorption intensity depends on the concentration of the disperse phase and the refractive indices of the liquids constituting the disperse phase and the dispersion medium. Subsequent work by La Mer [6] and Langlois, Gullberg, and Vermeulen [7] has made it possible to determine the dispersity of emulsions from their light scattering.

As was stated above, the absorption of a monochromatic parallel beam by an emulsion depends on the refractive indices of the disperse phase and the dispersion medium, and the magnitude of the interphase area at which the light scattering actually occurs. Research has shown that the graphical relationship between these variables is represented by a straight line corresponding to the equation

$$\Phi_0/\Phi = aS + 1, \tag{1}$$

and hence

$$S = \frac{\Phi_0/\Phi - 1}{a}, \tag{2}$$

where S is the specific interfacial area (in cm^2/cm^3 of phase);* Φ_0 and Φ are relative quantities characterizing the intensities of a beam after passing through a layer of pure dispersion medium and a similar layer of emulsion; a is a slope factor, which depends on tan α; tan $\alpha = \varphi(K)$ is the tangent of the angle between the straight line and the abscissa axis; $K = \frac{n_p}{n_m}$ is the ratio of the refractive indices of the disperse phase and the dispersion medium.

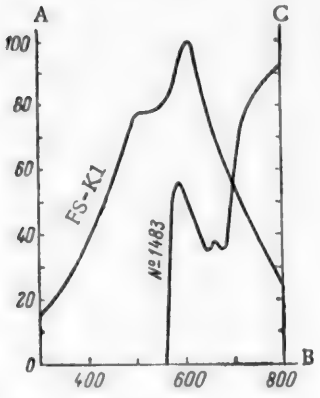

Fig. 2. Characteristics of FS-K1 photocell and light filter No. 1483. A) Photocurrent of FS-K1 (%), B) wavelength (mμ), transmission of light filter No. 1483 (%).

The above relationship is valid at a definite concentration of the disperse phase. Change of concentration must influence the interfacial area and hence the ability of the emulsion to absorb light. However, the specific interfacial area, which depends only on the dispersity, may remain constant with change of concentration.

At any degree of dispersion, the total area of the droplets of the disperse phase (the interfacial area) is proportional to the number of droplets, i.e., the concentration. This fully accounts for the experimental relationship

$$a = \frac{C}{C_0} \cdot \tan \alpha \qquad (3)$$

where C is the volume concentration of the disperse phase in the emulsion studied; C_0 is the corresponding value for an emulsion for which tan α is determined.

Substitution of the value of a into Equation (2) gives

$$S = \frac{\Phi_0/\Phi - 1}{\frac{C}{C_0} \cdot \tan \alpha}. \qquad (4)$$

The dispersity can also be expressed in terms of droplet diameter. Division of the droplet surface by its volume gives

$$S = \frac{6}{D}, \qquad (5)$$

and hence

$$D = \frac{6}{S}. \qquad (6)$$

It should be noted that unstable emulsions are markedly polydisperse [7]. The diameters of coexisting droplets may differ 10 to 15-fold. It is therefore more convenient to express the dispersity of emulsions in terms of the interfacial area and not of the average diameter, which is a very indefinite concept because of the high polydispersity.

EXPERIMENTAL

The apparatus for measurement of emulsion dispersity consists of a light source and a device for measurement of the intensity of the light beam. The apparatus, which we have named the "light probe," is shown schematically in Fig. 1. The small FS-K1 photoresistor was used as a photoelectric cell. In order to reduce the dimensions of the photoresistor, the projecting portions of the panel were removed and the contacts shortened. The characteristics of the photocell, which has high selectivity, are given in Fig. 2. The light filter No. 1483, made in the Dyes Department of the Lensoviet Technological Institute of Leningrad, was placed immediately in front of the photocell in order to protect it from heat emitted by the light source. The characteristics of the light filter are given in Fig. 2. The characteristics of the photocell after correction by means of the light filter are given in Fig. 3. The maximum sensitivity of the photocell is very close to the sodium

*Note the difference between this quantity and the usual expression for specific surface.

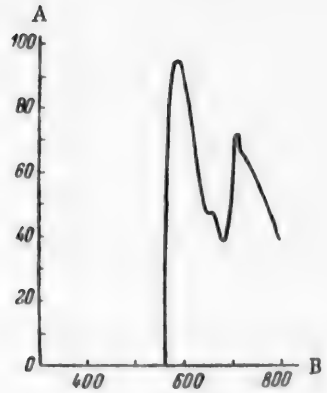

Fig. 3. Characteristics of photocell with light filter. A) Photocurrent of FS-K1 (%), B) wavelength (mμ).

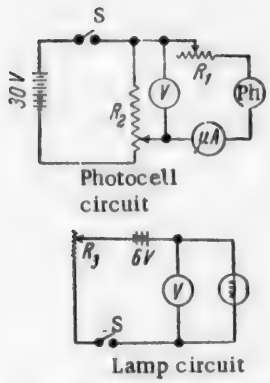

Fig. 4. Circuit diagrams.

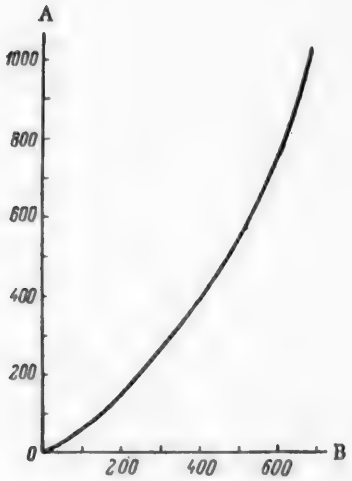

Fig. 5. Variation of the photocurrent (I) with the relative illumination $\Phi = \frac{1}{L^2}$. A) Light intensity Φ, B) photocurrent I (in ma).

line (5721 A). It is therefore permissible to substitute the refractive indices of the phase and medium measured against the sodium line, i.e., by means of the ordinary refractometers, into the expression $K = \frac{n_p}{n_m}$.

The aim in construction of the probe was to ensure the minimum dimensions, good streamlining, airtightness, and resistance to active solvents. The casing of the photocell was therefore made by electrolytic deposition of copper, while the joint between the lens and the casing of the light source was sealed with dental silicate cement.

The photocell and lamp circuits are shown in Fig. 4. The direct-current source consisted of high-capacity storage batteries, so that there were no voltage fluctuations in the circuits during operation. Constancy of the voltage was checked by means of voltmeters (testers of type TT-1), and the photocurrent was measured by means of a microammeter (MA-750). The voltage of the photocell circuit was maintained at 24 v.

Plotting of calibration curves. Compact photocells of the semiconductor type, which are considerably more sensitive than phototubes, have the important disadvantage that the relationship between the illumination and the photocurrent is not linear. Figure 5 is a plot of the illumination against the photocurrent for the FS-K1 photocell with the No. 1483 light filter. Since Equation (4) includes only the ratio of light intensities, the units in which these are measured do not influence the final result. The relationship in Fig. 5 is based on the law of inverse squares. Here the light source may be of any intensity, but the voltage in the photocell circuit must be of the nominal value (24 v in this instance).

The most difficult and vital part of the work is determination of the tan $\alpha = \varphi(K)$ relationship. The following relatively stable emulsions were used for this purpose: 1) water–petrolatum; 2) ligroine–glycerol; 3) mixture of octane with carbon tetrachloride–glycerol; 4) octane–glycol; 5) glycerol–petrolatum; 6) petrolatum–glycol; 7) mixture of octane with carbon tetrachloride–aqueous gelatin solution; 8) benzene–aqueous gelatin solution; 9) styrene–aqueous gelatin solution. The value of K varied from 0.899 to 1.156. The disperse-phase concentration (C_0) of all the emulsions was 10%.

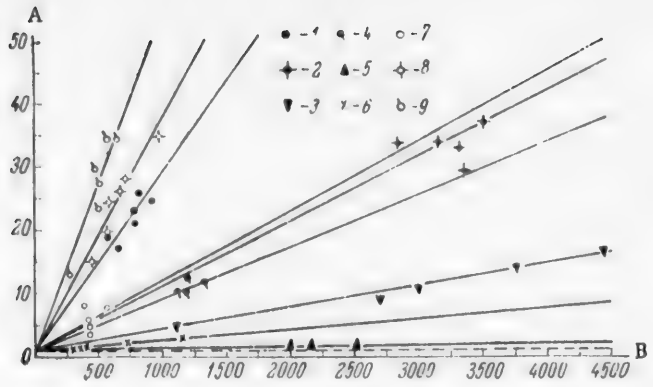

Fig. 6. Relationship between relative absorption of light (Φ_0/Φ) and specific interfacial area (S) at constant concentration of the disperse phase. A) Relative light absorption Φ_0/Φ, B) specific interfacial area S (cm^2/cm^3).

For determination of the tan $\alpha = \varphi(K)$ relationship, the pure liquid which was the dispersion medium was put into a vessel with a stirrer, shielded from external light. The probe was inserted and the photocurrent I_0 was measured. The graph in Fig. 5 was used to determine the corresponding value of Φ_0. The disperse phase was then added and the stirrer started. After the system had reached a steady state, the photocurrent I'_1 was measured, and the corresponding value of Φ'_1 found. At the same time a drop of the emulsion was removed and placed on a slide under a binocular microscope. The drop was photographed under the microscope at different magnifications. The stirrer speed was then increased, and I''_1, I'''_1 etc. and the corresponding values of Φ for different dispersities of the system were found. All nine emulsions were investigated as described. It should be noted that the values of the photocurrents I_0, I'_1, I''_1, I'_2, I''_2 etc., are the same whether the emulsion is in motion or stationary.

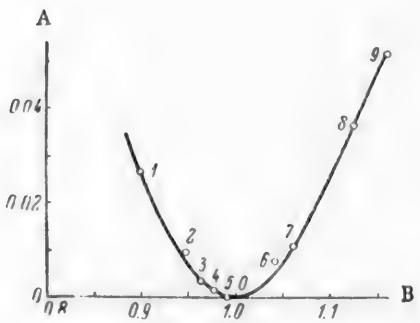

Fig. 7. Variation of tan α with the refractive indices of the liquids constituting the dispersion medium and the disperse phase. A) Tan α, B) ratio of refractive indices $K = \frac{n_p}{n_m}$.

The photographs were used to determine the average droplet diameters (the diameters of droplets of average volume). The specific interfacial area was then calculated and Φ_0/Φ was plotted against S. The result is presented in Fig. 6. Here $\underline{a}$ = tan α, because C = C_0 (Equation 3). The average value of $\underline{a}$ was taken from the graph. The refractive indices of the liquids forming the disperse phase and dispersion medium were measured by means of a refractometer, and the values of K_1, K_2, K_3, etc. were found. The results were then used to plot tan α against K, as shown in Fig. 7. Points 2 and 6 do not show a good fit, because of the relative instability of ligroine–glycerol and petrolatum–glycol emulsions, and of the insufficient enlargement when the microphotographs were taken. The scale of the graph in Fig. 6 was taken into account when Fig. 7 was plotted. The form of the curve depends on the characteristics of the light source and filter, the selectivity of the photocell, the voltage of the photocell circuit, etc.

Determination of emulsion dispersity. The following steps are necessary to determine the dispersity of any emulsion formed from colorless liquids: 1) find the value of $\underline{a}$ (Equation 3) from the emulsion parameters (C, n_p, n_m) and the tan α–K graph; 2) determine I_0 and I experimentally, and use the $I - \Phi_0/\Phi$ graph to find the corresponding values of Φ_0 and Φ; 3) calculate the interfacial area S (Equation 2).

When the probe is used, it should be remembered that the equations proposed for calculation were confirmed experimentally for emulsions containing from 10 to 40% of disperse phase by volume.

SUMMARY

1. The proposed method for determination of emulsion dispersity differs from that described in the literature by considerably higher sensitivity and simplicity of calibration.

2. The primary instrument ("light probe") of small dimensions can be constructed from standard units and components.

3. The proposed method and apparatus can be widely used for investigation of various heterogeneous systems (emulsions, suspensions, foams, mists, etc.).

LITERATURE CITED

[1] V. L. Ginsburg, Light Filters [in Russian] (ONTI, 1936).

[2] G. Meszaros, Z. Unters. Lebensm. 69, 321 (1935).

[3] T. Katsurai, Kolloid Z. 74, 287 (1936).

[4] E. D. Bailey, J. B. Nichols and E. O. Kraemer, J. Phys. Chem. 40, 1149 (1936).

[5] W. Clayton, Theory of Emulsions and Their Technical Treatment (Moscow, IL, 1950) [Russian translation].

[6] V. La Mer, Chem. Revs. 44, 245 (1949).

[7] G. E. Langlois, J. E. Gullberg and T. Vermeulen, Rev. Sci. Instr. 25, 360 (1954).

Received July 5, 1957

LIQUID–VAPOR EQUILIBRIUM IN THE BINARY MIXTURES ETHYL ALCOHOL–ISOPROPYL ALCOHOL AND CARBON DISULFIDE–METHYL IODIDE

G. A. Gaziev, Ia. D. Zel'venskii, and V. A. Shalygin

The present communication contains the results of liquid–vapor equilibrium studies of two binary systems: ethyl alcohol–isopropyl alcohol, and methyl iodide–carbon disulfide.

EXPERIMENTAL

Equilibrium was determined by the known single-evaporation method, based on the fact that the so-called "equilibrium still" yields a condensate the composition of which is equal to the composition of the vapor in equilibrium with liquid in another part of the apparatus. The composition was determined from the refractive index, which was measured by means of the IRF-23 refractometer to an accuracy of $3\text{-}5 \cdot 10^{-5}$. A calibration curve for the refractive index against the composition of the mixture was first determined by the gravimetric method.

The equilibrium still (Fig. 1) used in the work was a somewhat modified version of the apparatus described by Bushmakin [1]. The lower part of the apparatus, which acted as the evaporator, was fitted with an external electric heating coil. The vapor rose from the evaporator up the central tube, which was surrounded by vapor of the same liquid. This arrangement excluded both partial condensation and overheating of the vapor.

The working capacity of our apparatus was 130-140 ml of liquid. At an evaporation rate of about 100 drops per minute, the time to reach equilibrium did not exceed 30-45 minutes after the receiver had been filled with condensate.

The equilibrium still was previously tested with the system acetic acid–water, with chemical analysis of the equilibrium phases; good agreement with literature data was obtained.

The boiling points of the mixtures were determined by means of the ebulliometer shown in Fig. 2. The upper portion of the ebulliometer was large enough to contain a standard thermometer (TLN type) with a 0-50° or 50-100° scale. The apparatus was first tested and corrections determined, by means of redistilled water, cryoscopic benzene, and anhydrous diethyl ether. Operating conditions were found in which the thermometer readings are not dependent on the heating rate.

The materials used were obtained by thorough purification and drying of the commercial products (Table 1).

The System Ethyl Alcohol–Isopropyl Alcohol

The results of preliminary determinations of the refractive index as a function of the mixture composition at 20° are given in Table 2.

These results show that the actual refractive indices differ appreciably from the values calculated by the additivity rule.

Our experimental values for the boiling points of mixtures of ethyl and isopropyl alcohols at atmospheric pressure are given on next page.

Ethyl alcohol content (molar %)	0	1.7	20.7	30.5	34.7	47.0	58.1	69.7	86.60	100
Boiling point (°C)	82.45	82.3	81.4	81.0	80.8	80.3	79.85	79.4	78.65	78.35

Liquid–vapor equilibrium for mixtures of ethyl and isopropyl alcohols was investigated by the method described above, at atmospheric pressure in the concentration range of 18 to 92 molar % of ethyl alcohol (Table 3). The special method with the use of radioactive tracers, used for studies of dilute solutions of isopropyl alcohol in ethyl alcohol, is described in another paper [5].

Values of the separation coefficient

$$\alpha = \frac{y(1-x)}{(1-y)x}. \qquad (1)$$

are given in Column 3, Table 3.

In the range of 20 to 92% of ethyl alcohol, the separation coefficient may be regarded as approximately constant, with an average value of 1.078 ± 0.018.

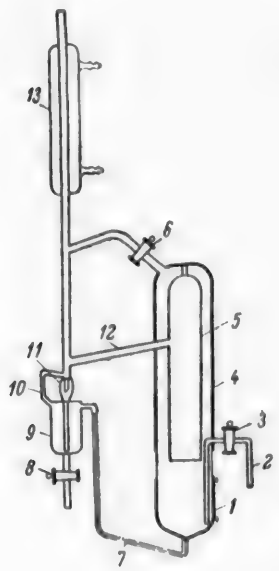

Fig. 1

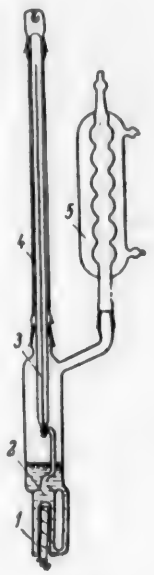

Fig. 2

Fig. 1. Equilibrium still. 1) Evaporator, 2) tube, 3) stopcock, 4) external insulation, 5) inner tube, 6) stopcock for displacement of air from system in discharge, 7) capillary tube for liquid circulation, 8) stopcock for taking condensate samples, 9) condensate receiver, 10) tube, 11) dropper for estimation of evaporation rate, 12) connecting tube, 13) condenser.

Fig. 2. Ebulliometer. 1) Electric heater, 2) evaporator, 3) standard thermometer, 4) thermometer jacket, 5) condenser.

This value differs appreciably from the vapor pressure ratio of the pure components (equal to the separation coefficient or relative volatility of an ideal solution).

Thus, at the boiling point of ethyl alcohol $\frac{P^{\circ}_{eth}}{P^{\circ}_{ipr}} = 1.161$,* and at the boiling point of isopropyl alcohol $\frac{P^{\circ}_{eth}}{P^{\circ}_{ipr}} = 1.169$.*

*Calculated from data in [4] and [6].

TABLE 1

Properties of the Substances Used

Substance	This investigation		Literature data	
	refractive index at 20°, n_D^{20}	normal boiling point (°C)	refractive index at 20°, n_D^{20}	normal boiling point (°C)
Ethyl alcohol	1.36245	78.35	1.36242 [2]	78.37 [2]
Isopropyl alcohol	1.37730	82.45	1.3776 [2]	82.5 [3]
Carbon disulfide	1.62738	46.30	1.6276 [4]	46.3 [2]
Methyl iodide	1.53030	42.50	1.5293 [4]	42.50 [2]

Figures 3 and 4 are t–x and y–x phase diagrams for the system ethyl alcohol–isopropyl alcohol, plotted from the experimental data.

Thermodynamic verification (conformity to the Gibbs–Duhem equation) of the experimental equilibrium data for the system ethyl alcohol–isopropyl alcohol was unsuccessful, probably because of deviation of the vapor phase from the ideal gas laws.

Investigation of liquid–vapor equilibria of binary mixtures of ethanol with methanol, normal and secondary butanol, and pentanol showed that ethyl alcohol does not form azeotropes with the other alcohols [7]. Our data for mixtures of ethyl and isopropyl alcohol are in agreement with this result.

TABLE 2

Refractive Indices of Ethyl–Isopropyl Alcohol Mixtures

Composition (molar % of ethyl alcohol)	Refractive index n_D^{20}		Composition (molar % of ethyl alcohol)	Refractive index n_D^{20}	
	experimental	calc. by additivity rule		experimental	calc. by additivity rule
100	1.36245	1.36245	58.88	1.36950	1.36856
91.97	1.36396	1.36364	51.02	1.37072	1.36950
85.42	1.36515	1.36462	39.80	1.37225	1.37139
77.22	1.36658	1.36583	30.70	1.37352	1.37274
62.46	1.36895	1.36802	13.96	1.37551	1.37523
61.21	1.36908	1.36821	0	1.37730	1.37730

The System Methyl Iodide–Carbon Disulfide

The results of preliminary determinations of the refractive index of mixtures of methyl iodide and carbon disulfide at 20° are given in Table 4.

The results obtained for the boiling points and equilibrium compositions of the liquid and vapor phases of the system $CH_3I–CS_2$ under atmospheric pressure are given in Tables 5 and 6 respectively.

These data were used to plot t–x and y–x diagrams (Figs. 5 and 6).

According to literature data, methyl iodide forms an azeotropic mixture with carbon disulfide; according to Lecat [8] this mixture contains 44.53 molar % methyl iodide, b. p. 41.55°; Horsley [9] gives b. p. 46.6°.

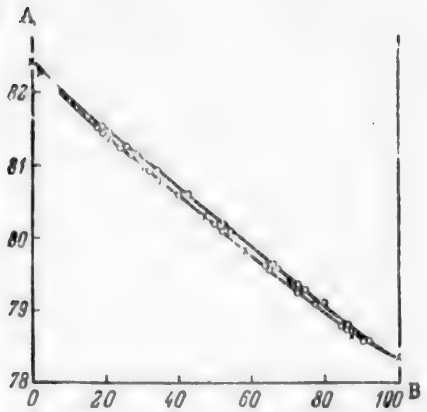

Fig. 3. Boiling points of mixtures of ethyl and isopropyl alcohols at atmospheric pressure. A) Boiling point (°C), B) composition of solution x (molar % C_2H_5OH).

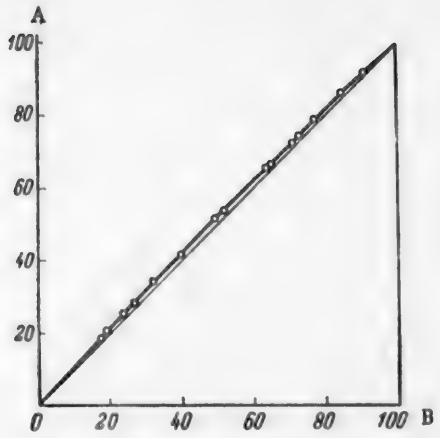

Fig. 4. Equilibrium compositions of vapor and liquid in the system ethyl alcohol–isopropyl alcohol at atmospheric pressure. A) Vapor composition y (molar % C_2H_5OH), B) liquid composition x (molar % C_2H_5OH).

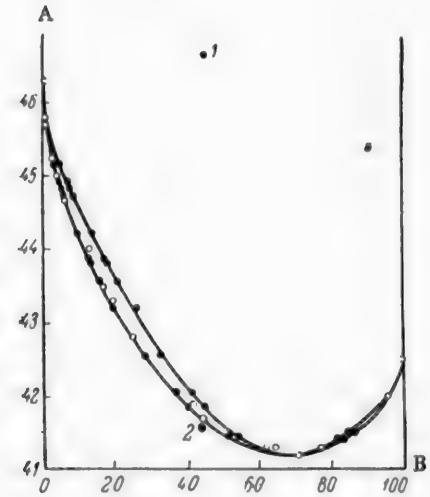

Fig. 5. Boiling points of mixtures of methyl iodide and carbon disulfide at atmospheric pressure. A) Boiling point (°C), B) composition of solution x (molar % CH_3I). 1) Horsley's data, 2) Lecat's data.

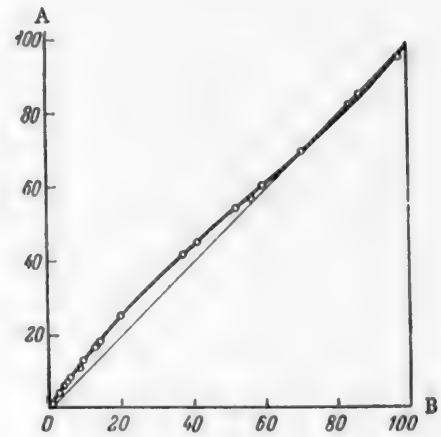

Fig. 6. Equilibrium compositions of vapor and liquid in the system methyl iodide–carbon disulfide. A) Vapor composition y (molar % CH_3I), B) liquid composition x (molar % CH_3I).

The tables and graphs show that by our results methyl iodide and carbon disulfide form an azeotrope containing 70 ± 1 molar % CH_3I, of minimum boiling point 41.2°.

For comparison with the experimental data, it was of interest to carry out calculations by means of Kireev's formula [10]

$$\frac{1}{x_2} = \sqrt{\frac{\log P_0 - \log P_2^0}{\log P_0 - \log P_1^0}} - 1, \qquad (2)$$

TABLE 3

Equilibrium Composition of Vapor and Liquid Phases of Isopropyl–Ethyl Alcohol Mixture

Ethyl alcohol content (molar %)		Separation coefficient $\alpha = \frac{y(1-x)}{(1-y)x}$	Ethyl alcohol content (molar %)		Separation coefficient $\alpha = \frac{y(1-x)}{(1-y)x}$
in liquid, x	in vapor, y		in liquid, x	in vapor, y	
91.45	92.00	1.075	50.00	51.79	1.074
85.32	86.20	1.075	39.97	41.70	1.074
77.50	79.20	1.105	32.40	33.80	1.065
72.96	74.60	1.089	26.70	28.20	1.078
70.91	72.30	1.071	23.74	25.40	1.094
65.27	67.10	1.085	19.60	20.50	1.058
64.00	65.65	1.075	18.35	19.00	1.044
52.10	53.90	1.075			

TABLE 4

Refractive Indices of Methyl Iodide–Carbon Disulfide Mixtures

Composition of mixture	Refractive index n_D^{20}		Composition of mixture	Refractive index n_D^{20}	
(molar % of methyl iodide)	experimental	calc. by additivity rule	(molar % of methyl iodide)	experimental	calc by additivity rule
0.00	1.62738	1.62738	23.78	1.60276	1.60429
0.543	1.62658	1.62685	27.02	1.59949	1.60115
1.26	1.62588	1.62615	30.37	1.59618	1.59790
2.53	1.62448	1.62492	34.76	1.59228	1.59363
4.46	1.62244	1.62305	44.61	1.58273	1.58407
6.49	1.62039	1.62108	61.15	1.56672	1.56892
8.53	1.61830	1.61910	67.16	1.55340	1.55306
13.34	1.61326	1.61443	72.58	1.55613	1.54692
20.88	1.60609	1.60711	89.96	1.54007	1.54014
21.59	1.60489	1.60642	100.00	1.53030	1.53030

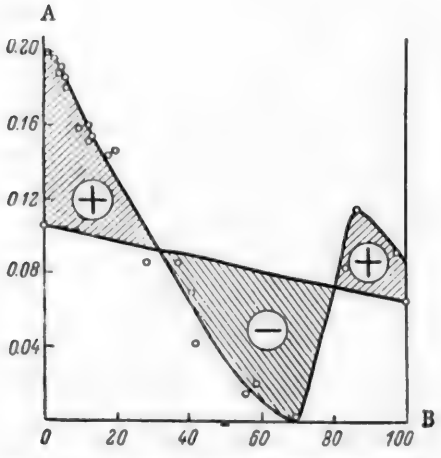

Fig. 7. Thermodynamic verification of the experimental data. A) Log α, B) liquid composition x (molar % CH_3I).

where x_2 is the content of the volatile component in the azeotropic mixture, P_1^0 and P_2^0 are the saturated vapor pressures of the pure components at the boiling point of the azeotrope, and P_0 is the total pressure.

The value of x_2 (methyl iodide content) calculated by means of this formula was 71.5%, which is in good agreement with our experimental data.

The experimental liquid–vapor equilibrium data for the system methyl iodide–carbon disulfide were subjected to a thermodynamic check.

According to Redlich and Kister [11], the following condition should hold:

$$\int_0^1 \log \frac{\gamma_1}{\gamma_2}\, dx_1 = 0, \qquad (3)$$

where γ_1 and γ_2 are the activity coefficients of the components.

TABLE 5

Boiling Points of Methyl Iodide–Carbon Disulfide Mixtures Atmospheric Pressure

Methyl iodide content (molar %)	0	0.3	0.45	2.40	3.85	6.02	10.10	12.24	16.47	19.08
Boiling point (°C)	46.3	45.8	45.7	45.25	45.0	44.7	44.25	44.0	43.50	43.3

TABLE 5 (continued)

Methyl iodide content (molar %)	24.90	41.40	44.10	62.00	64.50	70.99	77.13	96.04	100
Boiling point (°C)	42.8	41.9	41.7	41.3	41.3	41.20	41.28	42.0	42.5

If the vapor phase is assumed to be an ideal gas, we have

$$\gamma_1 = \frac{P_0 \cdot y_1}{P_1^0 \cdot x_1} \text{ and } \gamma_2 = \frac{P_0 \cdot y_2}{P_2^0 \cdot x_2}, \tag{4}$$

and hence, from (3) and (4)

$$\int_0^1 \left(\log \alpha - \log \frac{P_1^0}{P_2^0} \right) dx = 0. \tag{5}$$

Equation (5) may be represented graphically by the area contained by the abscissa axis and the curves for $\log \alpha$ and $\log \left(\frac{P_1^0}{P_2^0} \right)$ as functions of x. This graph, plotted from our data, is given in Fig. 7.

If the area is taken as positive when $\log \alpha > \log \left(\frac{P_1^0}{P_2^0} \right)$, and negative when $\log \alpha < \log \left(\frac{P_1^0}{P_2^0} \right)$ then, by Equation (5), the algebraic sum of the areas should be zero in the range of x from 0 to 100.

In Fig. 7 the positive and negative areas differ by 0.4%, and therefore the experimental data are in good agreement with the thermodynamic Equation (3).

TABLE 6

Equilibrium Composition of Vapor and Liquid Phases of Methyl Iodide–Carbon Disulfide Mixtures at Atmospheric Pressure

Methyl iodide content (molar %)		Separation coefficient	Methyl iodide content (molar %)		Separation coefficient
in liquid, x	in vapor, y	$\alpha = \frac{y(1-x)}{(1-y)x}$	in liquid, x	in vapor, y	$\alpha = \frac{y(1-x)}{(1-y)x}$
0.95	1.50	1.586	19.56	25.47	1.400
2.80	4.33	1.571	28.23	32.43	1.220
4.14	6.27	1.548	36.81	41.51	1.218
4.80	7.29	1.559	40.56	44.51	1.175
5.56	8.81	1.539	51.56	53.95	1.101
5.71	8.41	1.516	55.72	56.50	1.033
9.67	13.35	1.439	58.76	59.95	1.050
12.51	16.84	1.416	69.96	70.03	1.003
12.57	17.20	1.445	83.43	82.15	1.213
13.00	17.58	1.427	86.17	85.08	1.301
13.65	17.97	1.385	97.59	97.03	1.239

SUMMARY

1. The refractive indices, boiling points, and liquid–vapor equilibria have been determined for mixtures of ethyl and isopropyl alcohols; it was found that this mixture does not form azeotropes.

2. The refractive indices, boiling points and liquid–vapor equilibria have been determined for mixtures of methyl iodide and carbon disulfide. It was found that methyl iodide and carbon disulfide form an azeotrope with b. p. 41.2°, containing 70 ± 1 molar % CH_3I. These results are in agreement with values found by calculation from Kireev's equation, but not with literature data, which must be regarded as erroneous.

LITERATURE CITED

[1] I. N. Bushmakin and E. D. Voeikova, J. Gen. Chem. 19, 9, 1615 (1949).•

[2] Handbook of Chemistry and Physics, 33rd edn. (New York, 1952).

[3] D. R. Stull, Vapor Pressures of Individual Substances (IL, 1949) [Russian translation].

[4] Chemist's Reference Book [in Russian], II (Goskhimizdat, 1952).

[5] Ia. D. Zel'venskii and V. A. Shalygin, J. Phys. Chem. 31, 7, 1501 (1957).

[6] G. Parks and M. Barton, J. Am. Chem. Soc. 50, 25 (1928).

[7] L. Hellwig and M. Winkle, Ind. Eng. Ch. 45, 3, 624 (1953).

[8] M. Lecat, Tables azeotropiques 1, 406 (1949).

[9] L. Horsley, Azeotropic Data (Moscow, IL, 1951) [Russian translation].

[10] V. A. Kireev, J. Phys. Chem. 15, 4, 481 (1941).

[11] O. Redlich and A. Kister, Ind. Eng. Ch. 40, 345 (1948).

Received November 19, 1956

•Original Russian pagination. See C.B. Translation.

THE USE OF DIENOLS AS "HARDENING" ACCELERATORS FOR UNSATURATED POLYESTER RESINS

R. K. Gavurina, A. V. Mitrofanova, and N. S. Dmitrieva

Accelerators (activators) are generally used for "hardening" of unsaturated polyester resins at room temperatures. Different substances, belonging to different classes of chemical compounds, are used as accelerators, they include amines and their derivatives, resinates, oleates, and naphthenates of manganese and cobalt, and other compounds [1-4].

It is reported in the literature that any given accelerator acts only in conjunction with a quite definite catalyst, i.e., it acts selectively [2-4]. Therefore accelerators must be chosen in pairs with catalysts. Among the pairs most commonly recommended are: a) benzoyl peroxide and dimethylaniline; b) 1-hydroxy-1'-hydroperoxide – dicyclohexyl peroxide, referred to in brief as cyclohexyl hydroperoxide, with driers; c) methyl ethyl ketone hydroperoxide and driers.

The action mechanism of each such pair is specific. Recent investigations shed some light on this problem.

According to Horner et al., [5], benzoyl peroxide reacts with dimethylaniline according to the equation

$$PhCOOOCOPh + PhN(CH_3)_2 \rightarrow PhCOO^{\cdot} + [Ph^{\cdot}N^{+}(CH_3)_2]PhCOO^{-}. \quad (1)$$

In the opinion of these authors, the polymerization process is initiated by both types of radical formed. However, according to later work by Imoto et al., [6], only benzoate radicals initiate polymerization; this was confirmed by the fact that nitrogen could not be detected in the polymers either spectroscopically or analytically.

The interaction of hydroperoxides with driers is somewhat more complex.

Kern and Willersinn [7], who studied autoxidation of unsaturated compounds in presence of hydroperoxides and organometallic compounds, concluded that an oxidation–reduction system is formed

$$ROOH + Me^{+} \rightarrow RO^{\cdot} + Me^{++} + OH^{-}, \quad (2)$$

$$ROOH + Me^{++} \rightarrow ROO^{\cdot} + Me^{+} + H^{+}. \quad (3)$$

Reaction (3) is slower than (2), and is therefore the determining step. Similar conclusions were reached by other workers [8, 9]. The free radicals formed in Reactions (2) and (3) cause formation of active centers in polymerization.

The present work consisted of a study of the possible use of dienols as hardening accelerators for unsaturated polyester resins. The investigations described in the Experimental section show that dienols are active accelerators in conjunction both with peroxide and with hydroperoxide catalysts.

According to Dolgoplosk [9], the reaction of dienols with hydroperoxides can be represented as

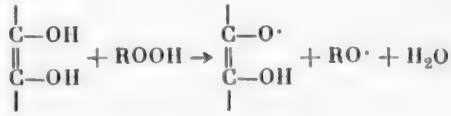

$$+ ROOH \rightarrow$$

$$+ RO^{\cdot} + H_2O \quad (4)$$

with liberation of free radicals; this accounts for their accelerating action.

EXPERIMENTAL

The compounds used in the study of dienols as accelerators of the copolymerization (hardening) of unsaturated polyester resins were ascorbic and dihydroxymaleic acids.

For elucidation of the selective action of these accelerators, they were used in conjunction with catalysts both of the peroxide and of the hydroperoxide type.

Five systems were studied: 1) benzoyl peroxide–ascorbic acid, 2) benzoyl peroxide–dihydroxymaleic acid, 3) cyclohexyl hydroperoxide–ascorbic acid, 4) cyclohexyl hydroperoxide–dihydroxymaleic acid, 5) cumene hydroperoxide–ascorbic acid.

The experiments were performed with two types of unsaturated polyester resins – ethylene glycol maleate–adipates (shortly, "adipates") and ethylene glycol maleate–phthalates (shortly, "phthalates").

The formulations of the polyester resins (in moles) are given below.

Components	Phthalates	Adipates
Ethylene glycol	1.1	1.1
Maleic anhydride	0.5	0.6
Phthalic anhydride	0.5	–
Adipic acid	–	0.4

The monomer used for copolymerization was styrene, 30% on the weight of the polyester being added. The polyesters were synthesized under the usual conditions, i.e., at 190-200° without catalysts or solvents, in a stream of inert gas (nitrogen or carbon dioxide). The course of esterification was indicated by the acid numbers. Phthalates of acid number 40-50 mg KOH per g, and adipates of acid number approximately 30 mg KOH per g, were used for the experiments.

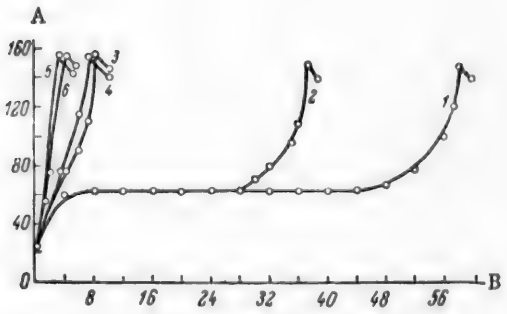

Fig. 1. Effect of the amount of ascorbic acid on the hardening of phthalates (hardened in presence of benzoyl peroxide at 64°). A) Temperature (°C), B) time (minutes). Amount of ascorbic acid (%): 1) 0, 2) 0.002, 3) 0.006, 4) 0.01, 5) 0.02, 6) 0.09.

Inhibitor (0.02% of hydroquinone) and part of the styrene was added to the freshly prepared resin. The mixture was stirred to yield a homogeneous mass, and kept in that form. Directly before the experiment the catalyst (1% on the weight of polyester), dissolved in a second portion of styrene, was added to a weighed portion of the mixture. The accelerator was added after brief stirring of the mixture in the cold. In view of the fact that ascorbic acid is insoluble in styrene, it was introduced in the form of solution in a mixture of ethanol and tricresyl phosphate. A 1% solution of ascorbic acid in ethanol was first prepared, and this was then diluted with a 7-fold volume of tricresyl phosphate. Freshly prepared solutions of ascorbic acid were used. Dihydroxymaleic acid was also introduced in solution form. The mixture with the accelerator was stirred for 4-5 minutes, and then poured into test tubes in which the hardening took place. The test tubes were previously coated on the inside with polyvinyl alcohol or silicone varnish. In all the experiments the hardening was carried out at two temperatures: at 64± 0.5°, and at room temperature.

The hardening process at 64° was studied by means of exothermic curves. The method used for plotting these curves is described in an earlier paper [4]. In cold hardening, it was in some instances difficult to determine the exothermic curves, as the process was very protracted and sometimes lasted several days. Therefore two other characteristics were used for the cold-hardening process – time of gel formation, and peeling time.

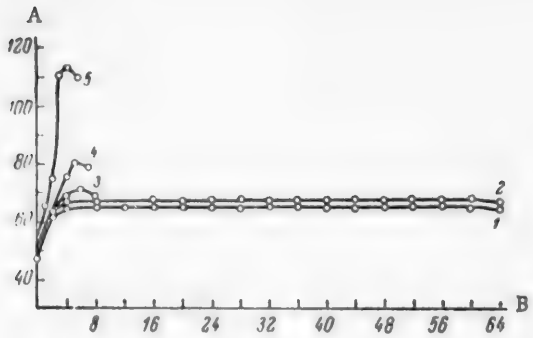

Fig. 2. Effect of the amount of ascorbic acid on the hardening of adipates (hardened in presence of benzoyl peroxide at 64°). A) Temperature (°C), B) time (minutes). Amount of ascorbic acid (%): 1) 0, 2) 0.006, 3) 0.01, 4) 0.02, 5) 0.09.

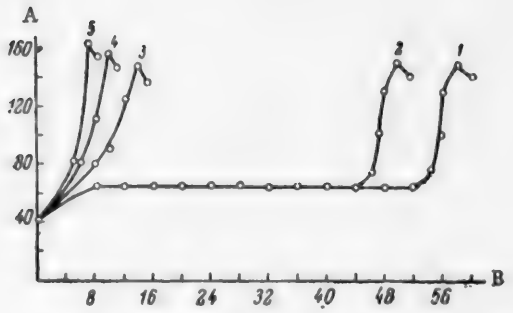

Fig. 3. Effect of the amount of dihydroxymaleic acid on the course of exothermic curves (hardening in presence of benzoyl peroxide at 64°). A) Temperature (°C), B) time (minutes). Amount of dihydroxymaleic acid (%): 1) 0, 2) 0.006, 3) 0.01, 4) 0.02, 5) 0.09.

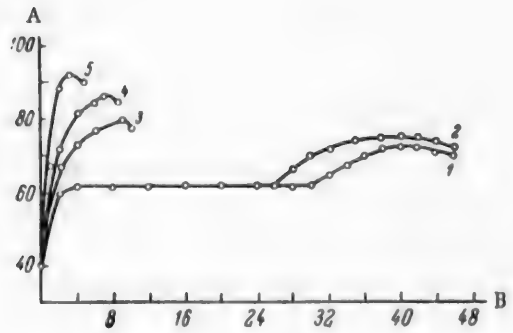

Fig. 4. Effect of the amount of ascorbic acid on the course of exothermic curves (hardening in presence of cyclohexyl hydroperoxide at 64°). A) Temperature (°C), B) time (minutes). Amount of ascorbic acid (%): 1) 0, 2) 0.006, 3) 0.01, 4) 0.02, 5) 0.09.

The time of gel formation was determined from the ascent of an air bubble. The time between the instant when the accelerator was added and the instant when an air bubble in an inverted standard test tube containing the resin could not ascend from the bottom of the tube was defined as the time of gel formation. The peeling time represented the time necessary for conversion of the resin into a hard state; it was determined visually from the distinctly visible peeling of the resin from the rube walls.

In the first two series of experiments benzoyl peroxide was used as catalyst and ascorbic acid as accelerator. The experimental results for two types of resin – phthalates and adipates – are given in Figs. 1 and 2 and Table 1.

The results show that ascorbic acid, in conjunction with benzoyl peroxide, is a highly effective accelerator which greatly shortens the hardening time; the

TABLE 1

Effect of Ascorbic Acid in Cold Hardening
Catalyst – 1% Benzoyl Peroxide

Am't of accel. (% on polyester)	Phthalates		Adipates	
	time of gel formation	peeling time	time of gel formation	peeling time
0.09	10 min	1.5 hrs.	10 min.	2 hrs.
0.02	1 hrs.	2 hrs.	1 hrs.	2.5 hrs.
0.01	2 hrs.	5 hrs.	2 hrs.	8 hrs.
0.006	4.5 hrs.	9 days	2 days	4 days
0.002	6 hrs.	12 days	—	—
0	16 days	20 days	2.5 days	4.5 days

accelerating effect is intensified with increase of the amount of ascorbic acid. This is especially prominent in the cold-hardening experiments, in which the time of gel formation was shortened from 16 days to 10 minutes for phthalates, and from 2.5 days to 10 minutes for adipates. There is an interesting difference in the behavior of the two types of resin. Whereas in the case of phthalates the induction period is greatly shortened while the height of the peaks on the isothermic curves remains almost unchanged by addition of ascorbic acid, in the case of adipates there is a distinct raising of the peaks.

TABLE 2

Effects of Ascorbic and Dihydroxymaleic Acids in Cold Hardening Catalyst – 1% Cyclohexyl Hydroperoxide

Amt. of accel. (% on polyester)	Ascorbic acid		Dihydroxmaleic acid	
	time of gel formation	peeling time	time of gel formation	peeling time
0.09	10 min.	1.5 hrs.	1 hr.	16 hrs.
0.02	20 min.	2.5 hrs.	3 hrs.	34 hrs.
0.01	30 min.	8—16 hrs.	3.5 hrs.	36 hrs.
0.006	2 days	6 days	14 hrs.	43 hrs.
0	2 days	6.5 days	2 days	6.5 days

TABLE 3

Effect of Ascorbic Acid on the Hardening of Phthalates in Absence of Catalysts

Amt. of accel. (% on polyester)	Hardening at 64°		Cold hardening	
	time to reach exothermic max. (gel formation)	maximum heat evolution (°C)	time of gel formation	peeling time
0.02	18 min.	72	30 hrs.	40 hrs.
0.01	25 min.	69	36 hrs.	48 hrs.
0	more than 2 days	—	more than 3 months	—

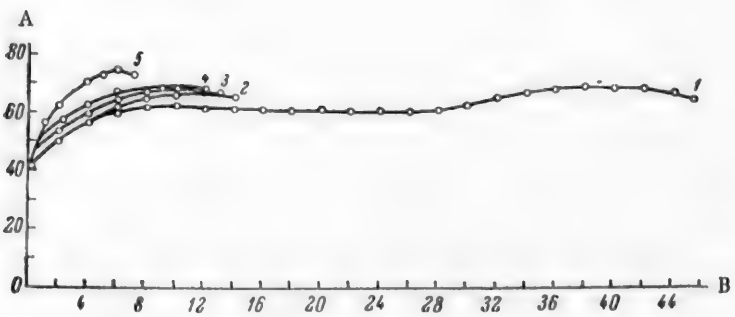

Fig. 5. Effect of the amount of dihydroxymaleic acid on the course of exothermic curves (hardening in presence of cyclohexyl hydroperoxide at 64°). A) Temperature (°C), B) time (minutes). Amount of dihydroxymaleic acid (%): 1) 0, 2) 0.006, 3) 0.01, 4) 0.02, 5) 0.09.

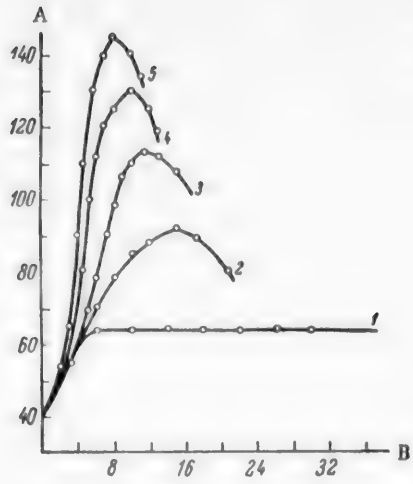

Fig. 6. Effect of the amount of ascorbic acid on the course of exothermic curves (hardening in presence of cumene hydroperoxide at 64°). A) Temperature (°C), B) time (minutes). Amount of ascorbic acid (%): 1) 0.005, 2) 0.01, 3) 0.2,* 4) 0.03, 5) 0.04.

Phthalates were used in the experiments on the accelerating effect of dihydroxymaleic acid in conjunction with benzoyl peroxide. The results of experiments on cold hardening are summarized below, and the exothermic curves are presented in Fig. 3.

Amount of accelerator (% on polyester)	Time of gel formation	Peeling time
0.09	2.5 hrs.	12 hrs.
0.02	3 hrs.	15 hrs.
0.01	7 days	14 days
0.006	8 days	15 days
0	16 days	20 days

It follows from these results that dihydroxymaleic acid has the same effect as ascorbic, i.e., it is also an active accelerator. In the next two series of experiments cyclohexyl hydroperoxide was used as catalyst. The experiments were performed on phthalates with the use of both accelerators – ascorbic and dihydroxymaleic acids. The results are given in Figs. 4 and 5, and Table 2.

In the case of cyclohexyl hydroperoxide both the accelerators showed the same activity as in the case of benzoyl peroxide. The absence of any selective action by accelerators of the dienol group was confirmed with another catalyst, cumene hydroperoxide. The experiments were performed on phthalates with the use of ascorbic acid.

The results of the cold-hardening experiments are presented below, and the exothermic curves for hardening at 64° are given in Fig. 6.

Amount of accelerator (% on polyester)	Time of gel formation	Peeling time	Maximum heat evolution (°C)
0.04	1.5 hrs.	5 hrs.	33
0.03	2 hrs.	7 hrs.	27
0.02	2.5 hrs.	8.5 hrs.	24
0.01	4 hrs.	18 hrs.	22
0.005	9 days	12 days	–
0	20 days	25 days	–

The experiments with cumene hydroperoxide provide additional confirmation of absence of any selective action of the accelerators studied. They proved active in conjunction with all the catalysts tested, both of the peroxide and of the hydroperoxide type.

It is interesting to note that ascorbic acid,** even in absence of catalysts, has a strong accelerating effect on the hardening of unsaturated polyesters; this is illustrated by the experimental data in Table 3. Similar results were obtained by us earlier with other accelerators [4].

By the use of ascorbic and dihydroxymaleic acids as accelerators in conjunction with catalysts, unsaturated polyester resins can be hardened in the cold, and the duration of the process varied over wide limits. In view of the possible technical utilization of such accelerators, their action was tested on casting compositions containing fillers. The filler used was quartz powder, 150% on the weight of polyester. The results of experiments on the system cumene hydroperoxide–ascorbic acid in cold hardening are presented on next page, and the exothermic curves are given in Fig. 7.

*As in original – Publisher's note.

**The action of dihydroxymaleic acid was not studied.

Amount of accelerator (% on polyester)	Time of gel formation	Peeling time	Maximum heat evolution (°C)
0.04	15 min.	50 min.	40
0.03	25 min.	1.25 hrs.	35
0.02	40 min.	2.25 hrs.	29
0.01	1.5 hrs.	7 hrs.	24
0.005	6 days	7 days	–
0	10 days	11 days	–

The experimental results show that the effect produced by ascorbic acid is the same as in pure resins without filler. Introduction of the filler naturally results in some lowering of the exothermic curves.

The filled compositions were cast in the form of standard specimens which were subjected to tests. The specimens were hardened in the cold (cumene hydroperoxide catalyst, ascorbic acid accelerator), followed by heat treatment in which the temperature was gradually raised from 35 to 130°. The test results are given below:

Static bending strength (kg/cm^2)	760
Compressive strength (kg/cm^2)	2000
Specific impact viscosity ($kg \cdot cm/cm^2$)	5-6
Heat resistance, Martens test (°C)	67
Heat resistance, Vicat test (°C)	190
Dielectric strength (kv/mm)	18-25

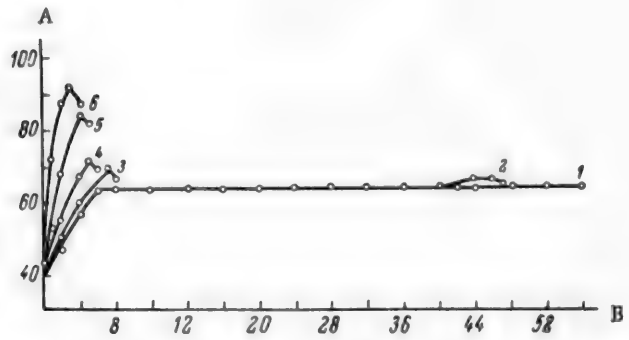

Fig. 7. Effect of the amount of ascorbic acid on the course of exothermic curves (filled compositions, hardening in presence of cumene hydroperoxide at 64°). A) Temperature (°C), B) time (minutes). Amount of ascorbic acid (%): 1) 0, 2) 0.005, 3) 0.01, 4) 0.02, 5) 0.03, 6) 0.04.

It should be noted that there was fairly considerable heat evolution during the cold hardening of the standard rods. The maximum temperatures were not measured.

SUMMARY

1. It was found that dienols, specifically ascorbic and dihydroxymaleic acids, are active accelerators of the hardening of unsaturated polyester resins, in conjunction with catalysts either of the peroxide (benzoyl peroxide) or the hydroperoxide (cyclohexyl hydroperoxide, cumene hydroperoxide) type.

2. It is shown that the pure resins and filled compositions can be hardened in presence of these accelerators at room temperature.

LITERATURE CITED

[1] H. Barron, Rubber Age Synth. 4, 162 (1953).

[2] F. S. Nichols and C. H. Bliss, Mod. Plastics, 29, 9, 124 (1952).

[3] B. Berndtsoon and L. Turunen, Kunststoffe, 44, 10, 430 (1954).

[4] R. K. Gavurina, P. A. Medvedeva and Sh. G. Ianovskaia, J. Appl. Chem. 31, 1, 116 (1958).*

[5] L. Horner and K. Scherf, Lieb. Ann. 573, 35 (1951).

[6] M. Imoto and K. Takemoto, J. Pol. Sci. XVIII, 89, 377 (1955).

[7] W. Kern and H. Willersinn, Makromol. Chem. 15, 1, 36 (1955).

[8] C. E. H. Bawn, Discussion Faraday Soc. 14, 181 (1953).

[9] B. A. Dolgoplosk, E. I. Tiniakova and V. N. Reikh, Vulcanization of Rubbers. Scientific and Technical Conference of the All-Union Scientific Society of Rubber Technologists [in Russian] (Goskhimizdat, 1954) p. 51.

Received January 16, 1957

*Original Russian pagination. See C.B. Translation.

POLYMERIZATION OF VINYLACETYLENE

I. M. Dolgopol'skii, Z. F. Dobler, A. P. Iashina, and P. N. Trofimova

Vinylacetylene is a highly active compound, because of the presence of a double bond in conjugation with a triple bond in its molecule. This peculiarity of vinylacetylene structure accounts for its ability to absorb oxygen with subsequent polymerization, or oxidation with formation of peroxides. From the work of Medvedev et al., [1], it may be concluded that both reactions (oxidation and polymerization) are initiated by the same mechanism under the action of free radicals formed in the decomposition of peroxides. There is no information in the literature on the polymerization of vinylacetylene, apart from the paper by Dykstra [2], but the prevention or retardation of this reaction is a very important problem.

The possibility of prevention of the polymerization of vinylacetylene depends on the nature of the polymerization process. Polymerization by a radical mechanism, known as initiated polymerization, may be interrupted by the use of inhibitors [3-5]. If inhibitors have no influence on polymerization, and polymers of low molecular weight are formed in the process, this proves that purely thermal polymerization occurs [6].

The present paper contains the results obtained in studies of certain properties of vinylacetylene polymers, polymerization rate of vinylacetylene in pure form and in chlorobenzene solution, and of the possible inhibition of vinylacetylene polymerization by the use of suitable compounds.

EXPERIMENTAL

Pure vinylacetylene was used, freed from traces of carbonyl compounds by treatment with 2% hydroxylamine hydrochloride solution. It was dried over calcined calcium chloride and then distilled through a Podbielniak column.

Method for vinylacetylene polymerization. The polymerization of vinylacetylene, both pure and in chlorobenzene solution, was carried out in sealed ampoules 20-25 ml in capacity, in absence of air.

Air was removed from the ampoules by repeated evacuation and evaporation of vinylacetylene from the system until a constant vacuum was obtained. The exact amount of vinylacetylene taken was determined by weighing. The vinylacetylene solutions were prepared in ampoules (Fig. 1). The amount of gaseous vinylacetylene introduced into the chlorobenzene (5 ml) was varied from 2.5 to 10%. The vapor pressure of vinylacetylene at 20° was determined for each vinylacetylene concentration. The vapor-pressure curve for vinylacetylene at different concentrations in solution is given in Fig. 2. The ampoules containing vinylacetylene or its solutions in chlorobenzene were sealed without access to air. The ampoules were placed in iron shells. The polymerization was effected with stirring in air thermostats. The duration and temperature of heating were varied, in order to vary the extent of polymerization.

Method for determination of the extent of polymerization of vinylacetylene. The polymer content in polymerization of pure vinylacetylene was determined gravimetrically from the weight of residue after evaporation of the unpolymerized vinylacetylene. The content of vinylacetylene polymers in chlorobenzene solutions was determined by a method based on determination of the vapor pressure of vinylacetylene before and after polymerization. In this method, at the end of polymerization the ampoule was cooled to −78°, opened, attached to a comb-shaped tube, and the air was pumped out. The ampoule was then placed in a water thermostat at 20°, and the constant pressure of vinylacetylene vapor was determined with shaking of the ampoule. The curve (Fig. 2) was used to determine the amount of unpolymerized vinylacetylene in solution.

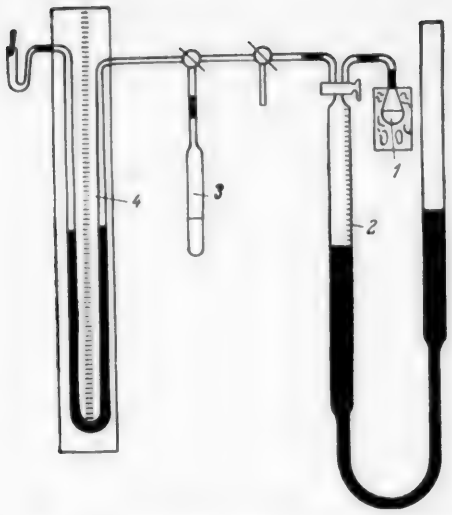

Fig. 1. Apparatus for determination of the vapor pressure of vinylacetylene over chlorobenzene solution. 1) Ampoule with C_4H_4, 2) mercury buret, 3) ampoule with chlorobenzene, 4) manometer.

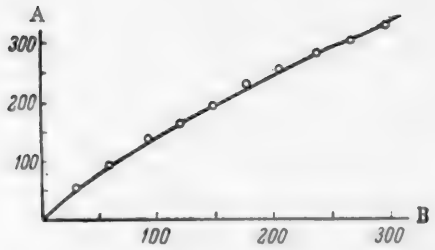

Fig. 2. Vapor pressure of vinylacetylene over chlorobenzene solution. A) Vapor pressure of vinylacetylene (mm Hg), B) content of vinylacetylene in solution (ml).

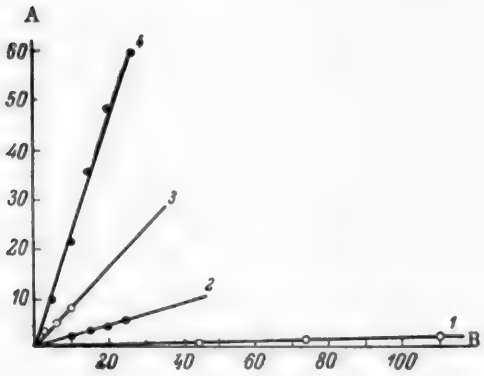

Fig. 3. Rate of vinylacetylene polymerization as a function of time. A) Extent of polymerization (% polymer), B) duration of polymerization (days). Polymerization of C_4H_4 at temperature (°C): 1) 20, 2) 40, 3) 50, 4) 60.

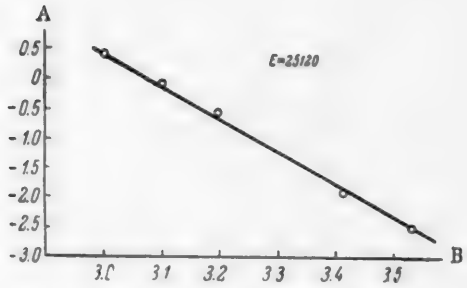

Fig. 4. Variation of log polymerization rate of vinylacetylene with the temperature. A) Log polymerization rate of C_4H_4, B) $\frac{1}{T} \cdot 10^3$.

Effect of temperature on the polymerization rate of pure vinylacetylene. Pure vinylacetylene was polymerized at 10, 20, 40, 50, and 60°.

The polymer contents obtained were used to calculate the extent and rate of polymerization of vinylacetylene at different temperatures. The extent of polymerization is a linear function of time (Fig. 3).

The reaction rate is a logarithmic function of the temperature (Fig. 4).

Data on the activation energy and the temperature coefficients of polymerization of vinylacetylene are given in Table 1.

Effect of impurities on the polymerization rate of vinylacetylene. The effects of water, acetaldehyde, chloroprene, and iron on the polymerization of vinylacetylene were studied. Water and acetaldehyde were introduced in the liquid state into the ampoules before the vinylacetylene. To prevent oxidation of chloroprene during its introduction into the ampoules, it was introduced by means of evaporation and subsequent condensation. In the experiments with oxygen, the latter was introduced into ampoules containing vinylacetylene. In studies of the influence of iron, iron plates were placed in the glass ampoules. The polymerization of vinylacetylene in presence of impurities was effected at 20, 40, and 60°.

TABLE 1

Calculated Activation Energies and Temperature Coefficients of Vinylacetylene Polymerization

Calculation data	Polymerization temperature (°C)				
	10	20	40	50	60
Reaction rate (% per day)	0.0033	0.013	0.23	0.85	2.4
Log reaction rate	—2.48	—1.88	—0.639	—0.071	0.38
1000/T	3.53	3.41	3.19	3.09	3.00
Activation energy	23000	25700	26000	22900	
Temperature coefficient		3.9	3.7	2.8	

TABLE 2

Polymerization of Vinylacetylene in Presence of Catalysts

Catalysts of vinylacetylene polymerization	Duration (hours)	Extent of polymerization (%)	Polymerization rate	
			% per day	average
Vinylacetylene without catalysts at 60°	72	6.0	2.0	2.0
	144	12.8	2.1	
	288	23.6	1.9	
	360	30.3	2.0	
with 1% azobisisobutyronitrile at 60°	120	21.1	4.2	4.1
	240	36.3	3.6	
	360	66.8	4.4	
without catalysts at 70°	72	13.6	4.5	4.4
	120	23.6	4.6	
	216	37.1	4.1	
	240	47.0	4.7	
	360	63.5	4.3	
with 2% benzoyl peroxide at 70°	4	4.7	26.4	26.0
	6	6.8	26.4	
	8	8.6	26.4	
	10	10.2	24.0	
	12	12.6	26.0	

The results showed that the polymerization rate of vinylacetylene is doubled only in presence of oxygen (0.005 mole). The effects of a number of impurities on the polymerization rate of vinylacetylene are shown in Fig. 5. Increase of the polymerization rate of vinylacetylene in presence of oxygen is evidently due to the influence of the peroxides of vinylacetylene or chloroprene formed during the process.

Initiation of vinylacetylene polymerization. To test the effects of catalysts, vinylacetylene was polymerized in presence of benzoyl peroxide and azobisisobutyronitrile (Table 2).

These results show that on addition of 1% of asobisisobutyronitrile the polymerization rate of vinylacetylene at 60° is doubled, while with 2% of benzoyl peroxide at 70° the polymerization rate is increased 5 to 6-fold.

It should be noted that vinylacetylene polymers obtained in presence of catalysts are insoluble in benzene even at a relatively low degree of reaction (13-15%), whereas polymers of pure vinylacetylene are readily soluble even at 40% conversion.

Polymerization of vinylacetylene in chlorobenzene solution. The polymerization rate of vinylacetylene in 2.5, 5, 7.5, and 10% solutions in chlorobenzene at 80, 100, and 120° was determined. Variations of the

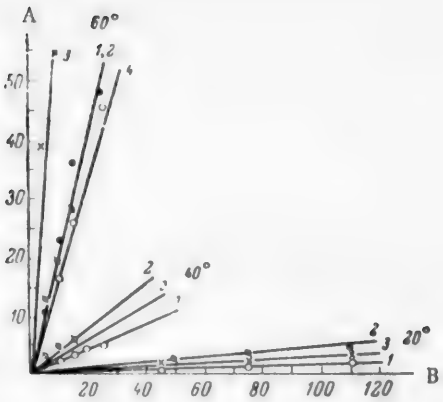

Fig. 5. Effect of impurities (C_4H_5Cl, H_2O, O_2) on the polymerization rate of vinylacetylene. A) Extent of polymerization (% polymer), B) duration of polymerization (days). Curves: 1) pure C_4H_4, 2) C_4H_4 + 0.005 mole O_2, 3) C_4H_4 + + C_4H_5Cl, 4) C_4H_4 + H_2O.

polymerization rate of vinylacetylene with the reaction temperature and solution concentration are plotted in Fig. 6. The results indicate that increase of the vinylacetylene concentration in solution leads to an increase of the polymerization rate, especially at higher temperatures.

Inhibition of vinylacetylene polymerization. To determine the possibility of preventing or retarding the polymerization of vinylacetylene, experiments were performed with addition of various inhibitors, both in presence of oxygen or other catalysts, and in their total absence (Table 3).

It follows from these results that addition of inhibitors in absence of catalysts has no effect on the polymerization of vinylacetylene. Addition of inhibitors in presence of catalysts lowers somewhat the polymerization rate of vinylacetylene.

Determination of the molecular weight of vinylacetylene polymers. The molecular weight of vinylacetylene polymers was determined by the cryoscopic method. Variations of the molecular weight of the polymers with the extent of polymerization are given in Table 4.

These results indicate that polymerization of pure vinylacetylene yields products of low molecular weight, and even when the extent of reaction is 63% the polymer molecule does not contain more than 10 vinylacetylene molecules.

The molecular weight of the polymerization products formed in presence of benzoyl peroxide (extent of polymerization not higher than 13%) is approximately 3-4 times that of vinylacetylene polymers obtained in absence of peroxide.

TABLE 3

Effect of Inhibitors on the Polymerization Rate of Vinylacetylene at 60°

Components	Time (days)	Extent of polymerization (%)	Polymerization rate: % per day	Polymerization rate: average
Vinylacetylene + 1% Neozone "D"	3	6.8	2.2	2.10
	10	22.0	2.2	
	15	32.0	2.0	
Vinylacetylene + 1% wood-tar antioxidant "(AO")	5	10.1	2.0	1.95
	10	18.8	1.9	
Vinylacetylene + 0.005 moles oxygen + 1% Neozone "D"	5	5.5	1.1	1.2
	10	12.5	1.3	
	15	18.0	1.2	
Vinylacetylene + 0.005 mole oxygen + 1% wood-tar antioxidant ("AO")	5	5.2	1.0	1.1
	10	10.7	1.1	
	15	16.7	1.1	

• The polymerization rate of pure vinylacetylene is 2.1.

Introduction of inhibitor (Neozone "D") in presence of benzoyl peroxide terminates chain growth at the vinylacetylene tetramer stage.

The variation of molecular weight with the extent of polymerization is plotted in Fig. 7.

Fig. 6. Effect of temperature on the polymerization rate of vinylacetylene in chlorobenzene solution. A) Vinylacetylene polymerization rate, B) polymerization temperature (°C). C_4H_4 contents in chlorobenzene (%): 1) 2.5, 2) 5.0, 3) 7.5, 4) 10.0.

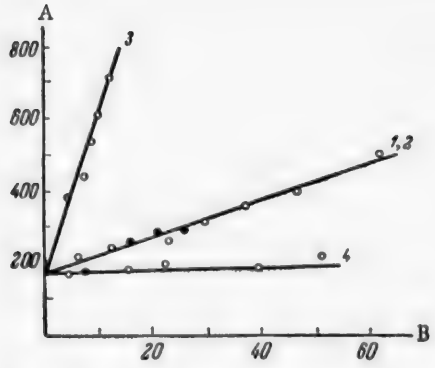

Fig. 7. Effect of extent of polymerization of vinylacetylene on the molecular weight of the polymer. A) Molecular weight, B) extent of polymerization of vinylacetylene (%). Curves: 1,2) pure C_4H_4, and with 1% Neozone "D;" 3) C_4H_4 + 2% benzoyl peroxide; 4) C_4H_4 + 2% benzoyl peroxide + 1% Neozone "D."

TABLE 4

Molecular Weight of Vinylacetylene Polymers

Components	Extent of polymerization (%)	Molec. wt. of polymers	Deg. of polymerization (monomer units)
Pure vinylacetylene at 60°	5.9	212	4
	12.6	240	5
	23.7	260	5
	30.2	309	6
The same, at 70°	37.0	362	7
	48.0	400	8
	63.0	507	10
Vinylacetylene + 1% Neozone "D" at 60°	8.3	175	4
	14.2	245	5
	21.1	264	5
	25.0	288	6
Vinylacetylene + 2% benzoyl peroxide at 70°	4.7	386	7
	6.8	435	8
	8.6	550	10
	10.2	625	12
	12.6	725	14

DISCUSSION OF RESULTS

The absence of inhibition and the stepwise character of the polymerization of pure vinylacetylene show that the mechanism of this reaction differs from the mechanism of formation of high polymers, and is probably analogous to ordinary dimerization by the Diels–Alder reaction.

The fact that trimers to pentamers, and not dimers, are formed in the polymerization of vinylacetylene may be attributed to structural peculiarities of vinylacetylene.

Many workers at the present time explain the reaction of diene synthesis in terms of a polar mechanism.

This reaction mechanism is in good agreement with the fact that inhibitors have no influence on vinylacetylene polymerization (the polymerization rate and molecular weight of the polymers formed are unchanged).

As the extent of reaction increases, the primary dimer, which contains two easily-polarized acetylene bonds conjugate with the cyclobutane ring, combines with other vinylacetylene molecules to form polymers.

The process is much more complicated in presence of catalysts. The latter should have no influence on the rate of consecutive diene synthesis. Nevertheless, additions of catalysts considerably increase the rate and degree of polymerization of vinylacetylene.

The molecular weights of the vinylacetylene polymers, even at 4-12% extent of reaction, correspond to 7-14 molecules of vinylacetylene per polymer molecule. On further increase of the extent of reaction, insoluble polymers are formed. The formation of insoluble polymers is characteristic of structure formation, which may be prevented by means of inhibitors.

The results suggest that in presence of catalysts 2 parallel processes take place simultaneously: 1) consecutive diene synthesis, and 2) radical polymerization with formation of short chains.

It is possible that the products of diene synthesis themselves favor chain termination by virtue of their structural peculiarities. It must be noted, however, that the data available at present are inadequate for a complete judgement of the mechanism of the reaction and of the structure of the polymers formed in presence of catalysts. These questions require further investigation.

SUMMARY

1. The influence of various factors on the polymerization of vinylacetylene was studied, and it was shown that vinylacetylene polymerization cannot be prevented by addition of inhibitors of the aromatic amine and phenol type.

2. The polymerization rate of vinylacetylene is increased severalfold by addition of substances which initiate radical processes.

3. The molecular weights of vinylacetylene polymers were determined, and it was shown that polymerization of pure vinylacetylene, and also in presence of inhibitors, yields low-molecular products corresponding to vinylacetylene trimers to hexamers.

LITERATURE CITED

[1] S. S. Medvedev and P. Tseitlin, J. Phys. Chem. 18, 1-2, 13 (1944).

[2] H. B. Dykstra, J. Am. Chem. Soc. 56, 1625 (1934).

[3] B. A. Dolgopolsk, Trans. All-Union Sci. Res. Inst. Synth. Rubber (1948).

[4] G. A. Parfenova, Dissertation (All-Union Sci. Res. Inst. Synth. Rubber, 1952).

[5] D. S. Korotkina, Dissertation (All-Union Sci. Res. Inst. Synth. Rubber, 1950).

[6] Schulz and Husemann, Ber. 43, 385 (1939); Walling, Briggs, and Mayo, J. Am. Chem. Soc. 68, 1145 (1946).

Received June 10, 1957

PREPARATION OF 8-(TRICHLOROMETHYL)-THEOBROMINE AND THEOBROMINE*

E. S. Golovchinskaia, V. M. Fedosova, and A. A. Cherkasova

The S. Ordzhonikidze All-Union Chemico-Pharmaceutical Scientific Research Institute

8-(trichloromethyl)-theobromine (II) is formed by chlorination of 8-methyltheobromine (I), and is the last intermediate in the synthesis of theobromine (III) from uric acid [1].

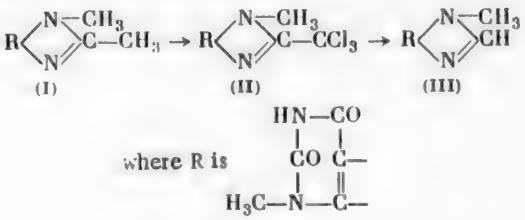

(I) (II) (III)

where R is

The preparation of (II) by the reaction of (I) with three molecules of chlorine in phosphorus oxychloride at room temperature was first described in 1901 [2]. To avoid the use of phosphorus oxychloride, one of us worked out conditions for the preparation of (II) by the passage of excess chlorine through a suspension of (I) in nitrobenzene at 11-13° [3], while another of us, jointly with Magidson, recommended the use of tetrachloroethane or trichloroethane as a reaction medium [4]. Because of the toxicity of nitrobenzene and tetrachloroethane, the need to use large amounts of trichloroethane as solvent, and other difficulties mainly of a technological character, it was necessary to seek other methods for the chlorination of (I). The possibility of the greatest interest was preparation of (II) in dichloroethane, which is a low-boiling solvent, more easily available and considerably less toxic than those named above.

Attempts to carry out the reaction in dichloroethane with cooling, i.e., under conditions analogous to the conditions of chlorination of (I) in nitrobenzene, and also of methylcaffeine in chlorobenzene [5], were not successful, as (I) reacts much less vigorously than methylcaffeine with chlorine. A considerable proportion of the chlorine introduced into the reaction was not retained in the reaction mass, and liberated iodine from aqueous KI solutions placed at the reactor exit. Even when a large excess of chlorine was passed through a suspension of (I) in dichloroethane at 11-13°, the reaction mass contained a mixture of the original unreacted (I) with a roughly equal amount of (II). The expected intermediate products, namely, 8-(monochloromethyl)- and 8-(dichloromethyl)-theobromine, were never detected in the mixture obtained.

The subsequent experiments on the chlorination of (I) at a higher temperature were based on the results of a study of the chemistry of conversion of methylcaffeine into 8-(trichloromethyl)-caffeine [6], which showed clearly that if the amount of chlorine does not exceed 3 moles per mole of methylcaffeine, chlorination can be successfully carried out at a higher temperature without the risk of formation of the 7-(chloromethyl) derivative as an impurity.

Chlorination of (I) in dichloroethane at various temperatures showed that a small rise of temperature (to 30°) resulted in even greater loss of the chlorine taken, and in an increase of the content of unchanged (I) in

*Communication IV in the series on the synthesis of purine alkaloids from uric acid.

the mixture, whereas at 60-80° (I) reacted much more vigorously with chlorine, and the chlorine introduced into the reaction mass was absorbed almost completely. The reaction product formed at 80° did not contain any unchanged starting substance, and consisted of (II), of which the yield did not exceed 63%, and of an oily by-product from which an individual compound could not be isolated.

A futher substantial improvement in the results of chlorination of (I) was achieved by the addition of aluminum chloride or crystalline iodine to catalyze the process. Introduction of small amounts of these substances into the reaction mass at once raised the yield of (II) sharply to 78-81%.

Experiments carried out in order to find the optimum chlorination conditions showed that the reaction is best carried out at 60° with (I) and dichloroethane in 1 : 10 ratio. It was also found that aluminum chloride and crystalline iodine have equally favorable effects on the course of the process; replacement of one by the other does not affect the yield of (II), which reaches 86-87% of the theoretical in the given conditions.

The use of excess chlorine (over 3 moles) at the chosen temperature results in substitution of hydrogen in the methyl group in position 7 by chlorine, i.e., in partial conversion of (II) into 3-methyl-7-monochloromethyl-8-trichloromethylxanthine. Hydrolysis of the latter is accompanied by removal of both chloromethyl groups and formation of 3-methylxanthine:

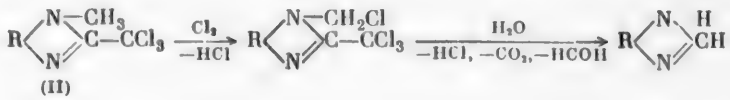

(II)

Therefore exact calculation of the amount of chlorine taken, and reliable determination of the end of the reaction in which (II) is formed, so that the chlorine supply can be stopped in time, are especially important for this reaction.

For development of a method for determination of the end of the reaction, use was made of the fact that (II) is much more soluble than (I) in chlorinated organic solvents. When 5 ml of the chlorinated reaction mixture (after the introduction of about 3 moles of chlorine) is diluted with dry dichloroethane to a volume of 250 ml and the product is shaken, the crystals of (II) suspended in dichloroethane dissolve. If no original (I) is present in the mixture, a clear solution is formed. However, if the solution formed contains turbidity or a suspended precipitate, this indicates the presence of (I), and the amount of undissolved substance gives a fairly exact idea of the approach of the end of the reaction (by comparison with a standard).

According to patent data [7], hydrolysis and decarboxylation of (II) take place when it is heated with a 130-fold amount of water.

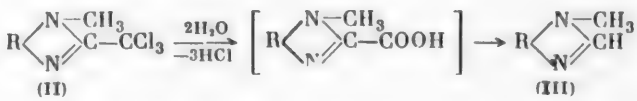

(II) (III)

The hydrochloride of (II), formed with the hydrogen chloride liberated in the reaction, is completely hydrolyzed at this dilution, and therefore theobromine is precipitated on cooling from the hydrolyzed solution without preliminary neutralization of the latter.

A disadvantage of this method of hydrolysis, from the practical aspect, is that large volumes are used. Attempts to decrease the amount of water 5 to 6-fold and to carry out the hydrolysis of (I) in suspension proved unsuccessful, although the amount of HCl liberated, as indicated by the results of titration of the solution with alkali, approached 3 moles in all cases. Experiments showed that the reason for the failure lies in the fact that a necessary condition for normal completion of the process is complete dissolution of the substance, accompanied by subsequent separation of (III) from solution, whereas in suspension the reaction is arrested at an intermediate stage.

The minimum amount of water which ensures the formation of a solution is 50 parts per one part of (II). The product (III) isolated from such a solution on cooling proved identical with natural theobromine, while

the filtrate could be used for the subsequent hydrolysis. The solubility of (III) in such filtrates increases with each hydrolysis operation because of accumulation of hydrochloric acid in them. Accordingly, when (II) was heated with 6-7% hydrochloric acid instead of water, a further considerable reduction of the volume of the reaction mass was achieved (in 1 : 15 ratio).* This method of hydrolysis, in its turn, ensures a high yield and good quality of (III).

In some cases the (III) crystallized from the hydrolyzed solution contains a small admixture of 3-methylxanthine. The latter may be formed both because of the presence of 3,8-dimethylxanthine as an impurity in the original (I), and as the result of an accidental excess of chlorine in the preparation of (II), with a consequent substitution of hydrogen in the N-methyl group in position 7 by chlorine. This impurity is easily removed by treatment of an aqueous suspension of unpurified (III) with calcium oxide at 60°: the readily soluble Ca salt of (III) passes into solution, while the sparingly soluble Ca salt of 3-methylxanthine is separated by filtration. The theobromine obtained by acidification of the filtrate conforms to pharmacopoeia specifications in all respects.

EXPERIMENTAL

Preparation of 8-(trichloromethyl)-theobromine (II). 1. 6.1 g of chlorine, made from $KMnO_4$ and technical HCl, and dried by means of concentrated sulfuric acid, was passed during 1 hour 25 minutes with vigorous stirring into a suspension of 5 g of 8-methyltheobromine (I) in 100 ml of dry dichloroethane (containing 0.004% moisture), heated to 80-81°. Most of the substance dissolved, yielding an almost clear solution. 0.326 g of chlorine was not absorbed in the reaction mass (as determined by titration of KI solution, placed at the reactor exit, with 0.1 N $Na_2S_2O_3$).

The solution was filtered; the weight of the residue was 0.18 g, m. p. 270-280°. The filtrate was cooled on ice; 4.4 g of (II) of m. p. 198° crystallized out. The dichloroethane was evaporated from the filtrate under vacuum, the residue was treated with alcohol, separated off by suction, and crystallized from ethyl acetate. The weight was 0.45 g, m. p. 196-198°. The total weight of (II) was 4.85 g, or 63.2% of the theoretical yield.

2. Into a suspension of 30 g of (I) and 0.15 g of $AlCl_3$ in 300 ml of dichloroethane (containing 0.02-0.03% moisture), heated to 60° , 35-36 g of dry chlorine was passed with vigorous stirring (of this amount, 2 g was not absorbed in the reaction mass, and liberated I_2 from 5% KI solution at the reactor exit). During the passage of chlorine, the mobile milky-white reaction mass thickened and then liquefied again; the (I) suspended in dichloroethane then dissolved completely and large, heavy, transparent crystals of (II) separated out. The liquid phase became completely clear and acquired an intense straw-yellow color. The chlorinated reaction mass was stirred for 1 hour more at 60°, then cooled at 2-4° for 4-5 hours, filtered, the residue was washed with 30-35 ml of dry dichloroethane and dried first at 60° and then at 90°. The weight of (II) obtained was 38.1 g, or 82.9% of the theoretical yield; m. p. 202-203°.

Dichloroethane was distilled from the filtrate; the distillate could be used for subsequent experiments without further purification. The residue was treated with alcohol; the crystals which formed were separated off and crystallized from 25 ml of ethyl acetate. This gave 2 g of (II) of m. p. 201-203°, or 4.3% of the theoretical yield. The total weight of (II) was 40.1 g, or 87.2% of the theoretical yield.

3. The reaction was carried out exactly as in Experiment 2 except that 0.03 g of crystalline iodine instead of 0.15 g of $AlCl_3$ was used. From the cooled chlorinated solution 37.0 g of (II), 80.3% of the theoretical yield, crystallized out; m. p. 202-204°. After evaporation of dichloroethane, treatment of the residue with alcohol, and crystallization from ethyl acetate, 2.6 g of (II), or a futher 6% of the theoretical yield was obtained; m. p. 200-203°. The total yield of (II) was 39.6 g, or 86.3% of the theoretical.

Properties of 8-(trichloromethyl)-theobromine. The substance consists of white prismatic crystals, m. p. 211-213° (after repeated crystallization from ethyl acetate). It crystallizes from ethyl acetate in 1 : 18 ratio, and from benzene in 1 : 16 ratio. It is soluble in boiling alcohol, but after a short time the boiling alcoholic solution deposits the ester of theobrominecarboxylic acid, almost insoluble in alcohol, m. p. 287-289°.

Preparation of theobromine. 1. 50 g of (II) (m. p. 202-204°) was boiled on a gauze under reflux with

*In this case the solution should be neutralized after the end of hydrolysis for complete separation of (III).

750 ml of 6% hydrochloric acid. After the (II) was completely dissolved, which required 2-3 hours, the liquid was boiled for 1 hour more with 2.5 g of charcoal, filtered, and the hot filtrate was neutralized by caustic soda solution to pH 6.2. After 8 hours of cooling at 6-8° the separated theobromine (III) was separated off by suction, washed with cold water, and dried. The weight of dry crude (III) was 24.7 g. It was put into a suspension of 4.3 g of calcium oxide in 500 ml water at 50-60°, stirred for 15-20 minutes to dissolve theobromine (the solution was turbid), 1 g of charcoal was added, and the liquid was stirred at the same temperature for 30 minutes more. The heated solution of the Ca salt of (III) was filtered and neutralized with dilute hydrochloric acid (1 : 1) to pH 6.2-6.5. The liquid was cooled for at least 8 hours at a temperature below 8°, the (III) which separated upon neutralization was separated off by suction, washed with water to a negative reaction for chloride in the filtrate, and dried. The yield of (III) conforming to pharmocopoeia specifications, was 22.4 g, or 74.3% calculated on (II) and 64.2% on the original (I).

2. Ten g of (II) (m. p. 202-204°) was boiled with 500 ml of water until dissolved, 0.3 g of charcoal was added, the liquid was boiled for 30 minutes more, filtered, and cooled for 8 hours at 6-8°. The crystallized (II) was filtered off by suction, the filtrate was boiled with the next 10 g of (II), the (III) formed by hydrolysis was isolated, and the same operation was repeated 3 more times (5 times altogether). The total weight of crude dry (III) was 23.54 g, from 50 g of (II). It was purified by way of the calcium salt, as in Experiment 1. The yield of theobromine, conforming to pharmocopoeia specifications, was 21.72 g, or 71.7% calculated on (II) and 61.9% on the original (I).

The acid filtrate after five hydrolysis operations contained 3.02% HCl. A further 1 g of (III), which is 3.3% of the theoretical yield calculated on (II), or 2.7% on (I), was obtained from the filtrate by neutralization (amount of NaOH required, 17.6 g), condensation under vacuum to 100 ml, and purification of the precipitate deposited after cooling, by way of the Ca salt.

SUMMARY

1. 8-(Trichloromethyl)-theobromine can be obtained in good yields by the introduction of 3.1 moles of dry chlorine into a suspension of 1 mole of 8-methyltheobromine in dry dichloroethane. The reaction should be performed at 60° in presence of small smounts of aluminum chloride or crystalline iodine.

2. 8-(Trichloromethyl)-theobromine can be converted into theobromine by heating with dilute hydrochloric acid (rather than water), whereby the volume of the reaction mass during hydrolysis can be reduced considerably.

LITERATURE CITED

[1] German patent 121,224 (1899) and 128,212 (1901); E. S. Golovchinskaia, Author's Certif. 63,603 (1943); E. S. Golovchinskaia, J. Appl. Chem. 30, 9, 1374 (1957);* E. S. Golovchinskaia and R. G. Glushkov, J. Appl. Chem. 30, 12, 1806 (1957).*

[2] German patent 146,714 (1902).

[3] E. S. Golovchinskaia, J. Appl. Chem. 19, 1173 (1946).

[4] V. M. Fedosova and O. Iu. Magidson, Author's Certif. 99,992 (1954).

[5] E. S. Golovchinskaia, O. Iu. Magidson and T. N. Kudinova, Author's Certif. 66,308 (1941).

[6] E. S. Golovchinskaia, J. Appl. Chem. 31, 6, 918 (1958).*

[7] German patent 151,133 (1902).

Received August 29, 1956

*Original Russian pagination. See C.B. Translation.

MECHANICAL PROPERTIES OF CASEIN FILMS

V. I. Eliseeva and E. V. Kuz'mina

Casein is widely used as a binder in leather finishing. The behavior of coatings on leather, which determines their quality and purpose, depends considerably on their mechanical properties. The work of the Central Scientific Research Institute for the Leather Industry has shown that the most important mechanical characteristics of coatings on leather, with regard to service behavior, are hardness and elasticity. According to these properties, coatings on leather are classified in this paper into elastic or film coatings, which persist as continuous films during deformation of the leather, and inelastic or adhesive films, which lose continuity when the leather is subjected to the usual deformations. The practical purpose of the former type is improvement of the service properties of leather (heat insulation, water proofness), application of an artificial surface, "refining," lacquering; the practical purpose of the latter is to confer luster to the surface and to attach pigments to it.

Hardness of the surface, on the one hand, makes the surface capable of withstanding various mechanical influences and harsh polishing operations (glazing) which confer luster on it. On the other hand, hard surfaces do not have high elasticity, so that they are incapable of considerable elongation and cannot withstand repeated deformations. This applies to casein coatings on leather, intended for glazing and having considerable hardness. They are not retained as continuous films during deformation of the leather, and therefore cannot be used as film coatings. The mechanical properties of casein films are directly related to the configuration of casein molecules. Pasynskii [1] considers that the protein molecule has an essentially stable configuration which is retained by fairly considerable forces, the total energy of which per amino acid residue is close to the energy of the peptide bonds themselves. Relative displacement of the units in the polypeptide chain during deformation is very difficult, so that the protein molecule has a stable and rigid configuration. To alter this specific configuration of the polypeptide chain, considerable forces are required, which must influence the system of bonds between the units in the polypeptide chain and overcome the potential barriers between them. Denaturation of proteins exerts an influence of this type. These effects can be produced by various means – action of heat, irradiation, change of pH, action of solvating substances (detergents), etc. Pasynskii considers that considerably portions of the coiled chain remain unchanged in protein denaturation, and complete uncoiling does not occur. His study of the asymmetry of protein molecules in urea solution showed that the change of asymmetry is only 1 to 2.5 % of the original.

Bresler [2], Lundgren [3], and Astbury [4] put forward the opinion that when proteins are mixed with certain detergents, they form complexes with the latter, and the protein molecules become uncoiled. In presence of sufficient detergent, when the protein chains are uncoiled, the detergent is attached along the chains, thereby facilitating their relative slippage during deformation, and acting as a plasticizer. Similar views have been put forward by many other workers. Thus, there are two different opinions with regard to elasticity increase of protein gels. According to the first, protein molecules have a stable and rigid configuration, which changes little on denaturation, including denaturation by solvating substances; according to the other opinion, elasticity can be increased by formation of protein complexes with suitable detergents, with simultaneous blocking of polar groups and decrease of intermolecular interaction.

Because of their hardness, good adhesion, vapor permeability, and the ability to give a high gloss in glazing, casein coatings are used in leather finishing. The cracking of casein coatings under tensile stresses, caused by their low elasticity, restricts their use of leathers made from the best hides only. Among the range of raw hides now used for conversion into leather for shoe uppers, there are numerous leathers which must be coated with continuous films in order to cover surface defects. Such coatings must have high elasticity.

The purpose of our work on casein coatings was to improve their elasticity, so that their range of application could be extended.

The films made by the drying of casein solutions (ammonium caseinate) have the following physical properties (at 7% moisture content): tensile strength 1200 g/mm^2, elasticity modulus[1] up to 80,000 g/mm^2, elongation at break in the range of 5-7%, 2-hour soaking in water 310%, 24-hour soaking in water 400%.

The moisture content of casein films is of primary importance in mechanical testing. On the one hand, in the light of modern views on plasticization [5] any liquid absorbed by a polymer acts as a plasticizer, the activity of which increases with increasing compatibility of the liquid with the polymer. The most active plasticizers are liquids which dissolve the polymers; in this instance water, which dissolves ammonium caseinate. On the other hand, dehydrated casein films are of practical importance as leather coatings. They become dehydrated during drying, in glazing operations (temperature up to 300°), and during pressing (at 60°). The moisture content of a casein coating varies according to the storage conditions. The variations of elongation (a measure of elasticity of casein films) with moisture content are given below:

Moisture content (%)	0	6	8.2	9.3
Elongation at break (%)	0	5	10.4	18

Determinations of the mechanical properties of air-dried casein films, with their moisture content disregarded, led some workers to erroneous conclusions concerning the similarity of casein to film formers with high elasticity [6].

The principle of our method for increasing the elasticity of casein coatings was the introduction into casein solutions of certain detergents which, according to the above-mentioned workers [2, 4] increase the asymmetry of protein molecules. The degree of asymmetry was found from the viscosity of 0.5% casein solutions, and calculated by means of Kuhn's formula [7, 8] for the degree of asymmetry (a/b) in terms of solution viscosity.

The relative viscosity (η / η_0) of casein solutions was determined by means of an Ostwald viscosimeter, with a water efflux time of 44.8 seconds.

Changes in the molecular asymmetry of casein under the influence of solvating substances, in solutions containing 0.005 g protein per cc, are given below:

Composition of film	Amount of solvating substance (% on casein)	η/η_0	(a/b)
Solution of casein in water	Nil	1.136	22.5
Casein solution with addition of MK•	50	1.205	27.9
Alizarin oil	50	1.170	25.2
MK	10	1.156	24.4
Alizarin oil	10	1.150	23.6
Monopole soap	10	1.136	22.5
Nekal••	10	1.118	20.8
Petrov's contact•••	10	1.134	22.4
OP 10••••	10	1.134	22.4
OS 20•••••	10	1.125	21.5
Urea	10	1.134	22.4
Glycerol	10	1.129	21.8

•MK consists of sodium salts of aliphatic sulfonic acids.

••Nekal is sodium isobutylnaphthalene sulfonate, $C_{14}H_{15}SO_3$.

•••Petrov's contact consists of sulfonaphthenic acids.

••••OP 10 is made by treatment of high-molecular alkyl phenols with ethylene oxide.

•••••OS 20 is a condensation product of octodecyl alcohol and ethylene oxide – $C_{18}H_{37}(OC_2H_4)_nOH$.

[1] The elasticity modulus was determined with the films extended by 0.05 of the original length, and the result was extrapolated to 0.1 of the length, to contain data comparable with those for other film formers.

It follows from the above data that the asymmetry of casein molecules is influenced only slightly by addition of detergents.

TABLE 1

Effect of Detergent Content on the Elasticity of Casein Films

Amount of detergent (% on weight of casein)	Viscosity of 10% solution	Tanning of 10% formaldehyde solution	Film properties	
			moisture content (%)	elongation (%)
MK emulsifier, 10%	90.58	No	8.2	0.65
Without detergent	13.08	"	8.8	1.29
MK emulsifier, 10%	90.58	Yes	7.8	4.00
Without detergent	13.08	"	9.2	2.7
Alizarin oil, 10%	61.88	No	7.3	0.35
Same	61.88	Yes	8.1	Brittle

Films were prepared from the solutions containing various detergents, and their mechanical properties and moisture contents were determined. Some of the films were tanned by formaldehyde (Table 1).

It follows from Table 1 that the presence of detergents has no appreciable effect on the elasticity of casein films. On the other hand, as Table 2 shows, the mechanical properties of the same films are strongly dependent on their moisture content.

TABLE 2

Type of film	Moisture content (%)	Elongation at break (%)
Casein	0	0
	6.2	5.2
	8.2	10.4
	9.3	22.9
Casein tanned by immersion of film in 10% formaldehyde solution for 20 seconds	0	0
	8.7	7.9
	9.6	12.5
Casein with MK detergent (10% on casein weight)	0	0
	6.0	6.2
	6.5	5.5
	8.6	10.8
Casein with MK detergent (10% on casein weight), tanned by immersion of film in 10% formaldehyde solution for 20 seconds	0	0
	5.9	11.7
	8.4	13.3

Next, a study was made of the elasticity of casein films with various detergents, containing a hygroscopic substance – glycerol, the commonest plasticizer for casein. The results are presented in Tables 3 and 4. It follows from the results that casein films are elastic in presence of glycerol only if they contain moisture; in absence of moisture casein films containing glycerol are not extensible. This is illustrated especially clearly by the data in Table 4. Comparison of the elongation data for casein films of different composition with and without glycerol shows that glycerol acts as a nongelating plasticizer (i.e., one which does not dissolve the polymer), and raises the elongation of the films only in presence of moisture. Water, which in itself increases film elasticity, is a gelating plasticizer which solvates the polar groups in casein and decreases intermolecular interaction.

TABLE 3

Effect of Moisture on the Elasticity of Casein Films Plasticized with 50% of Glycerol

Detergent (% on casein weight)	Tanning by formaldehyde solution	Air-dried		Drying temperature, followed by air humidification			
				60°		130°	
		moisture content (%)	elongation (%)	moisture content (%)	elongation (%)	moisture content (%)	elongation (%)
MK emulsifier, 10%	No	10.3	40.0	8.8	11.1	16.6	68.7
Without emulsifier	"	10.2	25.8	13.1	12.9	13.5	25.0
MK emulsifier, 10%	Yes	8	17.5	19.1	64.2	12.0	79.0
Without emulsifier	"	8.3	11.6	11.3	7.9	8.7	Very brittle
MK emulsifier, 10%	By addition of 1% formaldehyde to casein solution	17.9	90.8	11.2	68.0	9.2	19.4
Without emulsifier	The same	18.4	42.5	14.4	57.0	11.1	18.0
Alizarin oil, 10%	No	28	96	22.7	69	19	28.0
The same	Yes	24	69	13.2	18.7	10.0	17.7

TABLE 4

Effect of Moisture Content of Casein Films of Different Composition on Elongation

Film composition	Moisture (%)	Elongation (%)
Casein with 50% glycerol	0	0
	13.1	12.9
	13.5	25.0
Casein with 50% glycerol and 10% MK detergent (on casein weight)	8.8	11.1
	10.3	40.0
	16.8	68.7
Casein with 50% glycerol and 10% MK detergent (on casein weight), tanned by immersion in 10% formaldehyde solution for 10 seconds	0	0
	8	17.5
	19.1	64.2
Casein tanned by addition of 0.1% of formaldehyde on the weight of casein, in the form of 10% solution	0	0
	9.9	9.1
	12.8	6.6
Casein with 10% MK detergent (on casein weight), tanned by addition of 0.1% of formaldehyde in the form of 1% solution	0	0
	8.6	10
	9.3	18.7
Casein with 50% glycerol, tanned by addition of 0.1% of formaldehyde in the form of 1% solution	0	0
	13.4	42.5
	14.4	57.0
Casein with 50% glycerol and 10% MK detergent (on casein weight), tanned by addition of 0.1% of formaldehyde in the form of 1% solution	0	0
	9.2	19.4
	11.8	68.0
	17.9	90.3

TABLE 5

Variation of Properties of Pigmented Casein Films During Storage

Film characteristics			Freshly prepared film			Film after 6 months of storage			
tanned by formaldehyde	detergent content (%)	glycerol content (%)	moisture (%)	elongation at break (%)	elasticity modulus (g/mm²)	moisture (%)	elongation at break (%)	elasticity modulus (g/mm²)	surface shrinkage (%)
Yes	OS 20 10%	100	7	6.6	–	8.8	2.6	44240	38.3
		200	23	17.5	2900	7.4	2.6	74880	40
		300	14.2	10.3	8400	7.6	2.0	7140	62
No	No	No	10.8	14.2	20180	11.1	4.3	29820	18.4
Yes		100	11.6	14.5	4500	9.8	3.7	37520	20.8
"		200	18.7	35.0	1100	10.5	4.6	66520	48.3
Yes	MK 10%	No	15.2	21.7	18060	5.6	11.8	37400	13.6
		100	21.5	30	760	8.4	5.6	26640	41.2
No	MK 10%	No	9.2	7.5	18000	8.0	11.1	19020	2.0
		100	17.1	18.7	960	13.3	9.2	10920	28.0

Comparison of the elongation of casein films with glycerol, with and without detergents respectively (Tables 3 and 4), shows that the latter have an appreciable effect on elasticity; when sufficient moisture is present, the detergents produce some increase in the elongation of casein films.

An important practical property of casein coatings on leather is their hardness, which makes glazing possible and renders the films resistant to various mechanical influences. It is known from practical experience that formaldehyde tanning of casein coatings, performed in order to confer water repellence, increases hardness; this is confirmed by the data on the elasticity modulus, presented below:

Detergent content	Tanning by 10% formaldehyde solution	Moisture content (%)	Elasticity modulus (g/mm²)	Elongation (%)
Without detergent	No	6	29000	5
The same	Yes	8.7	42000	7.9
10% MK	No	6.8	30200	6.2
The same	Yes	5.9	38180	11.7
10% alizarin oil	No	9.1	20580	15.4
The same	Yes	8.5	29860	15.0

Variations of the elasticity modulus with moisture contents of the films are shown below:

Moisture content	Elasticity modulus (g/mm²)	Elongation (%)
7.1	27460	9.5
9.2	32700	19.4
11.8	11260	68
17.9	5020	90.8
20.0	6840	112.5

The above data show that the changes in the properties of casein films with increase of moisture content consist of an increase in elongation and a decrease in hardness. It follows that it is necessary in practice to dry casein coatings before glazing, in order to make them hard. Thus, a casein coating prepared for glazing must have considerable hardness, which is associated with low elongation. Further experiments showed the variations of mechanical properties of casein coatings on leather during storage.

Pigmented casein films of different composition were made, and their mechanical properties were determined immediately after formation, and after 6 months of storage under normal conditions of temperature and humidity. It was found that storage of the casein films resulted in surface shrinkage the extent of which depended on the film composition. The data in Table 5 show that the greatest shrinkage of film area, up to 62% of the original, occurs with films having a high glycerol content. The smallest area shrinkages, 2, 13, 6, and 18.4%, were found in films without glycerol. This effect is due to migration of glycerol from the films and a consequent decrease of the dry film content. Loss of glycerol is accompanied by a decrease of moisture content, which leads to loss of elasticity and increased hardness, as shown by the data in Table 5.

SUMMARY

1. The possibility of obtaining water-resistant and elastic casein films by addition of detergents to casein solutions was investigated and it was shown that addition of detergents, and in particular alizarin oil, to casein does not produce any significant changes of molecular asymmetry, calculated by the Kuhn formula. The mechanical properties of casein films also remain without appreciable change.

2. Introduction of a plasticizer which does not dissolve casein (glycerol) into casein films does not in itself increase film elasticity. Elasticity increases in this case only in so far as the moisture content of the film increases; removal of moisture causes brittleness. At a given moisture content, glycerol increases film elasticity, acting as a nongelating plasticizer. The elasticity of films containing glycerol is increased by addition of detergents. When casein films containing glycerol are stored, migration of glycerol occurs, resulting in brittleness and surface shrinkage of the films.

3. It is shown that casein films are elastic only in presence of moisture; this leads to the conclusion that only water solvates the polar groups in casein molecules, increasing their flexibility. The elasticity of casein films is a direct function, and hardness and water resistance are inverse functions, of the moisture content. The same applies to films tanned by formaldehyde. In view of the fact that hardness and water resistance are the principal characteristics of the quality of casein coatings, the use of casein as a polymeric binder is suitable only for the production of hard but inelastic coatings.

LITERATURE CITED

[1] A. G. Pasynskii, Conference on Proteins. Proteins in Industry and Agriculture [in Russian] (Izd. AN SSSR, 1944) p. 91.

[2] S. E. Bresler and D. L. Talmud, Proc. Acad. Sci. USSR 43, 326 (1944).

[3] H. P. Lundgren and R. A. O'Connell, Ind. Eng. Ch. 4, 370 (1944).

[4] W. T. Astbury, Nature, 141, 747 (1938).

[5] S. N. Zhurkov, Proc. 2nd Experimental Conference on High Polymers [in Russian] (1945).

[6] R. A. Metlitskaia, Light Ind. 2, 28 (1956).

[7] W. Kuhn, Koll.-Z. 76, 258 (1936).

[8] R. Simha, J. Phys. Chem. 44, 25 (1940).

[9] V. I. Eliseeva, Theoretical Principles and Practical Methods of the Surface Dyeing and Lacquering of Leathers [in Russian] (State Light Industry Press, 1954).

Received February 25, 1957

COKE FORMATION IN CATALYTIC DESTRUCTIVE HYDROGENATION OF PETROLEUMS AND PETROLEUM RESIDUES

Ia. R. Katsobashvili and N. V. Sidorova

Institute of Petroluem, Academy of Sciences USSR

Destructive hydrogenation of petroleums and petroleum residues is carried out industrially under pressure of 300-700 atmos. The reason for the use of high pressures is that pressure intensifies hydrogenation reactions, and thereby retards and ultimately prevents polymerization and coke formation [1]. In the opinion of a number of authors [1-4], high pressures are necessary to shift the equilibrium in the direction of hydrogen addition to unsaturated and aromatic hydrocarbons, which become inert to polymerization and condensation reactions, and therefore at high pressures destructive hydrogenation of petroleum products should not be accompanied by coke formation. However, this is not confirmed by literature data or practical experience. For example, Sakhanov and Tilicheev [2], on the basis of data on destructive hydrogenation of Groznyi paraffinic heavy oil in autoclaves at 460-480 atmos pressure, concluded that destructive hydrogenation can be effected without coke formation by the use of high pressures. However, coke formation took place in their experiments, and the yield of carboids reached 1%.

Ipat'ev, Belopol'skii, and Nemtsov [4] studied the cracking of Groznyi paraffinic heavy oil in autoclaves in presence of hydrogen in order to determine the influence of pressure, and found that in noncatalytic cracking in presence of hydrogen the yield of coke, calculated on the oil, fell from 11 to 2% with increase of the initial pressure from 0 to 100 atmos, which corresponds to operating pressures from 60 to 240 atmos, while in presence of catalysts under analogous conditions the coke yield was from 0.9 to 3.0%. It is reported in the paper that the catalyst rapidly lost activity as it became coated with the products of extensive condensation of asphaltenes and other high-molecular compounds in the oil.

Puchkov's work [5] on hydrogenation of Ishimbai heavy oil in autoclaves at pressures up to 300 atmos in presence of molybdenum sulfide also showed that the process is accompanied by coke deposition on the catalyst weight. Calculated on the raw material, the minimum coke yield was 0.3 wt. %. From this the author concluded that coke formation is virtually absent. He failed to take into account or verify the fact that coke would accumulate on the catalyst during the process, and the catalyst activity would fall.

Diner and Nemtsov [6] showed that in the destructive hydrogenation of Groznyi paraffinic heavy oil in autoclaves the yield of carboids fell from 2.0 to 0.48% on the oil weight with increase of initial pressure from 50 to 150 atmos, which corresponds to operating pressures of 125-370 atmos,* and the amount of coke on the catalyst never fell below 4-5%. As the result of three consecutive experiments with spent catalyst they advanced the hypothesis that a kind of dynamic equilibrium becomes established during hydrogenation between formation and hydrogenation of coke, and coke formation virtually ceases.

Karzhev [7] described the results of liquid-phase hydrogenation of heavy oil from Eastern petroleum over an active stationary catalyst in a flow system. Despite the low space velocity and high operating pressure (300 atmos), the catalyst became coated with an asphaltlike film in 48 hours, and became unserviceable.

Katsobashvili and Kurkova [8-10] showed that in the destructive hydrogenation of Tuimazy heavy oil and semiasphalt in autoclaves under 300 atmos pressure coke is always deposited on the catalyst, and the coke

*Pressures recalculated for the experimental temperature.

yield, calculated on the raw material, is 4-6 wt. % according to the oil–catalyst ratio and the extent of the process.

Katsobashvili, Volynskii, and Kuz'mina [11] also showed that the use of high pressures, about 250-270 atmos, in the catalytic hydrogenation of heavy oil neither leads to "equilibrium" catalyst operating conditions nor stops coke formation. Thus, it was found as the result of 21 consecutive experiments with the same catalyst sample that the amount of coke on the catalyst increased by about 0.1-0.3% with each experiment, and reached 6.1% by weight in the last experiment.

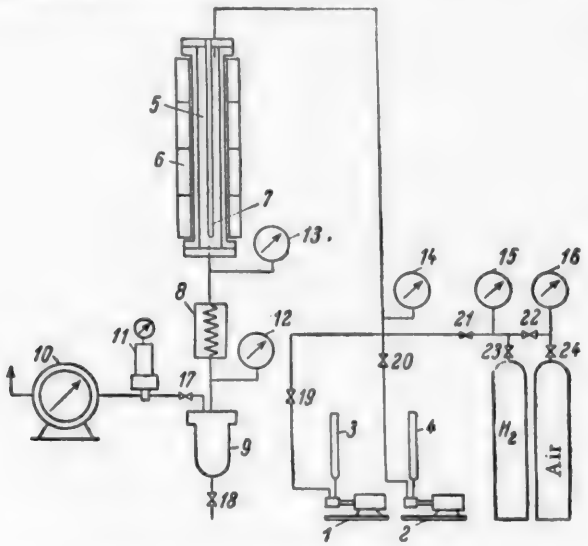

Fig. 1. Diagram of apparatus. 1) Raw-feed pump, 2) water pump, 3) raw-feed buret, 4) water buret, 5) reactor, 6) sectional electric furnace, 7) thermocouple socket, 8) condenser, 9) receiver, 10) gas meter, 11) pressure regulator, 12-16) manometers, 17-24) valves.

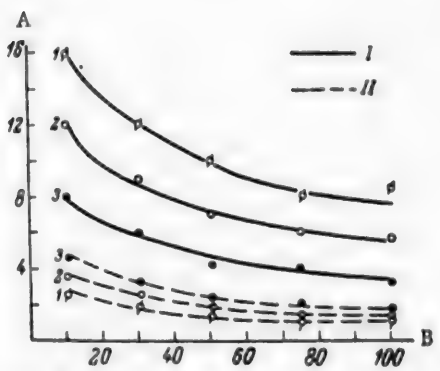

Fig. 2. Effects of pressure on the coke content of the catalyst and coke yield on the raw material. A) Coke content and yield (wt. %), B) pressure (atmos). Space velocity (kg/liter · hour): 1) 2.0, 2) 1.0, 3) 0.5. I) Content of catalyst, II) yield on raw material.

The above data on the destructive hydrogenation of heavy petroleum residues at high pressures, both in autoclaves and in flow systems, show that catalytic destructive hydrogenation is always accompanied by coke formation.

In view of recent reports on processes for hydrogenation of petroleums and petroleum residues under moderate pressures [8, 10, 12-18], it was desired to determine the main effects of pressure on coke formation, quality of the products formed, and catalyst activity in flow conditions.

The present paper contains the results of a study of the effects of pressure between 10 and 100 atmos of space velocities from 0.5 to 2.0 kg/liter · hour.

EXPERIMENTAL

The raw material used for the experiments was Tulmazy (Devonian) petroleum: specific gravity 0.847, sulfur content 1.34 wt. %, asphaltenes 2.82 wt. %, residue above 300° 53.3 wt. %. Aluminum–molybdenum catalyst No. 7360, containing 14% of molybdenum oxide, was used for the experiments.

Experimental procedure. The experiments were performed under dynamic conditions in a pilot unit of the flow type (Fig. 1), with a reactor 38 mm diameter and 250 ml in capacity. The temperature was

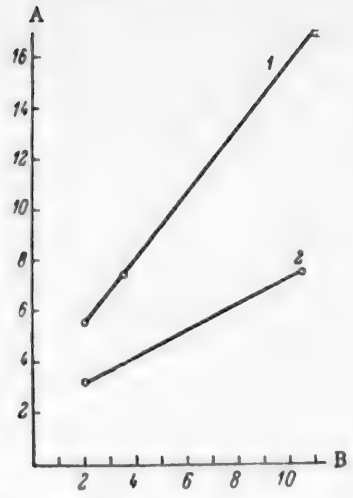

Fig. 3. Effect of duration of experiment on the amount of coke on the catalyst. A) Coke content (wt. %), B) duration of experiment (hours). Pressure (atmos): 1) 30, 2) 100.

regulated automatically, and measured by means of 4 thermocouples placed at different heights of the catalyst layer. At the end of the raw feed, steam was blown through the catalyst. The coke content of the spent catalyst was determined by combustion of a weighed sample in a quartz tube in a current of oxygen. Each experiment was performed with a fresh portion of catalyst. A series of experiments was carried out, at pressures of 10, 30, 50, 75, and 100 atmos, and space velocities of 0.5, 1.0, and 2.0 kg/liter·hour, at a constant temperature of 445-450°, hydrogen rate of 1000 liters per kg of raw feed per hour, and 2 hours duration.

DISCUSSION OF RESULTS

The effect of pressure on the coke content of the catalyst and the coke yield on the raw material are plotted in Fig. 2. The effects conform to a number of general laws: 1) at a given space velocity, the coke content of the catalyst and its yield on the raw material decrease with increase of pressure; 2) at a given pressure, the coke content of the catalyst increases while its yield on the raw material decreases with increase of space velocity, irrespective of the pressure in the range studied, i.e., from 10 to 100 atmos. It is seen from the graph that, at the same space velocity, the coke content of the catalyst and the yield on the raw material are approximately halved with increase of pressure from 10 to 100 atmos. Accumulation of coke deposits on the catalyst, at any pressure between 10 and 100 atmos, takes the same course with increase of space velocity – a 2-fold increase of space velocity increases the coke content of the catalyst 1.3 to 1.5-fold and a 4-fold increase of space velocity, 2 to 2.5-fold. Consequently, of coke formation on the catalyst, in relation to decrease of contact time and degree of conversion occurs to a lesser extent than the increase of the amount of raw material passed.* Therefore, despite the increase in the amount of coke deposited on the catalyst, with increase of space velocity, the yield of coke on the raw material falls considerably. This decrease is not directly proportional to the pressure. For example, at a space velocity of 2.0 kg/liter·hour the coke yields are 2.0 and 1.3 wt. % at 30 and 100 atmos respectively. To determine the effect of time on coke formation, prolonged experiments were performed under pressures of 30 and 100 atmos at a space velocity of 0.5 kg/liter·hour.

The results, plotted in Fig. 3, show that the coke content of the catalyst increases to about the same extent, 2.5 to 3-fold, with increase of the experimental time both at 30 and at 100 atmos. These experiments in a flow unit confirm the results obtained in autoclave experiments [11], which indicate that the coke contents of the catalyst increases with the amount of raw material passed, irrespective of the pressure in the process.

Figures 4-8 show the effects of pressure and space velocity on the yields and quality of hydrogenation products and fractions isolated from them. Pressure variations in the range of 10 to 100 atmos have little effect on the degree of decomposition of the raw material. The yields of hydrogenation products, fractions up to 180°, 180-300° fractions, and residue above 300° are changed very little if at all. Variations of space velocity have more effect. At space velocities of 0.5, 1.0, and 2.0 kg/liter·hour the yield of fractions up to 180° are respectively 30, 28, and 24 wt. % of the hydrogenation product; the 180-300° fractions comprise 42, 38, and 35 wt. %, and residues above 300°, 28, 36, and 41%. The yields of hydrogenation products, calculated on the original oil, are 85-89, 88-91, and 89-93 wt. % respectively. The density sulfur content, and iodine numbers of the hydrogenation products diminish with increase of pressure, and increase with increase of space velocity. For a given space velocity, these properties of the hydrogenation products change little with variation of pressure from 30-50 to 100 atmos. The densities of the fractions up to 180°, and 180-300° fractions, are almost independent of the pressure. The densities of residues above 300° diminish from 0.912 to 0.882 with increase of pressure from 10 to 100 atmos, and increase with increasing space velocity. It is significant that at pressures of 10, 30, and 50 atmos this increase in the density of the residue with increasing space velocity is not large, whereas at pressures of 75 and 100 atmos it is appreciable (one unit in the second place). Data on the quality

*As in original – Publisher's note.

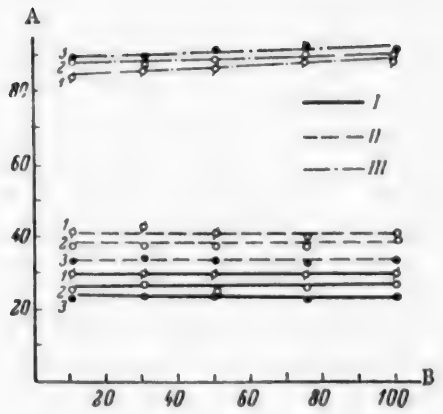

Fig. 4. Yields of hydrogenation products and fractions at different pressures. A) Yield (wt. %), B) pressure (atmos). Space velocity (kg/liter · hour): 1) 0.5, 2) 1.0, 3) 2.0. I) Fraction up to 180°, II) 180-300° fraction, III) hydrogenation products.

of the fractions also show that increase of pressure affects the quality of the products only in the range from 10 to 30-50 atmos, while with further increase of pressure the quality of the products changes very little. Comparison of the properties, given in Figs. 6-8 and Table 1, of the 180-300° fractions and residues above 300° obtained from the hydrogenation products, with the properties of 180-300° fractions and residue above 300° obtained from the raw material (Tuimazy oil), shows that the degree of decomposition and hydrogenation of the raw material, and the degree of desulfurization of the reaction products, are considerable under all the conditions studied, and pressure has a considerable influence up to 30-50 atmos, while further increases to 100 atmos produce only slight changes.

The results obtained in the study of the destructive hydrogenation of Tuimazy oil may be extended to the conversion of petroleum residues and heavy distillates by destructive hydrogenation with an evaporating diluent [10, 12], and to destructive hydrogenation of residues and distillates with recycled products, as the physicochemical properties of petroleum residues diluted to a certain extent by light fractions from the hydrogenation product are close to the properties of crude oil. Therefore in the conversion of heavier petroleum products than the petroleum itself there cannot be any essential differences from the behavior found in the conversion of petroleum.

The foregoing experimental results can be regarded as showing conclusively that increase of the operational pressure to 100 atmos in catalytic destructive hydrogenation of petroleums or similar types of raw material (diluted or undiluted residues, heavy distillates, etc.) does not fully suppress coke formation, and the process is accompanied by deposition of coke.

TABLE 1

Properties of 180-300° Fractions and Residues Above 300° from the Original Oil and from Hydrogenation Products Formed at Different Pressures and Space Velocities

Space velocity (kg/liter · hour)	Pressure (atmos)	180-300° fraction							Residue above 300°	
		density d_4^{20}	sulfur content (wt. %)	iodine number	sulfonable product (vol. %)	unsat. substances (wt. %)	aromatic (wt. %)	paraffin + naphthene (wt. %)	density d_4^{20}	sulfur content (wt. %)
From original oil		0.8160	0.69	8.5	29	5.7	25.8	68.5	0.9525	2.20
0.5	10	0.8277	0.16	6.0	36	4.5	35.5	60.0	0.9123	0.40
0.5	30	0.8264	0.08	3.0	33	2.0	35.0	63.0	0.8960	0.17
0.5	50	0.8272	0.04	2.0	31	1.0	33.0	66.0	0.8900	0.13
0.5	75	0.8250	0.02	1.0	30	0.5	33.0	66.5	0.8783	0.14
0.5	100	0.8219	0.03	2.0	29	1.5	30.8	67.7	0.8822	0.10
1.0	10	0.8237	0.30	8.0	35	5.4	33.0	61.6	0.9025	0.65
1.0	30	0.8231	0.17	5.0	30	3.0	31.0	66.0	0.8900	0.43
1.0	50	0.8226	0.08	2.5	30	1.7	31.6	66.7	0.8926	0.21
1.0	75	0.8237	0.06	1.0	30	0.9	32.3	66.8	0.8846	0.15
1.0	100	0.8260	0.03	1.5	32	1.0	33.0	66.0	0.8820	0.10
2.0	10	0.8222	0.43	13	35	8.7	29.1	62.2	0.9076	1.02
2.0	30	0.8235	0.26	6.0	30	4.5	28.5	67.0	0.8990	0.62
2.0	50	0.8227	0.14	3.0	29	2.0	30.0	68.0	0.8926	0.30
2.0	75	0.8210	0.07	1.0	30	0.8	31.6	67.6	0.8942	0.29
2.0	100	0.8200	0.06	2.0	27	1.0	29.0	70.0	0.8930	0.25

Coke accumulates on the catalyst with increasing duration of the process, irrespective of the pressure.

An "equilibrium state" of catalyst operation is not reached in the process, and the catalyst loses its activity in a relatively short time (2-10 hours). The process gives a coke yield from 4.7 to 1.3 wt. % on the

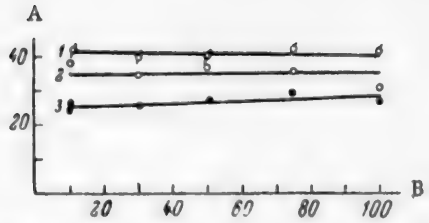

Fig. 5. Effect of pressure on the yield of residue above 300° (calculated on hydrogenation product). A) Yield (wt. %), B) pressure (atmos). Space velocity (kg/liter·hour): 1) 2.0, 2) 1.0, 3) 0.5.

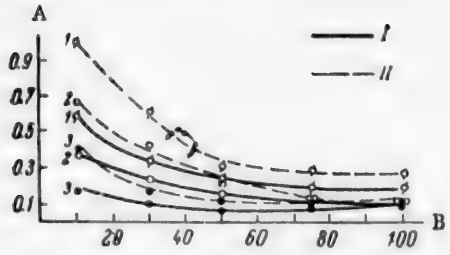

Fig. 6. Effect of pressure on the sulfur contents of hydrogenation products and residues above 300°. A) Sulfur content (wt. %) B) pressure (atmos). Space velocity (kg/liter·hour): 1) 2.0, 2) 1.0, 3) 0.5. I) Hydrogenation products, II)residues above 300°.

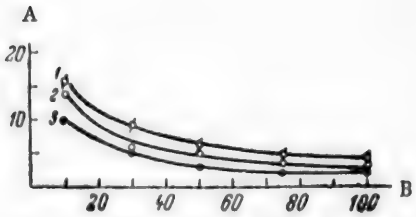

Fig. 7. Effect of pressure on iodine numbers of hydrogenation products. A) Iodine number, B) pressure (atmos). Space velocity (kg/liter·hour): 1) 2.0, 2) 1.0, 3) 0.5.

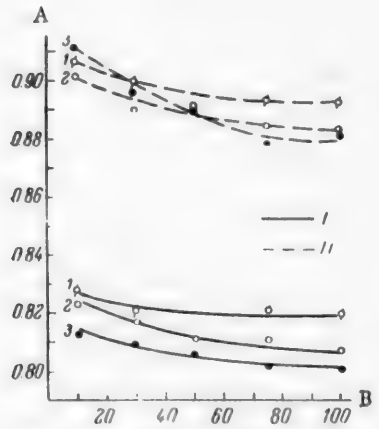

Fig. 8. Effect of pressure on the density of hydrogenation products and residues above 300°. A) Density (d_4^{20}), B) pressure (atmos). Space velocity (kg/liter·hour): 1) 2.0, 2) 1.0, 3) 0.5. I) Hydrogenation products, II) residues above 300°.

original raw material, according to the operating pressure (in the range of 10 and 100 atmos). Therefore the optimum pressure for catalytic hydrogenation of petroleums, petroleum residues, and heavy distillates must be chosen with regard to the conditions and characteristics, both of the destructive hydrogenation itself, and of catalyst regeneration, maintenance of catalyst activity, power consumption, metal requirements, etc. Evaluation of all these factors including product yields and quality, regeneration conditions and costs, showed that the optimum pressure is in the 30 atmos range.

SUMMARY

1. The influence of pressure in the 10-100 atmos range and space velocities from 0.5 to 2.0 kg/liter·hour on coke formation and properties of products formed in destructive hydrogenation of Tuimazy (sulfurous) petroleum was studied at 445-450°, in the presence of aluminum–molybdenum catalyst No. 7360; it was found that the degree of decomposition of the raw material depends little on the pressure.

2. Destructive hydrogenation of this petroleum, both at 10 atmos and at 100 atmos, is accompanied by coke formation, although increase of pressure from 10 to 100 atmos results in approximately a 2-fold decrease of the coke content of the catalyst and the coke yield on the raw material; increase of pressure from 30 to 100 atmos produces a 1.5-fold decrease.

3. The degree of hydrogenation and coke formation are influenced by pressure only in the range of 10 to 30-50 atmos; further increase of pressure has little effect either on the coke yield (on the raw material) or on the product quality.

4. Under the conditions studied, the coke yield did not fall below 1.3% on the raw material, and did not exceed 4.7% in experiments lasting 2 hours. Further accumulation of coke on the catalyst occurs with increase of the experimental time.

5. In all cases coke accumulation is so considerable that it is impossible to carry out continuous destructive hydrogenation of petroleums, petroleum residues, and similar types of raw material without a stage of catalyst regeneration.

LITERATURE CITED

[1] V. I. Karzhev and D. I. Orochko, Trans. All-Union Sci. Res. Inst. of Gas and Synthetic Liquid Fuel, 3, 80 (1951).

[2] A. N. Sakhanov and M.D. Tilicheev, Proc. Conf. on Cracking and Hydrogenation [in Russian] (Groznyi, 1931), p. 147.

[3] M. S. Nemtsov, Progr. Chem. 7, 2, 1617 (1938).

[4] V. N. Ipat'ev, M. A. Belopol'skii, and M. S. Nemtsov, Proc. Conf. on Cracking and Hydrogenation [in Russian] (Groznyi, 1931).

[5] P. V. Puchkov, Petroleum Economy 3, 51 (1935).

[6] I. S. Diner and M. S. Nemtsov, Chem. Solid Fuel 3, 9-10, 727 (1932); 3, 11-12, 838 (1932); 4, 2, 136 (1933); 3, 4, 231 (1932).

[7] V. I. Karzhev, Trans. All-Union Sci. Res. Inst. of Gas and Synthetic Liquid Fuel 4, 87 (1952).

[8] Ia. R. Katsobashvili, N. S. Kurkova, and A. R. Brun-Tsekhovoi, Sci. Report Inst. Petroleum Acad. Sci. USSR (1952).

[9] Ia. R. Katsobashvili and N. S. Kurkova, Trans. Inst. Petroleum Acad. Sci. USSR 1, 89-103 (1954).

[10] N. S. Kurkova, Candidate's Dissertation, Inst. Petroleum Acad. Sci. USSR (1956).

[11] Ia. R. Katsobashvili, N. P. Volynskii and T. N. Kuz'mina, Sci. Report Inst. Petroleum Acad. Sci. USSR (1954-1955).

[12] Ia. R. Katsobashvili and N. S. Kurkova, Sci. Report Inst. Petroleum Acad. Sci. USSR (1956).

[13] Ia. R. Katsobashvili, N. S. Kurkova, and A. R. Brun-Tsekhovoi, Sci. Report Inst. Petroleum Acad. Sci. USSR (1953).

[14] Ia. R. Katsobashvili, Author's Certif. 14, 057 (1953).

[15] Refiner, 34, 5, 156, V 1955.

[16] Petrol. Processing, IV, 11, 4, 47 (1956).

[17] Oil and Gas J., 54, 53, 84 (1956).

[18] Chem. Eng. News, 34, 9, 4686 (1956)

Received June 28, 1957

INVESTIGATION OF THE COMPOSITION OF PHENOLS FROM THE THERMAL LIQUEFACTION OF PEAT

M. K. D'iakova and N. A. Davtian

Institute of Combustible Minerals, Academy of Sciences USSR

In the thermal liquefaction of peat a considerable proportion of the oxygen present in its organic matter enters into liquid products, forming valuable oxygen-containing compounds, among which low-boiling phenols are of special interest. These phenols (phenol, cresols, and xylenols) can be successfully used in the chemical industry for the production of plastics, synthetic resins, etc.

There have been a number of investigations of the composition of phenols formed formed from peat by semicoking and gasification, and of methods for their separation and purification [1]. The following compounds have been identified in peat phenols: phenol, o-, m-, and p-cresols, 1,2,3-, 1,2,4-, and 1,3,5-xylenols, o-, m-, and p-ethylphenols, guaiacol, resorcinol, pyrocatechol, and hydroquinone [1, 2]. Peat tar contains about 12% phenols, or 1.4% on the organic matter of the peat; about one half of this consists of lower phenols [3].

Thermal liquefaction of peat yields 2-3 times as much of low-boiling phenols as semicoking.

The present investigation deals with the composition of phenols, boiling up to 225°, made by the thermal liquefaction of upper and lowland peats.

TABLE 1

Isolation of Phenols, Bases, and Carboxylic Acids from Ligroine Fractions Obtained by Thermal Liquefaction of Peat

Fraction of b. p. 225°, made by liquefaction of:	Yield (% on ligroine fraction)			
	phenols	bases	carboxylic acids	neutral oils
Lowland peat in hydrogenated peat tar	14.0	3.0	0.7	82.3
Upper peat in solar oil	9.0	1.2	0.5	89.3

EXPERIMENTAL

Raw materials, methods for isolation and purification of phenols. The phenols used for the study were isolated from the ligroine fractions boiling up to 225°, obtained by thermal liquefaction of lowland peat from "Redkii Rog" (Minsk province) in hydrogenated peat tar boiling in the 225-360° range, and by thermal liquefaction of upper Redkin peat (Kalinin province) in petroleum solar oil boiling in the 254-360° range. The liquefaction was performed in a continuous unit at 400-405°, with the peat paste remaining 30-45 minutes in the reaction zone, at 25 atmos. Under these conditions lowland peat yields (calculated on the peat organic matter) 18.5% of a ligroine fraction containing 9% of phenols.

Before isolation of the phenols, nitrogen compounds were removed from the ligroine fractions by treatment with 20% sulfuric acid saturated with sodium chloride [4]. Phenols were isolated by addition of 10% aqueous caustic alkali. The phenolate solution was washed 2-3 times with benzene to remove neutral oils present in the phenolates, and the residual benzene was then blown out in steam. The oil-free phenolates were decomposed by 30% sulfuric acid. The free phenols were extracted in ether, and the ether was distilled off (Table 1).

Carboxylic acids present in the crude phenols were extracted in saturated sodium bicarbonate solution by the action of heat on a water bath at 60°. The treatment of phenols with sodium bicarbonate solutions was repeated until the color of the extract became pale yellow. The phenols, freed from carboxylic acids, were further purified by means of 50% metaphosphoric acid (1.5% on phenol weight) under the action of heat for an hour, and the phenols were then distilled off under 2-3 mm Hg pressure [5]. The yield of purified phenols was 93.3%.

Isolation and purification of phenols from the ligroine fraction obtained by thermal liquefaction of lowland peat in hydrogenated peat tar yielded 13% of purified phenols by weight. The elementary composition was (%):C 77.54, H 7.5, O 14.96; nitrogen and sulfur absent.

The yield of purified phenols from the ligroine fraction obtained by thermal liquefaction of upper peat in petroleum solar oil was 8.4% by weight. The elementary composition was (%): C 77.95, H 7.86, O 14.19; no nitrogen or sulfur were found.

Investigation methods. The purified phenols were separated into narrow fractions by means of a column with an efficiency of 35 theoretical plates. The narrow fractions were characterized by their physical constants; the density, refractive index, and molecular weight were determined. The latter was found from the molecular weight of the methyl ethers formed on methylation of the phenol fractions by dimethyl sulfate [6]. The fractionation results and the physical constants of the fractions are given in Table 2.

TABLE 2

Characteristics of Phenols Formed by Thermal Liquefaction of Peat

Lowland peat in hydrogenated peat tar					Upper peat in solar oil				
boiling ranges of fractions (°C)	yield (%)	n_D^{20}	d_4^{20}	molecular weight	boiling ranges of fractions (°C)	yield (%)	n_D^{20}	d_4^{20}	molecular weight
180—183	13.3	1.5420	1.0683	100	181—183	12.1	1.5420	—	98
183—189	7.6	1.5450	1.0514	—	183—185	7.2	1.5420	—	—
189—192	5.5	1.5442	1.0420	109	185—189	1.9	1.5468	1.0581	—
192—199	14.1	1.5408	1.0354	—	189—194	3.0	1.5438	1.0436	110
199—204	20.8	1.5395	1.0282	112	194—198	2.4	1.5420	1.0424	—
204—206	3.2	1.5368	1.0219	—	198—203	13.8	1.5400	1.0416	—
206—212	12.3	1.5366	1.0158	121	203—206	2.2	1.5360	1.0385	112
212—215	7.6	1.5353	1.0080	124	206—209	12.5	1.5362	1.0188	—
215—217	0.9	1.5342	1.0038	—	209—212	5.0	1.5358	1.0188	120
217—219	4.0	1.5335	1.0036	128	212—215	2.6	1.5328	1.0156	—
219—221	1.4	1.5333	1.0025	—	215—218	7.6	1.5325	1.0130	126
221—225	2.9	1.5320	1.0012	—	218—220	5.0	1.5328	1.0127	—
225—230	2.8	1.5310	1.0020	—	220—221	12.2	1.5324	1.0113	—
Residue in flask, and losses	3.6				221—225	4.3	1.5310	—	—
					225—230	2.5	1.5285	—	—
					Residue in flask, and losses	5.7			
	100.0					100.0			

Individual phenols were identified by sulfonation of the narrow phenolic fractions with subsequent fractional decomposition of the phenolsulfonic acids by means of steam [7], in conjunction with formation of arylglycolic acids and separation of the latter by crystallization [8, 9].

The phenolsulfonic acids were prepared as follows: 10 or 20 g of the narrow phenolic fraction was sulfonated with an equal weight of sulfuric acid of sp.gr. 1.84 for 3 hours at 100-103°. After extraction of unchanged phenols in benzene, the sulfonation products were diluted with 20% sulfuric acid to a volume at which the boiling point of the mixture did not exceed 100°. The sulfonic acids were decomposed by a continuous stream of

TABLE 3

Investigation of Narrow Phenolic Fractions Made by Thermal Liquefaction of Lowland Peat in Hydrogenated Peat Tar

Boiling range of fraction (°C)	Characteristics of aryloxacetic acids				Corresponding acids	Literature data for acids				Shows presence of
	melting point (°C)	acid number	elementary composition C	elementary composition H		melting point (°C)	acid number	elementary composition C	elementary composition H	
180—183	97	365.5	—	—	Phenoxyacetic	98	368.4	—	—	Phenol
183—189	96.5—97	333	—	—	Phenoxyacetic	98	368.4	—	—	Phenol
	151—151.5	—	—	—	o-Cresoxyacetic	151—152	337.3	—	—	o-Cresol
189—192	151—151.5	334.5	65.36	6.30	o-Cresoxyacetic	151—152	337.3	65.06	6.02	o-Cresol
192—199	151—152	—	65.52	6.28	o;Cresoxyacetic	151—152	337.3	65.06	6.02	o-Cresol
	136—137				p-Cresoxyacetic	135—136				p-Cresol
	101—102				m-Cresoxyacetic	102—103				m-Cresol
199—204	136—137	330	—	—	p-Cresoxyacetic	135—136	337.3	—	—	p-Cresol
	101—102	329	—	—	m-Cresoxyacetic	102—103	337.3	—	—	m-Cresol
206—212	139.5—140	308	66.68	6.42	2,4-Dimethylphenoxyacetic	142	311.1	66.67	6.67	2,4-Dimethylphenol
	96—97	306			p-Ethylphenoxyacetic	97				p-Ethylphenol
	140—141.5				o-Ethylphenoxyacetic	141				o-Ethylphenol
	117—118	304.6			2,5-Dimethylphenoxyacetic	118				2,5-Dimethylphenol
212—217	85—86	308	66.56	6.46	3,5-Dimethylphenoxyacetic	86	311.1	66.67	6.67	3,5-Dimethylphenol
	97	304			p-Ethylphenoxyacetic	97	311.1			p-Ethylphenol

TABLE 4

Investigation of Narrow Phenolic Fractions Made by Thermal Liquefaction of Upper Peat in Solar Oil

Boiling range of fraction (°C)	Melting point of fraction (°C)	Phenol content (%)	Characteristics of aryloxyacetic acids				Corresponding acids	Literature data for acids				Show presence of	Established from Raman spectrum
			melting point (°C) [8]	acid number	elementary comp. (%)			melting point (°C) [8]	acid number	elementary comp. (%)			
					C	H				C	H		
181—183	37.0	95.0	—	—	—	—	—	—	—	—	—	Phenol*	—
183—185	24.7	73.0	—	—	—	—	—	—	—	—	—	—	o-Cresol
185—189	—	—	151—151.5	334.5	65.18	6.22	o-Cresoxyacetic	151—152	337.3	65.06	6.02	p-Cresol	o-Cresol m-Cresol p-Cresol
189—194	—	—	151—152	335	65.10	6.23	o-Cresoxyacetic	151—152	337.3	65.06	6.02	o-Cresol	—
198—203	—	—	102—103	336	65.20	6.15	m-Cresoxyacetic	102	337.3	65.06	6.02	m-Cresol	m-Cresol
			134.5—135.5	332	65.26	6.10	p-Cresoxyacetic	135—136	337.3	65.06	6.02	p-Cresol	p-Cresol Guaiacol

steam at definite temperatures. In some instances the sulfonic acid were treated with saturated potassium chloride solution [10] before decomposition. The potassium sulfonates formed, insoluble in potassium chloride solution, were filtered onto a glass filter, and the sulfonic acids were then liberated by the action of 30% sulfuric acid and decomposed by steam at various temperatures. The separated phenols were converted into aryloxyacetic acids by the Koelsch method [8].

The aryloxacetic acids, in the case of xylenol fractions were prepared by the method of steinkopf and Hopner [8], who use dry substances, which increased the acid yields. The properties of aryloxyacetic acids prepared in the identification of phenols, and the corresponding literature data, are presented in Tables 3 and 4.

The phenols isolated from the ligroine fraction obtained in the thermal liquefraction of Redkin upper peat were also investigated by Raman spectroscopy.

The contents of phenol, and o-, m-, and p-cresols were approximately estimated from the data obtained by fractionation through an efficient column, from the yields of phenolic distillates after hydrolysis of phenolsulfonic acids, from the yields of aryloxyacetic acids, and the melting points of the narrow phenolic fractions. Phenol and o-cresol were determined quantitatively in the narrow fractions with the aid of Raschig's table [11], and m-cresol was determined by Qwist's method [12].

DISCUSSION OF RESULTS

The results obtained for the narrow phenolic fractions from the thermal liquefaction of lowland peat in hydrogenated peat-tar, presented in Table 3, show that these fractions consist of phenol, o-, m-, and p-cresols, o- and p-ethylphenols, and 2,4-, 2,5-, and 3,5-dimethylphenols. This was confirmed by preparation of aryloxyacetic acids which were very close in their melting points, acid numbers, and elementary composition to available literature data of individual aryloxyacetic acids.

*The tribromo derivative prepared from this fraction melted at 95°, which corresponds to tribromophenol.

The distillation data in Table 2 show that the phenols formed in the thermal liquefaction of lowland peat contain 64.5% of a phenol–cresol fraction. The contents of phenol and o-cresol were calculated from the melting point of the fraction boiling at 180-183° (it melted at 37°), and from the yields of phenoxyacetic and o-cresoxyacetic acids from the fractions boiling at 183-189°, 189-192° and 192-199°. The m-cresol content was determined in the aggregate fraction boiling at 183-206° by Qwist's method [12]. The p-cresol content was found by difference. From these calculations it was tentatively found that the phenols formed by the thermal liquefaction of lowland peat contain 14% phenol, 14% o-cresol, 9% m-cresol, and 27.5% p-cresol. The rest consists of ethylphenols and xylenols.

It follows from the data in Tables 4 and 5 that the phenols formed by thermal liquefaction of upper peat in solar oil contain phenol, o-, m-, and p-cresols, guaiacol, and 2,4-dimethylphenol; this was confirmed by preparation of tribromophenol from the fraction boiling at 181-183°, of aryloxyacetic acids from the fractions boiling in the 183-185°, 185-189° and 194-203° ranges, and by the Raman spectra.

The characteristic lines given in Table 5 for the fractions boiling at 185-189°, 198-203° and 203-209° show that individual phenols cannot be isolated with the aid of a column of an efficiency equivalent to 35 theoretical plates. The fraction boiling at 185-189°, which consists mainly of o-cresol, also contains p-cresol and possibly m-cresol. The fractions boiling at 198-203° and 203-209° contain guaiacol in addition to p- and m-cresols. The fraction boiling at 203-209 also contains 2,4-dimethylphenol.

TABLE 5

Characteristic Lines of the Raman Spectra of Phenols Made by Thermal Liquefaction of Upper Peat in Solar Oil, Compared with Spectral Lines for Individual Phenols

Frequencies (cm^{-1}) and intensities*							
fractions (°C)			literature data				
185–189	198–203	203–209	o-cresol [13]	m-cresol [13]	p-cresol [13]	guaiacol [14]	2,4-dimethylphenol [13]
273 (2)	—	—	274 (5)	—	—	—	—
340 (5)	338 (5)	340 (5)	—	—	337 (6)	346 (3)	345 (9)
—	—	385 (5)	—	—	—	—	—
—	—	447 (2)	—	—	—	—	450 (7)
—	—	460 (4)	—	—	—	458 (2)	—
469 (4)	468 (6)	—	—	—	464 (6)	—	—
511 (3)	503 (1)	490 (2)	—	—	—	500 (2)	490 (9)
—	522 (2)	519 (1)	—	521 (5)	—	—	—
528 (2)	—	—	530 (5)	—	—	—	—
—	534 (1)	—	—	—	—	534 (5)	—
—	544 (2)	542 (2)	—	541 (5)	—	—	—
559 (1)	568 (1)	568 (1)	—	—	—	—	570 (9)
590 (5)	585 (3)	585 (2)	—	—	—	583 (5)	—
649 (4)	644 (6)	646 (5)	—	—	646 (5)	—	—
718 (2)	718 (4)	715 (4)	—	—	—	—	710 (10)
734 (3)	733 (5)	735 (4)	—	735 (8)	736 (1)	—	—
748 (10)	—	—	749 (12)	—	—	—	—
—	760 (2 b)	764 (4)	—	—	—	758 (10)	765 (9)
	823 (5)	821 (3)	—	—	825 (4)	—	—
843 (4)	845 (10)	845 (10)	847 (2)	—	841 (9)	—	—
		929 (2)	989 (3)	—	—	—	930 (9)
1004 (8)	1001 (10)	1001 (7)	—	998 (10)	—	1024 (3)	—
	1037 (3)	1037 (3 b)	—	—	—	1039 (7)	1035 (1)
1046 (8)	1050 (3)	1058 (2 b)	1044 (8)	—	—	—	—
—	—	—	—	1084 (4)	—	—	—
1117 (2b)	1117 (2 b)	1117 (3)	—	—	—	—	—
1155 (3)	1158 (4)	1155 (3 b)	1153 (3)	1160 (2)	—	1154 (6)	—
1178 (2)	1170 (5)	1173 (4)	—	—	1170 (3)	—	—
1205 (4)	1206 (2)	1202 (4)	—	—	—	—	—
1217 (4)	1215 (5)	1214 (4)	—	—	1213 (4)	—	—
1237 (2)	—	—	1238 (4)	—	—	—	—
1264 (5)	1264 (5)	1265 (6 b)	1256 (4)	—	1251 (3)	—	—
—	—	—	—	1277 (5)	—	—	—
1331	1326 (1)	1321 (3)	—	—	—	—	—
1384 (8)	1383 (6)	1382 (6)	1380 (3)	—	1380 (3)	—	—

*The intensities for the fractions were estimated visually on a 10-point scale.

According to the distillation data in Table 2, 42.6% belongs to the phenol–cresol fraction. The approximate quantitative composition of this fraction, calculated as described above, is (in %): phenol 17, o-cresol 7, m-cresol 10, and p-cresol about 9, calculated on the phenolic fraction.

The elementary composition of the narrow phenolic fractions, boiling at 215-218°, 218-220° and 220-221°, is in the range: C 78.10-78.58%, H 8.10-8.20%; this is in good agreement with the calculated elementary composition of xylenols and ethylphenols (C 78.7%, H 8.19%).

SUMMARY

The composition of phenols formed in the thermal liquefaction of lowland peat in hydrogenated peat tar, and of upper peat in solar oil, has been studied; it is shown that the phenols obtained from lowland peat contain about 14% phenol, 14% o-cresol, 9% m-cresol, and 27% p-cresol. In the fraction boiling above 206°, o- and p-ethylphenols and 2,4-, 2,5-, and 3,5-dimethylphenols were detected.

Phenols formed by thermal liquefaction of upper peat in solar oil were found to contain approximately 17% phenol, 7% o-cresol, 10% m-cresol, and 9% p-cresol. Phenol, o-, m-, and p-phenols, guaiacol, and 2,4-dimethylphenol were identified.

LITERATURE CITED

[1] V. E. Rakovskii and P. M. Ioffe, Trans. Inst. Peat 19, 27 (1939); M. V. Bulochnikov, ibid 19, 10 (1939); E. V. Voznesenskaia, ibid 19, 10 (1939); E. V. Voznesenskaia, ibid 19, 40 (1939); E. V. Voznesenskaia, ibid 19, 134 (1939); E. V. Rakovskii, Kh. I. Rivkina, S. I. Beniushevich, and G. D. Konontseva, Trans. Moscow Peat Inst. 2, 136 (1953).

[2] E. Börnstein and F. Bernstein, Z. ang. Ch. 27, 71 (1914); V. A. Lanin, Proc. 6th Conf. on Aniline Dye Chemistry [in Russian] Moscow–Leningrad, Izd. AN SSSR, 1942), p. 17.

[3] U. I. Kizner, Peat Industry 1, 27 (1940).

[4] C. H. Tischer and A. Eisner, Ind. Eng. Ch. 9, 213 (1937).

[5] V. A. Lanin, L. M. Mokhun' and N. D. Edemskaia, Bull. Acad. Sci. USSR, OTN 10, 128 (1956).

[6] S. Caplan, I. Ross, M. G. Sevag and M. Switz, Ind. Eng. Ch. 6, 1, 7 (1934).

[7] H. Brückher, Z. ang. Ch. 41, 1064 (1928); O. Kruber and A. Schmidt, Ber. 64, 2270 (1931); N. M. Karavaev, A. N. Bashkirov, and L. P. Kraeva, Collected Papers on Coal Chemistry [in Russian] 1, 97 (1934); I. B. Rapoport, Z. Vasil'eva and K. Zhirnova, Chem. Solid Fuel 7, 634 (1935).

[8] W. Gluud and P. K. Breuer, Abh. Kohle, 2, 236 (1917); 3, 242 (1918); W. Steinkopf and T. Hopner, J. pr. Ch. 113, 137 (1926); F. Koelsch, J. Am. Soc. 53, 304 (1931).

[9] S. S. Nametkin, N. N. Mel'nikov, Iu. A. Baskakov and K. S. Bokarev, J. Anal. Chem. 5, 1 (1950).

[10] A. N. Bashkirov and L. P. Kraeva, Collected Papers on Coal Chemistry [in Russian] 1, 99 (1934).

[11] F. Raschig, Abh. Kohle, 2, 178 (1917).

[12] W. Qwist, Z. anal. Ch. 65, 289 (1924); 68, 257 (1926).

[13] K. W. F. Kohlrausch and A. Pongratz, Monatsh, 63, 427 (1933); 64, 361 (1934).

[14] Landolt, 1, 2, 536 (1951).

Received January 8, 1957

BRIEF COMMUNICATIONS

THERMODYNAMIC PROPERTIES OF LIQUID ALLOYS IN THE SYSTEM SODIUM–LEAD

A. G. Morachevskii

The M. I. Kalinin Polytechnic Institute, Leningrad

The literature contains very little information on the thermodynamic properties of liquid alloys in the sodium–lead system. Measurements of the activity of sodium, carried out by Hauffe and Vierk [1], relate only to alloys in which the atomic fraction of sodium is between 0.9 and 0.4; i.e., they do not cover the lead-rich region, and cannot be used for reliable calculation of the integral thermodynamic characteristics of the system.

We carried out an electrochemical investigation of the sodium–lead system over a wide range of sodium concentrations at 375, 425, and 475°. The electromotive force (e.m.f.) of the following cell was determined:

Na | electrolyte with Na^+ ions | Na + Pb.

As in studies of other binary and ternary alloys of sodium [2, 3], the electrolyte used was glass containing sodium oxide. The methods used for the measurements, the apparatus, and preparation of the metals are described in an earlier paper [3].

The results of e.m.f. (E) measurements were used to calculate the activity of sodium from the equation

$$\ln a_{Na} = -\frac{F}{RT} E,$$

where F is the Faraday number.

The partial molar isobaric potential of sodium is

$$\Delta\bar{Z}_{Na} = RT \ln a_{Na}.$$

Correspondingly, the excess partial molar isobaric–isothermal potential of sodium is

$$\Delta\bar{Z}^{x}_{Na} = RT \ln a_{Na} - RT \ln N_{Na} = RT \ln \gamma_{Na}.$$

The partial molar entropy of mixing and heat of mixing are, respectively

$$\Delta\bar{S}_{Na} = F\left(\frac{dE}{dT}\right),$$

$$\overline{\Delta H}_{Na} = \overline{\Delta Z}_{Na} + T\Delta\bar{S}_{Na}.$$

The activity of lead in alloys with sodium was calculated from the equation [4]

$$\lg \frac{a_{Pb}}{N_{Pb}} = \lg \gamma_{Pb} = \int_0^{N_{Na}} \frac{\lg \gamma_{Na}}{(1-N_{Na})^2} dN_{Na} - \frac{N_{Na}}{1-N_{Na}} \lg \gamma_{Na}.$$

The excess integral molar isobaric–isothermal potential was found from the equation

$$\Delta Z^x = (1 - N_{Na}) \int_0^{N_{Na}} \frac{\overline{\Delta Z}^x_{Na}}{(1 - N_{Na})^2} \, dN_{Na}.$$

Analogous equations were used to determine other integral thermodynamic characteristics of the system.

DISCUSSION OF RESULTS

The results of the e.m.f. determinations, and the activities and excess partial molar isobaric–isothermal potentials of sodium at 425° are given in Table 1.

TABLE 1

Values of e.m.f., Activity, and Partial Molar Isobaric–Isothermal Potential of Sodium

N_{Na}	E_{375}	E_{425}	E_{475}	$\frac{\Delta E}{\Delta T} \cdot 100$ (mv/deg.)	a_{Na} 425°	$\overline{\Delta Z}^x_{Na}$ 425° (cal.)
0.901	—	8.2	—	—	0.872	— 44
0.851	—	15.9	17.6	3.4	0.768	— 143
0.800	—	33.1	34.8	3.4	0.570	— 470
0.734	—	74.1	71.3	—5.6	0.292	—1280
0.700	—	83.7	81.7	—4.0	0.248	—1440
0.601	—	132.4	—	—	0.110	—2350
0.598	141.4	137.5	133.5	—8.0	0.102	—2460
0.503	—	196.6	192.8	—7.6	0.038	—3580
0.500	201.8	197.2	192.8	—8.8	0.038	—3580
0.409	—	262.6	258.6	—8.0	0.013	—4770
0.402	271.0	268.0	265.0	—6.0	0.012	—4850
0.354	—	297.4	294.9	—5.0	0.007	—5420
0.300	340.6	337.1	334.2	—5.8	0.004	—6110
0.222	—	386.4	383.8	—5.2	0.0016	—6840
0.205	—	400.5	399.6	—1.8	0.0013	—7040
0.200	408.5	407.2	405.8	—2.8	0.0011	—7170
0.177	—	425.7	426.6	1.8	0.0008	—7420
0.149	—	450.5	452.4	3.8	0.0006	—7750
0.131	450.7	452.0	453.2	2.4	0.0005	—7620

The activity isotherms of sodium and lead at 425° are given in Fig. 1. The activities of sodium calculated from the data of Hauffe and Vierk [1] are also given; the agreement with our values is quite satisfactory.

Curves for the partial molar excess isobaric–isothermal potentials of sodium and lead at 425°, and the corresponding integral curve, are given in Fig. 2. The ΔZ^x curve has a very flat minimum, owing to the presence of a number of compounds with similar melting points. In fact, the compounds Na_4Pb, Na_5Pb_2 and NaPb, with melting points of 376, 400, and 368° respectively, are formed in the system sodium–lead.

Figure 3 shows the curve for the partial molar entropy of mixing for sodium ($\overline{\Delta S}_{Na}$). Even at the composition corresponding to Na_4Pb, $\overline{\Delta S}_{Na}$ decreases sharply and then passes into the negative region. It is clear from Fig. 4 that the integral molar entropy of mixing is negative for all the region of metallic-compound formation. Negative values of the entropy of mixing in liquid binary metallic alloys are observed if compounds with bonds of a partial ionic character are formed in the systems. According to Vetter and Kubaschewski [5] the entropy is negative in the region of medium concentrations in the systems Mg-Bi (700-800°) and Mg-Sb (860-920°). The strong polarity of bonds in the compounds Mg_3Bi_2 and Mg_3Sb_2 was experimentally demonstrated by Kubashewski and Reinartz [6]. According to Roeder and Morawietz [7], the entropy of mixing is also negative over a definite concentration region in the K–Hg system. All this indicates that the entropy of mixing in metallic alloys can be approximately regarded merely as a measure of particle order and arrangement; the most important factor influencing the magnitude and sign of ΔS is the nature of the bonds in the intermetallic compounds formed in a given system.

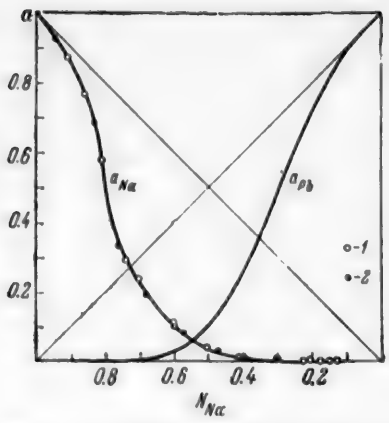

Fig. 1. Activity isotherms of the components in sodium–lead alloys at 425°. 1) Our data, 2) data of Hauffe and Vierk.

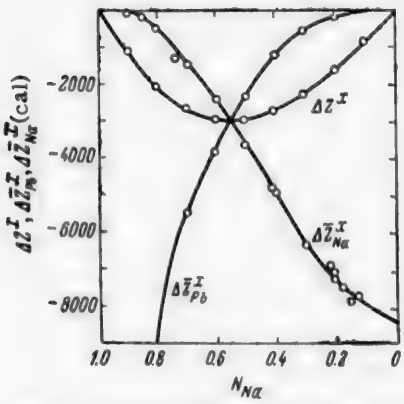

Fig. 2. Excess partial molar isobaric-isothermal potentials in the system sodium–lead at 425°, and the integral curve.

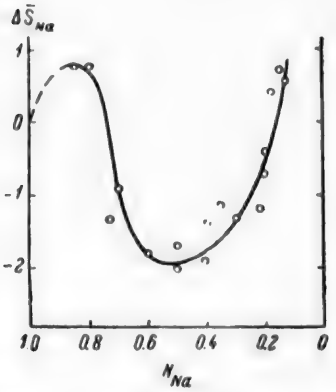

Fig. 3. Partial molar entropy of mixing of sodium (in cal/degree · ·g-atoms).

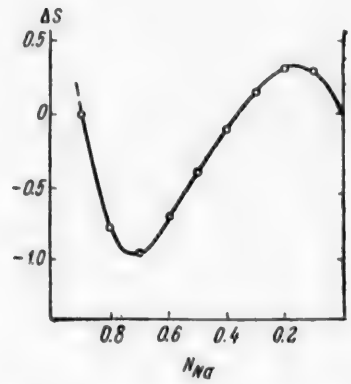

Fig. 4. Integral molar entropy of mixing (in cal/degree · g-atoms).

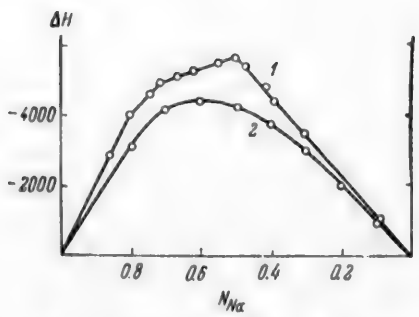

Fig. 5. Integral molar heats of formation (in cal/g-atom) of solid alloys (Curve 1), and of mixing of liquid alloys (Curve 2).

From the thermodynamic standpoint, the entropy of mixing can perfectly well be negative. It is known that

$$\Delta Z = \Delta H - T\Delta S < 0, \qquad (1)$$

where ΔH is the heat of mixing.

In the present instance the values of ΔZ, ΔH, and ΔS characterize the formation of alloys in isothermal–isobaric conditions from the corresponding pure components in the same state of aggregation. For such irreversible processes the second law of thermodynamics merely indicates the sign of the change of isobaric potential ($\Delta Z < 0$), while the question of the signs of the heat of mixing and entropy of mixing remains open. It follows from Equation (1) that when $\Delta H < 0$ (exothermic mixing), ΔS may have either

positive or negative values. It must be noted, however, that if $\Delta S < 0$, then $|\Delta H| > |T\Delta S|$.

The heat of mixing in the system sodium–lead is negative for all compositions (Fig. 5, Curve 2). Its greatest value is −4350 cal/g-atom at $N_{Na} = 0.6$. The scattering of the points in Fig. 3 shows that the accuracy in determinations of ΔS_{Na} is low because of the small value of the temperature coefficient of e.m.f.; as a result, the accuracy in determinations of the integral entropy of mixing is not high. However, it seems that errors in determinations of ΔS do not seriously affect the value of ΔH. The integral molar isobaric potential and heat of mixing, and the values of $T\Delta S$ at 425°, are given below.

N_{Na}	ΔZ	$T\Delta S$	ΔH
0.8	−2770	−540	−3310
0.7	−3500	−660	−4160
0.6	−3870	−480	−4350
0.5	−3900	−290	−4190
0.4	−3620	− 70	−3690
0.3	−3110	100	−3010
0.2	−2260	220	−2040
0.1	−1240	200	−1040

It follows from the foregoing that the role of the entropy component is relatively small for all compositions.

Figure 5 (Curve 1) also shows the heat of formation of solid alloys in the system sodium–lead, as a function of concentration, based on the data of Seith and Kubaschewski [8]. The inflections on the curve are associated with the existence of the compounds Na_4Pb, Na_5Pb_2, NaPb. There are no calorimetric data on the heats of mixing for the system sodium–lead in the liquid state.

In conclusion, I thank Professor A. F. Alabyshev for his guidance of this work.

SUMMARY

1. The e.m.f., of the concentration cell Na | electrolyte with Na^+ ions | Na + Pb was measured; the results were used to calculate the activities of sodium and lead, the partial and integral molar excess isobaric–isothermal potentials, entropy of mixing, and heat of mixing of the system. The system shows considerable negative deviations from Raoult's law.

2. The extremal values of the isobaric potential and heat of mixing lie in the region of intermetallic-compound formation.

LITERATURE CITED

[1] K. Hauffe and A. L. Vierk. Z. Elektroch. 53, 151 (1949).

[2] A. F. Alabyshev and A. G. Morachevskii, Proc. Acad. Sci. USSR 111, 369 (1956).•

[3] A. F. Alabyshev and A. G. Morachevskii, J. Inorg. Chem. 2, 669 (1957).

[4] C. Wagner, Thermodynamics of Alloys, Cambridge, Mass. (1952).

[5] F. A. Vetter and O. Kubaschewski, Z. Elektroch. 57, 243 (1953).

[6] O. Kubaschewski and K. Reinartz, Z. Elektroch. 52, 75 (1948).

[7] A. Roeder and W. Morawietz, Z. Elektroch. 60, 431 (1956).

[8] W. Seith and O. Kubashewski, Z. Elektroch. 43, 743 (1937).

Received October 29, 1956

•Original Russian pagination. See C.B. Translation.

EXPERIMENTAL INVESTIGATION OF THE GAS REDUCTION OF Na_2SO_4 TO Na_2CO_3 IN A SHAFT FURNACE*

A. I. Gorbanev

Our investigations [1-4] showed that the reduction of sodium sulfate to sodium carbonate is effected most economically and conveniently by means of semiwater gas. Therefore our further experiments with a large-scale shaft-furnace unit were carried out with semiwater gas as reducing agent.

The large experimental unit is shown schematically in the diagram.

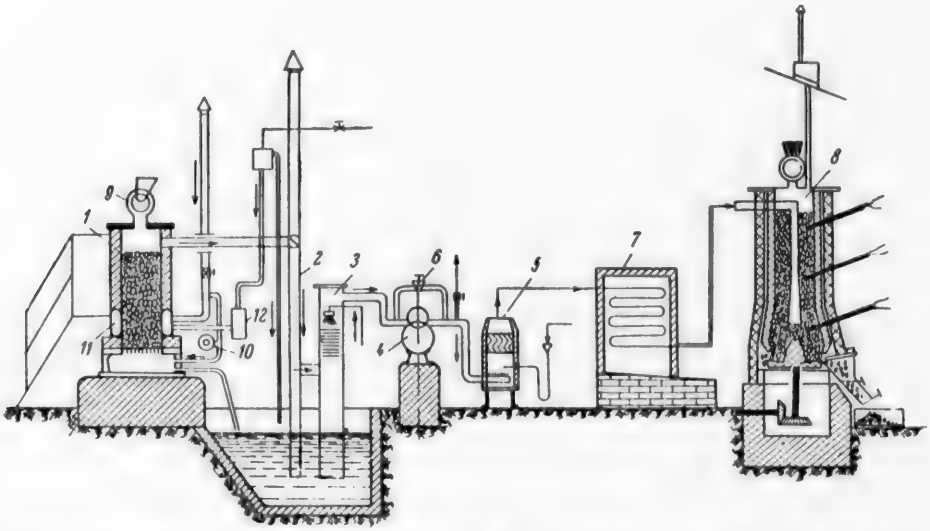

Large experimental unit. 1) Gas producer, 2) dust separator, 3) scrubber, 4) pump, 5) humidifier, 6) pressure regulator, 7) gas preheater, 8) shaft furnace, 9) sluice feed, 10) fan, 11) water jacket of gas producer, 12) float regulator.

The mixed producer gas used for sulfate reduction is made in the gas producer 1 by gasification of coke. The composition of the gas depends on the steam content of the steam–air mixture. The gas from the producer enters the water-spray dust separator 2, where solid particles (soot, ash) are removed, and then, for further removal of mechanical tar and carbon impurities it passes into the scrubber 3, packed with horizontal plates sprayed with water from above.

The purified gas is drawn out of the scrubber by means of the rotary pump 4, and enters the humidifier 5. The amount of gas entering the humidifier, and therefore used for reduction, is regulated by the pressure regulator 6 and measured by means of a differential manometer placed in the gas pipe between the pump and humidifier. The sprayed gas, after passing through the layer of water in the humidifier, is saturated with water vapor to a partial pressure P_{H_2O} = 0.35-0.40 atmos. The temperature of the gas, saturated with water vapor, is measured by means of a thermometer situated in the exit pipe.

*Communication V.

The reducing gas mixed with water vapor enters the preheater 7. The latter consists of a system of bent pipes made from stainless heat-resisting steel enclosed in a brick chamber and heated by flue gas or producer gas. The temperature of the gas leaving the preheater is measured by means of a thermocouple, and is approximately equal to the reduction temperature of sodium sulfate, i.e., 610-670°. The preheated gas then enters the shaft furnace 8.

The shaft furnace consists of an iron cylinder conically widened at the lower end. The furnace is lined with shaped fireclay blocks; its outer diameter is 350 mm, the internal diameter is 286 mm, and the height is 1800 mm. Cylindrical briquets, 15 mm in diameter and of approximately the same height, are fed into the top of the shaft through a sluice feed. The furnace can hold 250 kg of briquets at a time. The briquets are discharged continuously from the bottom of the furnace by means of a revolving platform with a scraper knife. As the converted material is discharged, the briquets lying above gradually settle under gravity and descend down the shaft. The discharge orifice of the furnace is made air-tight by means of a conical closing device. Calculations show that the briquets remain in the furnace for about 16 hours; the furnace output is 10 kg/hour. The briquets, containing catalyst (Fe), are made in a special roller press.

TABLE 1

Reduction of Na_2SO_4 to Na_2CO_3 in the Shaft Furnace Unit

Duration of expt. (hours)	Composition of producer gas %				Composition of mixed gas %				Average gas rate (m^3/hour)	Humidifier temp. (°C)	Exit gas rate (m^3/hour)	Temp. of gas entering furnace (°C)	Furnace temp. (°C)		Temp. of exit gas (°C)
	CO_2	CO	H_2	O_2	CO_2	CO	H_2	O_2					bottom	top	
1	7.2	20.1	—	—	—	—	—	—	35.0	76.0	23.0	593	603	560	367
2	6.3	20.6	6.5	0.2	—	—	—	—	35.0	76.0	23.0	593	617	570	382
3	—	—	—	—	—	—	—	—	19.0	76.2	20.2	586	617	573	356
4	7.6	19.0	8.0	0.5	—	—	—	—	21.5	77.2	17.9	592	622	587	388
5	5.0	21.2	9.3	0.5	—	—	—	—	27.7	77.5	17.8	580	615	603	412
6	—	—	—	—	—	—	—	—	27.5	77.5	18.3	597	622	512	445
7	—	—	—	—	9.4	16.0	16.2	0.6	30.0	78.6	18.4	584	648	608	470
8	—	—	—	—	8.6	14.6	18.4	0.4	33.2	79.3	21.1	563	650	602	465
9	—	—	—	—	8.4	11.8	21.4	0.5	32.2	77.2	18.1	572	637	587	447
10	—	—	—	—	5.5	18.7	16.0	0.2	29.7	78.7	17.8	603	655	585	437
11	—	—	—	—	—	—	—	—	19.3	83.7	18.1	552	668	600	398
12	—	—	—	—	9.0	7.4	32.0	0.4	21.1	80.1	17.2	545	660	615	397
13	—	—	—	—	4.9	18.6	18.8	0.1	24.7	79.0	21.1	550	658	630	413
14	—	—	—	—	8.6	17.8	29.4	2.2	29.2	82.5	24.0	557	662	633	438
15	—	—	—	—	—	—	—	—	26.6	84.3	22.7	563	655	637	437
16	—	—	—	—	10.4	18.4	18.2	1.0	28.6	77.7	22.7	583	660	637	450
17	—	—	—	—	—	—	—	—	27.2	76.0	20.6	570	663	643	450
18	—	—	—	—	7.4	21.6	12.7	0.3	29.3	76.0	18.7	565	658	648	450
19	—	—	—	—	—	—	—	—	29.6	76.0	19.2	605	662	615	445
20	—	—	—	—	8.0	20.8	11.2	0.2	18.4	76.0	17.3	590	662	610	428
21	—	—	—	—	—	—	—	—	22.0	76.0	20.0	590	660	617	413
22	—	—	—	—	9.6	19.4	12.0	0.5	29.6	76.0	20.1	597	660	623	420
23	—	—	—	—	—	—	—	—	23.7	78.3	17.9	593	662	632	413
24	—	—	—	—	11.5	12.1	10.8	0.3	27.5	78.3	18.9	577	655	633	422
25	—	—	—	—	—	—	—	—	38.0	76.0	22.1	603	650	613	433
26	—	—	—	—	8.0	21.3	13.2	0.4	41.0	76.0	24.3	610	647	603	440
27	—	—	—	—	5.4	20.2	11.4	0.8	35.3	76.5	22.6	622	663	585	428
28	—	—	—	—	—	—	—	—	38.0	77.0	23.8	545	668	590	379
Mean	6.5	20.2	7.9	0.4	8.2	17.05	17.2	0.5	26.3	77.7	20.2	581	648	605	420

The reducing gas passes along a pipe situated in the center of the shaft furnace to the lower end of the furnace, is distributed across it between the briquets, and ascends countercurrent to the slowly descending briquets. The spent gas passes through a moisture trap into the air.

The temperature at various heights of the furnace is measured by means of chromel–amanil thermocouples.

Experiments With the Pilot Unit

Some tens of experiments performed in the pilot shaft furnace demonstrated that the conversion of over 90% of sodium sulfate into carbonate is perfectly possible; this confirmed our results obtained in the laboratory unit.

In view of the fact that the degree of reduction of sodium sulfate to carbonate depends mainly on the furnace operating conditions, the concentrations of carbon monoxide and hydrogen, furnace temperature, and moisture content of the gas, the results of all the experiments are not given in this paper, as they differ only in the degree of reduction and experimental conditions. For this reason, the results of only one experiment, of the greatest duration and most characteristic of the process, are given here. During this experiment, which lasted 28 hours, 170 kg of sodium sulfate in the form of briquets mixed with catalyst was converted.

TABLE 2

Analytical Data for Briquets at Different Heights in the Furnace

Sampling point	Composition (%)					Deg. reduction of Na_2SO_4 (%)	Yield of Na_2CO_3 (%)
	Na_2CO_3	Na_2SO_4	Na_2S	Na_2SO_3	Other impurities and insoluble matter		
Top briquet layer	67.50	24.35	0.79	0.40	6.96	79.15	77.45
Briquets in middle of furnace	69.81	24.03	0.62	0.27	5.27	79.82	78.56
Briquets above gas entry into furnace	72.90	20.70	0.92	0.40	5.08	82.81	81.12
Bottom of furnace	89.10	5.10	0.56	0.40	4.84	95.44	94.19

The most important process conditions – composition and temperature of the reducing gas, its flow rate, and temperatures at the top and bottom of the shaft furnace – are given in Table 1.

The following data were obtained from the experiments and subsequent calculations.

1) The consumption of reducing gas per kg of $NaSO_4$ was 4.56 m^3, the excess of reducing agent being 160% of the theoretical amount.

2) The average degree of utilization of the reducing agent over 28 hours was 52%.

3) Comparison of the gas compositions at the furnace entry and exit shows that utilization of the reducing agent was far from complete, as thermodynamic calculations and laboratory experiments both show that the CO and H_2 contents of the final gas can be reduced to 1-2%, or even to tenths of one per cent. Therefore in this case, as in the laboratory experiments, some of the excess carbon monoxide and hydrogen is lost as the result of side reactions.

4) Experience showed that it is not necessary to use a large excess of reducing agent. It was found that when the gas rate was lowered to 15-16 m^3/hour from an average rate of 26.3 m^3/hour the reduction continued at the same rate.

Analytical data for briquets taken from different heights of the furnace after the experiment, presented in Table 2, also indicate that the excess of gas was too great.

Briquets taken from the furnace bottom, near the gas entry, had 89.1% Na_2CO_3, 5.1% Na_2SO_4 and 0.56% Na_2S; the degree of sulfate reduction was 95.44%, and the yield of carbonate was 94.19%. This is quite a satisfactory result from our point of view. The reduced briquets retained their strength and shape.

A very noteworthy fact is that the carbonate briquets made from Na_2SO_4 by the proposed method can be ground to give products of different particle size and high bulk density; this is especially important for the glass industry, where the use of soda of low bulk density results in phase separation of the charge.

It is to be expected that some design improvements in the shaft furnace, and modifications of temperature conditions, should lead to a further increase of the soda yield accompanied by a considerable decrease of the specific consumption of the reducing gas.

SUMMARY

1. A technological process for the production of sodium carbonate from sodium sulfate has been worked out from the experimental results. The process consists of the following main stages: a) preparation of the raw materials (catalyst preparation, briquetting of the sulfate, and drying of the briquets); b) preparation of the reducing gas, preheating of the gas to the reaction temperature, and humidification; c) reduction of sulfate by means of humidified semiwater gas.

2. In trials of the proposed method in a shaft-furnace pilot unit a product with a soda yield of 94% was obtained. The soda is quite suitable for a number of industries.

3. Adoption of the process for conversion of sodium sulfate into sodium carbonate should make it possible to establish the manufacture of soda in regions unsuitable for operation of the ammonia–soda process, and thereby to lower considerably transportation costs and the cost to consumers in the enormous territories of Eastern and Southeastern USSR.

LITERATURE CITED

[1] A. I. Gorbanev, J. Chem. Ind. No. 4 (1952).

[2] A. I. Gorbanev, J. Appl. Chem. 27, No. 8 (1954).•

[3] A. I. Gorbanev, J. Appl. Chem. 27, No. 9 (1954).

[4] A. I. Gorbanev, J. Appl. Chem 27, 10 (1954).•

Received December 17, 1956

•See C.B. Translation.

SYNTHESIS OF CATION-EXCHANGE RESINS BY SULFONATION OF PHENOL-FORMALDEHYDE NOVOLACS AT ELEVATED TEMPERATURES

A. A. Vasil'ev and A. A. Vansheidt

Institute of High-Molecular Compounds, Academy of Sciences USSR

It was shown in our first communication [1] that phenolsulfonic catin exchangers may be easily made by sulfonation of phenol-formaldehyde novolacs and treatment of the soluble sulfonated novolacs with formaldehyde, when their molecules become cross-linked through methylene groups, and are converted into insoluble space polymers. In our studies of the sulfonation of novolacs, however, it was found that insoluble polymers can also be formed in absence of formaldehyde if the sulfonated mass formed from the novolacs is heated at temperatures above 150°. Sulfur dioxide is evolved in the process, and the liquid mass is converted into a dark gel which increases in strength with subsequent heating. Soluble impurities can be easily removed from it by repeated treatment with water (and dilute alkali). The product is a dark, hard, mechanically strong resin, insoluble in water, with pronounced properties of a strongly acidic cation exchanger. It was found to contain up to 14.5% of sulfur, most of which (12.5%) is present in the form of titratable sulfo groups. As a result (SN) has a considerable exchange capacity (up to 3.9 meq/g), the magnitude of which depends on the sulfonation conditions. On the other hand, by variations of the conditions of resin preparation it is possible to vary its swelling in water within certain limits (from 1.3 to 1.8). This resin is thus not inferior to other phenolsulfonic cation exchangers in its ion-exchange properties.

As regards the mechanism whereby the space polymer is formed from the soluble sulfonated-novolac resin, the existing data are as yet inadequate for a solution of this problem. However, the presence in these sulfonated-novolac resins of a considerable amount of bound sulfur which cannot be estimated by titration suggests that this sulfur is present in the resin in the form of $-SO_2-$ groups which effect the cross linkage of the sulfonated-novolac molecules to form a space polymer. On the other hand, it is possible that the conversion of the soluble sulfonated novolac into the insoluble polymer is also associated with the oxidation-reduction reactions which take place when the sulfonated mass is heated and which lead to partial reduction of sulfur trioxide to the dioxide. However, these hypotheses require verification.

Data on the formation conditions and properties of cation exchangers of this type (SN), made from sulfonated novolacs without the use of formaldehyde, are presented below.*

EXPERIMENTAL

The starting materials for the synthesis were novolac resins of medium molecular weight, from 300 to 500, made by condensation of phenol with formaldehyde in presence of hydrochloric acid. According to preliminary data, molecular weight variations of novolacs within these limits had little effect on the properties of the cation exchangers obtained from them.

The novolacs were sulfonated by means of 93-98% sulfuric acid or 8% oleum, in wide-necked flasks heated on an oil or glycerol bath with continuous stirring. The resin first dissolved completely. Novolacs of average molecular weight close to 400 dissolved at about 125°. At 165-175° the solution passed into a gelatinous mass, which was heated further at 160-180° for 8-16 hours. At the end of the heating the cooled gel was

*G. A. Petrova and V. S. Matrosova took part in the experimental work.

covered with water; as a result, it cracked and could be removed from the flask without difficulty. In other experiments the hot mass was poured onto iron trays which were placed in a thermostat, where the gel was formed and subjected to the subsequent heat treatment. After extraction from the flask or tray, the hardened mass was crushed, and simultaneously sifted and washed with water to remove excess sulfuric acid. The resin was then treated with 1 N alkali solution at room temperature, usually 2-3 times (with the alkali solution renewed every 3-4 hours), regenerated by 2 N hydrochloric acid solution, and washed with water to a neutral reaction to methyl orange. The final washings were carried out on suction filters. The moist swollen resin was spread in a thin layer and dried at room temperature.

The cation exchangers were analyzed quantitatively for sulfur by fusion with caustic alkali and potassium nitrate [2].

The total exchange capacity (E) of the resins (in meq/g of dry resin) was determined by the method described earlier [3]. The "active" sulfur content, present in the form of SO_3H groups, was calculated from the formula: $\%\, S_{act} = E \cdot 3.207$.

The moisture contents of the air-dry resins were determined by drying in an oven to constant weight, usually at 110°. The permissible drying temperature was estimated in the light of considerations advanced in another paper [4].

The swelling coefficient (K) of the resins was determined as the ratio of the bulk density of the air-dry resin to the bulk density of the resin swollen in water.

The resistance of the resins in aggressive media was estimated from changes of exchange capacity, weight, and swelling coefficient of specimens after the action of alkali, acid, and oxidizing-agent solutions at room and higher temperatures.

For determination of mechanical strength, the resin samples were shaken with water for 5 hours, and the average grain sizes of the dry resin before and after the test were compared [5].

Effect of the Conditions of Resin Formation on Their Properties

The cation exchangers made with the use of oleum and sulfuric acid of the concentrations given above had approximately the same properties.

In a number of experiments the sulfonation agent was used in considerable excess (4 weight parts to 1 of resin). It was found, however, that it is not necessary to exceed a 2:1 ratio of sulfonation agent to resin.

The sulfonated novolac mass can withstand fairly prolonged heating (up to 2 hours at 150-170°) without any appreciable effects on the properties of the cations exchangers.

Heat treatment temperatures above 180° are not to be recommended, as in such conditions the sulfo groups of the cation exchangers are split off more rapidly, and the exchange capacity therefore falls sharply (see table).

Heat treatment of the gels at 160-180° for 8-16 hours yields cation exchangers of exchange capacity about 3.2-3.6 meq/g, with low swelling coefficients and satisfactory mechanical strength.*

Heat treatment of shorter duration yields cation exchangers of higher exchange capacity, reaching 4 meq/g, but of lower mechanical strength.

Heat treatment of the gels at 100-140° did not give positive results, as even prolonged treatment at these temperatures yielded only strongly-swelling and mechanically weak resins.

The optimum conditions for heat treatment of the gel are a temperature of 180°, and a time of 8-16 hours. The particle-size reduction in mechanical tests of resins made under these conditions did not exceed 3%. Their exchange capacity did not fall after treatment with 1 N caustic soda solution on a boiling water bath for 20 minutes. SN cation exchangers are stable in concentrated hydrochloric acid at room temperature, but, like other phenolsulfonic ion exchangers, are broken down when treated with 1 N nitric acid. By variations of the preparation conditions, the swelling coefficients of SN resins can be easily varied from 1.3 to 1.8, and the total

*The recommended temperatures of heat treatment are not excessively high. For example, Kressman and Kitchener [6] heated a sulfonated phenol–formaldehyde gel for 15 hours at temperatures up to 150°.

Sulfonation agent	Ratio sulfonation agent: novolac	Heat treatment conditions		Swelling coef. of resin	Sulfur content (%)		Exchange capacity (meq/g of dry resin)	Particle-size reduction (%)
		temp. (°C)	time (hrs)		total	active		
H_2SO_4 98%- . .	4 : 1	180	2	—	13.81	12.06	3.77	—
		220		1.5	10.48	8.42	2.63	—
		260		1.2	5.37	2.02	0.65	—
Oleum, 8%	4 : 1	180	1	2.8	14.98	12.26	3.82	—
			3	—	14.77	12.03	3.76	2.9
			8	1.8	12.68	10.34	3.23	—
H_2SO_4 96.6%- . .	2 : 1	160	1	3.3	15.33	12.37	3.86	High
			4	2.3	14.94	12.77	3.98	16.4
			8	1.5	14.67	12.47	3.88	4.7
			16	1.4	13.84	11.62	3.62	2.7

The Influence of Temperature and Prolonged Heat Treatment on the Properties of SN Cation Exchanges.

exchange capacity (E) from 2.5 to 3.9 meq/g. Thus, they are not inferior in exchange capacity to the phenolsulfonic resins MSF (E = 2.7•) [7] and Duolite C_3 (E = 3.2•) [8], and are superior to the resins KU-1 (E = 2.3•) [7] and Amberlite IR-100 (E = 1.7•).

SUMMARY

1. Strongly acid cation-exchange resins can be synthesized by the action of heat, above 150°, on the sulfonation products of phenol–formaldehyde novolacs.

2. The sulfonated novolac cation exchangers are not inferior in their properties (exchange capacity, mechanical strength, chemical resistance, etc.) to the best phenolsulfonic action exchangers.

LITERATURE CITED

[1] A. A. Vasil'ev and A. A. Vansheidt, J. Appl. Chem. 31, 7, 1075 (1958).•

[2] R. P. Lastovskii, Technical Analysis in the Production of Intermediates and Dyes [in Russian] (Moscow-Leningrad, Goskhimizdat, 1949), p. 75.

[3] A. A. Vansheidt, A. A. Vasil'ev and O. I. Okhrimenko, in the book: Theory and Practical Applications of Ion-exchange Materials [in Russian] (Moscow, Izd. AN SSSR, 1955), p. 110; A. A. Vansheidt, A. A. Vasil'ev, O. I. Okhrimenko and G. A. Petrova, in the book: Chromatography [in Russian] (Leningrad University Press, 1956), p. 51.

[4] A. A. Vasil'ev, J. Appl. Chem. 30, 1022 (1957).•

[5] I. E. Apel'tsin, V. A. Kliachko, Iu. Iu. Lur'e, and A. S. Smirnov, Ion Exchangers and their Applications [in Russian] (Standards State Press, 1949), p. 113.

[6] T. R. E. Kressman and J. A. Kitchener, J. Chem. Soc. 1190 (1949).

[7] E. B. Trostinskaia, Trans. Commission on Anal. Chem. 6 (9),215 (1955).

[8] O. Samuelson, Ion Exchangers in Analytical Chemistry (Moscow, IL, 1955), p. 275 [Russian translation edited by K. V. Chmutov).

Received November 12, 1957

•According to our experimental data.

••Original Russian pagination. See C.B. Translation.

NEOABIETIC ACID – A PRIMARY ACID OF THE OLEORESIN OF PICEA EXCELSA LINK

I. I. Bardyshev and Kh. A. Cherches

Institute of Chemistry, Academy of Sciences, Belorussian SSR

Investigations of the chemical composition of spruce oleoresin are both of theoreti cal and of practical importance, as the problem of the industrial tapping of spruce will, in our opinion, be very soon successfully solved [1, 2].

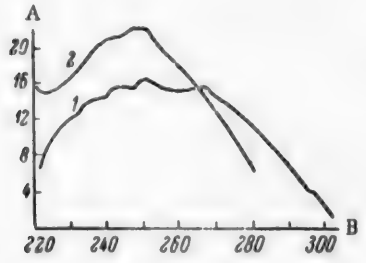

Fig. 1. Ultraviolet absorption spectra. A) Absorption coefficient α, B) wavelength λ (mμ). 1) Original resin acids, 2) resin acids after treatment with maleic anhydride.

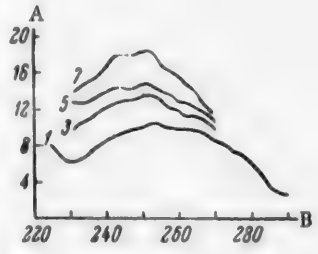

Fig. 2. Ultraviolet absorption spectra. A) Absorption coefficient α, B) wavelength λ (mμ). 1,3,5,7) Consecutive fractions of ethanolamine salts deposited in crystallization from alcohol.

Earlier investigations showed that spruce oleoresin contains levopimaric, dextropimoric, and α-sapinic acids [3], and abietic acid [4].

The present paper deals with a further study of the composition of spruce oleoresin. The investigation showed that, in addition to the above-named resin acids, unchanged fresh spruce oleoresin also contains neobietic acid, which was previously found in the oleoresin of different species of pine [5, 6].

EXPERIMENTAL

The oleoresin was obtained by tapping from spruce plantations in the Belorussian SSR, and stored in sealed jars.

For isolation of the original mixture of resin acids, the oleoresin was treated with 1.5 % aqueous caustic soda at 40°. Neutral substances were removed by means of repeated extraction of a solution of the salts with ethyl ether. The salts were decomposed by 1% aqueous acetic acid, and further treatment yielded the original mixture of resin acids melting at 116-130°, with $[\alpha]_D = -81.6°$ used for the investigation. The specific rotation was determined in 1% alcoholic solutions of the acids in all cases. The ultraviolet absorption spectrum of this acid mixture is given in Fig. 1 (Curve 1).

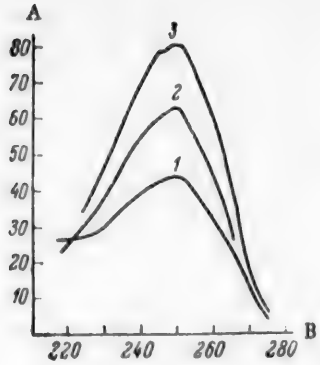

Fig. 3. Ultraviolet absorption spectra. A) Absorption coefficient α, B) wavelength λ ($m\mu$). 1) Ethanolamine salt precipitated from ether solution, 2) diethylamine salt of neoabietic acid, 3) neoabietic acid.

To remove levopimaric acid, the thoroughly dried mixture was treated in the usual way with redistilled maleic anhydride. 170 g of the original acid mixture yielded 60 g of resin acids which did not react with maleic anhydride, with $[\alpha]_D = +60°$, and absorption spectrum as shown in Fig. 1, Curve 2.

The acids prepared in this way were converted into their ethanolamine salts by the mixing of approriate amounts of the reagents dissolved in ethyl acetate. Recrystallization of the salts from alcohol yielded seven consecutive crystalline fractions of resin-acid salts, progressively richer in neoabietic acid (Fig. 2, Curves 1,3,5, and 7).

The 6th and 7th salt fractions, richest in neoabietic acid, were thoroughly washed with ethyl ether on the filter. After 24 hours the ether solution deposited a salt of m. p. 129-134° (Fig. 3, Curve 1). This ethanolamine salt fraction was converted by the usual method into the diethylamine salt; after ether washing, this salt had m. p. 142-146° $[\alpha]_D = +104°$ (Fig. 3, Curve 2). The diethylamine salt was recrystallized three times from acetone. The neoabietic acid isolated from the salt, after two recrystallizations from alcohol, had m. p. 172-175° $[\alpha]_D = +174°$ and specific absorption coefficient $\alpha = 80.5$ at 250 $m\mu$, which corresponds to 98% of neoabietic acid in the sample [6].

Elementary Analysis

Found %: C 79.2, 79.4; H 10.15, 10.15. $C_{20}H_{30}O_2$. Calculated %: C 79.42; H 10.0.

SUMMARY

Neoabietic acid is a primary acid of the oleoresin of the common spruce (Picea excelsa Link).

LITERATURE CITED

[1] I. Bardyshev and Kh. Cherches, Bull. Acad. Sci. Belorussian SSR 2 (1956).

[2] A. F. Mednikov and K. G. Gol'dman, Hydrolyt. and Wood Chem. Ind. 7 (1956).

[3] S. S. Malevskaia and S. D. Kharad, J. Appl. Chem. 23, 2 (1950).*

[4] I. I. Bardyshev and Kh. A. Cherches, J. Appl. Chem. 29, 1888 (1956).*

[5] G. C. Harris and T. F. Sanderson, J. Am. Chem. Soc. 70, 334 (1948).

[6] I. I. Bardyshev and Kh. A. Cherches, J. Appl. Chem. 31, 7, 1122 (1958).*

Received March 26, 1957

*Original Russian pagination. See C.B. Translation.

DETERMINATION OF CYCLOHEXANONE IN PRESENCE OF OTHER KETONES

A. S. Maslennikov

Laboratory of the Prophylactic Disinfection Division of the Gor'kii Regional Sanitary and Epidemic Station

Cyclohexanone is used more widely in technology than any other ketone. Being an excellent solvent for many technically valuable organic substances, cyclohexanone is also used to a considerable extent in the production of caprolactam, nylon, and many other synthetic organic products.

The existing methods for determination of cyclohexanone [1-3], based on the general reactions of carbonyl compounds, cannot be used for its determination in presence of other ketones.

We found that cyclohexanone can form a diazo dye with the diazonium salt of 1,8-aminonaphthol-3,6-disulfonic acid:

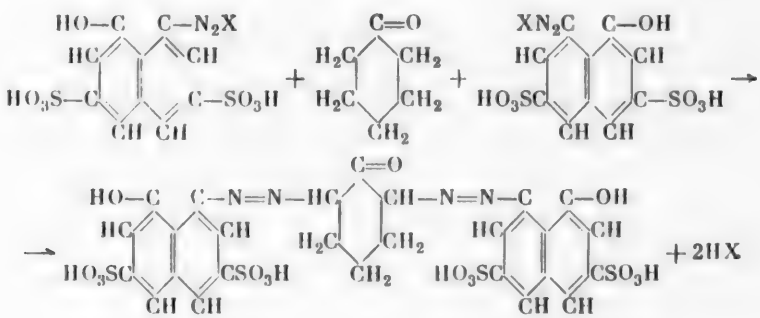

1,8-Aminonaphthol-3,6-disulfonic acid is usually known as H acid in the special literature on azo dyes. This designation is, for convenience, used in the present paper.

The azo dye formed by the reaction of cyclohexanone with the diazonium salt of H acid was isolated in the pure state; its composition was determined, and its most important physicochemical properties studied. The color of its solutions conforms to the Lambert–Beer law ($\log \frac{I_0}{I_d}$ is a linear function of the cyclohexanone concentration).

The maximum absorption is found in the 550 mμ region. The molar extinction coefficient, calculated from the formula $E = \xi \cdot l \cdot C$, is 15,700.

$$E = \xi \cdot l \cdot C$$

The reaction of dye formation from cyclohexanone and the diazonium salt of H acid has a pronounced specific character. Other ketones were found, in these conditions, to give only weakly colored substances, which were not isolated in the free state on acidification; H acid can therefore be used for determination of cyclohexanone in presence of other ketones.

It is known [4] that the diazonium salt of H acid can couple with itself in an alkaline medium, with

formation of compounds of an intense blue color. This makes the use of H acid as the diazo component in colorimetric analysis difficult. Introduction of sodium sulfite or bisulfite into the solution prevents the self-coupling of the diazonium salt of H acid without any adverse effects on its coupling with cyclohexanone.

EXPERIMENTAL

Preparation of an azo dye by the reaction of cyclohexanone with the diazonium salt of H acid. To 100 ml of a 2% suspension of the monosodium salt of H acid in 0.1 N sulfuric acid, 5 ml of 10% sodium nitrite solution was added dropwise. After 5 minutes 500 mg of cyclohexanone and 25 ml of an alkaline mixture made from 20% solutions of sodium sulfate and hydroxide in 1:1 ratio was added to the reaction mixture. On addition of the alkaline mixture the precipitated diazonium salt of H acid dissolved, and the solution acquired an intense cherry-red color. After 20 minutes 50% sulfuric acid was added dropwise to the solution until the color changed from cherry-red to brown and a precipitate of the azo dye was formed. The solution and precipitate were transferred to a No. 3 porous filter funnel, the precipitate was filtered off by suction, washed three times with alcohol, and dried in an oven at 100-105°. The yield was 2.04 g or 98.8% of the theoretical, on the assumption that the H acid content of the monosodium salt was 87%, as was established by analysis.

The azo dye retains some of the properties of H acid, has no definite melting point, decomposes when heated above 200°, and is insoluble in the common organic solvents: alcohols, ether, chloroform, and carbon tetrachloride; it has relatively high solubility in water – about 3.8% at room temperature. In aqueous solutions the color of the dye changes with pH from brick-red in the acid region at pH 4 to cherry-red in the alkaline region at pH 12. In concentrated sulfuric acid the color of the azo dye is green. On dilution with water the green color again passes into brick-red, typical of this dye in an acid medium. The action of salts of heavy and alkaline-earth metals on aqueous solutions of the azo dye yields sparingly soluble precipitates, while barium salts give virtually insoluble salts of the azo dye. The fact that the barium salts of the dye are insoluble was used for determination of the number of sulfo groups in the dye molecule, and of its nature.

Determination of the number of sulfo groups. To a definite volume of a 0.01 M solution of the dye (7.58 g/liter) 0.1 M barium chloride solution was added in small portions at 5-minute intervals, until the supernatant liquid became colorless. After 30 minutes the colorless solution was decanted through a filter funnel. The decantation was repeated three times. The precipitate was then transferred to the filter and washed until barium ions were no longer present in the wash waters. The excess barium chloride in the combined filtrate was determined by the usual method. The average ratio of the amount of 0.01 M solution of azo dye to 0.1 M barium chloride solution in precipitation of the azo dye was 10:1.99.

Elementary Analysis of the Azo Dye

Found %: SO_3H 42.59. $C_{26}H_{22}O_{15}S_4N_4$. Calculated %: SO_3H 42.74.

Determination of sulfur by Messenger's method [5].

Weight of substance taken (mg): 512, 456, 470.
$BaSO_4$ formed (mg): 639, 556.35, 572.15.

Found S %: 16.96, 16.77, 16.10. $C_{26}H_{22}O_{15}S_4N_4$. Calculated S %: 16.88.

Colorimetric determination of cyclohexanone by the reaction with the diazonium salt of H acid in presence of other ketones. To 1 ml of the aqueous cyclohexanone solution, containing certain amounts of other ketones, in a colorimetric tube, there were added 0.2 ml lots of 0.25% solution of the monosodium salt of H acid in 0.1 N sulfuric acid, 1% sodium nitrite solution, 5% sodium metabisulfite solution, and 10% caustic soda solution. The liquid was stirred before addition of the metabisulfite and alkali. Five minutes after addition of all the reagents the liquid was diluted to exactly 10 ml, and its color compared with a range of standards obtained under the same conditions. The results of colorimetric determinations of cyclohexanone by the reaction with the diazonium salt of H acid, in presence of other ketones, are given in Table 1.

It follows from the data in Table 1 that this method can be used for determination of cyclohexanone in presence of small amounts of other ketones, not more than 5 times the amount of cyclohexanone present. If large amounts of other ketones are present, the analysis can be performed by colorimetric titration with standard aqueous solutions of the azo dye.

TABLE 1

Colorimetric Determination of Cyclohexanone by the Reaction with the Diazonium Salt of H Acid in Presence of Other Ketones

Amount of cyclohexanone taken (μg)	Other ketones present (μg)		Cyclohexanone found (μg)	Error (%)
5.0	Acetophenone	25	5.4	+8.0
5.0	"	30	5.5	+10.0
10.0	"	50	11.4	+14.0
5.0	Acetone	25	4.9	− 2.0
5.0	"	40	5.2	+ 4.0
10.0	"	50	9.8	− 2.0
5.0	Methyl ethyl ketone	30	4.8	− 4.0
10.0	"	50	9.7	− 3.0
10.0	"	75	11.4	+14.0
5.0	Pentanone-2	30	5.1	+ 2.0
10.0	"	50	10.3	+ 3.0
10.0	"	75	11.5	+15.0
5.0	Methyl isobutyl ketone	25	4.9	− 2.0
10.0	"	50	10.5	+ 5.0
10.0	"	70	11.3	+13.0

TABLE 2

Determination of Cyclohexanone by the Reaction with the Diazonium Salt of H Acid in Presence of Other Ketones, by Means of Colorimetric Titration

Amount of cyclohexanone taken (μg)	Other ketones present (mg)		Cyclohexanone found (μg)	Error (%)
10.0	Acetophenone	0.15	10.47	+4.7
	Acetone	0.20	9.77	−2.3
	Methyl ethyl ketone	0.20	10.96	+9.6
	Pentanone-2	0.20	10.20	+2.0
	Heptanone-2	0.20	9.66	−3.4
	Methyl isobutyl ketone	0.20	9.87	−1.3
20.0	Acetophenone	0.30	19.3	−3.5
	Acetone	0.30	19.20	−4.0
	Methyl ethyl ketone	0.30	21.20	+6.0
	Methyl isobutyl ketone	0.30	18.40	−8.0
	Pentanone-2	0.30	20.92	+4.6
	Heptanone-2	0.30	21.40	+7.0
	Methyl ethyl ketone	0.60	21.10	+5.5
30.0	Acetophenone	0.60	28.20	−6.0
	"	0.90	30.12	+4.0
	Acetone	0.90	32.40	+8.0
	Methyl ethyl ketone	0.90	28.40	−5.34
	Methyl isobutyl ketone	0.90	28.50	−5.0
	Pentanone-2	0.90	31.40	+4.60
	Heptanone-2	0.90	29.0	−2.3

Determination of cyclohexanone in presence of other ketones, by colorimetric titration. To 2 ml of the unknown solution of a total ketone content not greater than 1 mg, contained in a test tube, 1 ml of 1% solution of H acid in 0.2 N sulfuric acid, and 0.2 ml of 5% sodium nitrite solution were added. The liquid in the tube was mixed. One ml of an alkaline solution made from 20% solutions of sodium sulfite and hydroxide was then added. In presence of cyclohexanone the solution became cherry-red. In presence of other ketones the solution was yellow or yellow-brown. After 10 minutes 0.5 ml of 50% sulfuric acid was added. The azo dye formed by the reaction of cyclohexanone with the diazonium salt of H acid was precipitated. The reaction products of the other ketones remained in solution. The precipitate was transferred onto a filter, filtered off, and washed twice with alcohol. The funnel with the filter was then inserted into a colorimetric tube and the precipitate was dissolved in 10 ml of water. Two ml of water was treated in the same way. A standard aqueous solution of the azo dye was then added to the control sample until the color was equal to that of the test sample. The amount of standard solution of azo dye taken for the colorimetric titration was used to calculate the cyclohexanone content of the sample (7.734 μg of azo dye corresponds to 1 μg of cyclohexanone). The results of determination of cyclohexanone by its reaction with the diazonium salt of H acid, by means of colorimetric titration in presence of other ketones, are presented in Table 2.

It follows from the data in Table 2 that cyclohexanone can be determined by colorimetric titration, by its reaction with the diazonium salt of H acid, in presence of 30-fold quantities of other ketones. The time required for each determination is about 30 minutes.

SUMMARY

1. The reaction of azo dye formation by the action of cyclohexanone with the diazonium salt of H acid has an appreciable specific character; it may be used for determination of cyclohexanone in presence of other ketones.

2. A method has been developed for determination of cyclohexanone in presence of other ketones, by its reaction with the diazonium salt of H acid. The determination can be performed by the usual colorimetric method, or by colorimetric titration with standard aqueous solutions of the azo dye.

3. The colorimetric method can be used for determination of cyclohexanone in presence of 5-fold quantities of other ketones. Determination in presence of 30-fold quantities of other ketones is possible by means of colorimetric titration.

LITERATURE CITED

[1] H. A. Jobes and A. W. Zow, Ind. Eng. Ch. 2, 102 (1939).

[2] S. D. Nagare and J. Mitchell, Anal. Chem. 9, 1376 (1953).

[3] A. S. Maslennikov, Factory Labs. 20, 1, 40 (1954).

[4] S. F. Fillipychev, Chemistry and Technology of Azo Dyes [in Russian] (1938), p. 231.

[5] J. F. Thorpe and M. A. Whiteley, A Student's Manual of Organic Chemical Analysis (1937), p. 67.

Received August 6, 1956

SIGNIFICANCE OF ABBREVIATIONS MOST FREQUENTLY ENCOUNTERED IN SOVIET PERIODICALS

FIAN	Phys. Inst. Acad. Sci. USSR.
GDI	Water Power Inst.
GITI	State Sci.-Tech. Press
GITTL	State Tech. and Theor. Lit. Press
GONTI	State United Sci.-Tech. Press
Gosenergoizdat	State Power Press
Goskhimizdat	State Chem. Press
GOST	All-Union State Standard
GTTI	State Tech. and Theor. Lit. Press
IL	Foreign Lit. Press
ISN (Izd. Sov. Nauk)	Soviet Science Press
Izd. AN SSSR	Acad. Sci. USSR Press
Izd. MGU	Moscow State Univ. Press
LEIIZhT	Leningrad Power Inst. of Railroad Engineering
LET	Leningrad Elec. Engr. School
LETI	Leningrad Electrotechnical Inst.
LETIIZhT	Leningrad Electrical Engineering Research Inst. of Railroad Engr.
Mashgiz	State Sci.-Tech. Press for Machine Construction Lit.
MEP	Ministry of Electrical Industry
MES	Ministry of Electrical Power Plants
MESEP	Ministry of Electrical Power Plants and the Electrical Industry
MGU	Moscow State Univ.
MKhTI	Moscow Inst. Chem. Tech.
MOPI	Moscow Regional Pedagogical Inst.
MSP	Ministry of Industrial Construction
NII ZVUKSZAPIOI	Scientific Research Inst. of Sound Recording
NIKFI	Sci. Inst. of Modern Motion Picture Photography
ONTI	United Sci.-Tech. Press
OTI	Division of Technical Information
OTN	Div. Tech. Sci.
Stroiizdat	Construction Press
TOE	Association of Power Engineers
TsKTI	Central Research Inst. for Boilers and Turbines
TsNIEL	Central Scientific Research Elec. Engr. Lab.
TsNIEL-MES	Central Scientific Research Elec. Engr. Lab.–Ministry of Electric Power Plants
TsVTI	Central Office of Economic Information
UF	Ural Branch
VIESKh	All-Union Inst. of Rural Elec. Power Stations
VNIIM	All-Union Scientific Research Inst. of Meteorology
VNIIZhDT	All-Union Scientific Research Inst. of Railroad Engineering
VTI	All-Union Thermotech. Inst.
VZEI	All-Union Power Correspondence Inst.

Note: Abbreviations not on this list and not explained in the translation have been transliterated, no further information about their significance being available to us. – Publisher.

RUSSIAN-ENGLISH

Cover-to-cover Translations by Bilingual Scientists

Bulletin of Experimental Biology and Medicine

Covers physiology, pathology, immunology, biophysics, pharmacology, oncology, morphology. Translation began with the 1956 volume, and is by special arrangement with the National Institutes of Health. Annual subscription, English translation, 12 issues, approximately 1000 pages –240 articles. Only $20.00

Pharmacology and Toxicology

By special arrangement with the American pharmaceutical industry; translation began with the 1957 volume. Annual subscription, English translation, 6 issues, approximately 600 pages – 150 articles. Only $25.00

Biochemistry

Most comprehensive Soviet biochemical journal; covers plant and animal biochemistry. Translation began with the 1956 volume, and is by special arrangement with the National Institutes of Health. Annual subscription, English translation, 6 issues, approximately 600 pages – 120 papers. Only $20.00

Soviet Journal of Atomic Energy

"Atomnaya Energiya" in complete English translation. Covers latest advances in peaceful uses, including biological-medical work with radioactive isotopes. Translation began with 1956 (first) volume. Annual subscription, 12 issues, approximately 1200 pages – 240 papers. Only $75.00

Soviet Pharmaceutical Research

Chemistry Collection No. 4 – Covers all aspects of Soviet pharmaceutical research; papers expertly selected from the following Russian chemical journals translated by Consultants Bureau, 1949-1955: Journal of General Chemistry; Journal of Applied Chemistry; Bulletin of the Academy of Sciences, USSR, Division of Chemical Sciences; Journal of Analytical Chemistry; Colloid Journal. Sections–may be purchased separately:

I. Pharmaceutical Chemistry: Solubility; stability; ion exchange; emulsions, suspensions, gels; miscellaneous. 74 papers, 447 pages, $95.00

II. Pharmacognosy: Alkaloids; oils; glycosides; miscellaneous. 87 papers, 399 pages, $90.00

III. Medicinal Chemistry: Structure-activity relationships; General. 91 papers, 556 pages, $100.00

Complete: 252 papers, 1402 pages $200.00
Single papers, $7.50–free table of contents on request.

RADIOBIOLOGY SYMPOSIUM–Seven reports by four famous Soviet biologists on X-ray irradiation of mice. English translation. 134 pages, $50.00

REMOTE CONSEQUENCES OF INJURIES CAUSED BY IONIZING RADIATION – Summaries of 22 papers; effects on dogs, rabbits, mice. 74 pages, $10.00

Text clearly reproduced by multilith process from IBM "cold type"–includes all diagrammatic and tabular material; books and journals staple bound in durable paper covers. Sample journal Tables of Contents on request.

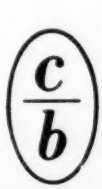

CONSULTANTS BUREAU, INC.
227 W. 17th St., NEW YORK 11, N.Y.

PROCEEDINGS OF THE FIRST ALL-UNION CONFERENCE ON RADIATION CHEMISTRY, MOSCOW, 1957

THIS UNPRECEDENTED RUSSIAN CONFERENCE on Radiation Chemistry, held under the auspices of the *Division of Chemical Sciences, Academy of Sciences, USSR* and the *Ministry of Chemical Industry* , aroused the interest of scientists the world over. More than 700 of the Soviet Union's foremost authorities in the field participated and, in all, fifty-six reports were read covering the categories indicated by the titles of the individual volumes listed below. Special attention was also given to *radiation sources used in radiation-chemical investigations.*

Each report was followed by a general discussion which reflected various points of view in the actual problems of radiation chemistry: in particular, on the *mechanism of the action of radiation on concentrated aqueous solutions,* on the *practical value of radiation galvanic phenomena,* on the *mechanisms of the action of radiation on polymers, etc.*

The entire "Proceedings" may be purchased as a set, or individual volumes may be obtained separately as follows:

Primary Acts in Radiation Chemical Processes
(heavy paper covers; 5 reports, approx. 38 pp., illus., $25.00)
Radiation Chemistry of Aqueous Solutions
(heavy paper covers, 15 reports, approx. 83 pp., illus., $50.00)
Radiation Electrochemical Processes
(heavy paper covers, 9 reports, approx. 50 pp., illus., $15.00)
Effect of Radiation on Materials Involved in Biochemical Processes
(heavy paper covers, 6 reports, approx. 34 pp., illus., $12.00)
Radiation Chemistry of Simple Organic Systems
(heavy paper covers, 9 reports, approx. 50 pp., illus., $30.00)
Effect of Radiation on Polymers
(heavy paper covers, 9 reports, approx. 40 pp., illus., $25.00)
Radiation Sources
(heavy paper covers, 3 reports, approx. 20 pp., illus., $10.00)

PRICE FOR THE 7-VOLUME SET
: $125.00

NOTE: *Individual reports from each volume available at $12.50 each. Tables of Contents sent upon request.*

CB translations by bilingual scientists include all photographic, diagrammatic, and tabular material integral with the text.

CONSULTANTS BUREAU, INC.
227 WEST 17TH STREET, NEW YORK 11, N. Y